THE BEHAVIOUR OF POLYTETRAFLUOROETHYLENE AT HIGH PRESSURE

by

Haroun Mahgerefteh

A dissertation submitted to the University of London for the degree of Doctor of Philosophy

Department of Chemical Engineering and Chemical Technology,

Imperial College,

London SW7 2BY.

October 1984

If a man will begin with certainties, he shall end in doubts, but if he will be content to begin with doubts, he shall end in certainties.
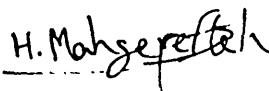
Robin Hyman

TO MY PARENTS

P R E F A C E

This dissertation is a description of the work carried out in the Department of Chemical Engineering and Chemical Technology, Imperial College, London between October 1981 and October 1984. Except where acknowledged, the material presented is the original work of the author and includes nothing which is the outcome of work done in collaboration, and no part of it has been submitted for a degree at any other University.

I am deeply indebted to Dr. Brian Briscoe for his excellent supervision during the course of my research. His help and guidance have been invaluable. It has been a pleasure to receive the help of many members of the Department, in particular Messrs. D. Wood and M. Dix of Electronics and Mr. B. Lucas of the Workshop. The help and support from all the members of my family especially my sister Deborah have been invaluable. I also thank Mrs. Joyce Burberry for patiently typing the manuscript.

H. Margerefteh

Imperial College,

London

H. Margerefteh

October 1984

CONTENTS

A B S T R A C T

This thesis describes a series of experimental studies on some of the effects produced when relatively large specimens of poly(tetrafluro-ethylene), PTFE, are subjected to gaseous and liquid pressures of up to 51 MPa in a temperature range between $0^{\circ}C$ and $70^{\circ}C$. The main measurements provide a precise value of the extent of gas sorption and the associated volume changes. Data for three gases, helium, nitrogen and argon together with mixtures of helium and nitrogen are presented to elucidate the influence of pressure and temperature on the gas sorption and linear contraction in this polymer. Comparative data are given for a liquid medium. Additional data on absorption of nitrogen in three other polymers, namely poly(ethylene), PE, poly(propylene), PP and poly(methylmethacrylate), PMMA, are also reported.

The gas sorption data indicate that relatively large quantities of gas are absorbed and that the amount is a function of the size of the gas molecule and the temperature of the matrix. In general, the least dense polymers sorb the most gas. The extent of gas sorption is not a marked function of the gross morphology or the pressure or thermal history of PTFE. The gas molecules appear to be associated with sites whose volume is in the order of the gas molecules dimensions and hence the sorption experiments detect, in a crude way, the molecular free volume sites in the matrix.

In spite of the large mass computed volume sorptions (ca. 16% V/V He in PTFE at $17^{\circ}C$ and 51 MPa), the polymers, PE and PTFE are found to contract under pressure and the compressibility is similar to that found using an hydraulic oil pressure medium in separate experiments. However, to a first order, it is found that the greater the gas sorption the

less is the compressibility. The linear contraction measurements allow the pressure dependence of the $20^{\circ}C$ transition in PTFE to be detected. The transition temperature increases with pressure but at a rate less than that observed in a liquid medium. This is tantamount to suggesting that under pressure, the gas molecules and atoms not only compress the polymer, but also facilitate molecular relaxations by effectively "lubricating" the molecular chains in the polymer. The magnitude of this effect is found to be dependent on the nature of the gaseous medium.

List of Symbols

Chapter 2

D	Diffusion constant
P	Pressure
L	Membrane thickness
E	Activation energy
a	Effective size of diffusing molecule
ℓ	Average jump length
ρ	Polymer density
A and B	Activation energy constants
f	Free volume
K	Boltzmann's constant
T	Absolute temperature
S	Gaseous solubility constant
R	Universal gas constant
Q	Gaseous uptake
t	Time
C_∞	Gaseous concentration at saturation
A	Accessible area
m	Mass of sample
P	Permeability
α	Degree of cystallinity
m	A constant
Pa	Permeability of amorphous polymer
r	Radial distance
ΔH	Heat of solution

Chapter 3

K	Thermal conductivity
C	Specific heat

V	Phonon velocity
X	Distance
t	Time
$\dot{Q}$	Flux rate of heat
ℓ	Specimen length
r	Specimen radius
γ_G	Isothermal Graneisen parameter
f_0	Fractional free volume
k	Boltzmann constant
Tg	Glass transition temperature

Chapter 4

τ	Maximum shear stress
α	Coefficient of increase in yield
P	Pressure
V	Velocity of craze propagation
T_b	Gaseous boiling point
D	Diffusion coefficient
Q_v	Heat of vapourisation
δ	Maximum depth in polymer invaded by gas
A and B	Constants
P_r	Relative pressure

Chapter 5

$\Delta\alpha$	Change in thermal expansion coefficient
$\Delta\beta$	Change in compressibility
ΔC_p	Change in specific heat
ε	Linear strain
ε_0	Linear strain at 1 atmosphere pressure
t	time
m and n	constants

ΔQ Enthalpy change

$B(T)$ Polymer melt parameter

Chapter 6

σ_u Ultimate tensile strength

σ Yield strength

K Aspect ratio

Chapter 7

HDPE   High density poly(ethylene)

PP   Poly(propylene)

PMMA   Poly(methylmethacrylate)

Chapter 8

DTA   Differential thermal analysis

K Thermal conductivity

Chapter 9

ρ/ρ_o Normalised gaseous density

F_o/F Frequency attenuation

B A constant

P Polymer

$A\ell$ Aluminium

A_c Compression area

M_o Mass of specimen

Δm Entrained or displaced mass of gas

$\Delta m'$ Gaseous uptake

ℓ_1 and ℓ_2 Dimensions of compression area

h Entrained layer thickness

Chapter 10

C Electrical capacitance

k_o Permittivity of free space

K	Relative permittivity
A	Capacitance area
t	Distance between capacitive plates
C_r	Reference capacitance
C_p	Polymer capacitance
ε_ℓ	Polymer linear strain in liquid
ε_g	Polymer linear strain in gas
ℓ	Polymer length
$a, b \ \& \ c$	Constants

Chapter 11

C	Electrical capacitance
V	Polymer volume
ΔV	Volumetric strain at transition
ΔQ	Enthalpy change

Appendix

P_y	Yield pressure
P_b	Burst pressure
HPSC	High pressure safety code
P_{max}	Maximum allowable working pressure
P_w	Maximum working pressure
A	Bolt head area
W_{max}	Maximum cap displacement
E	Young's modulus
σ_{max}	Maximum stress
$c', c'' \ \& \ a$	Constants
E_s	System energy
E_1	Fluid expansion energy
E_2	Chemically released energy
E_3	Elastic strain energy

ΔH Enthalpy change

S Entropy

RHO Density

E_{KE} Kinetic energy of cap

M Mass of cap

t Mild steel thickness

CHAPTER 1

INTRODUCTION

This thesis describes a series of experiments on the influence of gases at high pressures on the properties of organic polymers, in particular PTFE. A number of variables have been examined including the amount of gas absorbed, the volume change associated with absorption at high pressure, the thermal effects accompanying absorption, and the influence of the gas sorption on the room temperature transition in PTFE. Data are also reported on the influence of a conventional liquid pressure medium on PTFE in the same types of experiments. In addition, selected data are also presented for three other commercial polymers, namely poly(methylmethacrylate), poly(propylene) and high density poly-(ethylene).

This work was motivated, in the first instance, by a publication in the literature approximately 14 years ago. Billinghurst and Tabor (1971) had reported that under some circumstances a nitrogen gas environment could lead to what they termed a plasticisation of PTFE. This process had two interesting commercial implications. The first was that if this plasticisation could be proven and improved, it would form a useful basis for improving the fabrication of PTFE components. PTFE invariably has to be sintered at high temperatures, preferably under pressure, and this is both a costly and often ineffective fabrication technique. The second area of interest was less obvious and is associated with the operation of PTFE-based components in high-pressure media, particularly where PTFE is used as a piston ring. In these applications it has been known for many years that PTFE-based materials can suffer unexpected premature failure depending upon the gas environment in which they operate.

Early in the study, it is demonstrated that the apparent plasti-cisation process is an artifact due to the adiabatic compression which occurred during the previous studies. Chapter 8 reports this data and extends the analysis of the data to indicate the potential uses of the apparent plasticisation which is, in fact, associated with the trans-port of hot gas flux into the matrix. While the plasticisation is not of the form initially envisaged, it has some potential commercial value and indeed could explain some of the premature failures associated with the performance of dynamic PTFE-based seals.

During the preliminary studies on the apparent plasticisation pro-cess of PTFE in nitrogen, a number of interesting phenomena were revealed which are dealt with in the remainder of this thesis. Central to the whole of this study is the development of an experimental technique which can accurately determine the extent of gas sorption into polymer matrices. This topic is described in Chapter 9. During the course of this part of the study it was also possible to develop a useful probe for measuring the density of gases at high pressures and this is also described in Chapter 9. The experimental results were rather surprising and indicated, for example, that the amount of gas sorption was large and was also a function of the type of gas molecule. A rough correla-tion between the size of the molecules and the extent of mass sorption was detected. In addition, rather peculiar effects such as the tempe-rature dependence of the sorption of pure gases and the behaviour of gas mixtures were observed. These data were obtained primarily for PTFE but similar trends were seen with other polymers, the main diffe-rence being that other polymers absorb even more gas than the PTFE used in this study. A particularly interesting feature which emerged was that the extent of mass sorption was not a function of the morphology, or the thermal history or, indeed, the pressure history of the polymer.

During the course of these investigations it became a matter of interest to discover whether this volume sorption was accompanied by a contraction or expansion of the polymer matrix. In view of the large amount of gas sorption it did appear that the latter would be more favoured. A separate study is therefore described which measures the volumetric strain of PTFE and high density poly(ethylene) as a function of temperature and pressure both in gas and liquid media. Rather surprisingly it was discovered that the polymer is compressed in gaseous media by about the same amount as that observed in a liquid medium. There are some second order effects however which indicate that the extent of the compressibility is also a function of the gas species. These data are reported in Chapter 10.

The same volumetric measurement also facilitated a study of the effects of the pressure environment on the room temperature transitions of PTFE. These data are reported in Chapter 11. As might be expected, the pressure dependence of the transition temperatures is positive and it is also found to be extremely sensitive to the nature of the pressure medium.

Chapter 12 brings together the results from the gas sorption volumetric change measurements and the pressure dependence of the transition data and attempts to review the rather subtle problems associated with describing the influence of gas media on the properties of organic polymers. The early parts of the thesis comprise four Chapters which review the precedence in the areas of the diffusion and solubility of gases in organic polymers (Chapter 2), the effect of pressure on the thermal conductivity of polymers (Chapter 3), the effect of hydrostatic pressure on the mechanical properties of polymers (Chapter 4) and the effect of hydrostatic pressure on the compressibility of polymers

(Chapter 5). The hardware used to superimpose both a hydrostatic and
a pneumatic pressure media on polymers are described in Chapter 6.
The details of the experimental methods, in particular the transducers
for measuring volumetric strain and mass sorption are described in
detail in the appropriate Chapters. The Appendix to the thesis contains
an evaluation of the safety and design requirements for the pressure
vessels used in the current study. A general description of the poly-
mers used in this investigation is described in Chapter 7.

CHAPTER 2

THE DIFFUSION AND SOLUBILITY OF GASES IN ORGANIC POLYMERS

2.1 Introduction

This Chapter is a review of some of the important work published in the field of diffusion and absorption of gases in organic polymers. Typical experimental data have been selected to exemplify what is known about the diffusion mechanisms and the influence of various variables on the diffusivity and the solubility of permanent gases in a number of organic polymers. The review covers work reported both at atmospheric pressure and also at higher gas pressures. The main purpose of this review is to provide a background in which the data from the subsequent chapters may be interpreted and compared with previous studies. The studies at ambient pressure introduce the major feature.

2.2 Diffusion and Solubility of Gases in Polymers at Atmospheric Pressure

The classical way of describing the diffusion of condensable gases through thin polymeric films is that proposed in a publication by Graham (1866). In it, the process is described as the condensation and solution of gas at one end followed by diffusion through the matrix and finally evaporation at the other end. More than a decade later, Wroblewski showed that the gaseous solubility in a rubber membrane was proportional to the partial pressure above the membrane. Wroblewski (1879) also speculated that Fick's linear diffusion law applied and was able to formulate the well known permeability equation

$$Q = DS \, \frac{P_1 - P_2}{L} \qquad (2.1)$$

where Q is the amount of gas passing through unit area per second, D is the diffusion constant, S is the solubility coefficient and P_1 and P_2 are the partial pressures of the diffusing gas at the two sides of a membrane of thickness L. The product DS is termed the permeability constant and is applicable to permanent gases.

Perhaps the next important study was by Barrer (1939) who made use of the now famous time lag technique developed earlier by Dynes (1920) to determine both the solubility and diffusivity by measuring the time taken to acquire steady state of permeation of gases through a polymer membrane. From this study he was able to conclude that in general, using simple gases, Henry's law was obeyed and the diffusion constants were independent of gaseous concentration. The time lag technique has been useful in the present study.

By this time it was evident that the various factors concerning diffusivity of simple gases could be discussed in terms of the molecular dimensions of the gas and the structural characteristics, in particular, the holes in the polymer matrix. The specific interaction between the permanent gas molecules and the polymer matrix were of a weak nature and the diffusion process was Fickian in its character. This type of system is now known as case I diffusion. Alongside the simple case developed another type of system, case II, systems where very significant matrix gas interactions occur. Here, the gas modifies the properties of the matrix; the idea of gas plasticisation is introduced. These are comparatively complex systems although certain features are amenable to analysis. In this review we will not deal with the case II systems as these special features are not seen in the present study. There are however certain aspects of the current work which do resemble case II systems but they arise from an artefact

in the experimental method. Adiabatic compression of gas in the present studies produces a heated front in the matrix as the gas transports and the matrix is modified thermally rather than chemically.

Mears (1954) extended these ideas and proposed that the gas diffusion proceeded by discrete "jumps" of the diffusing molecules from one sorption site to the next. He then adopted a thermally activated model where the corresponding activation energy, E_d, was correlated to the polymer bond cohesive energy, E, in terms of an equation of the form:

$$E_d = a\ell\rho E \qquad (2.2)$$

The expression incorporates the "effective size", a, of the diffusing molecule, the average jump length, ℓ, and the density, ρ of the polymer which is a measure of its free volume. Mears was then able to derive an exponential variation of the penetrant diffusion coefficient with the polymer "free volume", f, and the diffusion activation energy, E_d. His equation took the form:

$$D = A\exp(-aB/f - E_d/KT) \qquad (2.3)$$

with A and B being constants which in first approximation are independent of the material. The constant B is also a function of the entropy of diffusion.

The idea of available or "free volume" is an important factor in both solubility and transport and was developed further by Michaels and Parker (1959)[†] who, in a comprehensive study, presented evidence that at $25^{\circ}C$ the solubility of N_2, O_2 and CO_2 in poly(ethylene) varied linearly

with the amorphous content of the polymer. No dependence on molecular

weight, mode of polymer synthesis, and sample preparation was observed.

It was speculated that the crystalline phase of poly(ethylene) did not

sorb gas molecules to any detectable extent and hence did not play a

constructive part in gas transport. The gaseous solubility constants,

S, were found to obey the Arrhenius type relationship with temperature

of the form:

$$S = S_o \, e^{-E_d/RT} \tag{2.4}$$

where S_o and E_d were the pre-exponential factor and activation energy

respectively. In a later publication, Michaels and Bixler (1961)

showed that the above criteria were generally obeyed using a wider

range of permanent gases. Also, the diffusion coefficients of gases

decreased almost universally with increasing gaseous molecular diameter

at the expense of an increase in activation energy. This is consistent

with the now generally accepted view of the thermally activated nature

of this diffusion process. Also larger holes need to be formed or be avai-

lable in the polymer for the diffusion of the larger molecules. These

hole formation processes will require a larger energy of formation

and hence the activation energy will be greater for the diffusivity

of large molecules.

These early studies emphasised the important notion of "holes"

as transport sites. The sum of these holes is often termed the free

volume of the matrix. This is a vague but useful notion which is

not only useful in transport and sorption studies but also in the

analysis of mechanical and dielectric data. Free volume can be

regarded as static distribution of discrete "holes". Alternatively,

a dynamic picture would see them as the probability of a hole of a given size occurring at a given point. For an analysis of equilibrium mass sorption the static picture is appropriate but in a transport problem a dynamic model is more appropriate. Current molecular dynamicists do not regard the notion of holes as useful nor do they approve of the Eyring type of analysis suggested by Mears (1954). The concept of "free volume" is certainly naive but it does explain trends and,perhaps of more importance in the context of this thesis, it gives a simple account of the influence of hydrostatic stress. Application of pressure increases density and hence reduces free volume. Increasing temperature reduces the density and thereby increases the free volume but also at the same time increases the rate of thermal activation. A linear relationship between the diffusion coefficient of octadocane with the coefficient of expansion of different elastomers as reported by Auerbach et al (1958) is in support of this view.

In the dynamic picture, the ease of hole formation primarily depends on chain mobility. It is therefore related to the glass transition temperature, Tg,and cohesive energy of the matrix. These are reflected in the degree of cross-linking, the crystallinity and the coefficient of thermal expansion.

The influence of Tg on the diffusion constants of Ar and O_2 in amorphous poly(vinylacetate) was investigated by Mears (1954). An abrubt increase in the gaseous diffusion constant was observed on passing through Tg. This was attributed to an increase in chain mobility and coefficient of thermal expansion around Tg. The latter induced an increase in the rate of increase in free volume.

The importance of the relative sizes of the penetrant gas mole-

cules and polymer sites on the above was highlighted in a publication

by Stannett and Williams (1966). They studied the diffusion of gases

with a range of molecular diameters in polyethylmethacrylate. No dis-

continuity in the diffusion coefficients of N_2, He, Kr and Ar

were observed at or around Tg. The gas CO_2 was an exception to this

rule. They proposed that around Tg, the average site size distribu-

tion increased while the number of sites remained unchanged. All

the former gases were already small enough to occupy most of the

sites so a discontinuity was not observed around Tg. CO_2 represented

a limiting size where the relative size of gas and molecular site

became important. Kumins (1961) and Roteman (1961) also obtained

similar results when studying the behaviour of poly(vinylchloride) and poly

(vinylacetate). Unfortunately, the significance of the observed increase

in the rate of change of diffusion coefficient with temperature for

increasing gaseous molecular diameter was ignored by all of the above

authors. Similar critical size effects are seen in the present work.

So far we have stressed the idea of relative sizes as the controlling

factor in diffusion and solubility of gases. Van Amerongen (1964)

showed that the log of the solubility coefficients of a number of

gases such as argon, nitrogen, carbon dioxide and a number of hydro-

carbon gases in natural rubber was a linear function of their boiling

points. This observation lends some support for a condensation mecha-

nism (Graham 1866). In the cases where the gaseous critical temperature

is below the ambient temperature this signifies a case II diffusion mechanism

and case I in the cases where the reverse is true. The idea of inter-

stitial condensation is interesting but is unlikely for permanent

gases. There have been attempts to model specific gas matrix inter-

actions. Michaels and Bixler (1961) reported a linear relationship

between the solubility of some permanent gases together with a range of hydrocarbon gases in amorphous poly(ethylene) and the Lennard Jones force constant. Their data were statistically parallel to the corresponding data obtained by Jolley and Hildebrand (1958) who studied the solubility of the same gases in benzene. They argued that the above implied an analogy between the solution process in poly(ethylene) and that in low molecular weight non-polar liquids. Specific interactions clearly cannot be ruled out; in the gross form they give rise to case II processes.

More recently Pasternak et al (1970) studied the permeation of the gases CO_2, O_2, N_2 and N_2O_4-NO_2 mixtures through PTFE. With the exception of the gas mixture, it was found that the generally assumed simple diffusion laws held; the independence of the coefficients of diffusion and permeability with membrane thickness in particular, proved that the sorption process on the membrane was fast. A close numerical agreement between the heats of solution and condensation of the simple gases in PTFE indicated that the solution process in PTFE was similar to a condensation process with minimal interaction between the polymer and the solute. Finally, a comparison was made between the PTFE data and those obtained by Michaels and Bixler (1961) using the structurally similar poly(ethylene), PE. On comparison, the activation energies for diffusion of gases in PTFE were lower than in PE. This was somewhat unexpected since PTFE has a stiff backbone chain of high viscosity. It was argued that the diffusion of gas molecules in PTFE proceeded through preformed channels and cavities and required little movement of polymer chains. The idea of short circuit diffusion paths has precedents in metals and may be important in a sintered polymer such as PTFE. The notion

of easy paths is just an extension of the Michaels and Bixler (1961)
idea of impervious crystalline domain where the matrix bears the
transport and solubility role.

In a later publication Pasternak et al (1971) made a study of the
diffusion of the same gases in a copolymer of hexafluoropropylene and
PTFE. The low melt viscosity of the copolymer allowed its fabrication
by conventional techniques. The finished product, although structurally
similar to PTFE, presented a more compact structure, presumably free
from micropores. The results indicated a higher diffusion activation
energy in the case of the copolymer than PTFE, thus lending support
to the previously proposed mechanism (Pasternak et al, 1970) of gaseous
transport through pre-existing short circuit pores and channels in
the previous PTFE sample used.

Gas transport and solubility have been used by several authors
to probe the internal structure of polymers. The short circuits and
crystalline barriers have been mentioned. Peterlin (1970) estimated
the accessible surface in drawn poly(ethylene) by studying the sorption
of methylene. To achieve this, he made use of the well known tran-
sient experiment (Park, 1952). This involved a plot of measured
weight gain Q of the sample versus the square root of time, t. An
initial linear relationship followed by a saturation point (corres-
ponding to a gaseous concentration C_∞) was obtained. The initial
slope was given by:

$$\left(\frac{dQ}{dt^{\frac{1}{2}}}\right)_{t=0} = C_\infty \, A(D/\pi)^{\frac{1}{2}} \qquad\qquad (2.5)$$

Using simple manipulation Peterlin (1970) was able to show that
the accessible area, A, per gram of the sample of mass m was

$$\frac{A}{m} = \frac{1}{\rho} (\frac{\pi}{D})^{\frac{1}{2}} (\frac{d(Q/Q_\infty)}{dt^{\frac{1}{2}}})_{t=0} \qquad\qquad (2.6)$$

where ρ was the sample density, Q_∞ was gas mass uptake at saturation and D was the measured value of the gaseous diffusion coefficient. A value of ca. 450 cm^2/g for the accessible area of drawn poly(ethylene) was obtained at $25^{\circ}C$. This was significantly lower (ca. 14 folds) than the corresponding value using undrawn specimen. The drawn sample also exhibited nearly twice as high limiting sorption. It was con-cluded that drawing poly(ethylene) resulted in the formation of a great many submicroscopic holes which would have been otherwise inaccessible to gaseous molecules.

Following the above observation Peterlin (1974) undertook a study of the extreme sensitivity of gaseous transport with molecular architecture by studying gaseous transport into a variety of morpho-logically different polymers. For example, he produced evidence that drawn materials with fibrous structures having a large fraction of highly aligned molecules with close packing exhibited a drastic decrease in diffusion and sorption. Subsequent annealing relaxed the amorphous component and restored the transort properties to values observed in undrawn material. Another example of the overwhelming influence of morphology were the hard elastomers where the formation of a great many submicroscopical holes yielded permeability increases by many orders of magnitude with no change in crystallinity. Finally, these effects were so enormous that it was proposed that the changes in transport properties could be used as an extremely sensitive tool for the study of micromorphology of the amorphous component where conventional X-ray techniques were rendered unreliable.

In the same study, Peterlin (1974) explored the possibility of

diffusion and absorption of gas molecules in the crystalline regions. He speculated that as a consequence of the fact that the crystalline lamella and blocks of the polymer were so extremely thin (ca. 100Å), they were easily permeated by the diffusant in a short time (ca. 1 sec). Hence, under the normal conditions of a permeability experiment the crystals exhibited equilibrium sorption corresponding to the local chemical potential of the diffusant in the adjacent amorphous regions. The permeability of a crystalline polymer was shown to be given by:

$$P = (1-\alpha)^{m+1} P_a \qquad (2.7)$$

where P_a was the permeability of the perfectly amorphous polymer and α was denoted as the degree of crystallinity. Prevorsek et al (1972) successfully verified the validity of the above equation using a number of polymer systems of similar morphology. The index 'm' was calculated for simple geometries of amorphous and crystalline phases and was found to vary between 0.3 to 0.9.

Klein (1977) studied the diffusion of linear molecules of broad structure $n(CH_2)_N$ in both semi-crystalline and molten poly(ethylene). N ranged between about 15 and 1000. From these studies, Klein highlighted the important concept of topological constraints imposed on diffusion of long molecules in solid poly(ethylene) and like Peterlin (1974) proposed that these measurements could provide information on the nature of the amorphous domains of semi-crystalline polymers.

The mechanism of diffusion in both solid and molten poly(ethylene) was shown to be primarily dictated by the length of the diffusant molecules. In the case of diffusion of long molecules (n>30) in both systems the diffusion mechanism was said to be constrained to

reptation in a virtual tube analogous to a snake slithering through an obstacle field. For values of N<30, the diffusion mechanism was said to approach that of gaseous molecules in which reptation was suppressed in favour of hops involving large portions of diffusant. In terms of the previous zoological analogy, the slithering snake movement became so short that it behaved more like a lizard and no longer moved by propagation of stored strength along its body.

These studies indicate that the transport and sorption of gases in polymers is a complex phenomenon. The idea of "free volume" is useful but specific gas-matrix interactions are sometimes evident. In addition the morphology of the matrix may often be a controlling factor.

2.3 Diffusion and Solubility of Gases in Polymers Under High Pressure

The diffusion and solubility mechanism of gases in polymers at above atmospheric pressure has not been studied extensively. The amount of literature available on this topic is small. It is perhaps ironic since this subject is of significant industrial importance. Examples include the blanketing of molten polymers under inert gas pressures during polymer finishing processes or techniques involving a high pressure polymerisation of gaseous monomers in equilibrium with the polymer. In this section, it is attempted to review most of the work reported in this field in the hope of building a picture of our current understanding of the subject. A survey of various experimental techniques used to obtain data is also embodied in this section.

Lundberg et al (1960) were one of the first people who made a series of comprehensive studies in this field. They studied the dependencies on pressure and temperature of the solubilities of nitro-

gen in molten poly(ethylene) up to a maximum pressure of 69 MPa and a temperature range of $125^{O}C$ to $226^{O}C$. The method involved exposing the polymer to a rapid increase in gas pressure and measuring the corresponding pressure drop following the absorption process. Their measurements indicated a high solubility of nitrogen (ca. 5% W/W max.) increasing with temperature and pressure. The pressure dependence however increased less rapidly than linearly as predicted by Henry's law. No dependence of the diffusion coefficients were reported.

The method of calculation of solubilities and diffusion coefficients together with additional data on the diffusion of methane and nitrogen in molten poly(styrene) and poly(ethylene) were reported in a later paper by Lundberg et al (1962). In it, the diffusion coefficients and the solubilities were estimated from a knowledge of the magnitude of the pressure drop and on the basis of modelling the sorption process by Fourier's (1955) radial differential equation of the form:

$$\frac{\partial C}{\partial t} = \frac{1}{r} \frac{\delta}{\partial r} (rD\frac{\delta C}{\delta r}) \qquad (2.8)$$

where C was concentration, t, the time and r, the radial distance. Assuming D was invariant with C, r and t, the solution of the diffusion equation, for the case of uniform radial diffusion into a cylinder (sample shape) proposed by Fourier (1955), was applied.

A serious limitation of the above procedure, apart from its extreme mathematical complexity, was of course the assumption that the diffusion coefficients were invariant with gaseous concentration. Another drawback was the applicability of a virial type equation of state to calculate the volume of gas dissolved from a knowledge of drop in pressure. The volume of the vessel and the volume of the polymer

(measured at atmospheric pressure) were also assumed to be constant. The effect of the change in the volume of the polymer and the inevitable decrease in pressure as a result of adiabatic compression of gas were ignored. This omission produces serious error. The results were however interesting. In general, the diffusion coefficients and gaseous solubilities increased with increasing pressure and temperature; the solubility again increasing less rapidly as expected from Henry's law. Typically at a pressure of 50 MPa and $100^{o}C$ an average increase of 70 $\pm$ 20% in diffusion coefficients from the corresponding atmospheric values were obtained. The deviation increased with temperature and was more pronounced in the case of CH_4 sorption where the departure from Henry's law was greatest.

These studies show that the concentration of gases in the polymer is low. It was estimated that approximately 2 molecules of nitrogen and about 6 molecules of methane were dissolved per 100 carbon atoms at about 69 MPa. On the same basis, methane was about twice as soluble in poly(ethylene) than it was in poly(styrene).

Lundberg et al (1962) used a free volume model for the sorption process. It was argued that the diluent molecules were accommodated in free or unoccupied volumes inaccessible to polymer segments, i.e. the gas molecules entered interstitially into a disordered array of polymer molecule segments.

The effect of change in volume of poly(styrene) following the application of pressure was considered in another publication by the same authors the following year (Lundberg et al, 1963). In this study the polymer volume at any pressure was estimated by using the compressibility data reported earlier by Matsuoka and Maxwell (1958) who used a liquid as the pressure transfer medium. The applicability of these data under gaseous environments is in serious doubt (see Chapter 10).

· Durill et al used a more sophisticated version of the technique employed by Lundberg et al (1960) to determine the solubilities and diffusivities for systems involving N_2, He, CO_2 and Ar in molten poly(ethylene), poly(isobutylene) and poly(propylene) up to a maximum pressure of 20 MPa. They found that, in general, Henry's law was obeyed and the diffusion coefficients were fairly independent of pressure.

The inevitable initial rapid decrease in pressure observed in most sorption studies carried out by Lundberg et al (1961-63) was examined in a further publication by the same authors (Lundberg et al, 1969). They blamed the effect on the relatively slow gas flow within the measuring system. This however did not explain why the effect was strongly gas specific. The explanation is also somewhat unacceptable considering the small volume of the pressure vessel (ca. 10 cm^3) and the relatively long duration of the transient effect (ca. 1 minute). In any event, one would expect that the slow gas flow would give rise to an opposite response (i.e. pressure increasing with time). The solubilities and diffusivities reported at short elapsed times were therefore re-estimated by extrapolation. These gave rise to no appreciable change in diffusivity but the solubilities decreased by an average of 30% compared to the previous data. The basic trend however remained unchanged. The solubilities and diffusivities of methane in poly(isobutylene) at a pressure range of 0.101 MPa to 35 MPa were also studied in the same paper. The results indicated that the diffusion coefficients for methane increased slightly with increasing methane concentration. The effect of gas pressure and concentration upon the gaseous diffusion coefficient, D in all the systems previously studied could be approximated by the relation:

$$lnD = A + BP \qquad\qquad (2.9)$$

with A and B being constants specific to the system under study. The above equation was used to estimate diffusion coefficients at one atmosphere.

The degree of change in gaseous diffusion coefficient with concentration in a particular system was associated with the plasticizability of the gas. For example, methane was said to plasticize linear poly-(ethylene) following an observed relatively large increase in diffusion coefficient with increasing concentration.

The relatively small gaseous temperature coefficients of diffusion and the relatively high diffusion coefficients observed in branched poly(ethylene) were attributed to its open structure. Finally, the solubility data were adequately represented by Langmuir's adsorption isotherm (Langmuir, 1918) in which sites were thought of as voids or unoccupied spaces in the polymer and multi-layer adsorption was permitted. The fact that the fitted isotherm did not incorporate an interaction parameter between adsorbed molecules and the substrate, and the observed increase in solubility with temperature led to the conclusion that polymer gas interactions within the cells were small.

Bonner and Cheng (1975) measured the solubility of N_2 in poly-(ethylene) at $125°C$ up to a maximum pressure of 15 MPa. Their technique involved the measurement of the resonance frequency of a piezoelectric crystal carefully coated with a thin layer of the polymer specimen. Their experimental results agreed reasonably well with those reported earlier by Lundberg et al (1960).

Atkinson (1977) carried out some crude solubility measurements by directly weighing the polymer specimen immediately after depressuri-

sation. He tested his experimental technique by measuring the solubility of N_2 in branched poly(ethylene) in the temperature range 130-190°C at gas pressures up to 100 MPa. He observed an abrupt decline in gaseous uptake near and above a pressure of 50 MPa in the 135°C isotherm. He proposed that the inflection represented the pressure at which the crystalline melting point had been shifted to 135°C from the normal melting point of 115°C and that the upper part of the isotherm (above 50 MPa) represented a partly crystallized poly(ethylene) which could not absorb so much gas.

It is of interest in this connection to note a similar behaviour in the original data of the paper represented by Lundberg et al (1969) for the same system as Atkinson's (1975). Although not highlighted, an inflection is evident in the 125.8°C isotherm at 17 MPa. This transition is somewhat lower than that reported by Atkinson (1977) and may be attributed with the higher crystalline melting point of the specimen used by Atkinson (1977).

Finally, Atkinson's (1977) isobaric studies indicated a linear relationship between gaseous uptake and temperature implying an endothermic heat of solution. The heats of solution were calculated from the relation:

$$S = S_o \exp\{-\Delta H/RT\} \qquad (2.10)$$

An observed systematic increase in heat of solution with pressure indicated that the activation energy required to introduce more gas molecules in poly(ethylene) increased with increasing pressure.

Cheng and Bonner (1978) fitted statistical mechanical correlations for the solubility of methane and nitrogen in molten low density poly-

(ethylene) up to a maximum pressure of 7 MPa. They used the solubility data reported by Lundberg (1969) and successfully modelled these with the corresponding state solutions applicable to mixtures of high and low density fluids.

2.4 Summary

Diffusion and absorption of permanent gases in polymers can be considered in terms of two important parameters; (a) the effective size of the penetrant gas molecules, and (b) the molecular architecture and the chain mobility of the polymer matrix. Specific interactions can be ignored to a first order. The extent of gaseous invasion primarily depends on the relative size of gas molecules to the average site size distribution in the polymer; smaller gas molecules find it easier to occupy a larger spectrum of sites. These sites can either pre-exist in the form of intramolecular voids as a consequence of molecular disorder (i.e. the amorphous region), and/or exist in the form of intermolecular spaces (i.e. the free volume). Sites can also be generated during gaseous transport. The latter process exclusively depends on chain mobility. The crystalline region inherits significant molecular order in its most energetically stable state. Gaseous transport in the crystalline region is therefore small and is mainly confined to the molecular free volume.

Increases in temperature can give rise to two thermodynamically opposing factors which affect the diffusion process. Temperature enhances chain mobility which in turn encourages gaseous absorption in the polymer, at the same time, temperature increases the average kinetic energy of gas molecules which reduces the probability of absorption at the expense of increasing the diffusion coefficient. Increase in pressure invariably increases gaseous absorption. It may

be argued that pressure reduces the average kinetic energy and the equilibrium distance of gas molecules thus increasing gaseous concentration in the polymer. At the same time, pressure plays the less important role of opposing absorption by reducing chain mobility and the available space for gaseous penetration. The effect of pressure on gaseous diffusion coefficients is not well understood.

The influence of molecular relaxations such as glass transitions on gaseous transport is somewhat ambiguous. A transition is accompanied by a rapid volumetric expansion which is usually reflected in an abrupt increase in sorption and diffusion in the case of relatively large gas molecules. In the case of small gas molecules no such observation is evident. It may be speculated that at the transition, the average site size distribution increases while the number of sites remains unchanged. The small gas molecules may be already small enough to occupy most of the sites so a discontinuity is not observed. For larger species things will be different. However, the general picture of the influence of pressure on gas sorption and transport is not precisely developed. The solubility coefficients and diffusion coefficients seem to increase with pressure but there must be concern about adiabatic heating factors in much published literature in particular in Lundberg's work.

C H A P T E R   3

EFFECT OF PRESSURE ON THE THERMAL CONDUCTIVITY OF POLYMERS

3.1   Introduction

The theory of heat conduction through solid dielectric materials at atmospheric pressure was first described in a publication by Debye (1914). He proposed that the heat flow through any dielectric material was governed by the motion of elastic waves. The scattering of these waves and hence the thermal conductivity, K, depended on the mean free path ℓ (defined as the distance which a wave of velocity, V travels before its intensity is reduced to 1/e of its initial value) and the specific heat, C, of the material. These variables were then correlated in terms of an expression analogous to the equation of state for gases. This was given by:

$$K = \frac{1}{4} C V \qquad\qquad (3.1)$$

Peierls (1929) developed a more refined theory of thermal conductivity in crystals by considering individual lattice vibrations rather than continuum as treated by Debye. He speculated that in the process of heat conduction, the total energy of these phonons was conserved but the direction of the energy current changed. He then speculated that at sufficiently low temperatures, the mean free path of the phonons was limited to the diameter of the crystal. For this reason, most of the thermal conductivity studies at atmospheric pressure in the following years were mainly reported at low temperatures.

3.2   Thermal Conductivity of Polymers at Atmospheric Pressure

Reese et al (1965) have measured the thermal conductivity and

heat capacity of a number of commercial polymers such as PTFE, PCTFE, nylon and three samples of PE of varying crystallinities at temperatures between $1^\circ K$ and $4.5^\circ K$. Values of K and C for cylindrical polymers were determined from a solution of Fourier's heat conduction equation of the form:

$$\frac{\partial}{\partial x} (K \frac{\partial T}{\partial x}) = C(\frac{\partial T}{\partial t}) \qquad (3.2)$$

where T is the temperature of the specimen measured at time t and at a distance x from a heat source placed at one end of the polymer specimen. The results indicated that in nearly all cases the specific heat was proportional to T^3. The variation of thermal conductivity with temperature was almost linear. In the case of the PE samples, the specific heat was found to decrease linearly with increasing density indicating that the amorphous regions have a higher specific heat than the crystalline regions. Unfortunately, no data on the effect of crystallinity on K was reported. A similar study over a wider temperature range (1.2 to 20K) was carried out by Kolough and Brown (1968). Thermal conductivity measurements on samples of PE with densities between 0.914-0.971 g cm^{-3} indicated a linear increase between log K and temperature. The constant of proportionality was greater in the case of the denser (more crystalline) specimens. The increase in K with temperature and crystallinity was explained in terms of the kinetic approach first suggested by Debye (1911). The authors argued that at lower temperatures, the phonons see the material as a somewhat disordered structure. This gives rise to an increase in phonon scattering which in turn results in a reduction in K. On the basis of the same argument, increasing crystallinity (more order) must have an opposite effect on K as

decreasing temperature.

Many more fundamental theoretical papers relating to the thermal conductivity of polymers with varying degrees of crystallinities have been published either at very low temperatures (Hansen et al, 1960 and Powell et al, 1957) or at room temperature (Eiermann, 1965). An excellent review of these works is carried out in a paper by Choy (1977).

3.3 The Effect of Pressure on the Thermal Conductivity of Polymers

The influence of pressure on the thermal conductivity of solid polymers has attracted little attention. This is somewhat surprising both from a practical and theoretical point of view. Many polymeric materials are used as thermal insulators in high pressure components. Any variation of thermal conductivity as a result of an imposed hydrostatic pressure must surely affect their performance. This, in turn, may also give rise to an adverse effect in mechanical properties following a pressure pulse. The phenomenon of the plasticisation of PTFE described earlier is partly a consequence of the above. From a theoretical point of view, any changes in bond angles, interaction distances or the local arrangement of the polymer molecules as a result of increasing pressure must severely effect the phonon mean free path during the heat conduction process. Clearly, the thermal conductivity of solid polymers must therefore be influenced by increasing pressure. One of the first studies of this kind was carried out by Barker and Chen (1970) who studied the effect of superimposed hydrostatic pressures of up to 420 MPa on the thermal conductivity, K, of tubular rods of PTFE and PC. Values of K were then calculated using the following expression:

$$K = (\dot{Q}/2\pi\ell\Delta T) \ln(r_2/r_1) \qquad\qquad (3.3)$$

where $\dot{Q}$ is the flux rate of heat in a cylindrical heater encapsulated

by the polymer specimen of length, ℓ. ΔT denotes the temperature difference across the walls of the sample of inner and outer radii of r_1 and r_2 respectively. Pressure was applied directly via a piston. The results for PTFE at $30^{\circ}C$ indicated a linear 100% increase in K over a pressure span of only 100 MPa. The corresponding increase for PC was non-linear (exponential) but of the same order. The non-linear behaviour was believed to be mainly an artefact due to imperfect contact at interfaces. The above problem was partly overcome by Andersson and Backstrom (1972) who used solid cylindrical PTFE specimens heated along their axis by an electrical current. Once again, the authors observed a rapid linear increase in K with increasing pressure. Typically, the value of K increased by ca. 200% over a pressure range of ca. 3000 MPa at $27^{\circ}C$. This rate of increase was considerably less (ca. 7 fold) than the corresponding data reported by Barker and Chen (1970). However, the authors somehow managed to conclude that the observed increase was comparable in magnitude to the values reported by the above authors. In addition, the phase change at 600 MPa (II to III transition) reported previously by Bridgman (1948) did not give rise to an abnormal behaviour in the variation of thermal conductivity. In the following year, Andersson and Backstrom (1973) reported data on the pressure dependence of the specific heat of HDPE (0.965 g cm^{-3}, 80% crystalline) and LDPE (0.926 g cm^{-3}, 55% crystalline) from simultaneous measurements of K and thermal diffusivity of a cylindrical geometry at $27^{\circ}C$ up to 2500 MPa pressure. The thermal conductivity increased strongly with pressure, the values at 2500 MPa for HDPE and LDPE being higher by factors of 2.75 and 2.19 than those at atmospheric pressure respectively. The specific heat of HDPE decreased by a factor of 0.8 over the same pressure range. It is worth noting that the increase in

K with pressure was almost exponential on both occasions. The larger pressure dependence of K for HDPE (more crystalline) compared to LDPE was explained by arguing that the interchain thermal conduction in the crystalline component grew more strongly with increasing pressure than the amorphous component. The proposed larger pressure dependence of thermal conductivity, $\frac{\partial K}{\partial P}$, in the crystalline component was successfully evaluated using an empirical relation previously proposed by Eiermann (1965) and later refined by Pastine (1970). The above expression allowed the measurement of K of the crystalline and amorphous components from a knowledge of the percentage crystallinity and the thermal conductivity of the polymer matrix measured at any particular pressure.

Dzhavadov (1975) was one of the first people who evaluated values of $\frac{\partial K}{\partial P}$ for polymers by studying the kinetics of the temperature field in a flat plate specimen during a one dimensional heating pulse. This new technique was said to be superior compared to other methods due to the small heat exchange between the specimen and its surrounding which would otherwise limit the applicability of the proposed equations required for the calculation of K. Dzhavadov used the above technique to report a linear 400% increase in K for PTFE up to 3000 MPa pressure. The same technique was also employed by Kieffer (1976) to study the pressure dependence of K for a cylindrical block of PTFE specimen compressed to a maximum pressure of 3600 MPa. Surprisingly, in contrast to previous data, the PTFE phase II to III transition was clearly reflected as a discontinuity in the thermal conductivity vs. pressure curve. This involved a sharp rapid increase (ca. 15%) in K between 700 to 800 MPa (see Figure 3.4). However, the overall rate of increase in K was the same as that reported by the previous authors. Kieffer

then argued that the absence of the discontinuity in the thermal con-
ductivity data reported by Andersson and Backstrom (1973) was due to
the differences in the sample crystallinity although the density of the
samples were nearly identical (2.15 g cm^{-3} compared to 2.144 g cm^{-3}).
Andersson and Backstrom (1976) on the other hand produced evidence in
support of the presence of a discontinuity in K around 6Kbar (ca.600MPa)
using a transient hot wire technique (see later). In the opinion of
the present author the absence of a discontinuity as reported by some
authors is partly due to the lack of sensitivity in the measurement
techniques and perhaps more importantly, as a result of the low number
of measurements especially around the phase II to III transition (600
to 700 MPa). The latter case is clearly evident comparing the thermal
conductivity data reported by Andersson and Backstrom (1973) (Figure
3.1) and Dzhavadov (1975) (Figure 3.2) to those reported by Andersson
and Backstrom (1976) (Figure 3.3) together with Kieffer (1976) (Figure
3.4). Similar proposals may also be forwarded in order to explain the
disagreement between Andersson and Sudquist (1975) and Eiermann (1964)
concerning the presence of a discontinuity in the thermal conductivity
of atatic PP as a result of a phase change from a rubbery to a glassy
state around 200 MPa pressure (Passaglia, 1964). Andersson and Sudquist
(1975) also determined values of $(\frac{\partial K}{\partial P})_T$ for amorphous PMMA, PS and iso-
tactic PP together with semicrystalline atactic PP. In the case of
the amorphous polymers, the authors reported similar values for $(\frac{\partial K}{\partial P})_T$
up to a maximum pressure of 2500 MPa. The corresponding values of
$(\frac{\partial K}{\partial P})_T$ for the semicrystalline polymer was however larger. To explain
the above, the authors proposed that as atactic PP is more compressible
than isotactic PP, then on application of a hydrostatic pressure, the
resulting reduction in free volume in the case of the more compressible

atactic PP will be greater. Considering the free volume as posing a resistance to the passage of phonons during the heat conduction process, it is then not surprising to expect a larger value of $(\frac{\partial K}{\partial P})_T$ for the semi-crystalline polymer.

A clever variation of the heat pulse technique was developed by Andersson and Backstrom (1976) who abandoned the use of a separate temperature probe and measured K by monitoring the change in resistance of the heating probe (0.1 mm Ni wire) immediately after a heat pulse (ca. 1 sec duration). Sandberg et al (1977) employed the same technique to study the thermal behaviour of glycerol (a glass former). Their data revealed a behaviour for K similar to that for polymers. Figure 3.5 shows the reported variation for K(T) for liquid, glass and crystalline glycerol at 10 MPa pressure. For the liquid phase, $(\frac{\partial K}{\partial T})_P$ is weakly negative down to the glass transition temperature of about 210K after which the sign is reversed. The peak around the glass transition temperature, Tg, was discounted as an experimental artefact. It is also evident from the data that as expected (van Krevelen, 1972), the crystalline phase has a much higher thermal conductivity than the disordered amorphous phase.

3.4 The Role of Free Volume on the Process of Heat Conduction in Polymers

The important concept of free volume in the process of heat conduction was first highlighted in a publication by Barker et al (1977). The authors reported measurements of the influence of pressure on the thermal conductivities of four vitreous acrylates, poly(alkyl methacrylates): PMMA, poly(ethylene methacrylate) (PEMA), poly(n-butyl methacrylate) (PnBMA) and poly(i-butyl methacrylate) (PiBMA). As expected, positive values of $(\frac{\partial K}{\partial P})_T$ were recorded in all cases. However, with the exception of PnBMA, the absolute magnitudes of K were found to decrease as the

number of carbon atoms attached to the side chain increased. It was argued that this result is consistent with the fact that chain packing is less efficient for the higher members of the homologous series thus giving rise to a larger effective volume of the polymer. Since free volume should be sensitive to pressure, it seemed reasonable to suppose that $(\frac{\partial K}{\partial P})_T$ should be greatest in those polymers having the largest free volumes. A more quantitative approach on the effect of free volume on $(\frac{\partial K}{\partial P})_T$ was undertaken by Frost et al (1978) in a subsequent publication the following year. On the basis of the assumption that the fractional free volume, f_0 was temperature invariant below Tg (Haldon and Simha, 1968) and that dilatancy was represented by changes in f_0, the authors were able to show that the fractional change in K following the application of pressure was given by:

$$\frac{\Delta K}{K(P)} = \gamma_G \; |f_0 \; (0, \; T) - f_0 \; (P, \; T)| \qquad (3.4) \qquad or$$

$$= \gamma_G \; f_0 \; (0, \; Tg) \; |1 - \exp \; (- \frac{P}{B^*})|. \qquad (3.5)$$

where γ_G is the isothermal Gruneisen parameter (Barker et al, 1970) given by:

$$\Upsilon_G = |\frac{\partial \ln K}{\partial \ln V(P,T)}| \qquad (3.6)$$

V(T,P) is the volume of the polymer and $B^* = kTg/V_0$ with k denoting Boltzmann constant and V_0, the volume at 101 KPa and 273K. Equation (3.4) states that the fractional change in thermal conductivity is directly proportional to the change in free volume. This is consistent

with the previous observation (Barker et al, 1977) that the thermal

conductivity for the densest polymers having the smallest fractional

free volume must be least affected by the application of a hydrostatic

pressure. The reported (Andersson and Backstrom, 1973) larger $(\frac{\partial K}{\partial P})$

for HDPE compared to LDPE is however in contrast to the above view.

Also, equation (3.5) predicts that $\Delta K/K(P)$ should approach a limiting

value $(\gamma_G f_0)$ as the free volume is squeezed out of the specimen. This

is in agreement with most previous observations described above in

which the K vs P curve reaches a plateau (see Figure 3.2 as an example).

The effect of a phase transition from a liquid to a glassy state

on $(\frac{\partial K}{\partial T})_P$ for PVA was investigated in a publication by Sandberg and

Backstrom (1980) using the hot wire technique. Typical results at

an isobaric cooling rate of 15 K/hr are reproduced in Figure 3.6. The

general features of the data are similar to those reported by Sandberg

et al (1977). There is a moderate increase in K up to the temperature

region of Tg, followed by an equally moderate decline above this region.

The Tg is associated with a rather sudden peak in K which decreases

in height and moves to higher temperatures as the pressure is increased.

The value of $(\frac{\partial Tg}{\partial P})$ extracted from these data was found to be 264K GPa^{-1}

which is in close agreement with a value of 266K GPa^{-1} as reported by

McKinney and Goldstein (1974) obtained from mechanical measurements.

3.5 Summary

The large increase in the thermal conductivity of polymers with

increasing pressure has been somewhat unexpected. As the amount of

data in this field is comparatively small, it is difficult to forward

any definitive arguments in order to establish the responsible mecha-

nisms. We may however conclude by considering the free volume as a

barrier to the transfer of heat in polymers. Increasing the imposed

hydrostatic pressure results in a reduction in the free volume hence an increase in the thermal conductivity. The more compressible polymers may therfore be expected to exhibit a larger pressure dependence of thermal conductivity. Indeed most of the reported data is in support of this view. The larger thermal conductivity observed for the more crystalline polymers suggests a mechanism of heat transfer similar to that for metals. In this case, the individual atomic vibrations and the orbital electrons play an important role in the process of heat conduction.
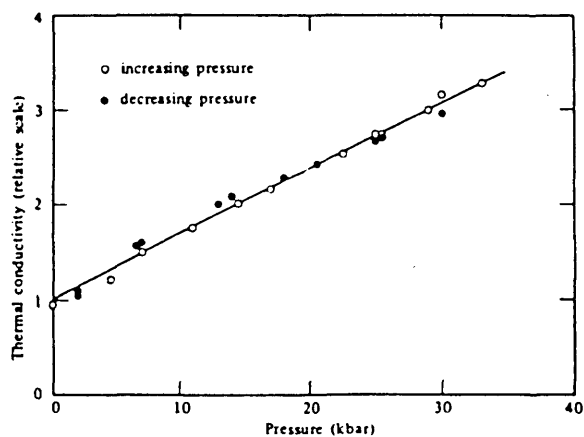
Figure 3.1. Thermal conductivity of PTFE as a function of pressure.
(Andersson and Backstrom 1973)
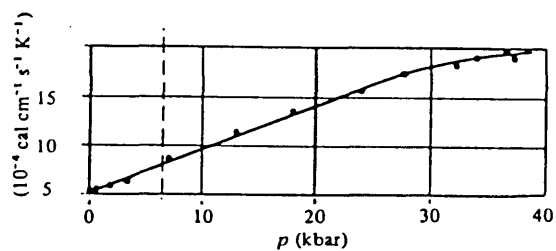
Figure 3.2. Thermal conductivity of PTFE as a function of pressure.
(Dzhavadov 1975)
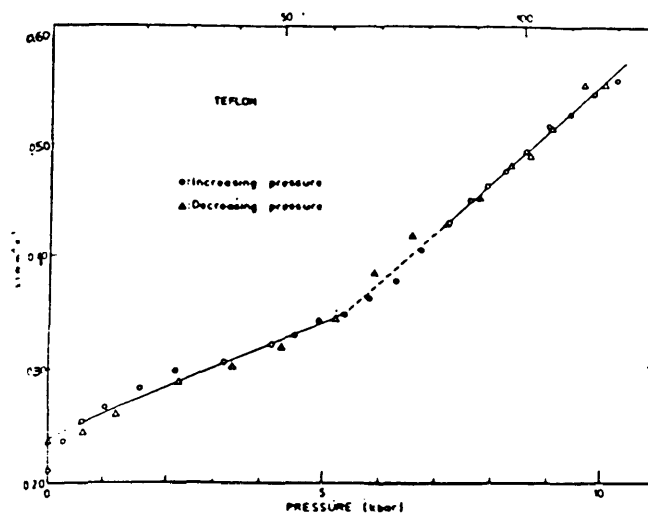
Figure 3.3. Thermal conductivity of PTFE as a function of pressure.
(Andersson and Backstrom 1976)
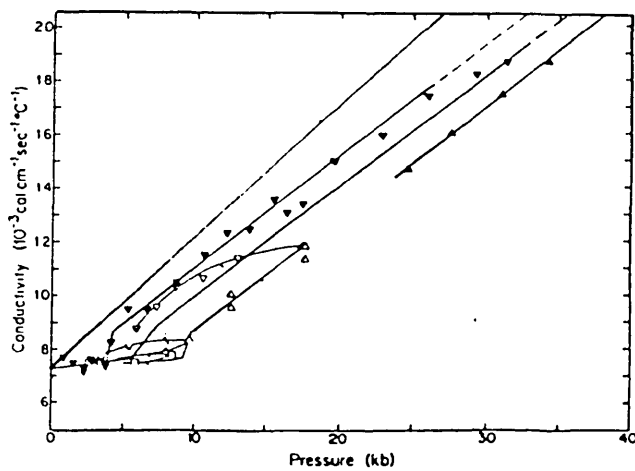
Figure 3.4. Thermal conductivity of PTFE as a function of pressure.
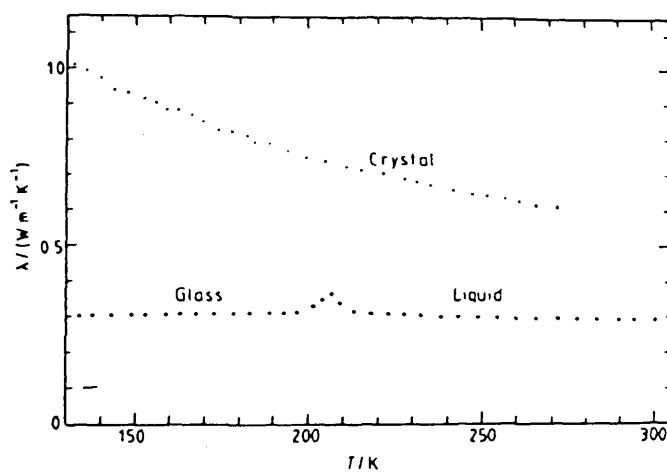(Kieffer 1976)

Figure 3.5. Thermal conductivity of amorphous and crystalline glycerol against decreasing temperature at atmospheric pressure (Sandberg et al 1977)
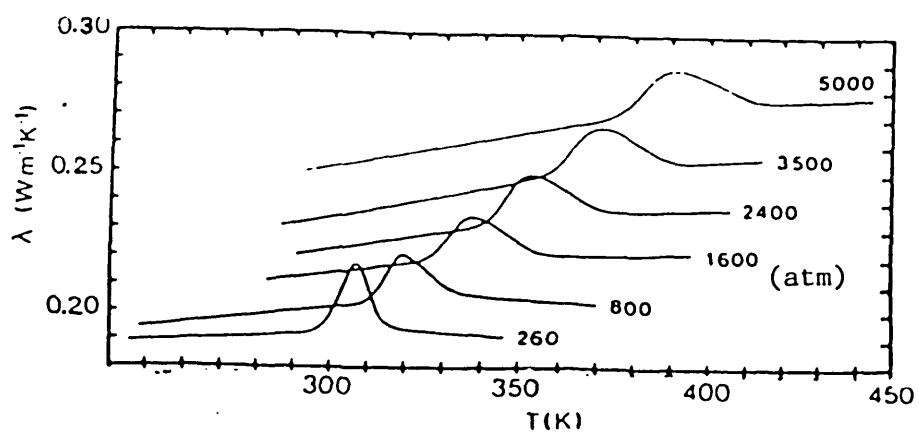
Figure 3.6. The effect of a phase transition on the thermal conductivity of PVA at various pressures (Sandberg and Backstrom 1980).

C H A P T E R 4

EFFECT OF HYDROSTATIC PRESSURE ON THE MECHANICAL
PROPERTIES OF POLYMERS

4.1 Introduction

The advent of polymeric materials in high pressure technology and in particular the significant susceptibility of their mechanical behaviour to high pressure environments has attracted the attention of many research workers in the recent years. Within our knowledge, Bridgman (1953) was one of the first people who conducted such tests on any polymeric material. His experiment involved carrying out tensile tests on copper sheathed melamine formaldehyde at three different pressures of 800, 2400 and 2800 MPa. The test specimen, renowned for its brittleness exhibited plastic yielding at a pressure of 800 MPa and fractured in a brittle manner at the higher pressures. In addition, his results indicated a remarkable increase in initial stiffness. For example, the specimen tested at 2800 MPa exhibited a ca. 3 fold increase in stiffness compared to the specimen examined at 800 MPa.

4.2 Polymeric Systems

Despite these reported marked changes, it was probably not until a decade later that a further similar investigation was undertaken by Holliday and his coworkers (1964) who conducted tensile tests on glassy poly(styrene) specimens at atmospheric pressure and 770 MPa. The brittle behaviour at atmospheric pressure changed at the high pressure to exhibit a yield stress and increased ductility. A broader study over a more limited pressure range was undertaken by Ainbinder et al (1965) who examined the tensile and compressive behaviour of PMMA, PS, PE and PTFE. The results indicated a substantial increase in Young's modulus

and the strain to fracture for all the polymers studied. Paterson
(1964) made a study of the effect of hydrostatic pressure on the com-
pressive modulii of a number of elastomers up to a maximum pressure of
1000 MPa at room temperature. Synthetic rubbers such as neoprene,
silicone, fluorosilicone, poly(urethane) and low nitrile rubbers were
selected for the study following their increasing use as rubber O rings
in high pressure equipment. The experimental technique involved the
measurement of the displacement of a piston which compressed the polymer
specimen in a confining pressure vessel containing petroleum ether as
the pressure transmitting fluid. The results indicated a typical glass
transition between 400 to 600 MPa involving between 1000 to 2000 fold
increase in the Young's modulus for all the elastomers studied. The
effects were reversible, however faster pressure cycles resulted in
the transition being shifted to slightly higher pressures. The impli-
cations of the above observed transitions are interesting. It may be
argued that pressure, in contrast to temperature, reduces chain mobility
and decreases intramolecular distances. Therefore, an amorphous polymer
which at atmospheric pressure may exist in a rubbery state may isother-
mally revert back to a glassy state characteristic of a lower temperature,
following the application of pressure. In simple terms, the polymer
is made to undergo a pressure induced transition which would have other-
wise occurred at a lower temperature at atmospheric pressure. The
above also tentatively proves that pressure increases the glass transi-
tion temperature. Sadar et al (1968) investigated the time stress-
strain behaviour of poly(oxymethylene) up to 800 MPa. The Young's modu-
lus, yield stress and fracture stress were found to increase by a factor
of three at the highest pressure. In addition, stress relaxation
experiments revealed the modulus increase was associated with the dis-

placement of the γ relaxation from $-75^{\circ}C$ to $20^{\circ}C$ at a pressure of 500 MPa.

4.3 The Effect of Hydrostatic Pressure on the Stress-Strain Behaviour of Polymers

The effect of hydrostatic pressure on the stress-strain behaviour of poly(ethylene) (PE) and poly(propylene) (PP) was investigated by Mears et al (1969). In these experiments, the specimens were tested under both tensile and compressive loads while the samples were simultaneously subjected to various hydrostatic pressures up to 680 MPa. They found that the yield stress and Young's modulii increased significantly with increase of pressure for both materials. However, the mode of yielding and fracture for both polymers was different. In PP fracture occurred by plastic tearing across the cross-section whereas PE deformed by shear and the necked region reduced to a fine point before separation. The authors qualitatively attributed these differences in yielding to the molecular structure of the polymers. In a subsequent publication, the same authors (Sauer et al, 1970) carried out similar experiments on the highly crystalline PTFE and amorphous PC. Once again, for both polymers, the yield stress was found to increase significantly with increase of pressure. Typically, for PTFE the yield stress was found to increase by a factor of five up to a maximum pressure of 680MPa. The increase was linear in the case of compressive strains and non-linear in the case of tensile loads. These effects were accompanied by large increases in the Young's modulii of both polymers; the magnitude being greater (ca. 3 times as much) in the case of PTFE. In addition, tensile tests carried out on PTFE revealed a decrease in the nominal strain at fracture. PC, on the other hand, exhibited a monotonic increase in strain at fracture with increasing pressure. Comparatively large

increases in modulii were observed at pressures above 700 MPa. These were qualitatively associated with the shifting of the low temperature secondary relaxations to around room temperature. For PTFE at atmospheric pressure, this transition occurs at $-80^{o}C$ (McCrum, 1959). The corresponding value for PC is $-110^{o}C$ (Reding et al, 1961). Finally, weight measurements on test specimens before and after pressurisation revealed negligible weight gain due to the absorption of the pressure medium.

The reported universal increase in the yield stress of the polymers studied with increasing hydrostatic pressure was in direct contrast to that observed for metals (see for example Bridgman, 1952). In these cases, according to Von Mises criterion (Nadia, 1950), the imposition of a hydrostatic pressure has no appreciable effect on the yield conditions of metals. Sauer et al (1970), proposed that the yield surface in polymers should more correctly be regarded as a closed surface in stress space, and subsequently proposed a modified Von Mises equation.

4.4 The Effect of Hydrostatic Pressure on the Molecular Relaxations in Polymers

As the dissipative processes during the polymer deformation involve the movement of chain segments or groups, the "free" volume available must therefore play an important part. For this reason one would expect the viscoelastic behaviour such as in shear to be significantly influenced by the application of pressure. The first comprehensive study of this kind was reported in a publication by Rabinowitz et al (1970). The polymers studied included amorphous poly(methyl methacrylate) (PMMA) and crystalline poly(ethylene terephthalate) (PET) and high density poly(ethylene) (HDPE). Torsion experiments were carried out up to a maximum pressure of 70 MPa using a liquid as the pressure medium. The

results indicated a two fold increase for the pressure dependences of shear modulii of PMMA and a three fold increase for HDPE over a range of 70 MPa pressure. The increase for PMMA was considerably less than that reported by Ainbinder et al (1965) who found a two fold increase in the tensile modulus at a pressure of only 20 MPa. Substantial increases in the yield stress and strain to yield were also recorded for all three polymers. The crystalline polymers, HDPE and PET for example, exhibited a monotonic linear increase in ductility with increasing pressure. Typically, HDPE exhibited a 300% increase in maximum shear stress (maximum stress to instigate non-linear behaviour) over a pressure range of 70 MPa. The corresponding increase in shear strain before fracture was 100%. The failure mode of the amorphous PMMA was more complicated. At first, the polymer followed the same pattern as the crystalline polymers; pressure enhancing ductility. At higher pressures than 200 MPa however, the polymer failed in a brittle manner. In an attempt to explain the ductile to brittle transition, the authors examined three alternative mechanisms of failure, none of which were found to be conclusive. The authors also observed that for all the polymers studied the maximum shear stress, τ, could be represented by the empirical relation:

$$\tau = \tau_o + \alpha P \qquad (4.1)$$

where τ_o was the shear stress yield at atmopsheric pressure and α was the coefficient of increase of yield stress with hydrostatic pressure. For the crystalline PET and HDPE, the value of α was found to be three times less than that for amorphous PMMA. These results confirmed the general views of Ainbinder et al (1965) that the rate of increase in

the yield stress of amorphous polymers with increasing pressure was greater than that for crystalline polymers. Finally, the PMMA specimens were tested in order to investigate the possibility of permanent compaction under hydrostatic pressure. This was carried out by conditioning the polymer at a maximum pressure of 70 MPa for 2 hours before use. The strain-stress behaviour of the conditioned specimen was found to be identical to that of an untreated specimen. Density measurements before and after pressurisation also revealed little densification. A conditioning period of only 2 hours for the detection of this permanent deformation seems to be too short (see paragraph 10.4.2).

The high pressure brittle fracture of PMMA reported by Rabinowitz (1970) was further investigated in a publication by Harris et al (1971) who used a rubber coated PMMA as the test specimen. This time, the coated polymer remained ductile throughout a pressure span of up to 70 MPa. The authors then proposed that the brittle high pressure fracture of uncoated PMMA was due to the pressure fluid penetrating through pre-existing cracks and channels on the polymer surface. These then gave rise to local stress concentrations which in turn encouraged crack propagation. The effect of environmental stress cracking such as crazing (see for example Olf and Peterlin, 1974) as a source of crack initiation following specific interactions between the polymer and the pressure fluid resulting in ultimate brittle failure was ignored. The unchanged ductile behaviour of coated and uncoated PET and PE reported in the same publication partly supports the existence of a crazing mechanism.

4.5 Interaction of the Pressure Fluid with the Mechanical Properties of Polymers

The role of the type of the pressure transfer medium on the fracture response of PMMA and PS in tension under superimposed hydrostatic

pressures of up to 200MPa was investigated by Vroom and Westover (1969).
Choosing mercury as an inert pressure environment, the authors reported
an increase in the brittle fracture of PS with increasing pressure.
This was in contrast to the data reported earlier by Sadar et al (1967)
who observed an increase in ductility of the polymer when using hydrau-
lic oil as the pressure medium. The authors therefore classified the
oil as a plasticizer for PS. Pugh et al (1971) on the other hand,
observed a brittle to ductile transition by rubber coating PS and using
castrol oil as the pressure medium. The results for PMMA were also
unexpected. Contrary to the data reported by Harris et al (1971) who
observed an increase in ductility of rubber coated PMMA with increasing
pressure, on this occasion,the uncoated polymer failed in a brittle
manner when exposed to an hydrostatic pressure of mercury. Finally, the
observed increase in brittleness of PTFE with increasing mercury pres-
sure as reported by the above authors (Vroom and Westover, 1969) was
in agreement with the data reported later by Sauer et al (1970) who used
an oil as the pressure medium.

The wide variation of the mode of failure with the type of pressure
medium as revealed in all the previous studies indicated significant
interactions between the polymer and the liquid pressure medium. To
overcome this, Billinghurst and Tabor (1971) chose an inert gaseous
pressure medium such as nitrogen to study the viscoelastic properties
of a number of common thermoplastic polymers using a torsion pendulum
up to a maximum pressure of .200 MPa. The torsion apparatus employed
was of standard design (see for example, Heigboer, 1956) where the
inertia mass was borne on a suspension wire and the polymer rigidly
clamped underneath. The system was then forced into mechanical oscil-
lations ($\sim$1 Hz) and viscoelastic properties of the polymer were studied

by monitoring the decay of the oscillations. The use of a gaseous pressure medium also had the added advantage of minimizing viscous drag experienced by the inertia mass. The above was achieved at the expense of having to use special gas pumps for pressurisation (see Chapter 6). These were much more complicated in design and operating procedures than conventional hydraulic pumps which were useless for gas pressurisation. The operation of the gas apparatus also involved much stricter safety requirements (see Appendix). Although the technique was primarily designed for the study of the effect of pressure on the glass transition temperatures, some shear studies however indicated a universal increase in the modulii of nearly all of the polymers studied. For example, poly(vinyl chloride)(PVC) which at atmospheric pressure and $50^{o}C$ exists in a rubbery state could isothermally be made to exhibit a modulus characteristic of its glassy state following an application of 100 MPa pressure. This was yet another example of pressure having an opposite effect to temperature. PTFE however was an exception to the above rule. Following the application of nitrogen gas pressure, the polymer exhibited a marked decrease in the shear modulus. The authors also observed that changing the pressure medium to helium or hydraulic oil resulted in an opposite response. The large drop in modulus was classified as plasticisation and the effect grew pronounced with decreasing crystallinity, time and increasing temperature and pressure (see Figures 4.1, 4.2 and 4.3). Typically for a 60% crystalline specimen at $80^{o}C$ a five fold decrease in modulus was obtained. An interesting point in the original data (see Figure 4.3) was the small initial increase in modulus which disappeared with time and increasing temperature. The mechanism of the so-called plasticisation process was speculated by proposing that nitrogen plasticised PTFE by

penetrating between individual grains from which the sintered polymer specimen was prepared. The authors also claimed similar plasticisation effects with PS although apart from the observed permanent expansion of the polymer noted after depressurisation, no detailed experimental evidence was ever advanced in support of this view. The above proposed mechanism of plasticisation however does not explain the reason for the absence of a plasticisation effect in the presence of helium. In this case, the polymer matrix must be much more susceptible to the invasion of the smaller helium atoms which in turn, following the above argument, should give rise to a larger plasticisation effect. The origin of this plasticisation phenomenon is investigated further in Chapter 8.

In a following publication, Parry and Tabor (1974) using the same torsion pendulum, with nitrogen as the pressure medium, reported that the pressure dependences of the shear modulii for all the polymers previously studied (Billinghurst and Tabor, 1971) were time dependent. In most cases, the modulus reached an equilibrium value within 10 minutes. Taking the data for poly(chlorotetrafluroethylene) (PCTFE) as an example, the shear modulus increased by ca. 12% following the exposure of the polymer to a hydrostatic pressure of 70 MPa for 8 minutes at 20°C. Doubling the temperature reduced the equilibrium time by half. It was argued that the time dependences arose partly because the application of pressure to a non-homogeneous medium produced shear which was time dependent and at higher temperatures the time to reach equilibrium was shorter. This suggested that thermodynamic treatments were unjustified in considering hydrostatic pressure as a simple variable.

Duckett and Joseph (1976), who used a hydraulic fluid as the pressure medium, reported large changes in the shear modulus of poly-(propylene) (PP) at times of up to three hours after a pressure change.

Typically, a 100% increase in modulus was obtained by exposing the

polymer to a pressure of 400 MPa for 25 minutes at $21^{\circ}C$. Although

these changes were accompanied by transient adiabatic heating effects

of comparatively long duration, the results were said to be consistent

with the expected changes in free volume occuring during dilational

creep under pressure. A more detailed examination of the nature of the

adiabatic heating effect and in particular its relevance to the pre-

viously reported PTFE "plasticisation" (Billinghurst and Tabor, 1971) will

be discussed in Chapter 8.

Subsequent papers in the following years mainly concentrated on

investigating the effect of the type of environment on the yield pro-

perties of polymers. Olf and Peterlin (1974) for example discerned

the role of different gaseous environments such as N_2, He, Ar, O_2 and

CO_2 in the crazing behaviour of poly(propylene). From a study of opti-

cal and scanning electron microscopy as well as stress-strain measurements,

the authors found that,in general, the gases promoted crazing, the

extent of which largely depended on the proximity of the test temperature

to the condensation temperature of the environmental gas. Also, gases

with greater thermodynamic activities were generally found to be more

efficient crazing agents. In conclusion, the crazing mechanism was

speculated by arguing that the gas was strongly absorbed at the craze

tip, where stress concentration increased both the equilibrium gaseous

solubility and the diffusion constant. This resulted in the formation

of a plasticised zone with a decreased yield stress for plastic flow.

Also gaseous adsorption resulted in a reduction in the polymer surface

energy which enhanced the ease of crack initiation involved in crazing.

Silano et al (1977) using an oil as the pressure medium reported a

linear increase in shear yield stress for poly(oxymethylene) with

increasing pressure but a non-linear increase for poly(propylene). They

found that the linear and the non-linear behaviour could be success-
fully predicted using the Pae yield criteria (Pae and Bhateja, 1975).
Duckett et al (1979) studied the effect of hydraulic pressure, strain
rate and environment on the shear behaviour of amorphous poly(vinylace-
tate) (PVA) and poly(carbonate)(PC). Hydrostatic pressures of up to
200 MPa superimposed on torsion tests carried out on PVA revealed an
increase in modulus with increasing strain rate. The change in modulus
was typical of a rubber-like material at low strain rates and a glassy
material at high strain rates. It was speculated that the transition
occured due to the shifting of the atmospheric glass transition to
the temperature of the experiment, i.e. increasing strain rate had the
same effect in shifting the transition temperature and shear modulus as
increasing the pressure. Both strain rate and pressure were therefore
thought of as making the polymer relaxation time longer than the experi-
mental time scale. Finally, crazing was found to occur with unsheated
PC. The effect became more pronounced at low strain rates and pressures.
The effect of different gaseous enviornments at atmospheric pressure
on the mechanical relaxations of HDPE was investigated by Barham and
Arridge (1979). Loss modulus measurements in tension using different
gaseous environments such as N_2, Ar, He and air revealed different
polymer responses, each being specific to the type of gaseous environ-
ment. In addition, a loss peak in tension was reported to occur at
$220^{\circ}K$ only in air. In torsion tests, however, none of these features
were observed and the loss modulus was found to be more or less inde-
pendent of the environment. It was argued that the fact that these
differences occured in tension but not in torsion was due to the
. dilation which accompanied any tensile test. It was also speculated
that a loss peak at 220K occured in air but not in N_2 due to the CO_2
content of air. This gas undergoes a phase transition near 220K which

would probably give rise to a measurable loss in the polymer.

Brown (1981) derived a complicated mathematical relationship to predict the velocity of craze propagation in an organic polymer in a state of stress exposed to a gaseous environment at atmospheric pressure. His expression took the following form:

$$\ln V = A - 1/RT \left| U_o - \nu\sigma - BP\exp\{-(Q_v/R)(1/T_b - 1/T)\} \exp\{-V\delta/D\} \right| \tag{4.2}$$

The physical parameters of the gas that enter the above equation are the diffusion coefficient, D, boiling point, T_b, the heat of vapourization Q_v and the partial pressure P. V is the crazing velocity and σ is the applied stress. δ denotes the minimum depth below the surface of the polymer permeated by the gas of activation energy U_o in order to initiate crazing. A and B are constants which may be determined experimentally. The above equation implies that the gaseous diffusion coefficient decreases with increasing applied stress, and also that the craze velocity is very sensitive to small temperature changes in the vicinity of T_b since $\ln V$ decreases exponentially with increasing temperature for T approaching T_b.

A more vigorous examination of the effectiveness of a gaseous environment in influencing the mechanical behaviour of PS at one atmosphere was undertaken in a study by Wu and Brown (1982). Electron micrographs of tested tensile specimens in He between 77K and 350K revealed an increase in craze intensity with increasing temperature. This was in contrast to the behaviour in N_2 where the rise in temperature was accompanied by a decrease in craze intensity. Increasing the partial pressure of N_2 and CH_4 in He at 77K resulted in a remarkable reduction in tensile strength (nominal stress at fracture) accompanied by an increase in craze intensity. Typically, a 12.7 x 5mm long and 0.8mm

thick PS specimen at 77K exhibited a 40% decrease in tensile strength
only by increasing the N_2 concentration from 0 to 100% at 1 atm. total
pressure. The ratio of the tensile strength at fracture in mixtures
of N_2/He and CH_4/He to the corresponding values in helium was found to
decrease linearly with square root of the partial pressures of N_2 and
CH_4 in He. Subsequent investigations revealed that a gas was effective
in reducing the tensile strength of the polymer compared to that measured
in helium at the same temperature as long as the test temperature was equal
to   or below the boiling point of the gas. In the order of their
decreasing effectivness in reducing the tensile strength the tested gases
were: N_2, Ar, CH_4, N_2O, CO_2 and H_2S. The variation of tensile strength
with increasing strain rate was also very interesting. For example,
at 77K, the tensile strength of PS in He was found to be practically
independent of strain rate. In N_2, however, a large increase in tensile
strength was observed with increasing strain rate. These results are
reproduced in Figure 4.4. A point worth noting in the original data
is that, as before, the tensile strength in N_2 always remained less
than that in He at all strain rates investigated. To explain the
difference in behaviour, the authors argued that, according to Brown
(1981), if the strain rate was above a critical value, there was not
sufficient time for N_2 to penetrate the polymer and plasticize it.
Hence the solubility of the plasticizer gas, N_2, in PS decreased with
increasing strain rate. In conclusion, the authors proposed that
their experimental evidence was in support of the previously held view
(Brown and Metzger, 1981) that the effectiveness of a gas in changing
the mechanical behaviour via crazing depended on its solubility which
in turn depended on the relative pressure P_r; the ratio of its pressure
to the vapour pressure in equilibrium with the condensed gas. This

was given by:

$$P_r = P\exp(-\frac{Q_v}{R}(\frac{T-T_b}{T_b T}))$$ (4.3)

where Q_v is the heat of vapourization, T_b the boiling point and T the environmental temperature. The above equation was used to estimate the temperature T, above which a particular gas was ineffective in altering the tensile strength. For N_2 and CH_4, the predicted temperatures were 143K and 207K whereas the experimental points were about 160K and 185K. Finally, the authors used a cumbersome thermodynamical argument involving an assumed linear variation between the log of gaseous solubility and its boiling point (Amergon, 1964), to predict a relationship between the degree of softening (the fractional change in tensile strength with reference to an inert He environment) of PS with N_2 concentration, C. The proposed expression took the form:

$$(\sigma_i - \sigma_c)/\sigma_i = 0.07C^{\frac{1}{2}}$$ (4.4)

where σ_i and σ_c were the tensile strength in the inert environment (He) and in N_2 respectively. From the equation they estimated that a degree of softening of 0.1 required a N_2 concentration of $2cm^3$ (STP) per cm^3 PS. Taking the density of PS as 1.05 gm cm^{-3}, it was estimated that 0.01 N_2 molecules per monomer unit of PS reduced the intrinsic tensile behaviour by 10%.

4.6 Summary

We may conclude that, in general, the application of pressure to polymers results in the strengthening of polymers. This is reflected in the large increases in modulii observed in tension, compression and

torsion. The influence of hydraulic pressure on the ductility of poly-
mers, however, varies markedly from polymer to polymer and in many cases,
the behaviour may to a large extent be dictated by the type of hydraulic
pressure medium employed. A number of yield criteria have been success-
fully evaluated to explain the difference in the yield behaviour of
polymers. The role of the type of the hydraulic pressure medium on
yield is however not fully understood. It has been proposed that (a) the
pressure fluid may give rise to a ductile behaviour following the
plasticisation of the polymer, or (b) the fluid may cause brittleness
following the initiation and pressure induced propagation of cracks
in the polymer surface. Similar environmental effects have been observed
with different gases at atmospheric pressure which may also be reflected
in comparatively large changes in mechanical properties. The role of
different gaseous environments on mechanical properties above atmospheric
pressure is, however, little understood.
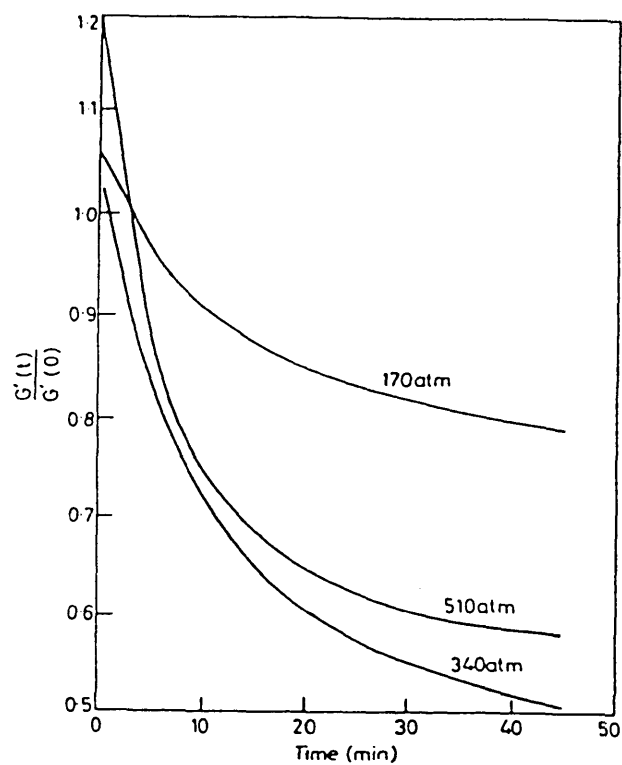
Figure 4.1. Plasticisation effect of N_2 pressure on PTFE at a constant temperature of $83^{\circ}C$ (Billinghurst and Tabor 1971).
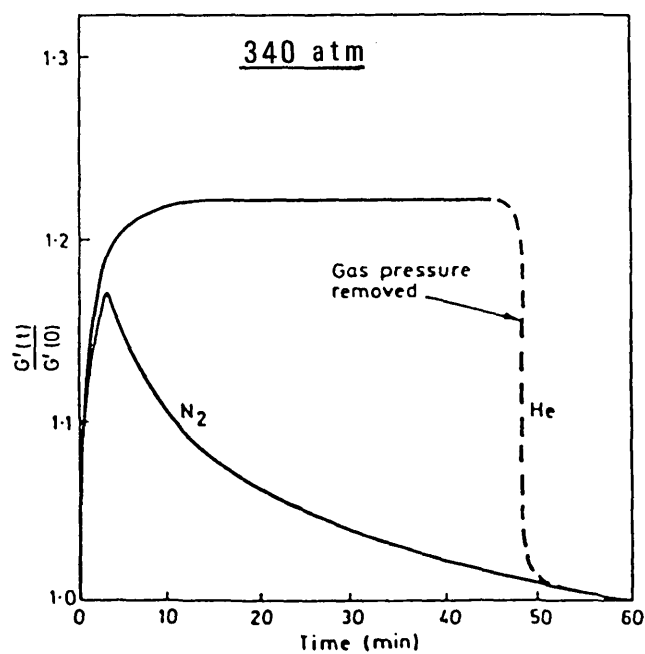
Figure 4.2. Softening of PTFE in N_2 and He pressure media at $20^{\circ}C$ (Billinghurst and Tabor 1971).
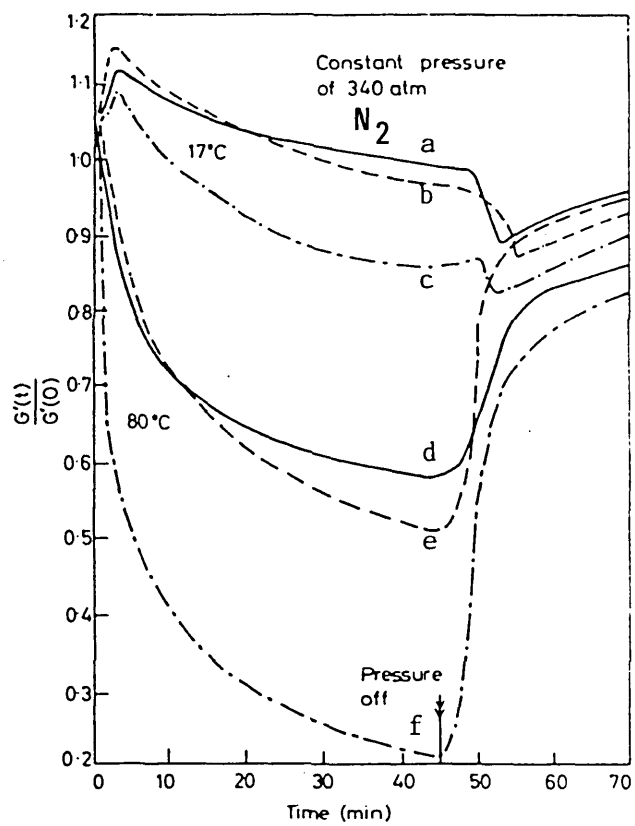
Figure 4.3.

PTFE plasticisation curves: ———,68% crystallinity;— — —,65% crystallinity ;—.—.—,60% crystallinity (Billinghurst and Tabor 1971).
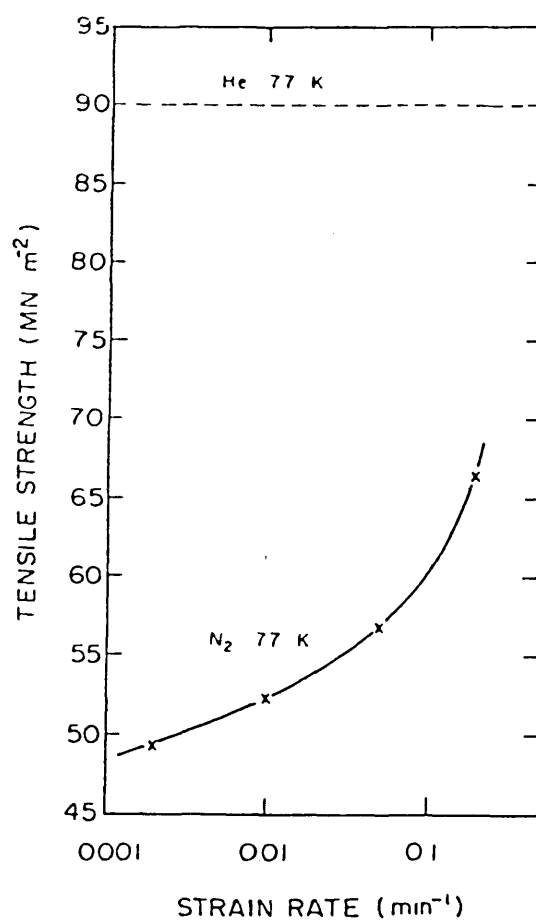
Figure 4.4. Tensile strength for PS in N_2 against strain rate at 77K.
Dotted curve is for He at 77K (Wu and Brown 1982).

CHAPTER 5

EFFECT OF HYDROSTATIC PRESSURE ON THE COMPRESSIBILITY OF POLYMERS

5.1 Introduction

Previous dilatometric studies on polymers have been mainly confined

to liquid hydrostatic media. This is largely due to the fact that

studies using gaseous pressure media require much more complicated equip-

ment. This section therefore reviews compressibility data obtained

using liquid pressure media and direct uniaxial compression only. It is

intended that the above together with the data obtained using gaseous

environments reported in the experimental section will be of some value

for comparing and contrasting the different effects of liquid and gaseous

pressure media on the compressibility of polymers.

5.2 Experimental Methods and Results

The most commonly used technique for studies under liquid pressure

media is that first developed by Weir (1950). Briefly, the experiment

consists of loading a "leak proof" piston into the bore of a cylinder

containing the specimen which is immersed in a suitable pressure trans-

mitting medium. A knowledge of the internal bore of the pressure vessel

and the displacement of the piston permits the calculation of the

change in volume of the polymer. Weir (1953) used this technique to

report some PVT data for PTFE up to a maximum pressure of 1000 MPa over

a temperature range of 10 to $80^{\circ}C$. The data revealed three distinct

transitions, namely phases I, II and III all of which intersected at

a triple point at approximately $70^{\circ}C$ and 5000 MPa pressure. This data

are represented in Figure 5.1. Weir found that at the transition lines,

phase III is approximately 2% denser than phase II and that phase I is

approximately 1% less dense than phase II. An important point to note

in Weir's original data (see Figure 5.2) is the larger compressibility of the polymer with increasing temperature; a feature which is universally reported in all the subsequent literature cited in the following sections.

Matsuoka and Maxwell (1958) avoided the use of a liquid pressure medium by directly compressing the polymer specimen at both ends using nitralloy steel plungers. Bulk compressibility studies on amorphous PS and crystalline PE were carried out up to a maximum pressure of 220 MPa at a temperature range of 40 to 180°C. In the case of PS, the glass transition temperature (associated with a large drop in compressibility) was found to shift at a rate of 40°C/100 MPa pressure. It was also found that the pressure required to induce such a transition increased with increasing temperature. This was attributed to the higher kinetic energy of the polymer chains. Increasing the rate of compression however gave rise to an opposite effect as increasing temperature, i.e. the faster the material was compressed, the less was the pressure required to induce a structural change. Similar behaviour was also observed in the case of PE. However, the amorphous PS was found to be more compressible than the crystalline PE.

Beecroft and Swenson (1959) employed a slightly more complex refinement of the above technique to extend the PVT data for PTFE to temperatures as low as 70K up to a maximum pressure of 2000 MPa. Yasuda and Araki (1961) used the same piston displacement technique to study the effect of superimposed pressures of up to 30 MPa on the 20 and 30°C room temperature transition of cylindrical PTFE specimens (2.162 to 2.230 gcm^{-3}) confined between the walls of a pressure vessel cylinder. Transition temperatures at various pressures were determined from the inflection points of volume vs temperature curves. Following the observation that

the lower transition predominated strongly over the upper, the lower

inflection point of the thermal expansion curve was referred to as the

room temperature transition and the higher one was unfortunately

ignored. However, the authors reported a linear relationship between

the shift in the $20^{o}C$ transition temperature and the applied pressure,

the rate of which varied between 20 to $16^{o}C/100$ MPa depending on the

type of the polymer. There was no apparent relationship between the

pressure dependence of the transition temperature, $\frac{dT}{dP}$ and the density

of the specimens. Passaglia and Martin (1964) slightly modified the

volume measurement technique first developed by Weir (1951) by fitting

the high pressure chamber with windows so that changes of mercury level

in a glass dilatometer sample cell could be followed directly with a cat-

hetometer. The authors used this technique to measure the variation

of the second order glass transition temperature in PP with increasing

pressure. Despite the fact that the glass transition temperature is a

consequence of relaxation times associated with molecular motions, the

authors used the compressibility data on PP to show that thermodynamic

principles   could be applied to the glass transition. To establish

this, the authors successfully predicted a value for $\frac{dT}{dP}$ using the Ehren-

fest equations. These are given by:

$$\frac{dT}{dP} = \frac{\Delta\beta}{\Delta\alpha} \qquad \text{or} \qquad \frac{dT}{dP} = \frac{T\bar{v}\Delta\alpha}{\Delta Cp} \qquad (5.1)$$

where $\Delta\alpha$, $\Delta\beta$ and ΔCp are the changes at the transition in thermal expan-

sion coefficient, compressibility and the specific heat respectively.

Values of Cp were obtained from literature (Dainton et al, 1962 and

Passaglia and Kevorkian, 1963). It is interesting to note a measured

reported value of $dT/dP = 20^{o}C/100$ MPa (see Figure 5.3) which is in close

agreement with the corresponding value reported (Yasuda and Araki, 1961) for the first order room temperature transition of PTFE. Also from Figure 5.3 the glass transition temperature obtained at atmospheric pressure is noticeably less than that predicted by the fitted straight line. The authors qualitatively attributed this to the slow rate used in the experiment. Martin and Eby (1968) used the same technique to study the effect of pressure on the $20^\circ C$ (II-IV) and $30^\circ C$ (IV-I) transitions in PTFE. It was found that the $20^\circ C$ and $30^\circ C$ transition pressure, P (Nm^{-2}) increased with temperature, T according to the second degree polynomials of the form

$$P = (-820 + 29.6T + 0.68T^2) \times 10^5 \text{ and}$$

$$P = (-91 - 57.8T + 1.99T^2) \times 10^5 \text{ respectively}$$

indicating a larger pressure dependence for the $20^\circ C$ transition (see Figure 5.4). These equations suggested a possible triple point near 260 MPa. However, the authors were unable to quantitatively establish above as the $30^\circ C$ transition could not be resolved above 200 MPa due to its small magnitude and also its overlapping with the much larger $20^\circ C$ transition. The relation between the $20^\circ C$ and $30^\circ C$ transition volumes, V (determined from a plot of the slopes of the specific volume-temperature curves against temperature and measuring the areas under the curves) and pressure is reproduced in Figure 5.5. It is interesting to note a large negative $\frac{dV}{dP}$ for the $30^\circ C$ (IV-I) transition whilst the corresponding value for the $20^\circ C$ transition (II-IV) is relatively small and positive.

Findley et al (1968) measured the hydrostatic creep of some solid plastics in an hydraulic oil medium by measuring the induced linear strain

via monitoring the change in the resistance of a strain gauge transducer cemented onto the surface of the sample. The polymers studied included PE, PVC, PMMA, PU (polyurethane) and EP (epoxy resin), all of which were tested up to a maximum pressure of 345 MPa. Surprisingly, the authors observed significant continuous increases in linear strain with time under constant superimposed hydrostatic pressures. The variation could be approximated in terms of an equation of the form:

$$\log(\varepsilon - \varepsilon_o) = \log m + n \log t \qquad (5.2)$$

where ε is the linear strain, t denotes the time and ε_o, n and m are constants which may be determined experimentally. Typically, a PE specimen was found to creep by ca. 70% following its exposure to a constant hydrostatic pressure of 345 MPa for 100 hrs. An interesting feature in all of the creep experiments was the initial rapid increase in ε over a span of 0.2 hrs. This was associated with the inevitable initial temperature rise in the polymer as a result of its adiabatic compression. The authors also observed reproducible changes in ε on reloading specimens provided sufficient time was allowed for the samples to recover. The time dependent strain phenomena and in particular the question of the stability of the reported apparent permanent densification of PTFE specimens (see for example Figure 5.2) following pressurisation were unfortunately not investigated by any of the above authors. Finally, the hydrostatic creep behaviour of the polymers was explained in terms of time dependent viscoelastic rearrangement of the polymer chains and molecules in response to the applied external pressure.

Hirakawa and Takemura (1968) measured the pressure dependence of the 30 and 130°C transitions in PTFE by determining the ultrasonic

absorption maxima corresponding to each transition. Surprisingly, no peak associated with the $20^{\circ}C$ transition was reported. This was attributed to the relatively long relaxation time of the $20^{\circ}C$ transition compared to the high absorption frequency (5 Mc/sec) of measurements. Using silicone oil/kerosene as the pressure transfer medium, the authors reported a shift of ca. $10^{\circ}C/100$ MPa in the $30^{\circ}C$ transition. The corresponding predicted values for the $30^{\circ}C$ and the $20^{\circ}C$ transitions using the Clapyeron-Glausius equation were 8.6 and $15^{\circ}C/100$ MPa respectively. This equation was given by:

$$\frac{dT}{dP} = T \frac{\Delta V}{\Delta Q} \tag{5.3}$$

where ΔV and ΔQ denote the total volume and enthalpy change at the transition respectively. Mizouki (1973) used a linear variable differential transformer (LVDT) to study the time dependent volumetric deformations in a glass up to a maximum pressure of 2200 MPa. The results exhibited similar trends to the hydrostatic creep data reported earlier by Findley et al (1968). An initial rapid increase in strain of approximately one hour duration was followed by a much slower uniform increase in strain over a prolonged period of time (ca. 50 hrs.). Spetzler and Meyer (1974) used another variation of the technique first developed by Passaglia and Martin (1964) to study the volumetric strain induced in PMMA exposed to a maximum pressure of 1000 MPa. This new method involved the measurement of the mercury level in the mercury sample cell ultrasonically. The results indicated compressibility values in close agreement with the previously reported data by Findley et al (1967) and Stephens et el (1972). It is interesting to note that the above agreement was obtained despite the fact that Findley et al used an hydraulic

oil as the pressure medium and also that the volumetric strains reported by Findley et al were estimated by assuming isotropic compression and multiplying the measured values of linear strain by three. Yet another variation of the technique first developed by Beecroft and Swenson (1959) was employed by Zoller et al (1976) to study the pressure volume relationship for PS. In this arrangement, the sample was contained in a rigid sample cell one end of which was closed by flexible bellows. The space not occupied by the sample was filled with mercury under vacuum. In this way the polymer was separated from the hydraulic pressure transfer medium. In a subsequent publication, Zoller (1978) used the above technique to report the PVT data for PTFE around its crystalline melting point. His data were in perfect agreement with those predicted using Tait's equation of state applicable to polymeric melts and glasses (Quach et al, 1971). This is given by:

$$V(P,T) = V(0,T) \{1 - 0.0894 \ln |1 + P/B(T)|\} \qquad (5.4)$$

where B(T) is described as a melt parameter which may be determined experimentally.

5.3 Summary

Relaxation processes in polymers are associated with time dependent short or long range reorganisations in the molecular architecture of the polymer matrices. These may involve the corporative rotation or displacement of side groups or chain segments requiring sufficient local space (free volume) and adequate vibrational energy to overcome the intermolecular cohesive forces. An increase in temperature fulfils both requirements. The role of pressure on the above is well established. We may conclude that a hydrostatic pressure, in contrast to temperature, reduces

free volume by compression and hence hinders chain mobility. This in
turn implies that a relaxation may occur at an increased temperature.
This is consistent with all of the previous observations in which
pressure increases transition temperatures. The precise role of a
pneumatic gas pressure on the molecular relaxations in polymers has
not been investigated.
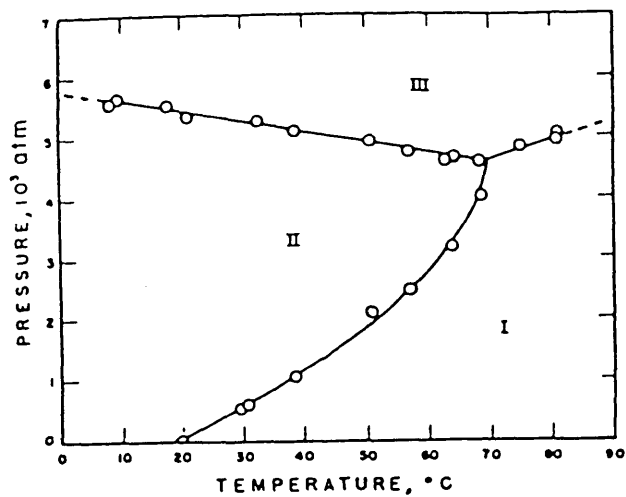
Figure 5.1. Proposed phase diagram for PTFE (Weir 1953)
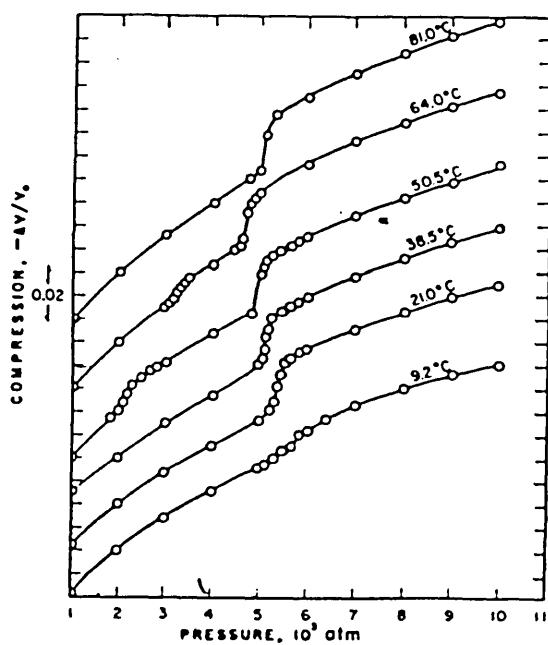
Figure 5.2. Compression curves of PTFE at various temperatures (Weir 1953)
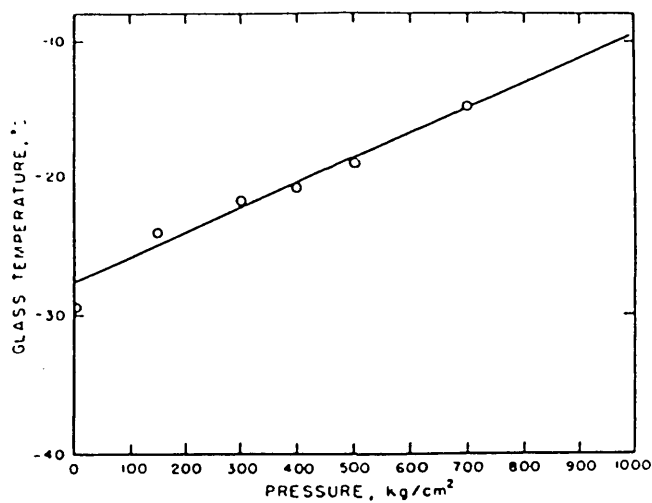
Figure 5.3. The glass temperature of PE as a function of pressure

(Passaglia and Martin 1964)
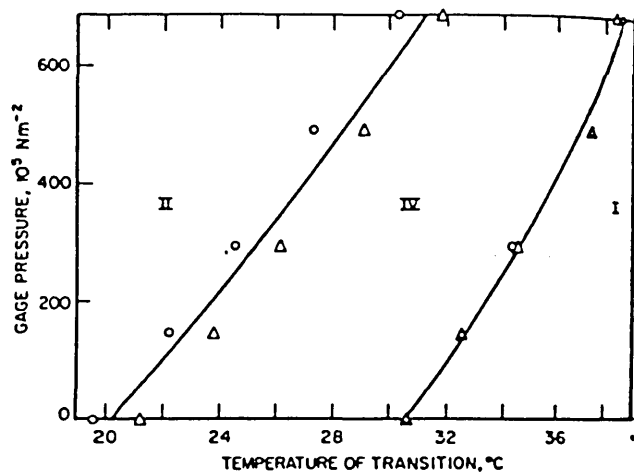
Figure 5.4. Relations between pressure and transition temperature for PTFE (Martin and Eby 1968)
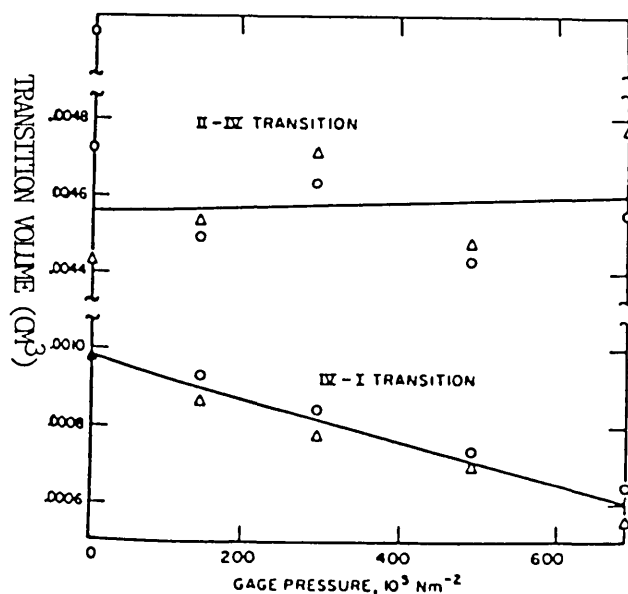
Figure 5.5. Changes in volumes of transition with pressure for PTFE (Martin and Eby 1968)

CHAPTER 6

HIGH PRESSURE APPARATUS : GENERAL DESIGN FEATURES

6.1 Introduction

The initial requirements for the design of gas and liquid pressure

systems were that both assemblies should be capable of producing and

safely containing a maximum pressure of ca. 55 MPa, working at a tempera-

ture range of between $0^{o}C$ and $75^{o}C$.

Following a survey of the type of equipment available, it was

eventually decided to use the apparatus designed and fabricated by

Billinghurst (1969) for gaseous studies. Major modifications in design

had to be made in order to make the equipment compatible with our pro-

posed studies.

A pressure vessel supplied by the Department was used for cases

were a liquid was employed as a pressure transfer medium.

6.2 The High Pressure Gas System

Plate 6.1 is a photograph of the high pressure gas apparatus.

Briefly, the unit consists of the high pressure chamber, an intermediate

gas receiver and a gas booster capable of delivering a maximum gas

pressure of 62 MPa from a   supply bottle pressure of ca. 6 MPa.

6.2.1 The gas booster pump; general design features

The pressure vessel was charged up to a maximum pressure of 55 MPa

using a slightly modified commercial gas booster pump (Charles Madan,

Altrincham; Plate 6.2) fed from conventional high pressure gas cylinders

fitted with commercial regulators. The gas was fed into a high pressure

cavity via a simple flap valve whose surface was fabricated from PTFE.

A simple piston, sealed with a single lipped neoprene ring of area

5.06 cm^{2} was moved in this cavity by a larger piston (486 cm^{2} area)

contained in a second chamber. This valve system was designed to fill

the higher pressure cavity at its maximum volume and to discharge the contents at maximum pressure (minimum volume). A second valve facilitated the latter. The second piston was driven by air pressure supplied by a 2.6 KW, 1450 R.P.M. hydrovane compressor (Whittaker Hall: Manchester) and a reservoir (0.52 m^3 volume). The air flow was supplied via a pressure regulator and a valve train connected to the large piston which ensured a proper reciprocating action was achieved in the high pressure chamber. This system was capable of pumping at ca. 84 kPa/sec. An important feature of this system was its ability to maintain isobaric conditions. Simple adjustments to the air pressure regulator connected to the driving stage pump allowed a balance condition to be maintained. The high pressure side was at a pressure 96 times that of the air pressure regulator. Small leaks and thermally induced volume changes were readily compensated to within $\pm$ ca. 140 KPa.

In practice the main experimental problems were associated with seal failure in the high pressure piston or in the two main high pressure flap seals. Certain modifications were made to design and materials throughout the study to improve the performance and longevity of these seals. Operation of the system at the maximum pump rating (ca. 5 MPa/min) gave rise to adiabatic heating (see Chapter 8). The problem was avoided to a large extent by limiting the maximum operating pumping rate to ca. 2 MPa/min.

6.2.2 The intermediate gas receiver

The intermediate gas receiver acted as a pressure stabiliser or buffer and was connected directly to the pressure vessel via a stop valve. It was designed to contain approximately five times the volume of gas in the pressure vessel. This ensured that small leaks in the pressure vessel did not give rise to a rapid drop in pressure when the two vessels were interconnected. The vessel was constructed from mild

steel and before use, it was tested hydraulically to a maximum pressure of ca. 86 MPa for 24 hours. Its safe working pressure was regarded as 138 MPa.

The chamber could be depressurised at will and at a controlled rate (7 minutes minimum for complete evacuation) by opening a release valve positioned between the pressure vessel and the chamber itself.

Madan stock high pressure tubing was used for the conveying of high pressure gas. These were made of alloy steel with an O.D. of 9.52 mm and an I.D. of 3.17 mm. Joints were made by machining tube ends to a 59° cone and screwing 9.52 mm dia. x 10 t.p.cm left hand threads.

6.2.3 The gas pressure vessel

Figure 6.1 is a dimensional drawing of the pressure vessel general assembly. Briefly, the unit consisted of two mushroom shaped caps which were secured to the body of the vessel (the chamber) via 6 high tensile bolts on each cap. The dimensions of the chamber were 61 cm long with an O.D. of 12.7 cm and an I.D. of 5.08 cm. This vessel was originally designed and fabricated by Billinghurst (1960). It was constructed from Vibrac 45; EN26 which is a high tensile steel. The material was hardened to 830^oC and tempered at 595^oC. Its useful operating temperature was -20^oC to 150^oC (Colbeck, 1933). The vessel had a safe working pressure of ca. 258 MPa and hydraulically tested at the same pressure for 24 hours.

A detailed safety and design analysis for the whole pressure vessel assembly assuming different modes of potential failure is presented in the Appendix. This appraisal was necessary as the vessel used was modified in design and also because of new safety regulations operating at the time of this work. Also. included in the Appendix is the design of the steel safety cabinet required by current regulations.

New pressure vessel's caps were designed as the previous pair were

not useful for the proposed experimental studies. Figure 6.2 is an

engineering drawing of the top cap. It was constructed from Vibrac 45;

a material with a hardness of 250 Hv corresponding to σ_u (ultimate

tensile strength) and σ_y (yield strength) of 9.45×10^3 kg cm^{-2} and

8.66×10^3 kg cm^{-2} respectively. The bottom cap was basically identi-

cal in design to the top cap with the exception that the latter contained

eight insulated electrical connections. The design of suitable insu-

lating plugs required for leading these electrical connections into

the pressure chamber presented considerable difficulties. Amagat (1911)

and Bridgman (1911) have suggested various techniques but these were

either too complicated in design or susceptible to failure after fre-

quent use. A schematic representation of the technique eventually

adopted here is included in Figure 6.2. Briefly, the connections were

made by machining 60° female cones into the caps. These holes were

sealed with 59° electrically insulating hollow ceramic cones. The

machining procedure was involved and expensive and I am grateful to

several members of the Department's Engineering staff for their assis-

tance. The central hole in the ceramic plug was then sealed off by

inserting a suitably machined Invar plug. All of the mating surfaces

were individually ground by hand. Insulated electrical leads were

previously hard soldered to each end of the Invar plug. Invar was

used as a very low thermal coefficient of expansion (ca. $9 \times 10^{-7}\text{°C}^{-1}$)

was required to reduce thermally induced stresses. Early attempts to

use mild steel for this purpose were fraught with premature failures.

The quality of the seals produced by these plugs were totally dependent

on the tolerance to which overlapping surfaces were machined. Gas

leaks did however occur and the problem was overcome by applying a

thin layer of slow setting epoxy (Araldite) onto adjoining surfaces

before final assembly. These were then cured in situ at 20 MPa for

8 hours, thus allowing sufficient time for the epoxy to set. This technique produced a leak tight and durable electrical connection.

The insulation resistance of these plugs were also high enough (ca. 10 meg-ohms) for the reported work. However, there was a considerable (1000 folds) decrease in electrical resistance when a cold cap was exposed to the outside environment following a low temperature experiment. This was found to be due to the hydroscopic nature of the epoxy resin; the resin simply absorbed moisture following atmospheric condensation and became too conductive. The above problem was cured by heating the cap for a few hours in an oven (80°C) prior to use.

The first experiments carried out using new caps failed because the main rubber seals (5.08 cm O.D., 4.12 cm I.D. and 5.36 mm thick) on the caps were extruded at comparatively low pressures. This gave rise to gas leaks and made the subsequent removal of the caps extremely troublesome. The problem was overcome by the use of bronze anti-extrusion rings placed above and below the rubber seals. The use of oil as a lubricant when assembling seals was also avoided. A schematic arrangement of these rings is presented in Figure 9.2.

6.2.4 The heat exchange system

The vessel's temperature and hence the temperature of the sample was varied and controlled externally. This was achieved by the use of an external heat exchanger which enveloped the whole body of the pressure vessel. This unit contained both the heating and cooling stages and was separated from the pressure vessel by the heat exchanger's inner wall which was in close proximity to the pressure vessel. The heat exchanger was filled with oil (type NS41, British Petroleum). The heating was obtained via two thermostatically controlled heaters. These heaters were capable of providing a maximum temperature of 150°C at an average rate of 0.2°C/min in the vessel. A platinum resistance tempera-

ture controller (type TCN-: Advanced Industrial Electronics) was used to maintain a constant temperature ($\pm$0.2°C precision). The heat exchanger was wrapped with several layers of glass wool to reduce heat losses to a minimum (see Plate 6.3).

Cooling was achieved by circulating a pre-cooled (-5°C) mixture of water and ethyleneglycol through a coil (5 mm I.D.) which was wound (50 turns) around the inner wall (adjacent to the pressure vessel) of the heat exchanger. The coolant temperature was lowered by the use of a 0.6 KW thermostatically controlled cryostat capable of providing a minimum temperature of -30°C. Typically, a time of ca. 16 hours elapsed before the vessel's temperature reached that of the coolant. The internal temperature in the vessel close to the specimen was monitored by measuring the potential across a platinum resistance film (type 158-328) supplied by Radio Spares. The change in resistance with temperature was calibrated according to BS 1904.

6.3 The Liquid Pressure Vessel Assembly

A schematic layout of the liquid pressure vessel assembly is presented in Figure 6.3. This system was much simpler in design and operating procedures than the gas pressure vessel assembly and only a brief account is given here. The unit consisted of a pressure vessel (supplied by the Department) surrounded by an oil bath and a cooling coil, a hydraulic manual pump (5.08 cm I.D., 200 MPa max; Taylor Hydraulic Engineers, Twickenham), a pressure gauge and an isolating valve. Two thermostatically controlled immersion heaters (3 KW each) were used for heating. Temperature was controlled and varied in exactly the same manner as in the gas pressure vessel assembly.

The vessel's safe working pressure was regarded as 300 MPa and Vibrac (V40) was used as the material of construction. The chamber had an I.D. of 2.59 cm, an O.D. of 18 cm with an overall length of 52.2 cm.

One end of the vessel (bottom end) was directly connected to the hydraulic pump via a pressure gauge and a stop valve. The other end was sealed off using a cap containing six electrical connections whose design and construction was similar to that in the gas pressure vessel cap. This cap was simply screwed on to the chamber.

High pressure tubing (5.2 mm O.D. and 3 mm I.D.) were used for the conveying of high pressure liquid. Joints were made by machining tube ends to 59° cones and screwing 5.2 mm dia. x 10 t.p.cm right hand threads.

Budenburg type pressure gauges were used for pressure measurements in both gas and liquid studies. These had a full scale deflection of ca. 70 MPa and were found to have typical accuracies of $\pm$340 KPa following appropriate calibration tests. Nitrogen gas was white spot oxygen free. All gases were supplied by British Oxygen Corporation.

TOP CAP

CHAMBER

BOTTOM CAP

BOLT

SCALE-CM

0   1   2   3
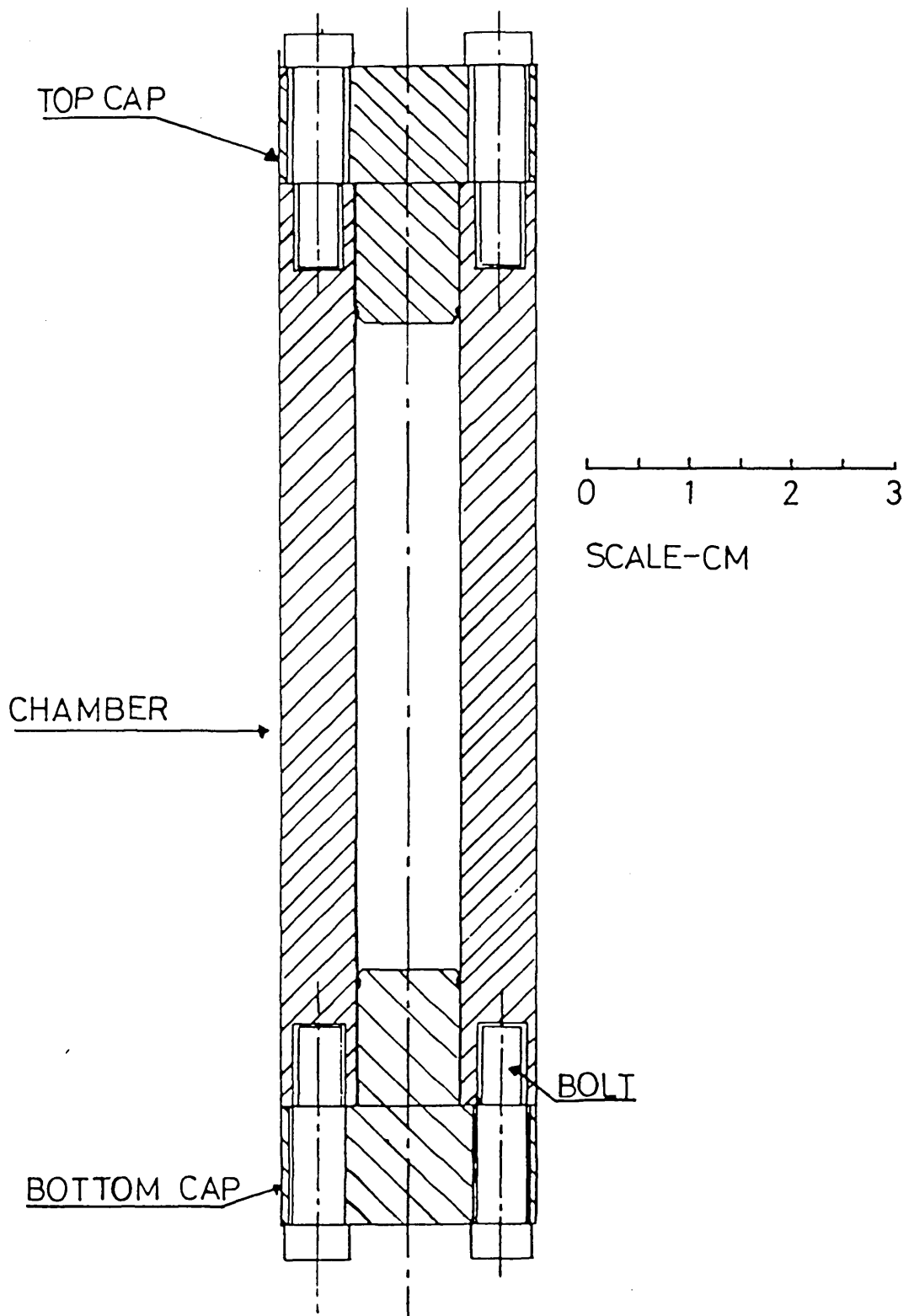
FIG.6.1: THE VESSEL GENERAL ASSEMBLY

FIGURE 6.2
DESIGN OF PRESSURE VESSEL
CAP

ELECTRICAL
CONNECTION

INVAR
PLUG

CERAMIC
CONE

INSULATING PLUG
ARRANGEMENT

2.295"

0.190"

1.0"

6 HOLES
1.10" DIA ON 3.500 PCD

5.00"

TOP VIEW

SECTION VIEW

0.750
20 T.P.I.

3/32
RAD

1.97"

2.76"

0.707"

26 T.P.I.

8 CERAMIC INSERTS
ON 1.250 PCD
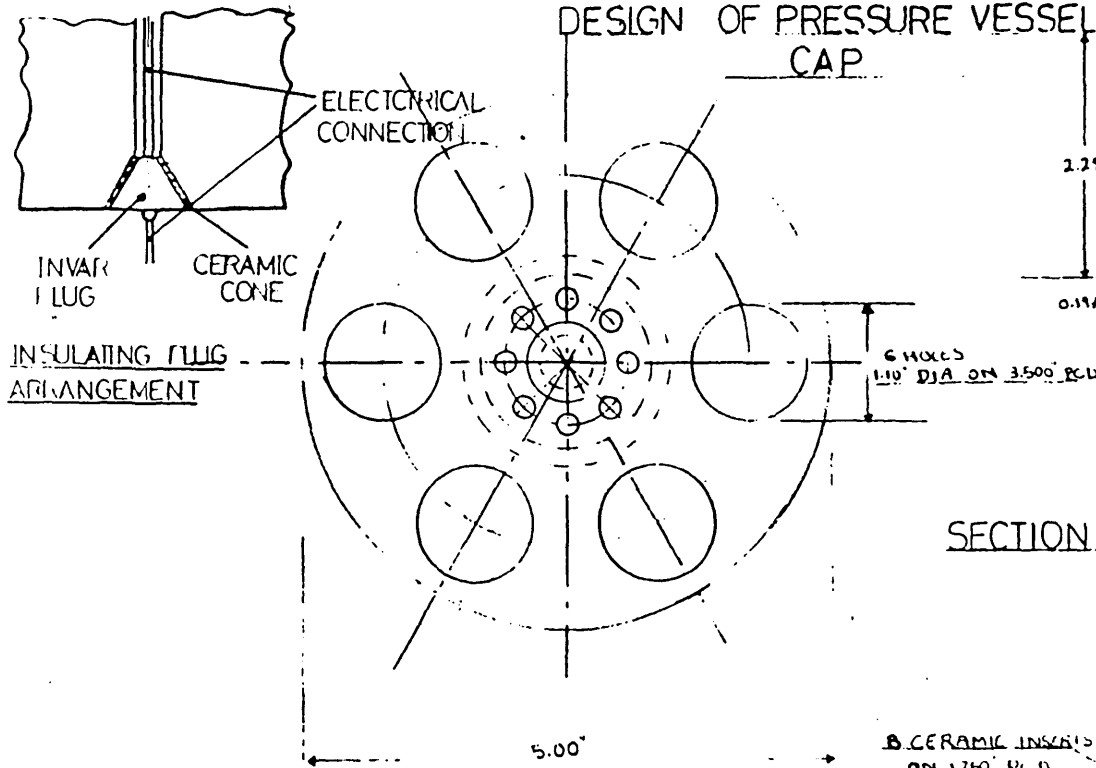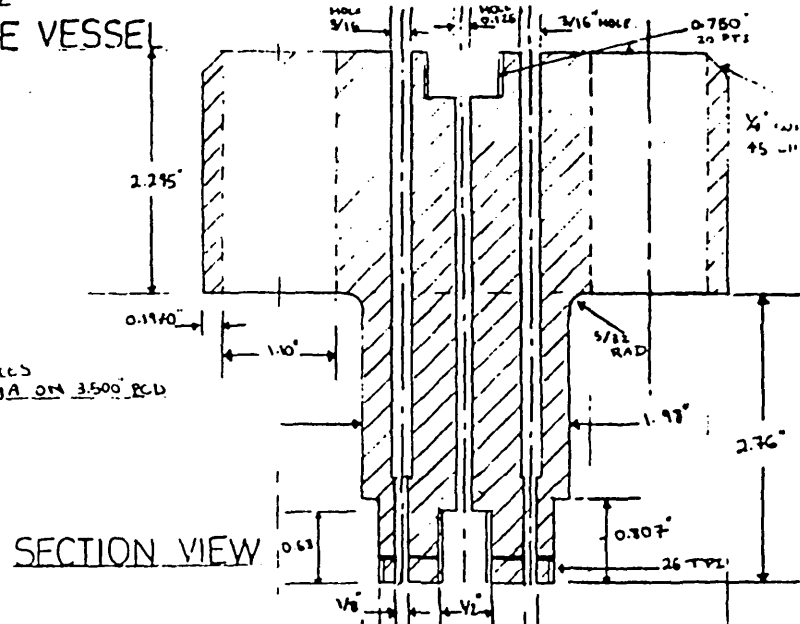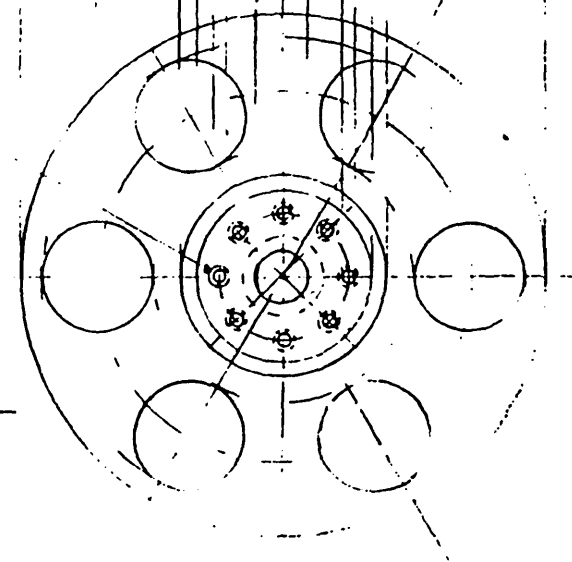
BOTTOM VIEW

MATERIAL OF CONST.	V45
DIMENSIONS	INCH
SCALE	1:1
DRAWING NO.	1

DRAWN BY H.MAHGEREFTEH
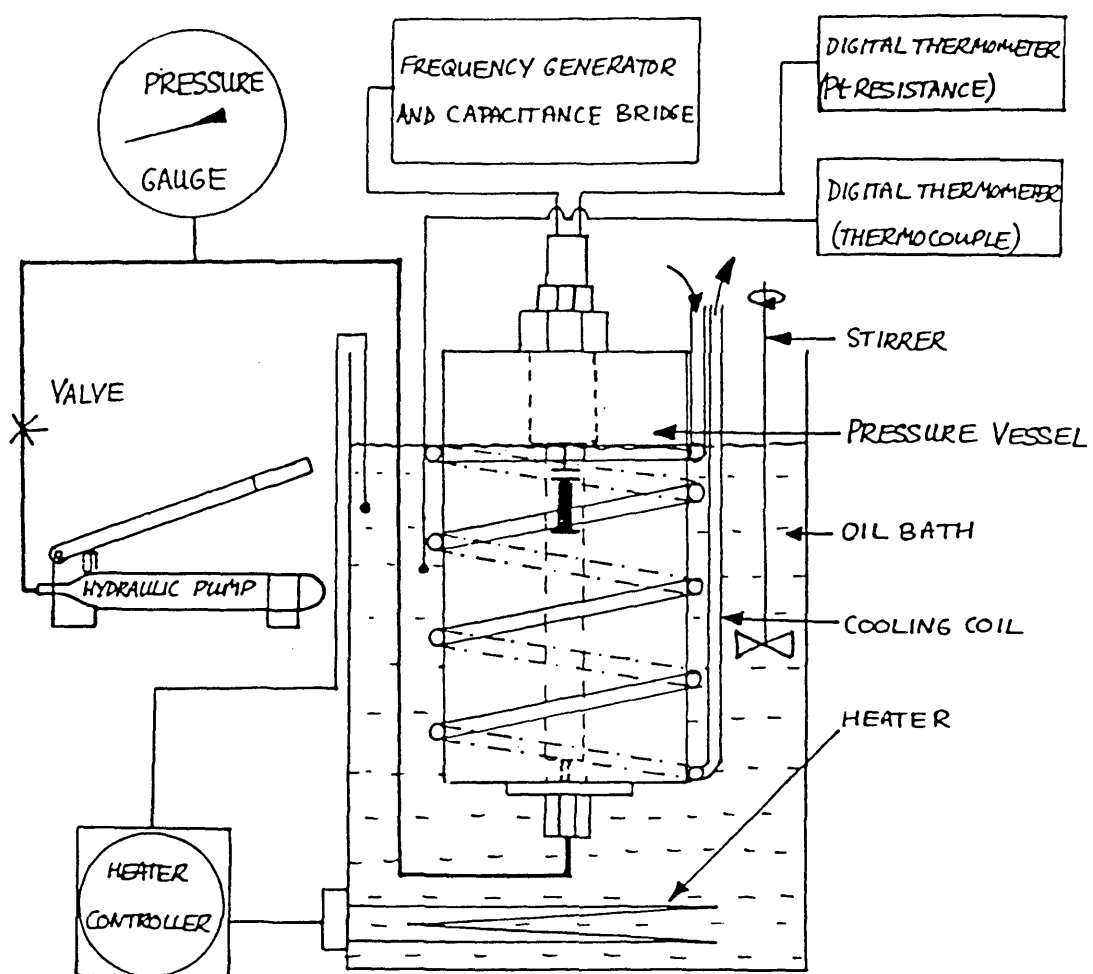
Figure 6.3. Schematic representation of the liquid pressure
vessel assembly.
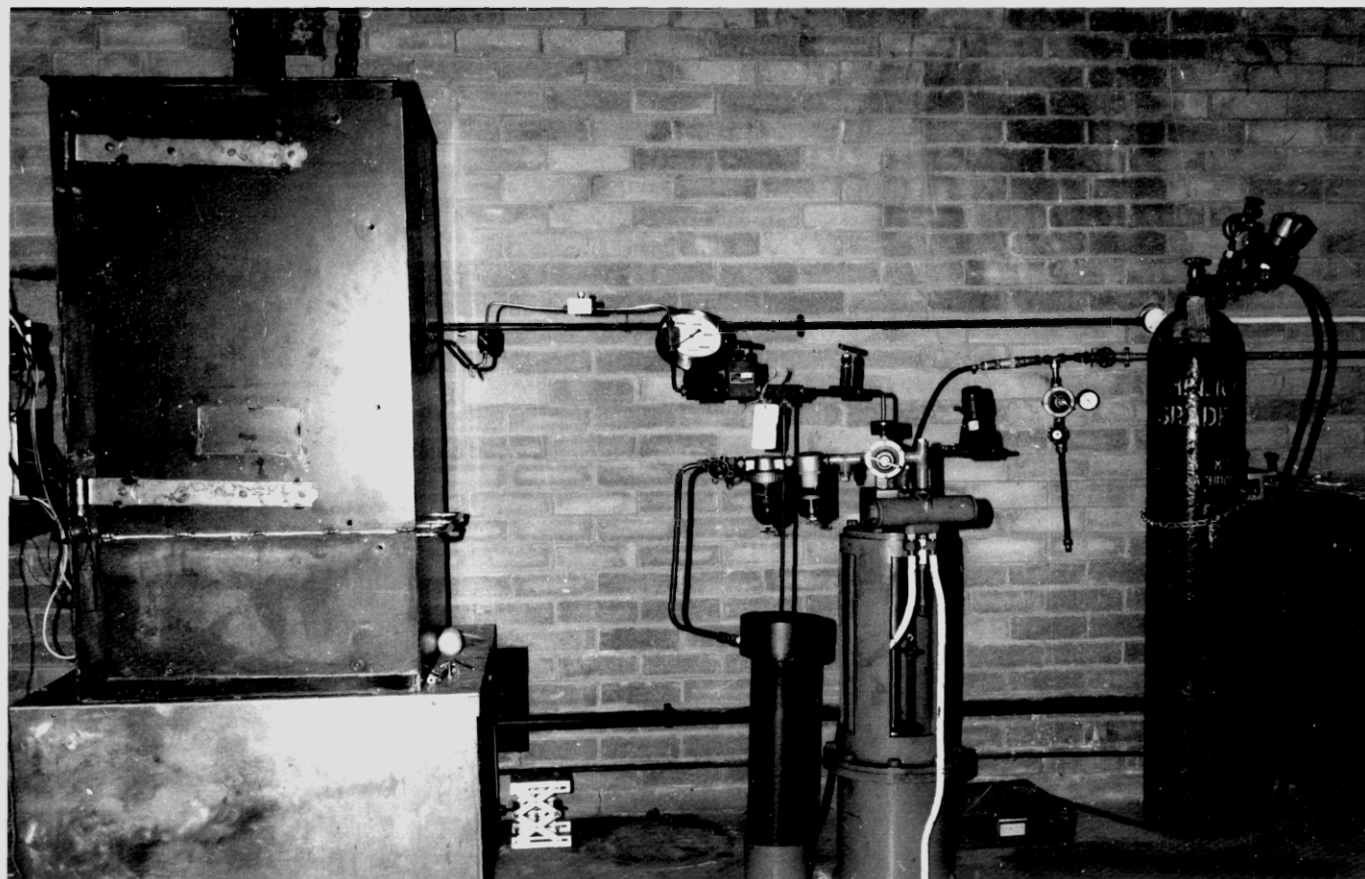
Plate 6.1. A photograph of the high pressure gas apparatus showing (left to right),the high pressure chamber, the intermediate gas receiver, the gas booster pump and a supply gas cylinder.
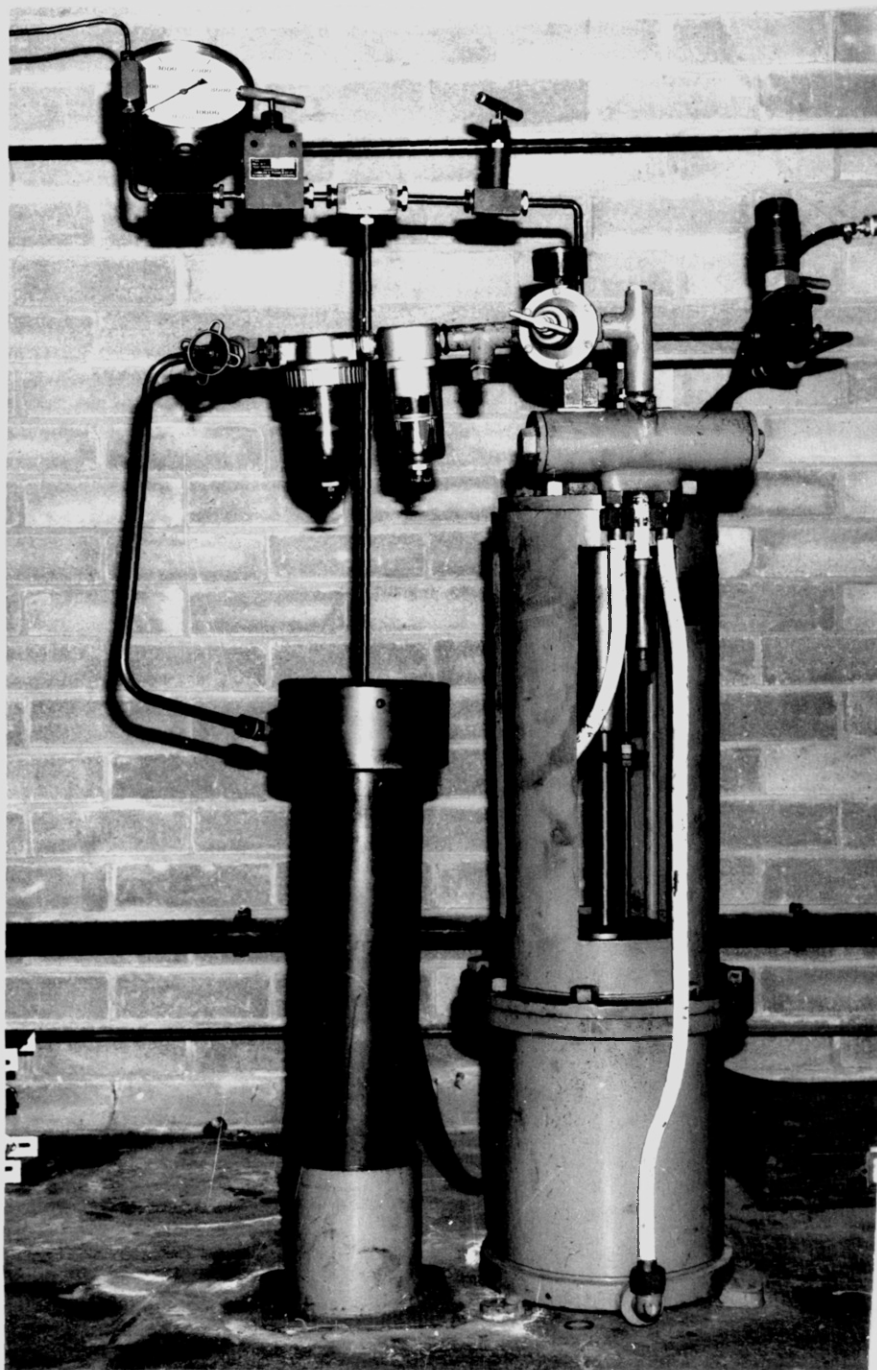
Plate 6.2. A photograph of the gas booster pump (right) and the intermediate gas receiver (left).
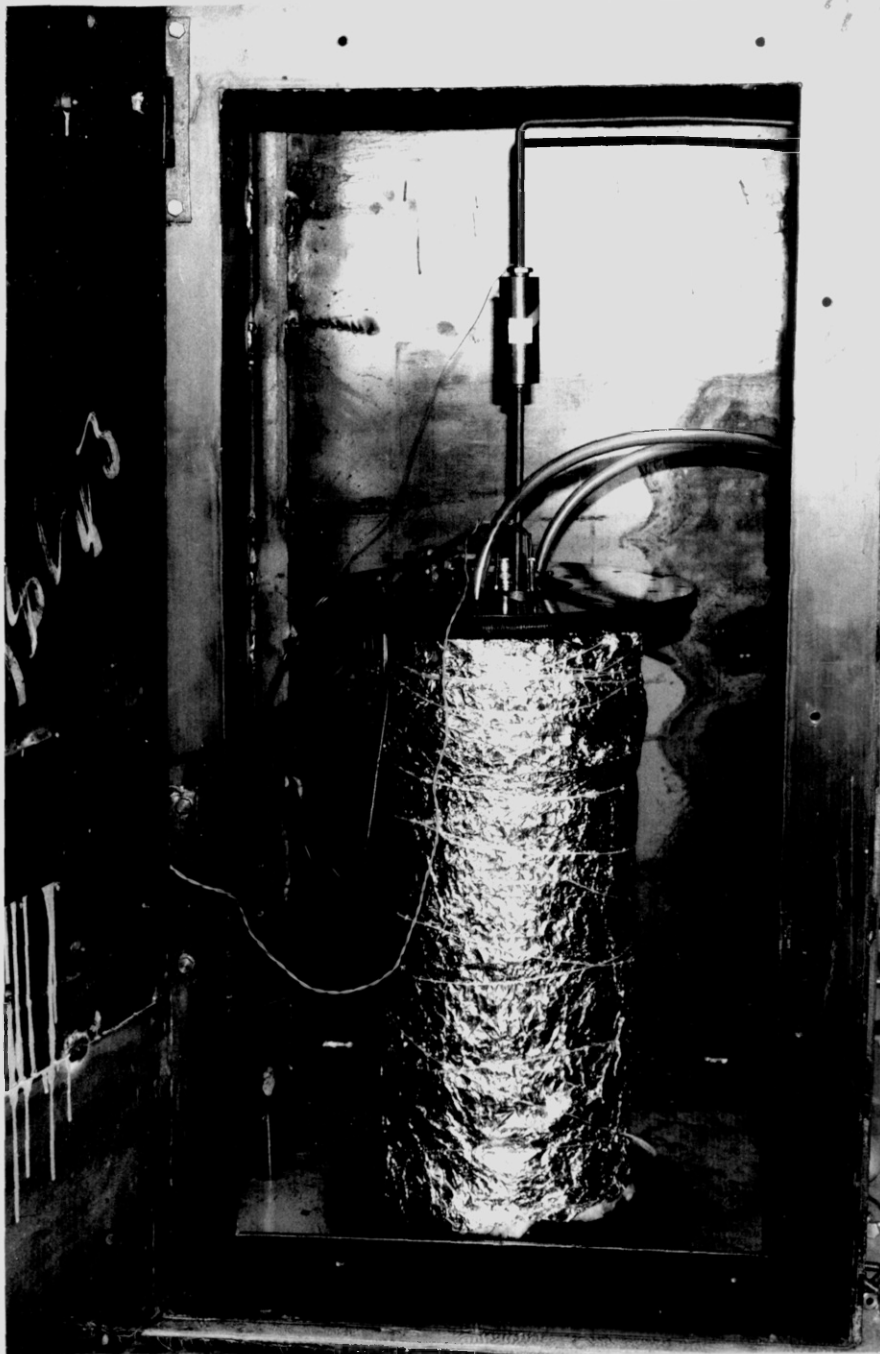
Plate 6.3. A photograph of the insulated heat exchanger
enveloping the high pressure chamber. The whole assembly
is contained in a mild steel blast cabinet.

CHAPTER 7

GENERAL PROPERTIES OF THE POLYMERS UNDER STUDY

7.1 Introduction

Most of this thesis is concerned with a study of poly(tetrafluoro-ethylene), PTFE. A few other commercially important polymers have been studied, namely:

High Density Poly(ethylene), PE

Poly(propylene), PP and

Poly(methyl methacrylate), PMMA

This section reviews briefly the preparation, properties and morphologies of the above polymers with particular emphasis on PTFE.

7.2 Poly(tetrafluoroethylene), PTFE

Poly(tetrafluoroethylene)s, PTFEs, are a generic class of perfluo-rinated ethylenes with the basic chemical formula $(CF_2-CF_2)_n$. The polymer contains 76% by weight fluorine. The most popular means of production (Plunkett, 1941) is from the monomer tetrafluoroethylene (TFE) gas which is polymerised in the presence of a free radical initiator and at moderate temperatures and pressures ($60^{\circ}C$ and 500-2500 KPa) to produce a fine white powder of an average particle size distribution varying from $0.2\mu m$ to a few hundreds of μm depending on the mode of poly-merisation (Speerschneider and Li, 1963). The powder is very highly crystalline (ca. 95% crystallinity) and has a crystalline melting point of $332^{\circ}C$ to $346^{\circ}C$ (Refer and Lewis, 1946). This is an unusually high value compared to other organic polymers of similar structure (Kantor, 1953). The practically useful polymer has a high weight average mole-cular weight (1-5 x 10^6: Doban, 1956) and the material will not readily

flow even above its crystalline melting point. Consequently conventional techniques of plastics fabrication such as injection moulding are not applicable and the fabrication process is limited to preforming followed by sintering (see Fluon Technical Service Note, F3). The finished product possesses an interesting combination of chemical and physical properties. It has an excellent chemical resistance and there are no known chemical plasticizers for PTFE (Rossa, 1964). In addition, it has a high temperature stability (Cox et al, 1964). The polymer also has excellent dielectric properties and possesses a dielectric factor of ca. 0.0002 which is virtually the lowest known amongst solid materials (Ehrlich, 1953). The low frictional properties are well known (a coefficient of friction of 0.04 at room temperature was reported by Shooter and Thomas, 1949) as is its poor affinity to adhere to solids (Schonhorn and Ryan, 1969) and liquids (Bernett and Zisman, 1959).

The study of the molecular structure of PTFE has received considerable attention. These studies have revealed that PTFE is a highly crystalline linear polymer. Evidence for its crystalline character was first provided from X-ray diffraction patterns reported by Hanford and Joyce, 1946. The linearity is revealed by analysis of the infra-red spectrum (Moyniham, 1958) or the fact that the polymer undergoes a sharp reversible transition at $327^{\circ}C$ changing from a stiff translucent substance to a transparent rubbery material, a behaviour which is a recognized characteristic of crystalline linear polymers (Meyer, 1942). Energetic considerations also suggest that branching by chain transfer is unlikely (Bryant, 1962).

The degree of crystallinity and hence the polymer density largely depends on the rate of cooling of the polymer from the sinter temperature (Thomas, 1956) and possibly its molecular weight. Estimations of

the degree of crystallinity have been made by X-ray (Howells, 1973),infra-

red (Miller and Willis, 1956) and density methods. Relative densities

of $2.30\,g\,cm^{-3}$ and $2.00\ g\ cm^{-3}$ have been reported for 100% crystalline

(Toshihiko and Sakami, 1958) and 100% amorphous PTFE (Sperati, 1961)

respectively at $25^{o}C$. The density of amorphous PTFE was estimated by

extrapolating to zero crystallinity.

The crystal structure and chain conformation have been discussed

by Bunn et al (1954-1958) and later by others (Pierce,et al, 1956 and

Clark et al, 1957). Bunn et al (1958), using electron microscopy,pro-

duced evidence for the formation of some very highly ordered spherelitic

fiberal structures of PTFE produced during slow crystallisation from

the melt of the granule material. These structures appeared as long

bands (see Figure 7.1), the width of which varied between $0.01-0.02\mu m$

with striations $300\overset{o}{A}$ apart and perpendicular to the length of the band.

The single crystals were hexagonal in form with step heights of $150\overset{o}{A}$

with the PTFE molecules folding back on themselves at regular intervals,

like firecrackers.

The crystalline melting point of sintered PTFE - a first order

transition from a partly crystalline to a completely amorphous polymer

is about $330^{o}C$. There are also two reversible first order transitions

at lower temperatures, $19^{o}C$ and $30^{o}C$ (Quinn et al, 1951) which together

involve a 1% change in density (Rigby and Bunn, 1949). The $19^{o}C$

transition accounts for 80% of this change. These transitions correspond

to three crystalline phases at atmospheric pressure: phase I ($<19^{o}C$),

phase II ($19^{o}C-30^{o}C$) and phase III ($>30^{o}C$). Below the $19^{o}C$ transition

(phase I), the chain repeat distance is $16.8\overset{o}{A}$ and the CF_2 groups are

equally spaced along the chain which is twisted to form a helix on

which successive carbon atoms lie, thirteen carbon atoms being involved

in a twist of 180° (Figure 7.2). A schematic representation of the
packing of a PTFE molecule in this phase is illustrated in a paper
by Klug and Franklin (1958). The diagram is reproduced in Figure 7.3.
Also drawn in the Figure are the sections of van der Waals spheres of
fluorine atoms (ca. 1.3Å in diameter) so that the diagram represents a
fairly realistic representation of intermolecular (ca. 1.5Å between
adjacent fluorine atoms) and intramolecular (ca. 3.2Å between adjacent
PTFE molecules) distances. Between 19°C and 30°C (phase II), the chain
repeat distance increases to 19.5Å (Pierce et al, 1956) corresponding
to a twist of 15 carbon atoms in 180°C. Above 30°C (phase III), further
disorder sets in and although the molecular conformation prevailing
at lower temperatures is maintained,the chains are displaced or rotated
along their long axes by variable amounts which increase as the tempera-
ture is raised further. The reason for the observed helical structure
of PTFE is the necessity to accommodate the bulky fluorine atoms (van
der Waals radius; 1.35Å) along the carbon chain. The rotation at each
chain bond, with the slight opening up of the bond angles to 116°C,
relieves the overcrowding and permits the shortest F-F distance to be
2.7Å (Bunn and Holmes, 1958).

The molecular motions at these transitions have also been studied
using internal friction: torsion pendulum (Smith, 1955 and Schultz,
1956), and nuclear magnetic resonance (Wilson, 1957). McCrum (1959)
was the first who investigated the effect of varying PTFE crystallinity
on the molecular motion. From the study, he was able to attribute these
relaxations to either the amorphous or the crystalline domains. Typi-
cal data are represented in Figure 7.4. In this, the relaxations are
denoted as α, β and γ in the order of decreasing temperature. Also
included is a relaxation at -113°C (160°K) which decreases in magnitude

with increasing crystallinity in a very clear manner and is therefore

identified with a transition in the amorphous region of the polymer.

The β relaxation (a composite of the $19^{\circ}C$ and $30^{\circ}C$ transitions) on the

other hand, increases in magnitude with increasing crystallinity and

is therefore associated with the crystalline region. There is no obvious

trend for the α transition. Kuroda and Sakami (1958) reported a con-

stant amorphous density of 2.00 g cm^{-3} around the $19^{\circ}C$ transition, thus

lending support to the above view that the room temperature relaxation

is associated with the crystalline domain.

7.3 High Density Poly(ethylene), HDPE

High density poly(ethylene), HDPE, is manufactured using a low

pressure (1 to 20 MPa) polymerisation of ethylene (Albright, 1974).

Its density varies between 0.955-0.970 g cm^{-3} (Doak and Schrage, 1965)

corresponding to a crystallinity often in excess of 75% (Wunderlich and

Dole, 1957). The polymer is highly linear: the number of branches is

often less than 5 per 1000 carbon atoms (Sella, 1959). It has a crystal-

line melting point of $137.5^{\circ}C$ (McCane, 1970) and possesses three relaxa-

tion temperatures of $\alpha(60^{\circ}C$-$80^{\circ}C)$, $\beta(-20^{\circ}C$ - $-30^{\circ}C)$ and $\gamma(-80^{\circ}C$ - $-90^{\circ}C)$,

all of which are associated with the amorphous regions of the polymer

(Boyer, 1966). In many ways HDPE resembles PTFE in its morphology.

7.4 Poly(propylene), PP

Poly(propylene), PP, possesses three distinct molecular configura-

tions described in the order of their packing ability as isotactic,

syndiotactic and atactic (Albright, 1974). Isotactic polypropylenes)

are those in which methyl groups are all arranged on the same side of

the principle chain of carbon atoms. For syndiotactic poly(ethylenes),

the methyl groups are arranged on either side of the principal chain

of carbon atoms. For atactic poly(propylenes), the methyl groups are

arranged randomly. Commercial polymers usually contain 75 to 98% (Jezl,

1969) isotactic sterio isomers corresponding to a crystallinity of 50 to 60% (Chen et al, 1960), they are spherulitic in morphology and have a melting point of ca. $167^\circ C$ (Fortune and Malcom, 1960). Poly(propylene) is slightly less dense than poly(ethylene). Its relaxation temperatures are (Groenewege et al, 1965): α, 30°-$80^\circ C$ (ambiguous in origin); β, $0^\circ C$ (amorphous dominated) and γ, $-80^\circ C$ (hindered movement of C-CH_3 units).

Gas phase polymerisation of poly(propylene) involves considerations similar to those for the production of poly(ethylene). In this case, the polymerisation of the liquid propylene monomer takes place in the presence of a Ziegler-Natta catalyst (Albright, 1974).

7.5 Poly(methyl methacrylate), PMMA

Poly(methyl methacrylate), PMMA, is manufactured using a low pressure polymerisation (ca. 300 KPa) of the monomer, methyl methacrylate in a stirred tank reactor at $95^\circ C$ to $110^\circ C$ in the presence of a suspending agent and buffers (Rodrigues, 1982). The polymer is transparent, amorphous in morphology, undergoes a glass transition temperature between 90-$100^\circ C$, and is more dense (ca. 1.19 g cm^{-3}: Wittmannand Kovac, 1969) than either poly(ethylene) or poly(propylene).

Crystal length
approx 40 μ

Amorphous layers
(folds, ends, etc.)

Dimension
not
known

Striation
length
approx 1 μ

Striations

0.0005 μ
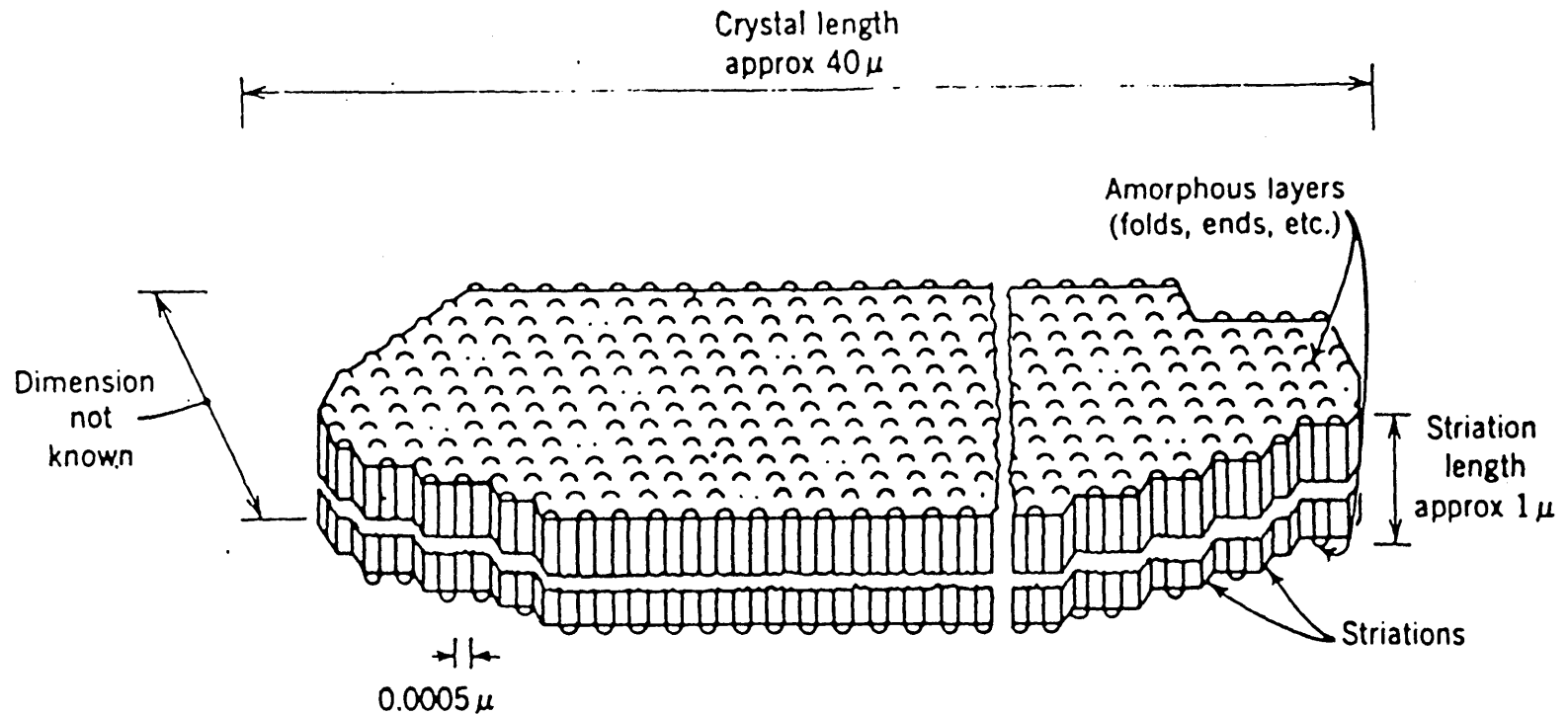
Figure 7.1. Schematic diagram, not to scale, showing a crystalline sheet in a sintered PTFE molding. A method is indicated for the formation of striations by zig-zag fracture. On the top face, molecular folds are drawn; the folds are probably not as regular in shape as shown and together with chain ends, and perhaps some chains which link crystals, could provide the basis for the formation of amorphous material on the hexagonal faces. The length of the striation would therefore include the thickness of the amorphous layers (Bunn et al 1958).
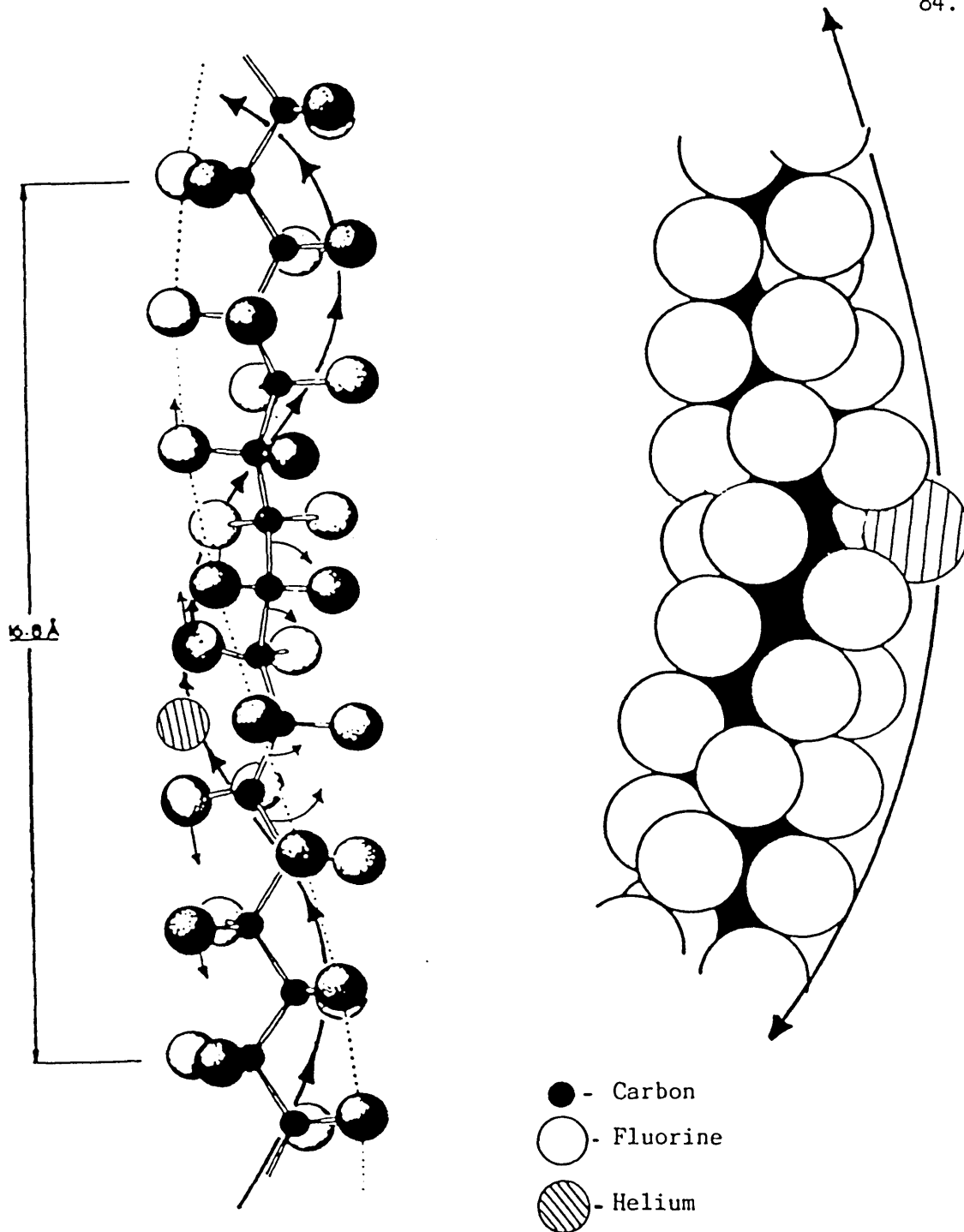
Figure 7.2. Schematic representation of the molecular conformation of
PTFE. The diagram also shows the supposed locality of a He atom
(2.7 Å) with respect to a PTFE chain. Preliminary calculations indicate
that on the basis of a 3-D model, every 8 $\{C_2F_4\}$ units are associated
with one He atom at a maximum pressure of 51 MPa and 17°C. These atoms
are assumed to move along the chains in a fashion not dissimilar to
to the movement of a dislocation or a point defect in the polymer matrix
(see conclusions).
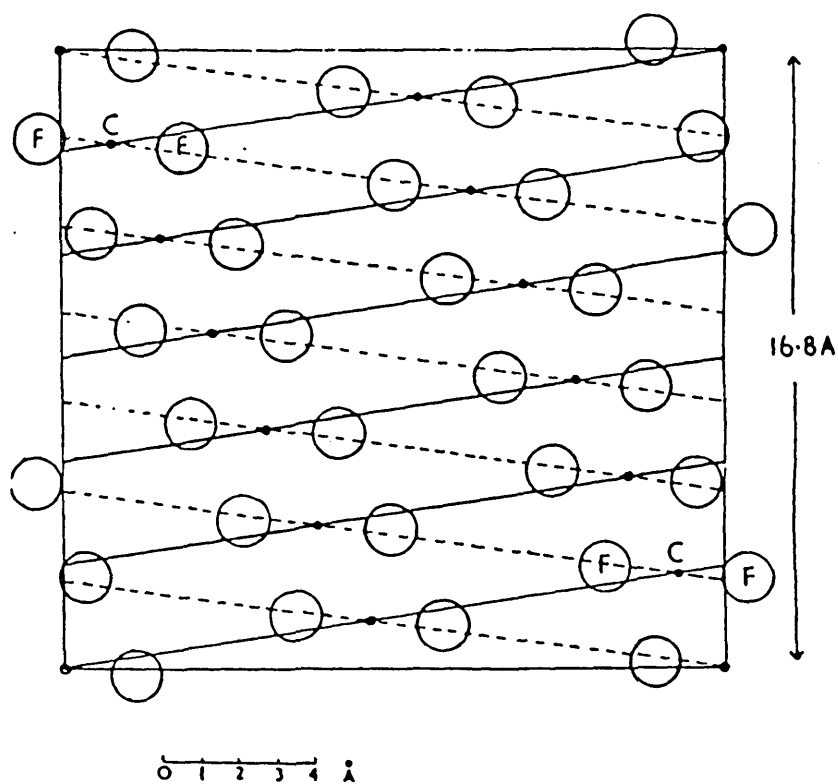
Figure 7.3. The radial projection (see text) of one axial repeat period of a molecule of polytetrafluoroethylene, drawn on a cylindrical surface of diameter equal to the inter-molecular distance. The sections of the van der Waals spheres of the fluorine atoms are shown as large circles. The full and dotted lines represent the helices (1,6) and (— 1,7) respectively (Klug & Franklin 1958).
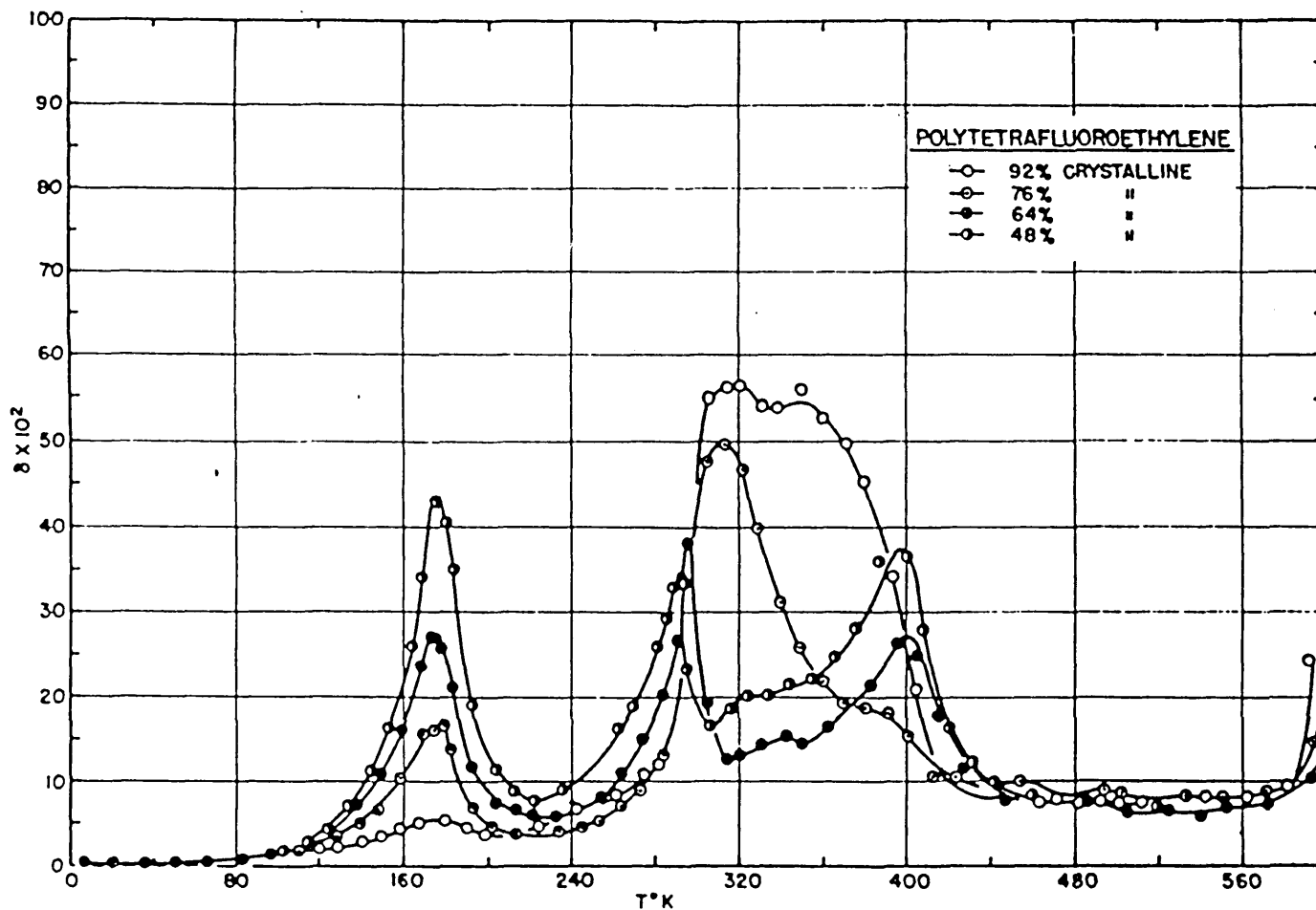
Figure 7.4. The internal friction of four samples of polytetrafluoroethylene of various crystallinities from 4.2 to 600°K (Mc Crum 1959).

C H A P T E R 8

THE APPARENT PLASTICISATION OF PTFE UNDER HIGH

PRESSURE NITROGEN ENVIRONMENT

8.1 Introduction

In Chapter 4 the previously reported phenomenon of apparent

plasticisation of PTFE (Billinghurst and Tabor, 1971) in a nitrogen pres-

sure environment was described. It was these unusual results which in part

stimulated the present study. This effect was manifested as an initial

small increase in shear modulus of short duration followed by a com-

paratively large decrease in modulus. The magnitude of this decrease

increased with time and was more pronounced at higher initial tempera-

tures and was found to decrease with increasing crystallinity (see

Figure 4.3). Changing the pressure medium to He or to an hydraulic

oil resulted in a linear increase in the shear modulus; no decrease

was observed. The initial conclusion was that N_2 plasticised PTFE.

In this Chapter a series of Differential Thermal Analysis (DTA) experi-

ments are used to show that the plasticisation process is a consequence

of the changes in the heat transfer properties of the polymer and the

surrounding environment following a rapid increase in pressure. The

plasticisation process is merely an artifact associated with adiabatic

effects. The experiments adopted to elucidate this process consist

of monitoring the temperature rise in the polymer matrix and that of

the surrounding environment following a rapid pressure increase (typi-

cally from 0.101 MPa and room temperature to 34.5 MPa in 15 seconds).

The results of similar dynamic experiments in which the polymer speci-

men is in thermal equilibrium with different pressure media and then

is externally and isobarically heated at a controlled rate are also

described.

The pressure ramp experiments are used to estimate the average equilibrium times required for the diffusion or sorption of nitrogen or helium gases in the polymer studied.

8.2 Experimental Method

The basic arrangement of the DTA experiment is schematically represented in Figure 8.1. The temperatures of the polymer and the pressure media are measured by monitoring the changes in the resistance of platinum resistance film thermometers (type 158-328; Radio Spares, $\pm 0.1^{\circ}C$ accuracy) placed inside and on the surface of the PTFE specimen. In the former case, the platinum film (ca. 30 x 4 x 0.5mm) is encapsulated by a cylindrical (ca. 42 x 17mm) block of PTFE specimen. This is achieved by firmly inserting the platinum film into a notch machined inside the smaller cylindrical block (ca. 3 0 x 8mm) which is drilled out of the original polymer. Finally, the unit is assembled by inserting the notched block containing the platinum film thermometer inside the original polymer and firmly sealing the top end using another suitably machined PTFE block. The various PTFE components are shown in Figure 8.2 before assembly. The temperature of the pressure medium is measured by simply fastening a platinum film onto the surface of the PTFE specimen using PTFE tape. Various attempts to mould the platinum film thermometer inside the PTFE specimen failed due to the breakage of the film during the polymer preforming process. The use of thermocouples as temperature probes was also unsuccessful due to the complications associated with the creation of spurious potentials at the additional junctions formed between the thermocouple wire (copper) and the electrical connections (invar) in the pressure vessel cap. The variation of temperature of the two probes with time was recorded using a double pen

chart recorded.

8.3 Results and Discussion

Figure 8.3 shows the results of the kinetic heat transfer experiments carried out on a medium crystallinity PTFE specimen (2.157 g cm^{-3}; 70% crystallinity) following its exposure to a pressure ramp in various pressure transfer media. Curves A, B and C are respectively the temperature versus time in the pressure medium for He, N_2 and hydraulic oil following the adiabatic compression initially at 17°C and 0.101 MPa to a final pressure of 34.5 MPa in 15 seconds. Curves a, b and c represent the corresponding temperature change in the PTFE specimen. These conditions simulate those employed by Billinghurst and Tabor (1971) when studying the apparent N_2 plasticisation of PTFE. The important features of the above results may be summarised as follows:

(a) The temperature of the pressure media can be attributed to the thermal energy released following the adiabatic compression process. The gases being more compressible than liquids evolve a larger amount of heat (Bett et al, 1975). The expected temperature rise associated with an adiabatic compression of a fixed number of moles of N_2 exposed to the above conditions is ca. 1200°C (see later).

(b) The detected rate of rise in the temperature of the pressure media is limited by the rate of change in the resistance of the platinum probe in response to a rapid change in temperature. The faster response in He (curve A) compared to N_2 (curve B) is partly due to the larger thermal conductivity of helium (ca. 5 folds greater than N_2 at 40°C and 34.5 MPa; Assael, 1980) together with a more efficient heat transfer by forced convection (Kreith, 1973) as a consequence of the larger atomic velocity and hence the smaller

viscosity of He atoms (Angus et al, 1975).

(c) The corresponding rise in the temperature of the polymer may be
due to tri-axial compression of the polymer (Findley et al, 1968
and Duckett and Joseph, 1975) as well as to the increase in ambient
temperature following compression. The latter process is complex.

The inevitable increase in the thermal conductivity of the polymer
as a result of a reduction in its free volume following the application
of pressure (Andersson and Backstrom, 1972 and Dzhavadov, 1975) especially
around room temperature (Andersson and Backstrom, 1976 and Kieffer, 1976)
may be important. Figure 8.4 is the response of a PTFE specimen heated
at atmospheric pressure in air or isobarically heated in a high pressure
(34.5 MPa) N_2 pressure medium. The faster rate of heat transfer in the
high pressure N_2 environment is evident. However, in the plasticisation
process, the time dependent absorption of a hot flux of high pressure
gas inside the polymer matrix (Lundberg et al, 1962 and 1969) is probably
more critical. It may be useful to bear in mind that the smaller He
atoms diffuse faster than the larger N_2 molecules. This is consistent
with the observed smaller rate of increase in temperature of the poly-
mer in the N_2 pressure medium (curve B). From curves a and b, the esti-
mated saturation time for N_2 and He diffusion are ca. 5 and 3 minutes
respectively.

The transfer of heat energy from the pressure media to the polymer
matrix via simple interface thermal conduction is also important.
The final temperature is limited by the total work, the heat capacity
and the rate of heat loss during the thermal equilibriation of the
polymer and the pressure media to the pressure chamber (at $17^{o}C$) at
the end of the compression cycle. This is proportional to the thermal
conductivity, K of each medium. The values of K for He, N_2 and an

hydraulic oil at 34.5 MPa and $40^{\circ}C$ are 0.172, 0.043 (Assael, 1980) and 0.09 $W/m^{\circ}C$ (Manashe, 1980) respectively (the variation of K with temperature is assumed to be small). The above is reflected in the rapid thermal equilibriation of the polymer in He pressure medium (curve a).

At this stage the data of Billinghurst and Tabor can be explained in simple terms. It is evident from Figure 8.3 that the polymer specimen in N_2 pressure medium reaches a temperature of $26^{\circ}C$ ($9^{\circ}C$ higher than the starting temperature) some 18 minutes after the completion of the almost adiabatic compression cycle. Billinghurst himself (1969) established a large temperature dependence for the shear modulus of PTFE at atmospheric pressure around the room temperature transition (Weir, 1953). These data are reproduced in Figure 8.5. It is evident that in the production of a $10^{\circ}C$ rise in temperature of PTFE from $17^{\circ}C$ to $27^{\circ}C$ (a condition similar to that produced by Billinghurst) will produce a 40% drop in shear modulus. Also the larger temperature dependence of the shear modulus for the more crystalline polymer is consistent with the reported larger effective plasticisation of the polymer with increasing crystallinity (see Figure 4.3).

The increase in the effective plasticisation with the initial temperature may be rationalised as follows. Considering an adiabatic compression of a fixed number of moles of N_2 from a temperature T_1 and pressure P_1 to a final pressure P_2, the rise in temperature, ΔT, assuming ideal gas is given by (Bett et al, 1975):

$$\Delta T = T_1 \ |(\frac{P_2}{P_1})^{0.286} - 1|$$

(8.1)

For an initial temperature $T_1 = 17^{\circ}C$ (curves a, b and c; Figure 4.3) and a pressure ratio, $P_2/P_1 = 340$, the rise in temperature,

$\Delta T = 1260^{\circ}C$. Alternatively, for the same conditions but with $T_1 = 80^{\circ}C$ (curves d, e and f; Figure 4.3), $\Delta T = 1500^{\circ}C$. The above argument indicates that the rise in the temperature of gaseous media and hence the temperature rise in the polymer directly increases with the initial temperature of the pressure medium before the compression cycle. This is consistent with the observed increase in the effective plasticisation of PTFE with the initial ambient temperature. The detected rise in the temperature of the pressure medium is, however, very much lower than the predicted values. This may be attributed to the loss of a significant proportion of the heat generated through the pressure vessel walls, the finite heat capacity of the temperature probe and an increase in the number of moles of gas at the end of the compression process (in this case pressurisation is achieved by increasing the number of moles of gas in a fixed volume). Calculation of the temperature rise, ΔT, for the above system proved to be extremely complicated. However, similar trends may be expected.

Finally, Billinghurst and Tabor were not able to detect these temperature rises, and hence incorrectly identify the origin of the PTFE plasticisation, due to the very slow response of the thermocouple temperature probes (2mm dia. copper wire) employed in their work. As an example, the equilibrium time for a 0.8mm dia. copper wire originally at $150^{\circ}C$ and then suddendly exposed to air at $40^{\circ}C$ is more than 30 minutes (Kreith, 1973). The corresponding equilibrium time for a 2mm dia. wire is considerably longer.

8.4 Summary

In this Chapter, the origin of a previously reported high pressure N_2 plasticisation of PTFE was investigated in some detail. The experimental data are consistent with the view that the plasticisation pro-

cess is a consequence of the temperature rise associated with an almost adiabatic compression process of the N_2 pressure medium and that of the polymer matrix. The magnitude and the duration of the plasticisation was found to depend, to a first order, on the thermal energy released during the compression cycle and on the rate of heat loss from the polymer to the surrounding medium respectively. There are important secondary factors such as the degree of crystallinity of the polymer and the degree of diffusion of the gas pressure medium in the polymer matrix.

From a practical point of view, the above result has some important implications. The conveying of many hydrocarbon gases in the process industry for example, involves high pressure reciprocating pumps incorporating self lubricating PTFE seals. The accumulative heat generated during the pulsating action of these pumps will expose the PTFE to a similar environment to the plasticisation process described above. It is known that the performance of these seals is often very sensitive to the environment, particularly the gas. Many systems fail unexpectedly and the failure seems to be thermally induced. Clearly the gas medium can influence the surface temperature in a subtle way and it is interesting to speculate that the sorption/desorption process described above is an influencial factor.

On a different topic, the final step in the manufacture of PTFE involves the sintering followed by cooling (Fluon Technical Note No. F3) of the compacted powder at a controlled rate. Rapid cooling or heating results in a non-homogeneous end product. The advantages in using a superimposed high pressure He environment during the finishing process are clear and potentially attractive.

Temperature
probes

Digital thermometers

Double pen chart recorder
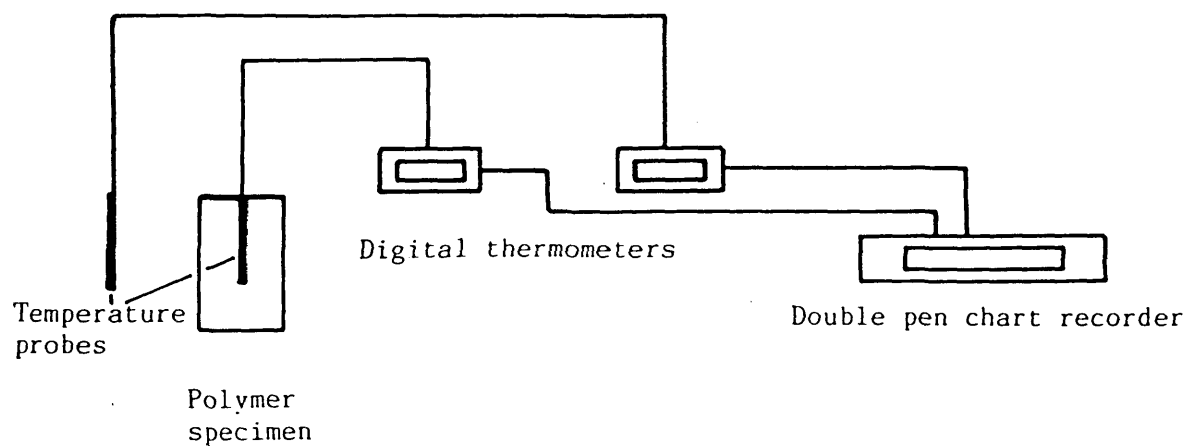
Polymer
specimen

Figure. 8.1. Schematic arrangement of the differential thermal analysis equipment used to monitor the temperature change in the polymer and the surrounding pressure medium.

Sealing polymer block

Platinum film

Notched specimen

Incapsulating polymer
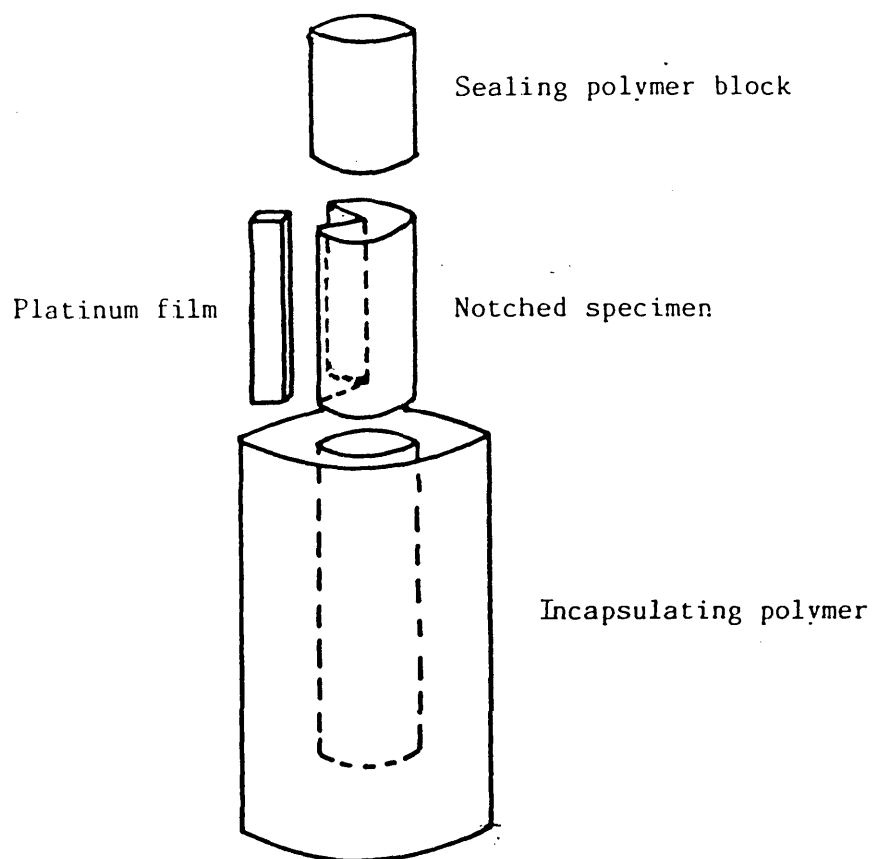
Figure 8.2. Schematic layout of the various componenets of a PTFE block used for the DTA experiments.
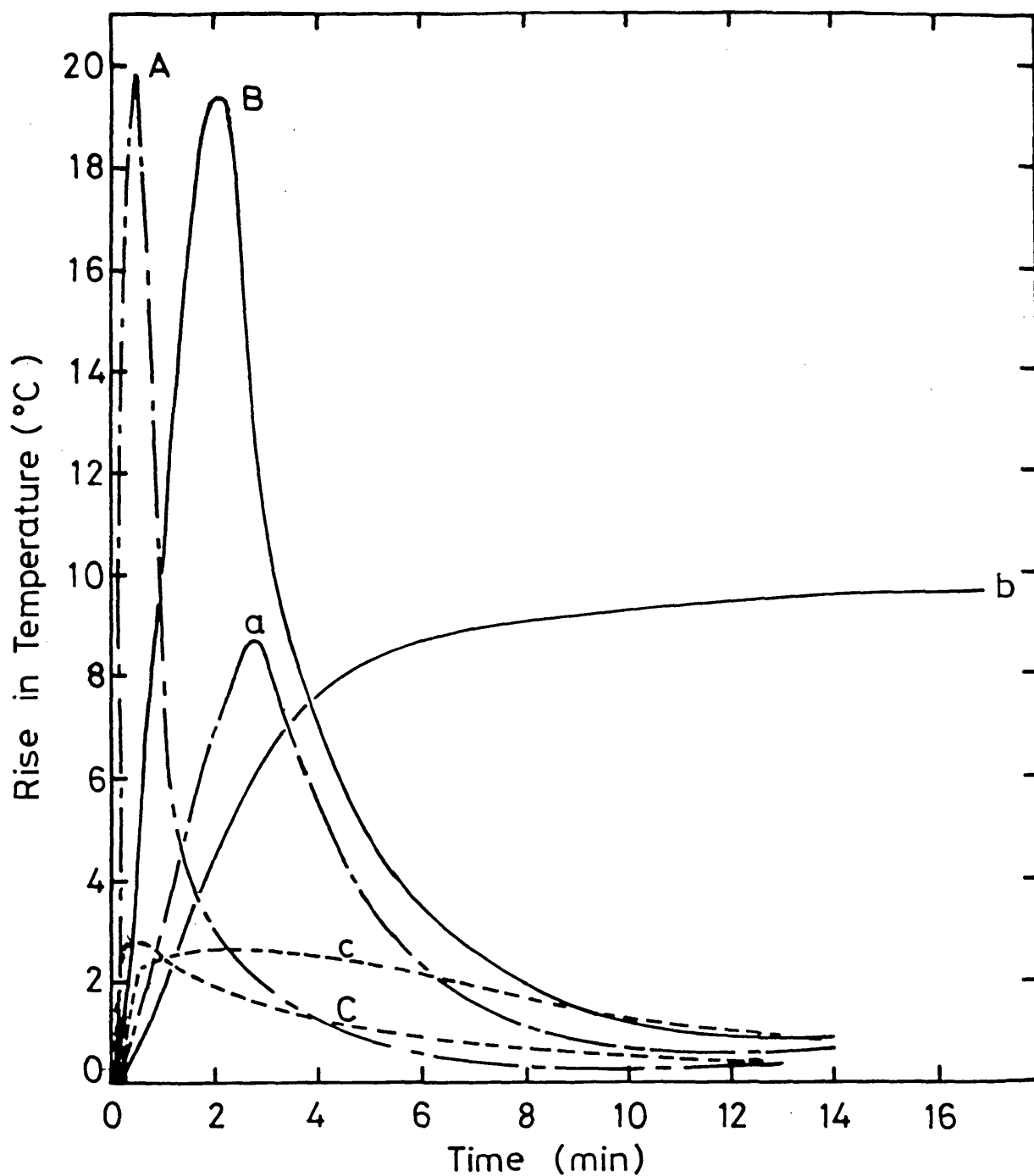
Figure 8.3. The rise in temperature of PTFE and various pressure
environments against time following a rapid pressurisation from 0.1 MPa
to 34.5 MPa in 15 seconds. Curves A,B and C are the response of He,
N_2 and hydraulic oil pressure media respectively. Curves a,b and c
respectively represent the corresponding PTFE response in the above
pressure environments.
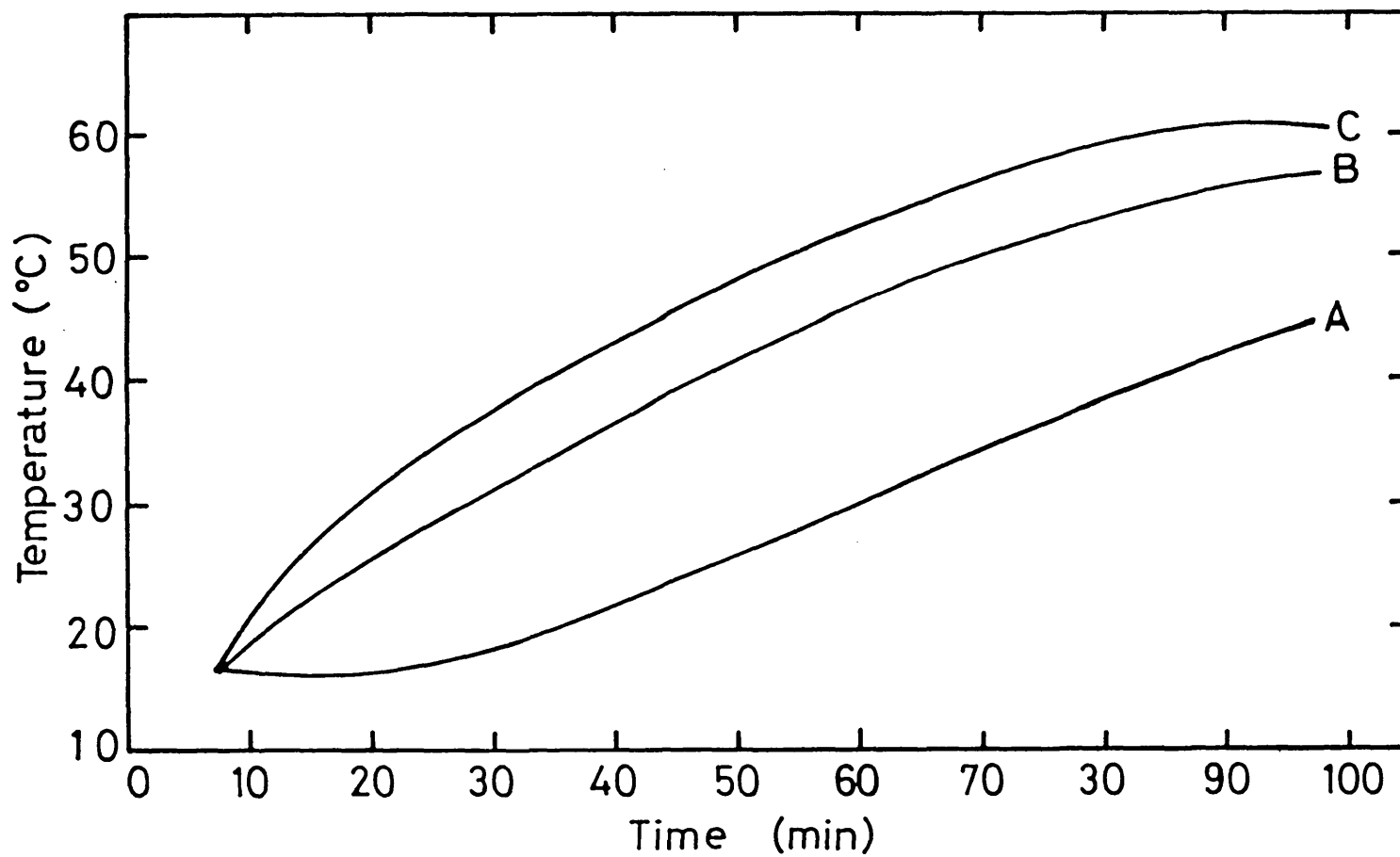
Figure 8.4. The rise in temperature of PTFE against time in air at atmospheric pressure (curve A) and in N_2 at 34.5 MPa (curve B) when heated at a controlled ambient heating rate represented by curve C.
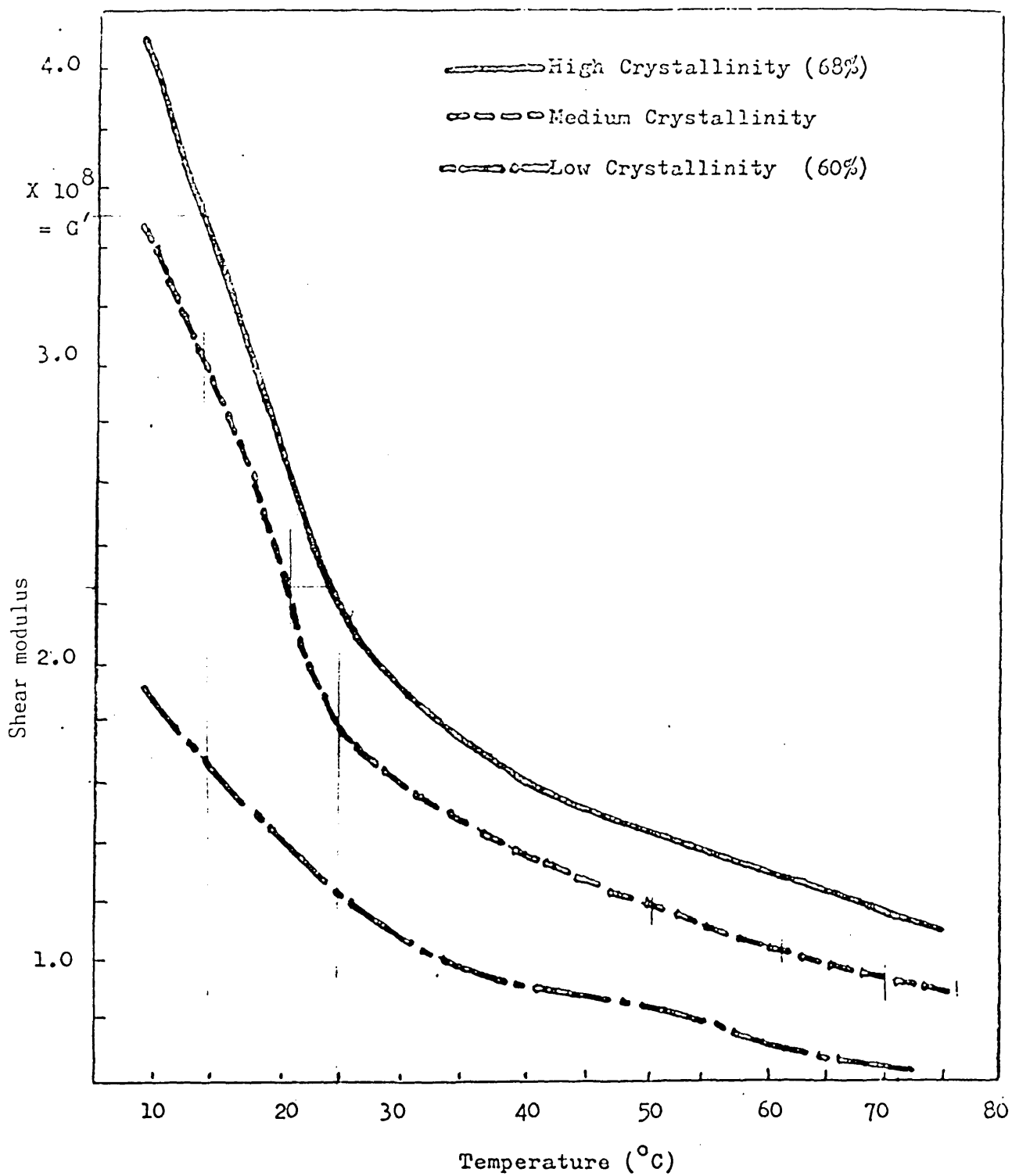
Figure 8.5. The variation of the shear modulus of PTFE with temperature at atmospheric pressure (Billinghurst 1969).

C H A P T E R 9

GASEOUS SORPTION IN ORGANIC POLYMERS UNDER

HIGH PNEUMATIC PRESSURES

9.1 Introduction

In Chapter 2 the various experimental techniques employed in the

past two decades for the measurement of solubility of gases in organic

polymers were reviewed. There are serious limitations in the value of

all of these techniques. The method adopted by Lundberg et al (1962)

and later by Durill et al (1966) for example, does not include a compen-

sation for the thermal effect produced during the almost adiabatic

compression process used in their studies. The resonance technique deve-

loped by Bonner and Cheng (1975) on the other hand, although more

sophisticated, is limited to thin polymeric films which must be carefully

deposited, usually from solvents on to a piezoelectric crystal; this

technique was also only evaluated to a pressure of 13.8 MPa. Thermal

fluctuations are also a problem in this approach. In addition, the

rather special morphologies generated during film preparation are not

characteristic of isotropic bulk polymers. The shortcomings associated

with the method employed by Atkinson (1977) which involved solubility

measurements by directly weighing the polymer specimen immediately

after depressurisation are all too apparent. This method probably

underestimates the sorption by ca. 50%.

The present work has devised a new technique to determine gas

solubility in polymers at high temperatures and gas pressures which

overcomes most of the limitations described above. The method is based

upon the measurement of the first harmonic resonance frequency of a

rigidly clamped vibrating steel spring on whose free end is attached

a rectangular block of the absorbing polymer. The technique relates the change in this resonance frequency to the effective mass change induced in the polymer specimen. This resonance frequency is found to be not only sensitive to the increase in mass within the polymer specimen but also to an increase in an entrained or displaced mass of gas which is also displaced by the vibrating assembly. The precise nature of the latter processes which produce this additional mass is uncertain. Three candidates may be identified; simple interface entrainment, remote circulation (Van Dyke, 1982) and inertia transfer. In this study the origin of these effects is not of importance and they will be described as entrained mass. It is necessary, however, to calculate an accurate quantitative effective entrained mass correction in order to deduce the mass sorption. The experimental data are consistent, to a good approximation, with an entrained mass which is provided by a fixed volume of gaseous mass which surrounds the vibrating assembly. This mass increases accurately, in a linear fashion, with the gaseous density. This volume is also found to be directly proportional to the surface area of the specimen normal to the plane of motion. It is this result that allows the precise but relative determination of the gas density. This is a necessary precursor for the determination of the absorbed mass and warrants a separate experimental section as it is the only technique available for the determination of gaseous density in a continuous manner at pressures above 20 MPa (see section 9.4).

The differences between absorbed mass and entrained mass are resolved by using inert aluminium specimens of similar geometry to that of the polymer. A simple relationship is given to assess the absorbed mass which is also found to be proportional to the gaseous density.

9.2   The Apparatus - the Vibrating Reed

The vibrating reed assembly which is housed inside the pressure vessel is depicted in Figure 9.1. Figure 9.2 shows a more detailed dimensional drawing of a typical spring steel beam with the polymer specimen attached to its free end. High-carbon magnetic steels of ca. 1mm thickness are suitable for this purpose. The reed is held in a hardened steel clamp whose jaws are highly polished on two faces of each pair. The jaw assembly is attached to a massive base which is in turn fastened to the upper cap of the pressure vessel. This cap contains the six electrical connections: two for the platinum resistance thermometer, two for a capacitance probe, and two for a magnetic drive. The free end of the reed has two holes to facilitate the attachment of the specimens to its surface by means of small (12 BA) screws. The specimens are suitably drilled and tapped to receive these screws. The basic electronic circuit   of the system is given in Figure 9.3. The reed is mechanically excited by a magnetic flux generated by a solenoid which is constructed from a rectangular (ca. 3 x 4 x 4mm) soft iron core wound with approximately 1500 turns of copper wire (ca. 0.1mm dia- meter). This is driven by a variable power amplifier (30W maximum). The frequencies of induced oscillations are measured with a capacitive plate transducer. The probe plate (ca. 3 x 9mm) is positioned near (ca. 0.5mm) the vibrating arm to obtain a high sensitivity. The capa- citive signal is amplified using a preamplifier with a gain of 30 and monitored with a frequency meter (see later) and an oscilloscope. This signal may also be fed back in a positive sense to the power amplifier thus forming a closed loop. A low pass filter at the input of the power amplifier reduces the loop gain at frequencies above 1kHz to prevent spurious oscillations due to stray electrical coupling. The system is

then automatically self-tuned to identify the primary resonance frequency of the vibrating assembly. Oscillations take place by regenerative feedback (Seely, 1958) at a frequency determined primarily by the resonance of the reed itself. This self-tuning feature is particularly useful for the detection of transient responses. The test period ca. 5 s, corresponds to 10^3 oscillations and is monitored using a digital frequency meter (Universal Timer Counter, Model 9903) having a 100 ns resolution. Prior to using the self-tuning arrangement described, a series of manual tuning experiments were carried out to locate the region where the resonance frequency was independent of the amplitude of the excited mechanical vibrations. This was made possible by the use of a wide-range R/C Marconi frequency oscillator (type TF1370) as a signal generator, having a 0.1 Hz resolution. A result is shown in Figure 9.4. In the current arrangement the amplitude range (capacitive transducer output) was limited to between 200 and 400 mV. This corresponded to a maximum displacement of ca. 0.1mm measured at the end of the vibrating beam. Significantly greater displacements produced a relatively small but unacceptable decrease in resonance frequency. This criterion is well known for vibrating beams and is termed as a softening spring behaviour (Timoshenko, 1937). In practice it is often necessary to progressively increase the driving power as the pressure is increased to compensate for the effect of viscous losses in the gaseous media. The viscosity of N_2 increases by ca. 20% in this range. Once the driving power range for an amplitude-insensitive resonance frequency had been identified the self-tuning mode was fixed at these displacement (power amplifier) levels. An oscilloscope was used for this purpose. It should however be pointed out that the voltage signal from the capacitive transducer output is not only a function of the amplitude of vibrations but it is also a function of the dielectric constant of the

gaseous media. Typically, a 20% increase in the dielectric constant of N_2 over a pressure range of 0.101 to 51 MPa may be expected (see Figure 10.4). This may give rise to a 20% over-estimate in the observed value of the amplitude of vibration. The corresponding value for He is smaller. However, the above effect is considered to be small and can be ignored provided one operates within the resonance frequency/amplitude insensitive region (see Figure 9.4). Figure 9.5 shows the effect of frequency on the amplitude of vibration in the vicinity of resonance at 1 atm ($\sim$101 kPa) and room temperature. A 'quality factor' of ca. 280 is typical.

9.3 Experimental Results and Mathematical Analysis

Figure 9.6 shows the results of experiments carried out with PTFE (density 2.157 g cm^{-3}; 70% crystallinity) and a number of rectangular aluminium samples of various sizes and masses in nitrogen gas at room temperature. The frequency attenuation, i.e. the resonance frequency at atmospheric pressure divided by that at the working pressure, for a polymer specimen as a function of pressure is presented by curve B. The change in frequency is significant and also greater than that of an inert aluminium specimen with an identical geometry as described by curve C. Curve A is an experimental model of the polymer; it represents an aluminium sample of the same size and mass (random holes were drilled in the metal to produce the same mass) as the polymer. The metal model of the polymer suffers from the fact that most of the pores in the structure of the polymer are in the form of interconnecting channels and also the voidage in the aluminium specimen exceeds the free volume available for gas absorption in the polymer. Curves D and E belong to aluminium samples of equal compression but different shear areas (see 9.3.1). From the plots in Figure 9.6 it is evident that

the frequency attenuation, F_0/F is not only a function of pressure, but it is also a function of the geometry of the samples. It is also clear that the curve A provides data which give a relatively good experimental description of the polymer specimen characteristics.

The variation of F_0/F with normalised density, ρ/ρ_0 (the ratio of the densities at the working pressure and at atmospheric pressure) for PTFE and an aluminium sample of identical geometry are presented in Figure 9.7. The physical properties of the gases nitrogen and helium were obtained at room temperature (Din, 1961, Angus et al, 1975). From these data it is observed that for both gases, the dependence of F_0/F is given to a good approximation by the empirical relation

$$F_0/F = B[(\rho/\rho_0) - 1] + 1$$

and for $B \ll 1$,

$$F_0/F = 1 + B(\rho/\rho_0). \tag{9.1}$$

(Typically B is 2×10^{-4}).

Considering the above relation it is evident that the instrument can be calibrated to indicate a continuous measurement of gaseous density with a high degree of precision (see 9.4).

9.3.1 The choice of a reference specimen

Considering a rectangular sample during vibration (Figure 9.2), there are two distinct faces which govern the effect of the gaseous medium on the sample. These are the two 'compression' or 'normal' areas, A_c which are normal to the direction of motion and the remaining areas which are in constant oscillatory shear with the gas molecules.

These are termed the 'viscous drag' areas. Figure 9.8 shows the effect of doubling the compression areas, A_c, on F/F_o for the same aluminium specimen at different pressures. This was achieved by mounting a specimen with an aspect ratio of ca. 2.1:1 so that the compression area could be changed by altering the clamping position of the specimen to the beam. It is observed that in the case of the larger A_c (curve A), also corresponding to a small viscous drag area, a larger reduction in frequency is obtained. The gradient of the two linear plots is in the ratio of 2.24:1. This ratio is somewhat greater than the ratio of the compression areas; clearly the compression face area is not the only factor. This tentatively indicates that the reduction in frequency is largely due to an entrainment or the displacement of a layer of gas, the mass of which depends mainly on the compression areas of the sample and the density of the gas medium (see also curves D and E in Figure 9.6). The effect of viscous drag on the samples is second order and the mass of gas entrained remains the same for geometrically similar specimens. The success of the gas sorption experiments clearly depends upon the calibration with a non-absorbing specimen of compatible geometry to the polymer.

9.3.2 Mass uptake formulation

Assuming that the resonance frequency, F, is inversely proportional to mass, then at atmospheric pressure and constant temperature, for geometrically identical samples of polymer and aluminium:

$$F_{o_p}/F_{o_{Al}} = (M_{o_{Al}} + M_o)/(M_{o_p} + M_o) \qquad (9.2)$$

where M_o is the effective mass of the beam (the entrained mass of gas is assumed to be zero at 1 atmosphere). $M_{o_{Al}}$ and M_{o_p} are the masses

of the aluminium and PTFE specimens where the subscripts P and Al
refer to polymer and aluminium respectively. For the aluminium speci-
men (no absorbed mass) under pressure having a resonance frequency, F,
we have:

$$(F_o/F)_{Al} = (M_{o_{Al}} + \Delta m + M_o)/(M_{o_{Al}} + M_o) \qquad (9.3)$$

similarly for PTFE at the same pressure

$$(F_o/F)_P = (M_{o_P} + \Delta m + M_o + \Delta m')/(M_{o_P} + M_o) \qquad (9.4)$$

where Δm is the mass of entrained gas, and $\Delta m'$ is the gas absorbed.

From equation (9.3)

$$\Delta m_{Al} = M'_{o_{Al}} |(F_o/F)_{Al} - 1| \qquad (9.5)$$

where $M'_{o_{Al}} = M_{o_{Al}} + M_o$.

Substituting for Δm in equation (9.4) and rearranging, the mass uptake
is given by

$$\Delta m' = M'_{o_P} |(F_o/F)_P - 1| - M'_{o_{Al}} |(F_o/F)_{Al} - 1| \qquad (9.6)$$

where $M'_{o_P} = M_{o_P} + M_o$.

Equations (9.2), (9.5) and (9.6) permit the calculation of the
gaseous uptake, $\Delta m'$, from $(F_o/F)_P$ and $(F_o/F)_{Al}$ as a function of pressure.

Alternatively, from equation (9.1), the corresponding equations for
the aluminium and the polymer specimen are respectively given by:

$$(F_o/F)_{Al} = 1 + B_{Al}(\rho/\rho_o) \tag{9.7}$$

$$(F_o/F)_P = 1 + B_P(\rho/\rho_o) \tag{9.8}$$

Substituting for $(F_o/F)_{Al}$ and $(F_o/F)_P$ in equation (9.6) and rearranging, the gaseous uptake is given by:

$$\Delta m' = (\frac{\rho}{\rho_o} - 1)(M'_{o_P}B_P - M'_{o_{Al}}B_{Al}) \tag{9.9}$$

Equations (9.2), (9.5) and (9.9) permit the calculation of the gaseous uptake, $\Delta m'$, from the measured slopes of the best straight lines through F_o/F versus ρ/ρ_o data for both aluminium and the polymer specimens respectively.

9.3.3 Entrained mass thickness and its physical significance

From equation (9.3), the frequency attenuation at constant pressure and temperature for an aluminium specimen is

$$F_o/F = (M'_o + \Delta m)/M'_o \tag{9.3a}$$

Assuming that the effective thickness of the entrained gas at each of the compression areas is 'h' (see Figure 9.2) and that no gas is entrained by either the shear areas or the arm, then at constant gas density, ρ, the entrained mass, Δm is given by:

$$\Delta m = 2\ell_1\ell_2\rho h = 2A_c h\rho \tag{9.10}$$

where ℓ_1 and ℓ_2 are the dimensions of the compression area.

From equations (9.3) and (9.10) we obtain

$$F_0/F = (M_0' + 2A_c h\rho)/M_0' = 1 + \rho/\rho_0(2A_c h\rho_0/M_0') \qquad (9.11)$$

Comparing equations (9.3a) and (9.11) the thickness of the entrained layer is given by:

$$h = (BM_0')/(2A_c \rho_0) \qquad (9.12)$$

The value of h is found to be approximately 3mm.

9.4 The Vibrating Reed as a Gas Density Meter

The accurate measurement of gaseous density over a wide range of temperature and pressure provides valuable information. The theoretician may use these data to evaluate the quality of equations of state and hence model intermolecular interactions. The process engineer is provided with a convenient transducer which can, for example, monitor the degree of conversion of gas phase chemical reactions such as the manufacture of ammonia, or the gas phase polymerisation of poly-(ethylene). He might also use such a transducer to sense the failure of a SF_6 transformer. The needs of the theoretician are served by traditional techniques (Brielles et al, 1975) but the process engineer often requires a relatively inexpensive continuous on-line device capable of operating in a wide range of conditions. Up to this time, apart from this vibrating reed technique, no reliable and convenient experimental technique has been available for this purpose.

Figure 9.9 shows the variation of frequency attenuation versus gaseous density for gases He, CO_2 and N_2. The ambient temperature and the pressure range for each gas are shown. Gaseous densities at any particular pressure were obtained from literature (IUPAC; 1973, 1974). It may be observed that to a very good approximation, the

decrease in the resonance frequency is not only proportional to the

gaseous density, but also rather independent of the nature of the gas.

At present I cannot confirm that this is a general result for all

gases and gaseous mixtures.

The system described has a capability of providing routine density

measurements to $\pm 1 \times 10^{-4}$ g cm^{-3}. However, this accuracy is limited

by the precision of the density data which are used for the calibration

purposes and the temperature fluctuations in the gaseous ambient.

It is envisaged that this device will be generally useful as a

gaseous density probe for both continuous and periodic sensing. It

will also be realised that the same principle may be used to monitor

the mass change of solids in a variety of environments. In this context,

it has potential value as a corrosion sensor or a sorption meter for

polymers or porous solids. A number of these applications as well as

the primary gas density application form the subject of further studies

following the completion of this work.

9.5 Gas Absorption Data

Typical gas absorption data in a medium crystallinity (2.157 g cm^{-3}; 70%

crystallinity) PTFE specimen are shown in Figure 9.10 for He and N_2 as

a function of ρ/ρ_0 at 17°C up to a maximum pressure of 51 MPa. These

results were obtained using both point by point calculation (equation

(9.6)) and also on the basis of the measurement of the slopes of F_0/F

vs. ρ/ρ_0 lines (equation (9.9)). The data indicate that the mass uptake

for both gases in PTFE is proportional to the density of the gaseous

media. This is despite the fact that the experiments were carried out

around the room temperature transition of PTFE. There is also a good

agreement between the results obtained using equations (9.6) and (9.9).

The gaseous uptake measurements described above are reversible although

distinct time dependencies are noted in the sorption and desorption processes. These kinetics are complicated by adiabatic effects created during pressure changes. Sorption during compression is rapid (ca. 3 minutes for He and 5 minutes for N_2) but desorption is comparatively slow (a few hours). Similar experiments carried out using high density (2.20 g cm^{-3}; 75% crystallinity) and low density (2.125 g cm^{-3}; 65% crystallinity) PTFE revealed that within experimental error the dependence of gaseous uptake with crystallinity was negligible. It was therefore decided to use the same medium crystallinity specimen for all the proceeding gaseous uptake experiments.

Figure 9.11 shows the results of the corresponding percentage volumetric uptake of N_2 and He in PTFE at room temperature up to 51 MPa pressure. Curves A and B were calculated using the respective mass uptake data obtained for N_2 and He using equation (9.9). Curves C and D, on the other hand, represent the corresponding data using equation (9.6). Gaseous volumes were calculated by assuming that ambient densities are appropriate in the interior of the polymer. It is interesting to note that on the basis of the linearized data (curves A and B), the volume of gas absorbed is insensitive of increasing pressure. This suggests that the gaseous atoms and molecules associate themselves with previously existing channels and pores in the polymer matrix (Pasternak et al, 1970). The volumetric data (curves C and D) obtained using equation (9.6), on the other hand, reveal that a rapid increase in the volumetric uptake up to a maximum pressure of 10 MPa is followed by a small and gradual decrease in volumetric uptake for both N_2 and He. According to curves A and B, the volume accessible by He atoms is ca. 24% greater than that available for N_2 molecules. This may be attributed to the smaller size of the He atoms. Also the maximum percentage

volume sorptions for N_2 and He are 12.5 ± 0.1 and 16.4 ± 0.1 res-
pectively. The density of a hypothetical 100% crystalline PTFE
(Ryland, 1958) is ca. 7% larger than the density of the specimen used
for these experiments. Assuming that this value represents an equiva-
lent of 7% free volume, the precise location of the remaining volume
of gas is problematical. Two interpretations are feasible; the diffu-
sion of gaseous atoms into the crystalline structure (Peterlin, 1974)
without matrix expansion or the swelling of the polymer matrix. Para-
llel results of volume measurement on PTFE together with some other
polymers under pressure in fact indicate a reduction in volume, the
magnitude of which depends on temperature, pressure and the type of
polymer and the pressure medium. These results are dealt with separately
in Chapter 10.

Figure 9.12 shows the results of gaseous uptake measurements in
PTFE in different gaseous mixtures of 3:1 and 1:1 Vol/Vol of N_2 and He
mixtures at 17°C (curve A). The gaseous sorption data are presented
by fitting the straight lines obtained from the linearized data (equa-
tion (9.9) to the data points obtained using equation (9.6). The uptake
in pure N_2 and pure He are also included in the same Figure for compari-
son. From the results, it is evident that the uptake in the case of
gaseous mixtures lies between the data for both pure gases. Also, the
gaseous solubility remains fairly independent of the relative concentra-
tion of N_2 and He in the bulk. The above suggests that the packing
configuration of N_2 molecules and He atoms in the polymer matrix remains
unchanged and is independent of the relative concentration of N_2 mole-
cules and He atoms in the bulk of the pressure medium.

Figure 9.13 shows the results of N_2 and He gaseous uptake measure-
ments (equation (9.9)) at different temperatures of 0, 17 and 67°C up

to a maximum pressure of ca. 51 MPa. The data indicate a relatively

large and positive temperature dependence for the solubility of N_2.

The variation of solubility of He with increasing temperature is

very small. The above trend is again confirmed by observing the isobaric

data presented in Figure 9.14. In this case the gaseous solubility is

measured (equations (9.6) and (9.9)) as a function of increasing tempera-

ture at a constant pressure of 37.9 MPa. The Figure also includes data

obtained for a 3:1 Vol/Vol gaseous mixture of N_2 to He (curve C). Once

again, a large and positive temperature dependence of N_2 solubility

(curve A) may be observed. Typically, the mass uptake of N_2 increases

approximately linearly by ca. 1.1 x 10^{-4} g/^{o}C over a temperature range

of 70°C. The corresponding rate of increase for He over the same

temperature range is 0.1 x 10^{-4} g/^{o}C. These results also indicate that

for a given rise in temperature, the increase in the accessible volume

in the polymer for N_2 molecules is almost 1.5 times that for the He

atoms. It is also interesting to note that from a linear extrapolation

of curves A and B, the temperatures corresponding to zero absorption

of N_2 and He in PTFE are -176°C and -350°C respectively. The larger

temperature dependence for the solubility of N_2 may be rationalized by

visualizing the polymer as a matrix having a spectrum of various sized

sites of an average site size distribution $\lambda(T)$ at a temperature T.

Lowering the temperature results in a reduction in $\lambda(T)$ and hence the

gaseous solubility is reduced. In the case of N_2 absorption, $\lambda(T)$ is

comparable in magnitude with the molecular size of N_2 and hence the

absorption of N_2 increases markedly with increasing temperature (curve

A). In the case of He absorption, however, $\lambda(T)$ is larger than the

average size of He atoms and hence an increase in temperature results

in a small increase in absorption (curve B). The required temperature

for zero absorption of He is lower than that for N_2 due to the smaller

size of He atoms. The gaseous mixture (curve C) shows a greater temperature dependency than for both pure gases; the mixture solubility approaches that for pure N_2 (curve A) at high temperatures. This suggests that as temperature increases, the absorption of N_2 in PTFE becomes more favourable than the absorption of He. This view is consistent with the present and the previous observation (Figure 9.12) of the larger temperature dependency for the solubility of N_2.

The temperature dependence of these gas sorptions is at least a factor of 10 greater than the temperature dependence of the bulk density of the polymer at 37 MPa pressure (McLaren and Tabor, 1963). This perhaps explains the absence of a discontinuity in the measured values of gaseous uptake around the room temperature transition of PTFE.

Figure 9.15 represents the results of the gaseous uptake per unit volume in HDPE, PP and PMMA at $17^{o}C$ up to a maximum pressure of ca. 51 MPa using N_2 gas. The appropriate densities for each polymer are shown. These results were calculated on the basis of point by point calculation (equation (9.6)) only as it was not possible to adequately approximate the F_o/F versus ρ/ρ_o data for the polymers by straight lines. The corresponding results for PTFE are also included in the Figure for comparison. The results indicate that the gaseous uptake per unit volume of the polymers (measured at atmospheric pressure) decreases with the density of the polymers, i.e. the least dense polymers absorb most gas. Also, at high pressures (>45 MPa), the gaseous uptake increases less rapidly than the pressure. This may be attributed to the saturation of the polymers around 45 MPa pressure at these temperatures.

9.6 Summary

These data show that under the influence of a pneumatic pressure, relatively large volumes of gas may be dissolved in a number of organic

polymers such as HDPE, PMMA, PP and PTFE. The extent of this gaseous sorption is found to decrease with the density of the absorbing polymer and increases with the gaseous density. In the case of PTFE (most dense of the above polymers), exposed to a maximum pressure of 51 MPa in N_2 or He pressure media, the mass sorption scales accurately, in a linear manner at a fixed temperature, with the density of the pure gases and two of their mixtures. The variation of gaseous mass sorption with temperature at a fixed pressure is also linear, the constant of proportionality increasing with the gaseous molecular/atomic diameter and at least a factor of 10 greater than the temperature dependence of the bulk density of PTFE at the same pressure. This perhaps explains the absence of a discontinuity in mass sorption as the room temperature transition of PTFE is passed. Studies on the uptake of various mixtures of N_2 and He in PTFE are in support of a view that sorption of N_2 becomes more favourable with increasing temperature. The converse may be speculated in the case of He sorption. A striking feature for both gases is that mass sorption is not a detectable function of the gross morphology of the polymer matrix. The above together with the apparent insensitivity of the gaseous uptake with the room temperature transition of PTFE, suggests that the free volume sites in the polymer matrix are of molecular dimensions.

Finally, the maximum absorbed volumes of N_2 and He exceed the free volumes generally ascribed to the polymers studied. Typically, in the case of absorption of N_2 in PTFE up to a maximum pressure of 51 MPa and room temperature, a 7% volumetric expansion is speculated. However, bearing in mind that gaseous sorption is accompanied by a superimposed triaxial pressure and that bulk densities may not be appropriate in the interior of the polymer, the above speculation is in doubt and its validity forms the subject of a further enquiry described in the following Chapter.
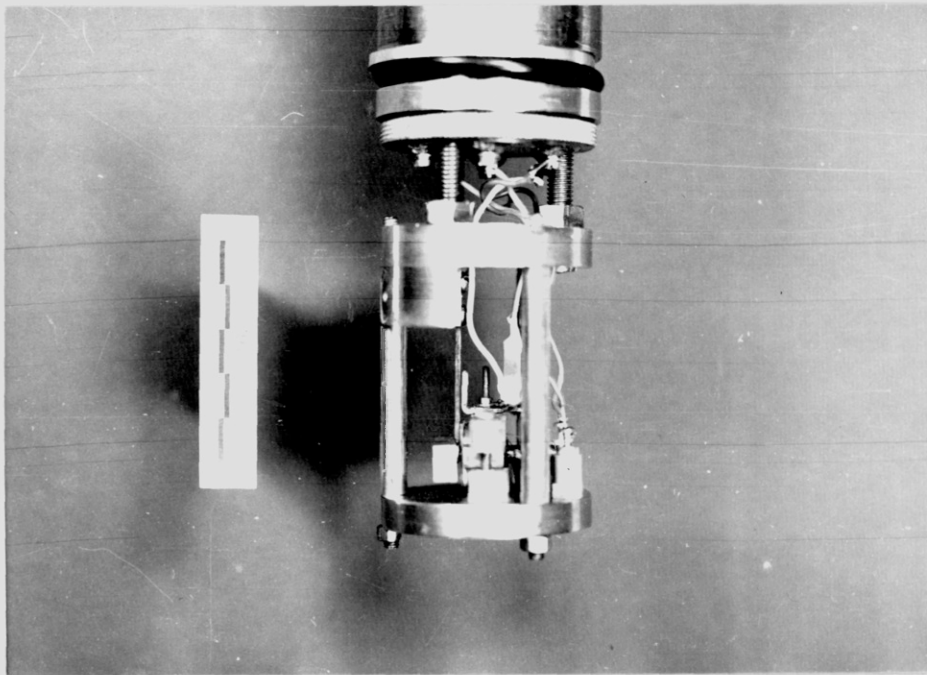
A photograph of the vibrating reed apparatus (see opposite page for detalis).
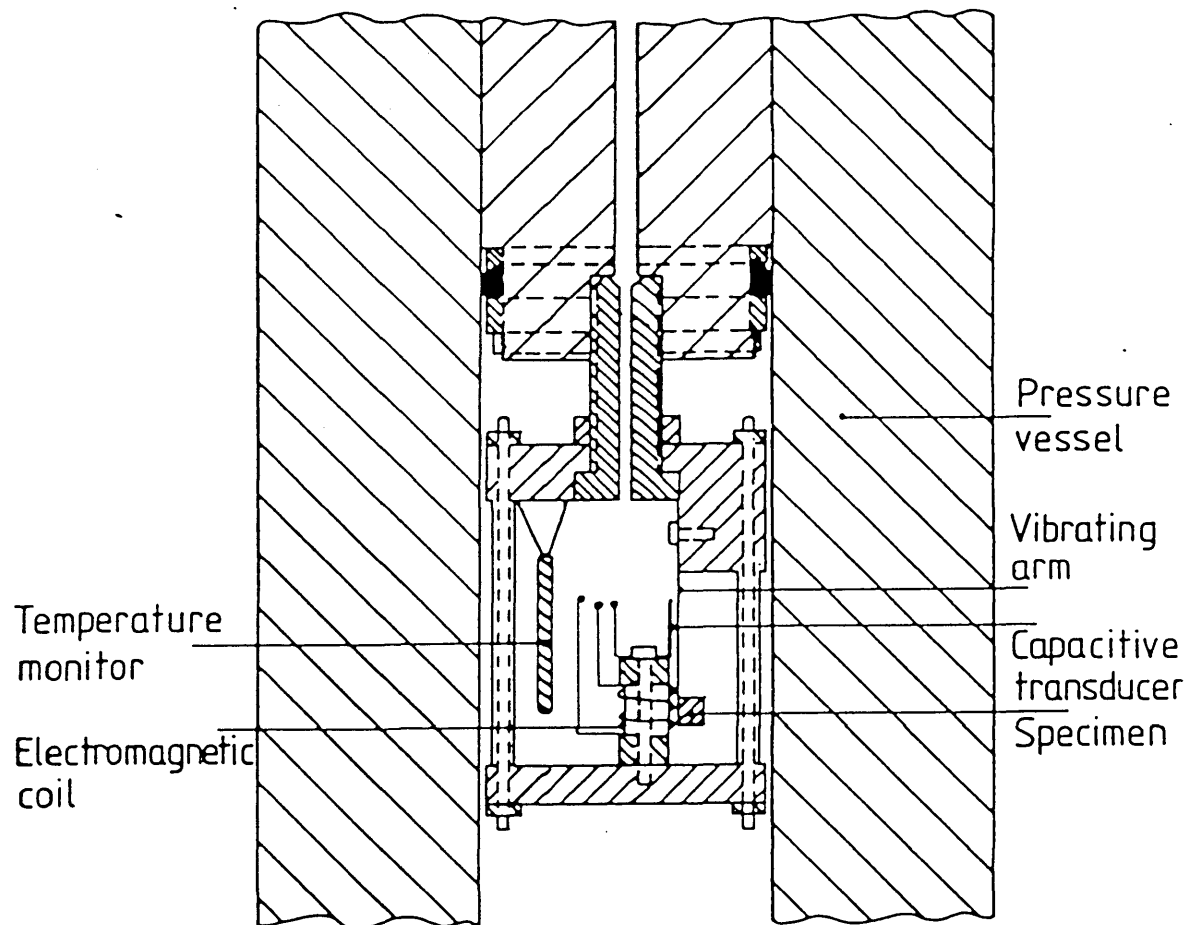
Figure 9.1. Schematic representation of the vibratng reed assembly housed inside the pressure vessel.
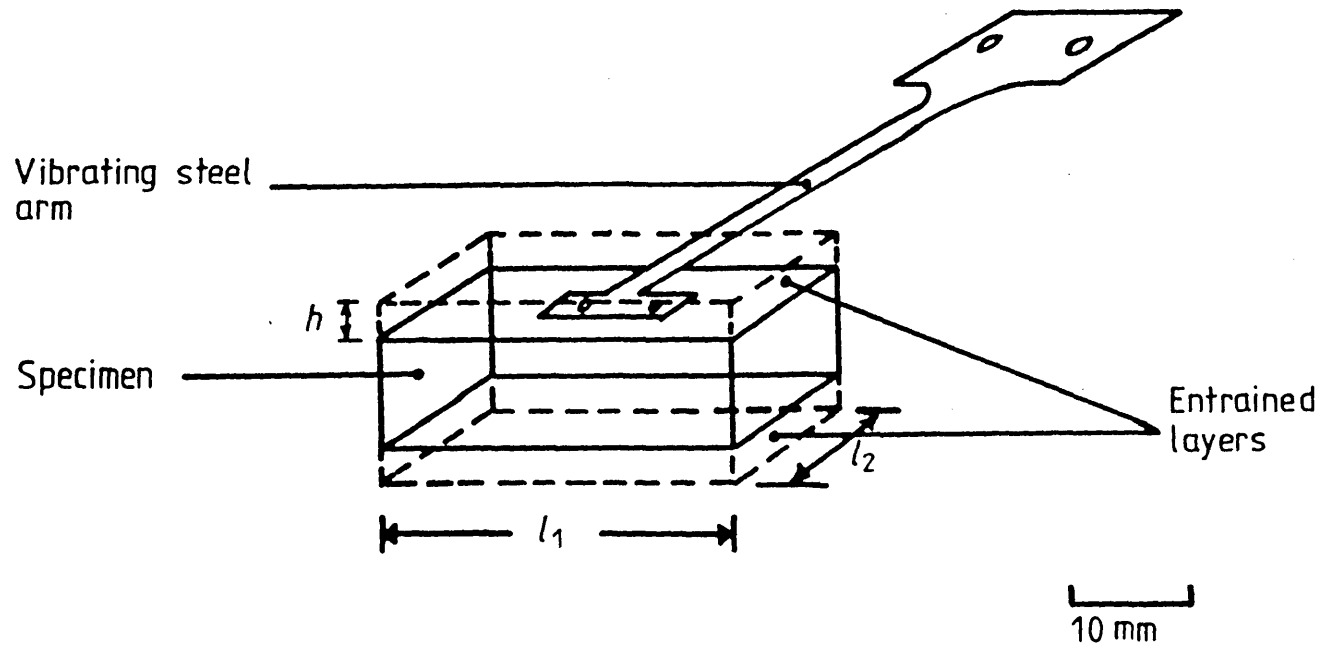
Figure 9.2. Schematic representation of the vibrating arm showing the entrained layers of gas.

Magnetic core

Reed

Capacitive
transducer

V_{bias}

V_{amp}

Pre-amplifier

Power
amplifier

Power supply

Frequency meter

Sensor
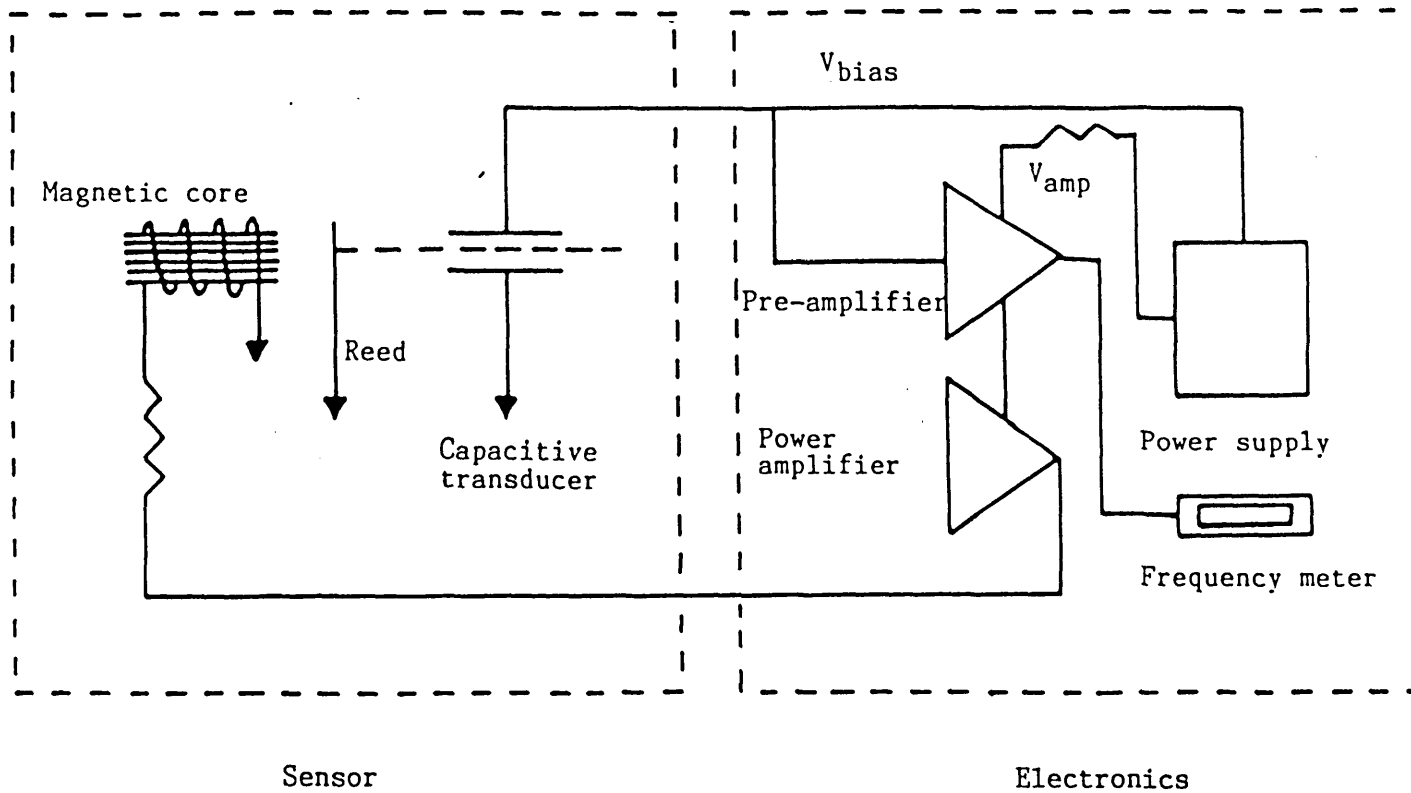
Electronics

Figure 9.3. The Vibrating Reed Electronic Circuitry
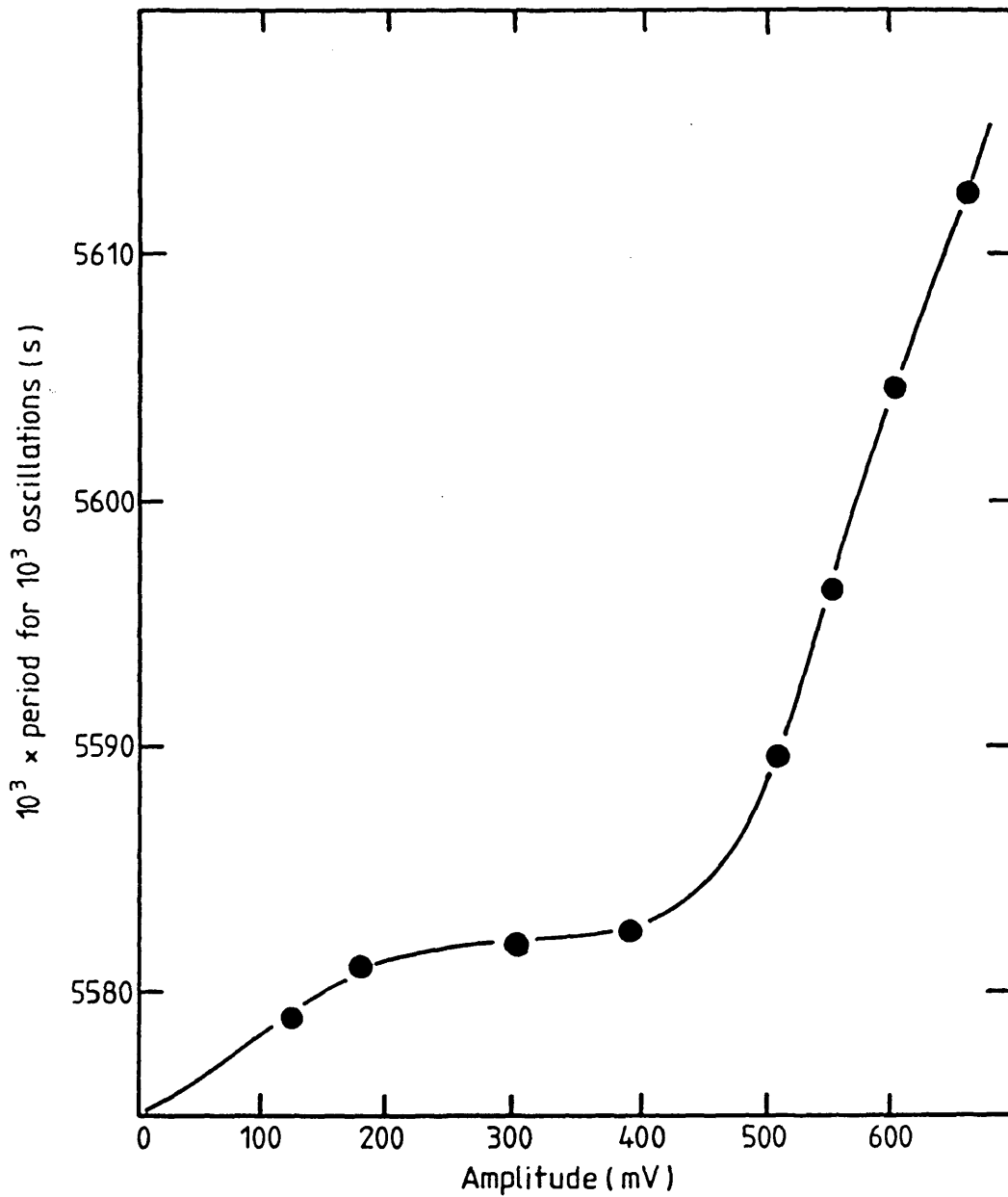
Figure 9.4. Effect of amplitude of vibration on the period of oscillation at atmospheric pressure and 17°C.
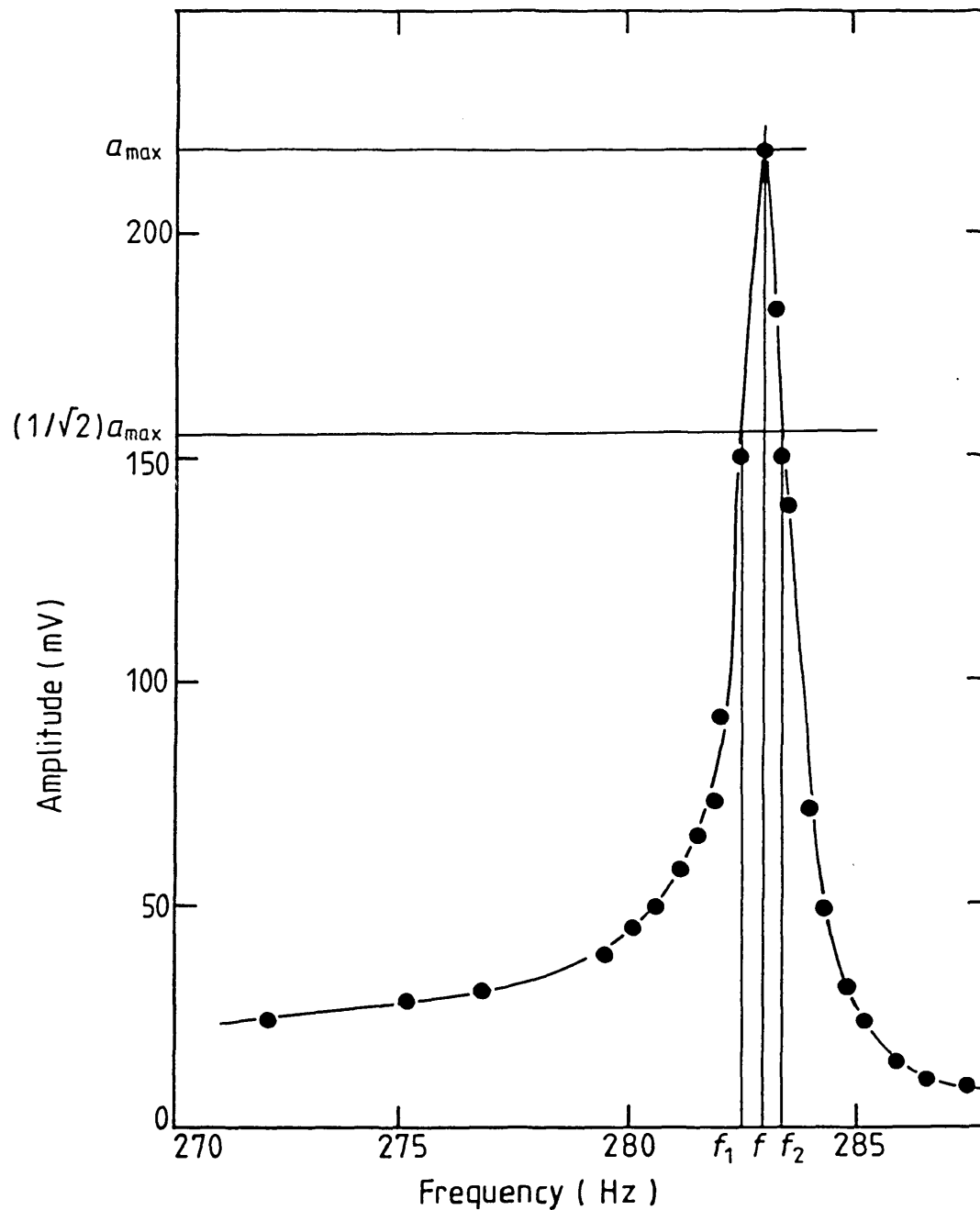
Figure 9.5. The vibrating reed 'quality factor', Q at atmospheric pressure and room temperature. This is calculated from the relation $,Q=f/(f_2-f_1),$(Beards 1981) where f is the resonance frequency corresponding to a maximum amplitude a_{max},and f_1 and f_2 are the frequencies at $(1/\sqrt{2})a_{max}$.
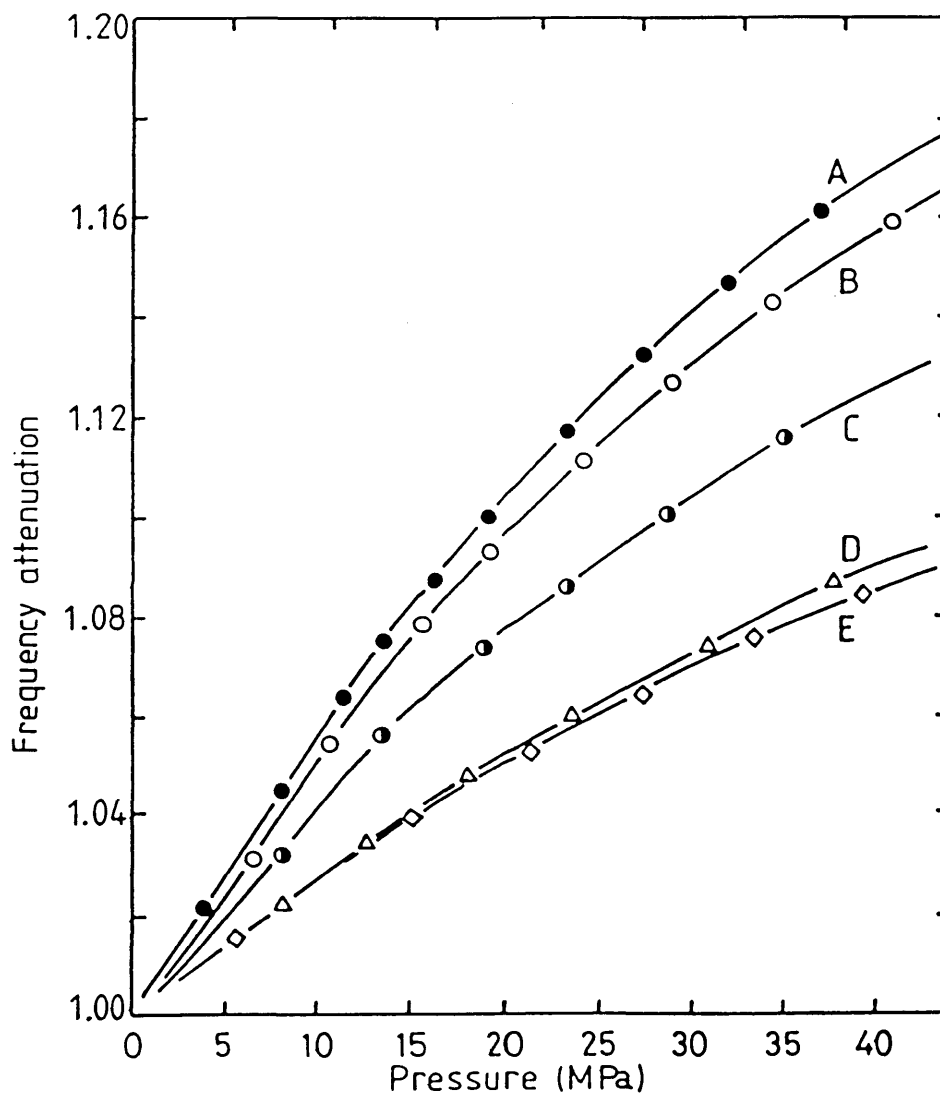
Figure 9.6. Variation of frequency attenuation with nitrogen gas pressure at 17°C:curve A,Al$_1$(2.6930g):sample with holes;curve B,PTFE (2.6920g):identical geometry to Al$_1$;curve C,Al$_2$(3.5296g):identical geometry to Al$_1$;curve D,Al$_3$(3.0527g):different geometry to Al$_1$; curve E,Al$_4$(2.6931):same compression area as Al$_3$.
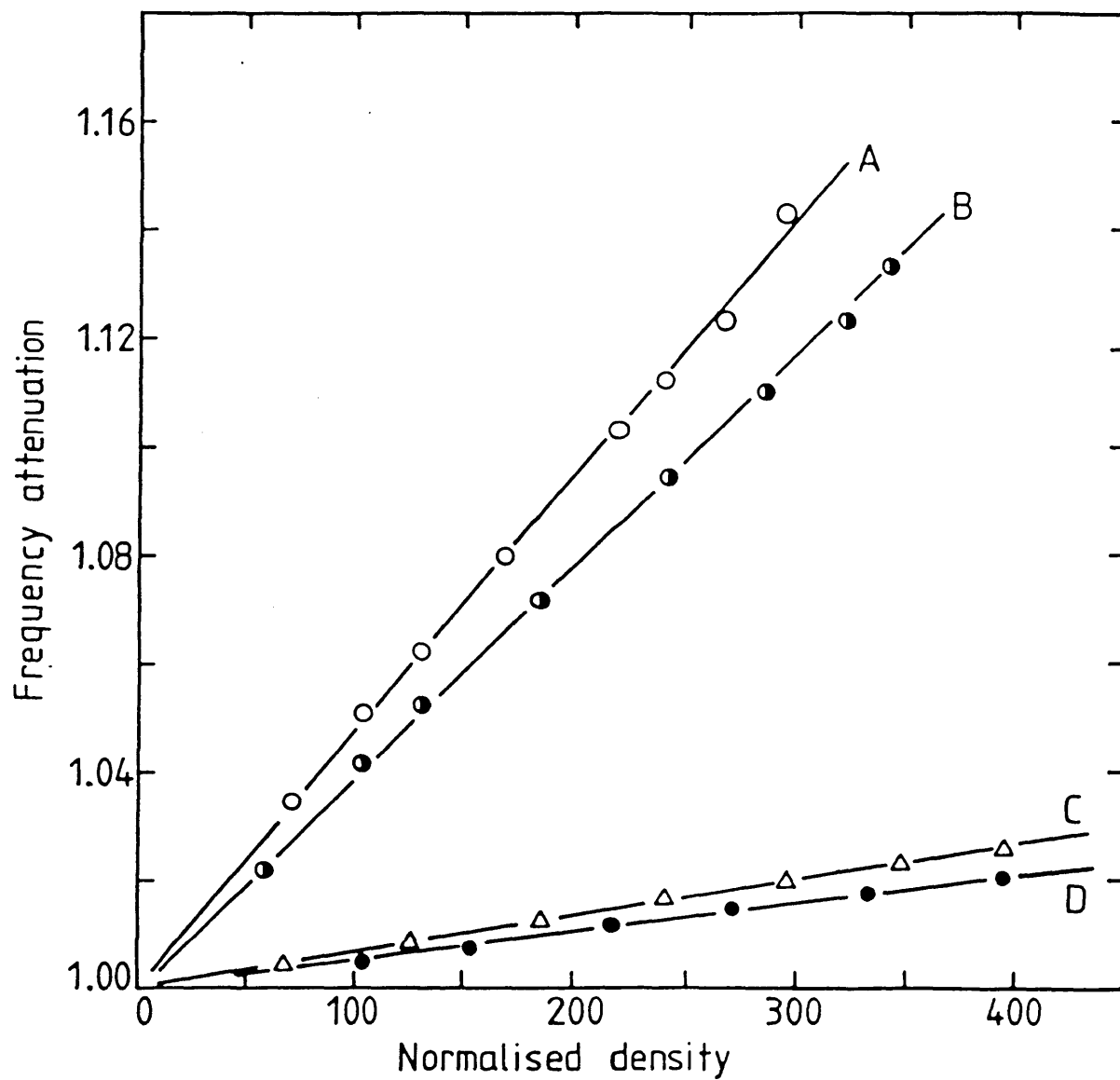
Figure 9.7. Variation of frequency attenuation with normalised gas density at 17°C: curve A,PTFE in nitrogen gas;curve B,aluminium in nitrogen gas; curve C,PTFE in helium gas;curve D,aluminium in helium gas.
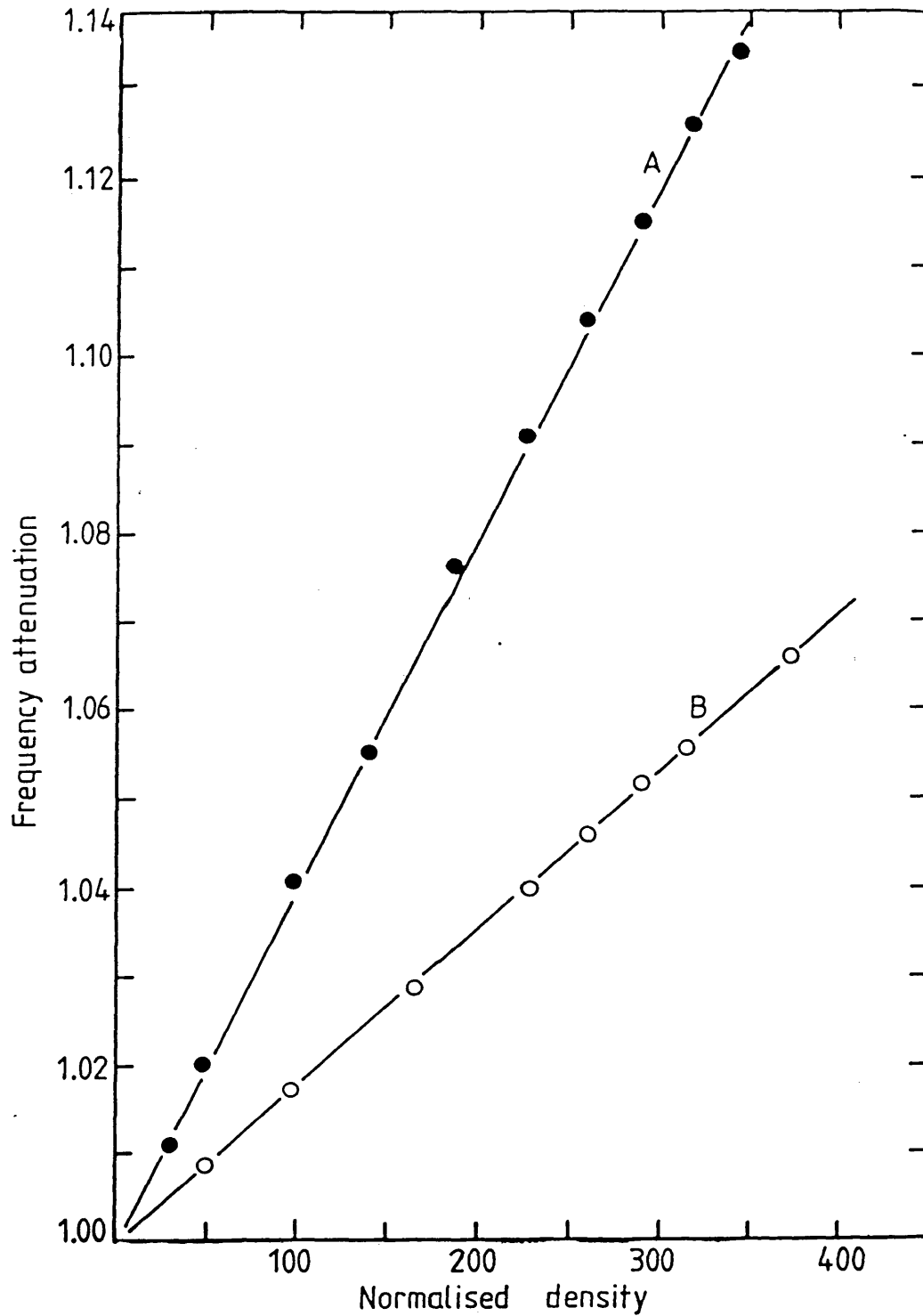
Figure 9.8. Variation of frequency attenuation with normalised nitrogen density at 17°C for aluminium specimen:curve A,A_c=180 mm^2;curve B,A_c=90 mm^2.
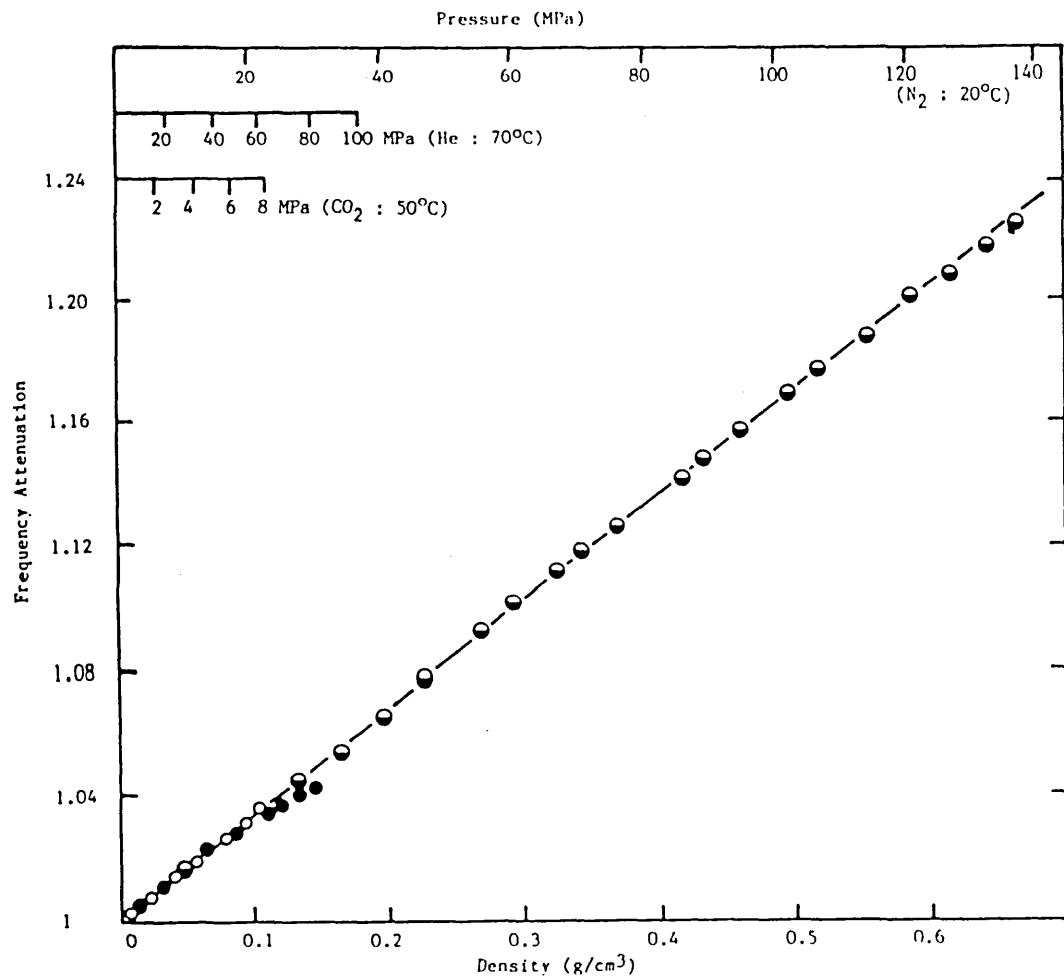
Figure.9.9. Variation of Frequency Attenuation with Gaseous Density:

O,He; ●,CO₂; ◑,N₂. A second gas booster pump was used

to reach a maximum pressure of 150 MPa.
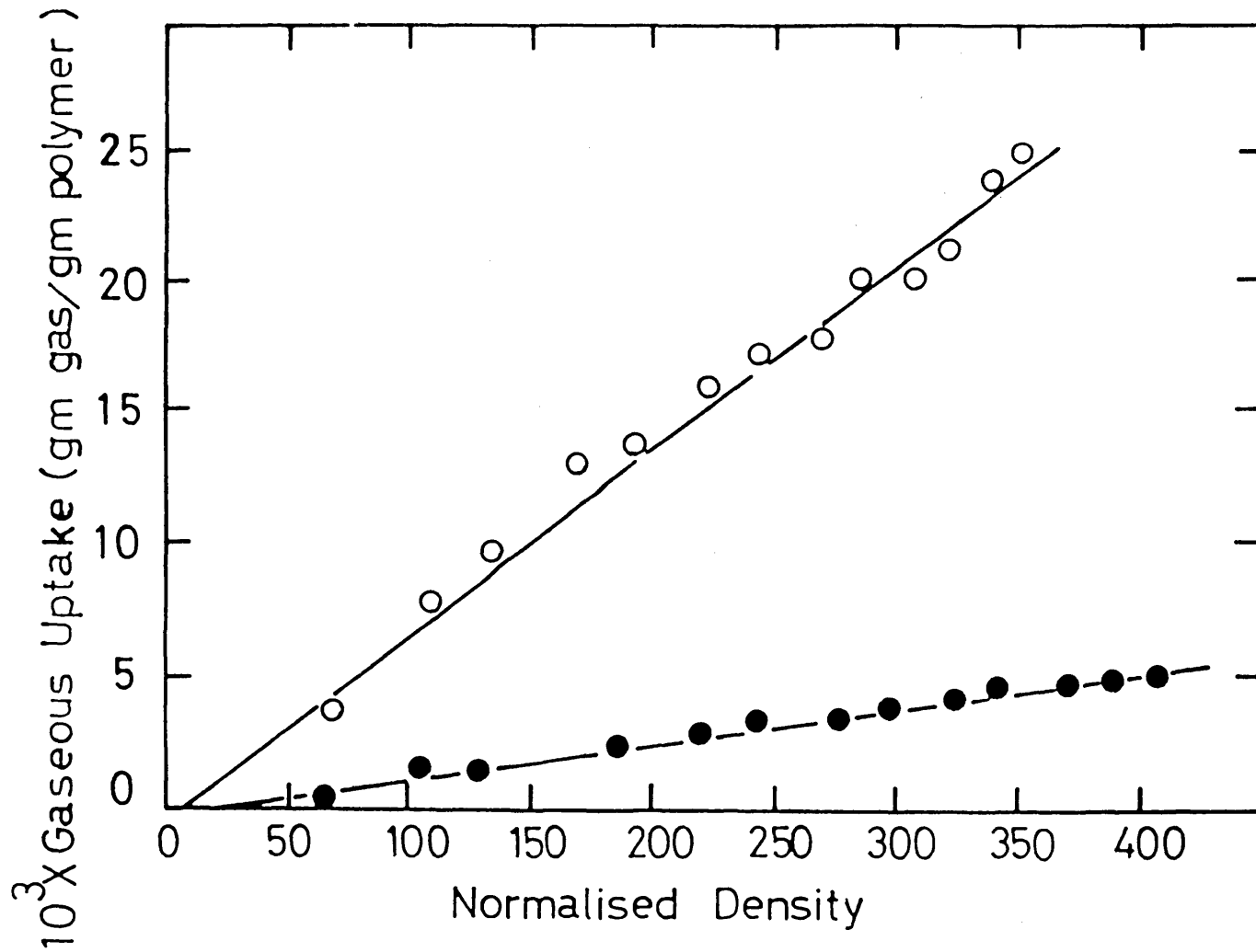
Figure 9.10. Gaseous uptake in PTFE as a function of normalised gaseous density up to a maximum pressure of 51 MPa at 17°C: O ,N$_2$; ● ,He.
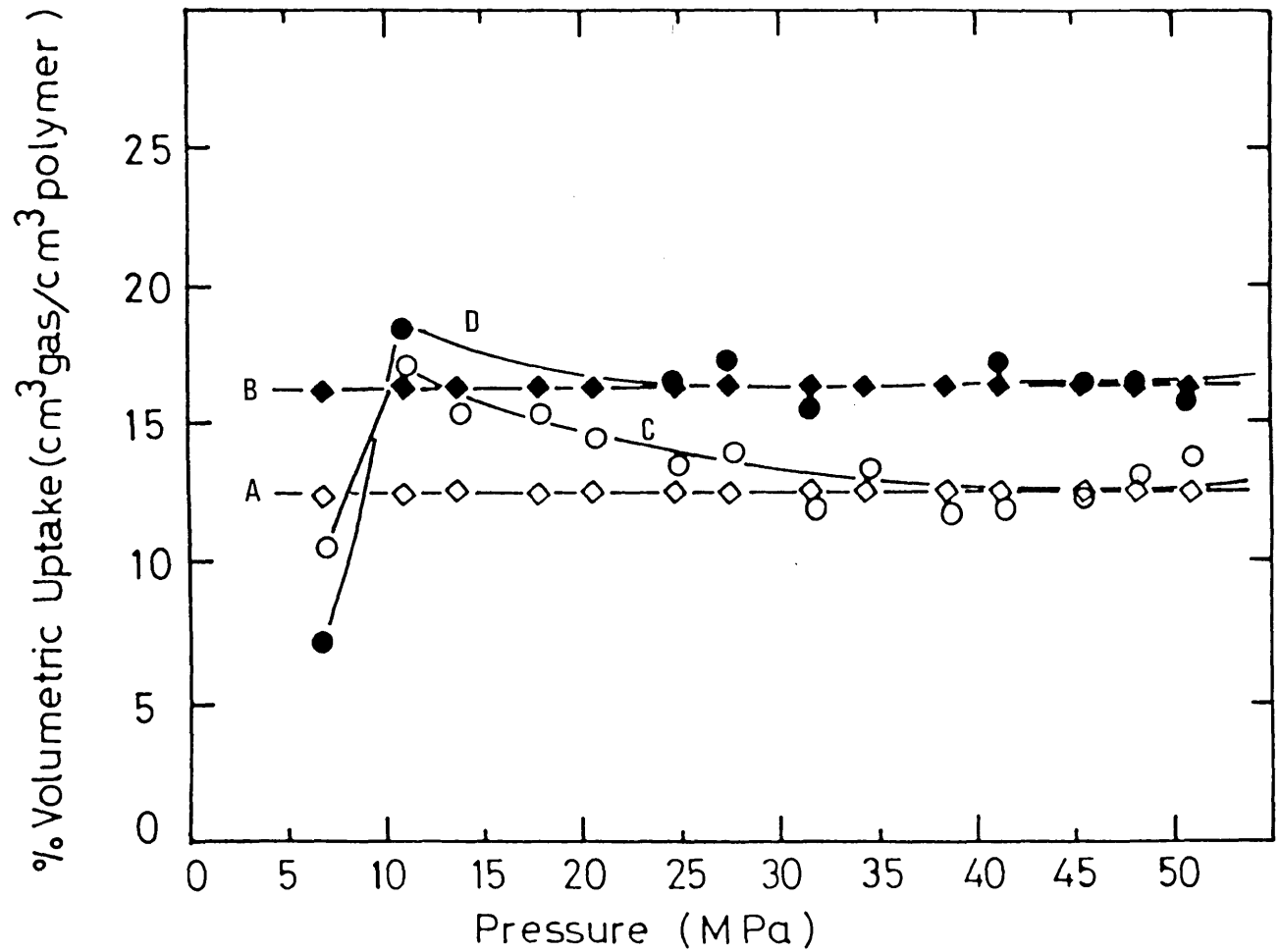
Figure 9.11. Percentage gaseous volumetric uptake in PTFE as a function of pressure at
17°C: ◆ ,He(equation (9.9)); ◇ ,N$_2$(equation (9.9));● ,He(equation (9.6)); ○ ,N$_2$(equation
(9.6)).
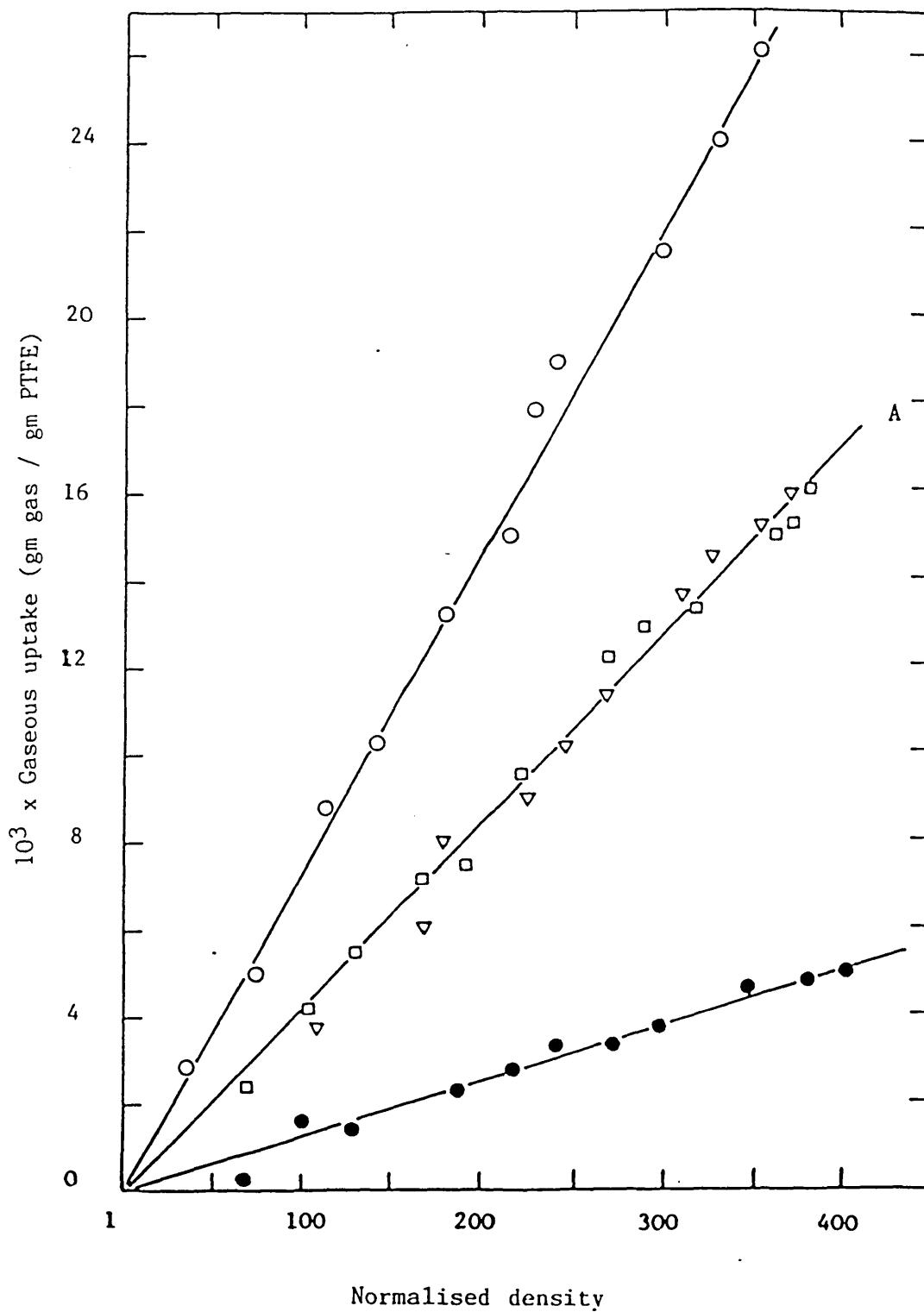
Figure 9.12. Gaseous uptake in PTFE as a function of normalised gaseous density at $17^{\circ}C$: ● ,He; O ,N_2; ▽ ,75% N_2-25% He; □ ,50% N_2 -50% He.
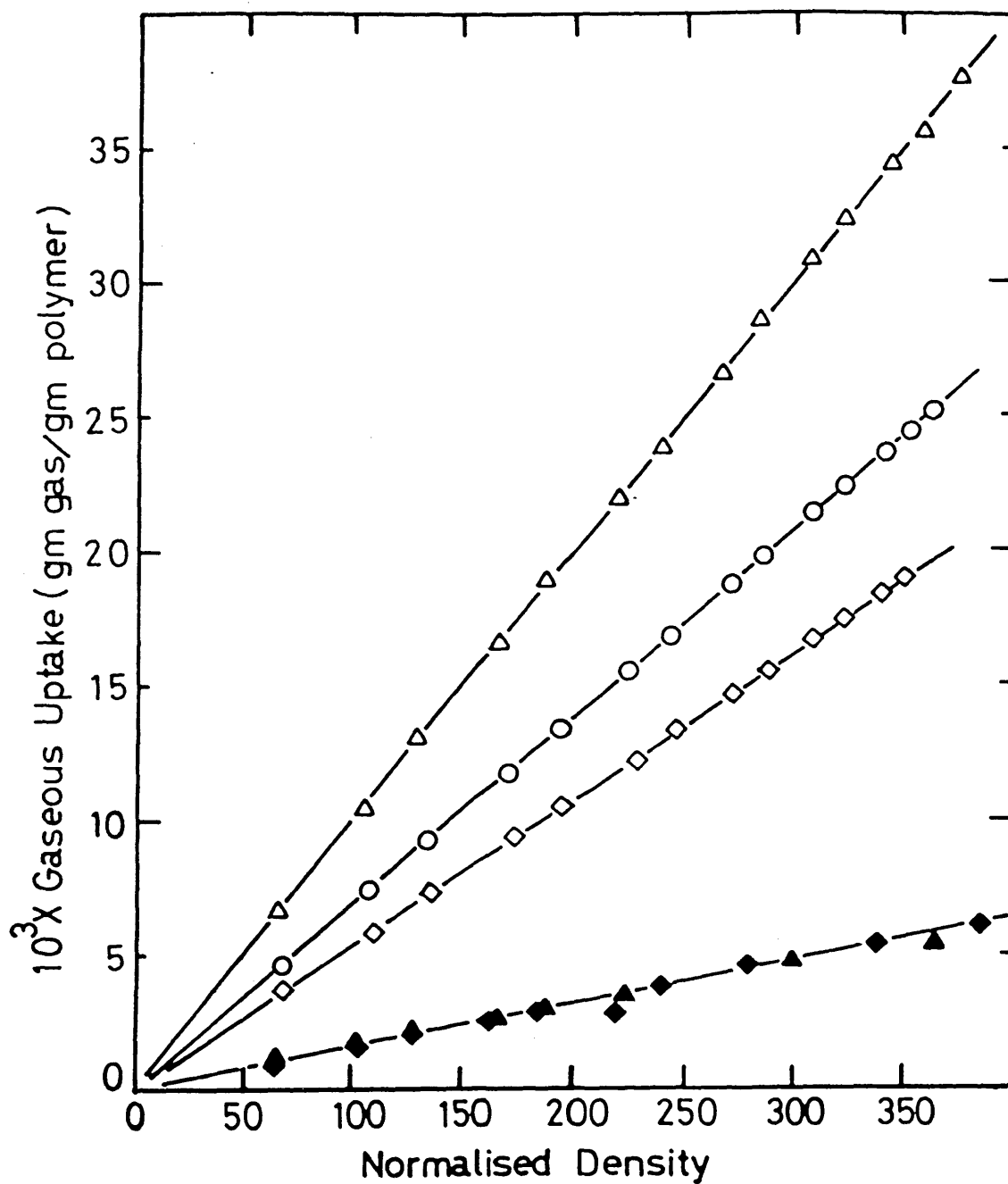
Figure 9.13. Gaseous uptake in PTFE as a function of normalised gaseous density at various temperatures up to a maximum pressure of 51 MPa: $\triangle$, N_2 67°C; $\bigcirc$, N_2 17°C; $\diamondsuit$, N_2 0°C; $\blacklozenge$, He 67°C; $\blacktriangle$, He 0°C.
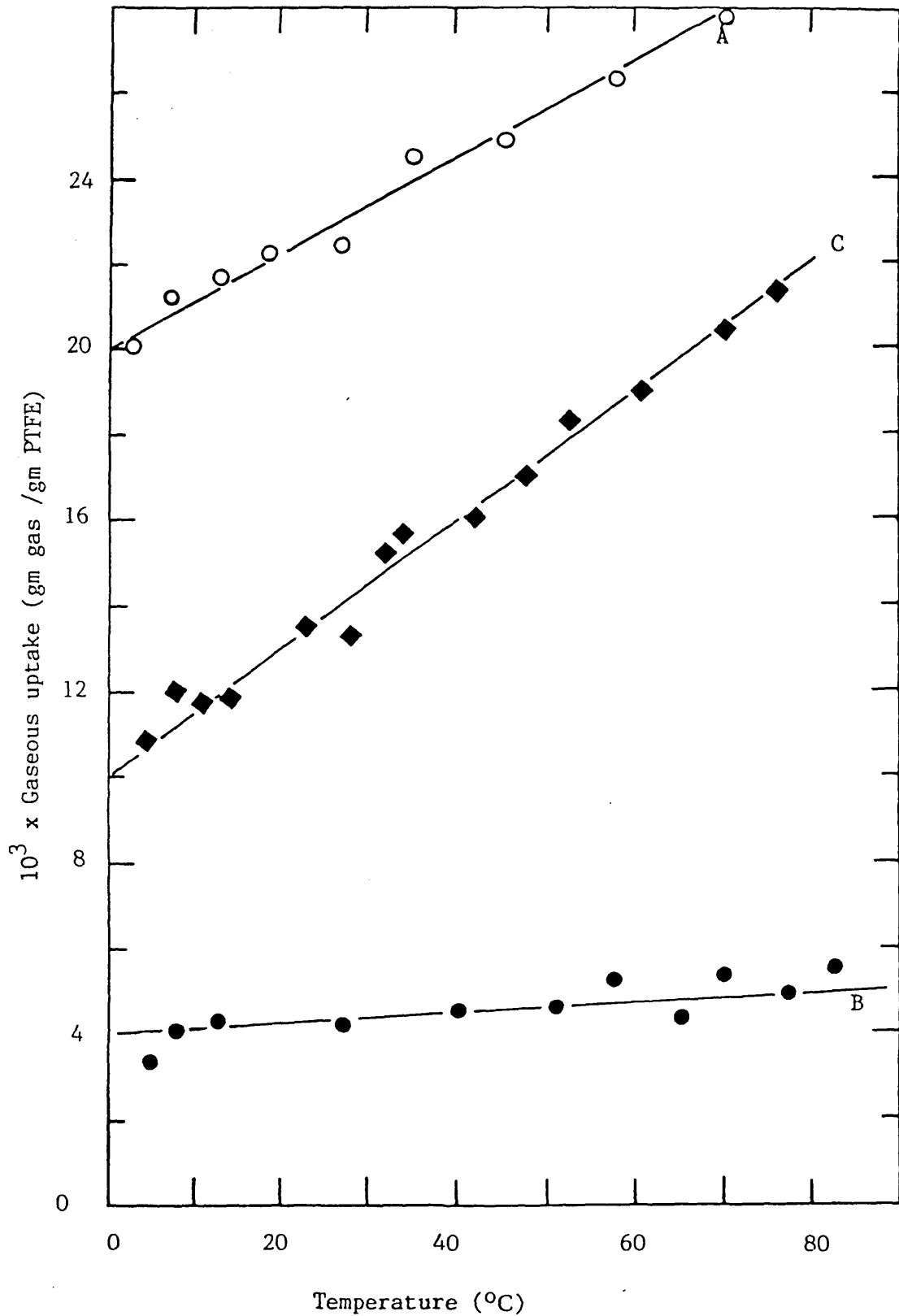
Figure 9.14. The variation of gaseous uptake in PTFE with increasing temperature at a constant pressure of 38 MPa: ○ ,N_2; ◆ ,N_2/He(3:1 v/v) ; ● ,He.
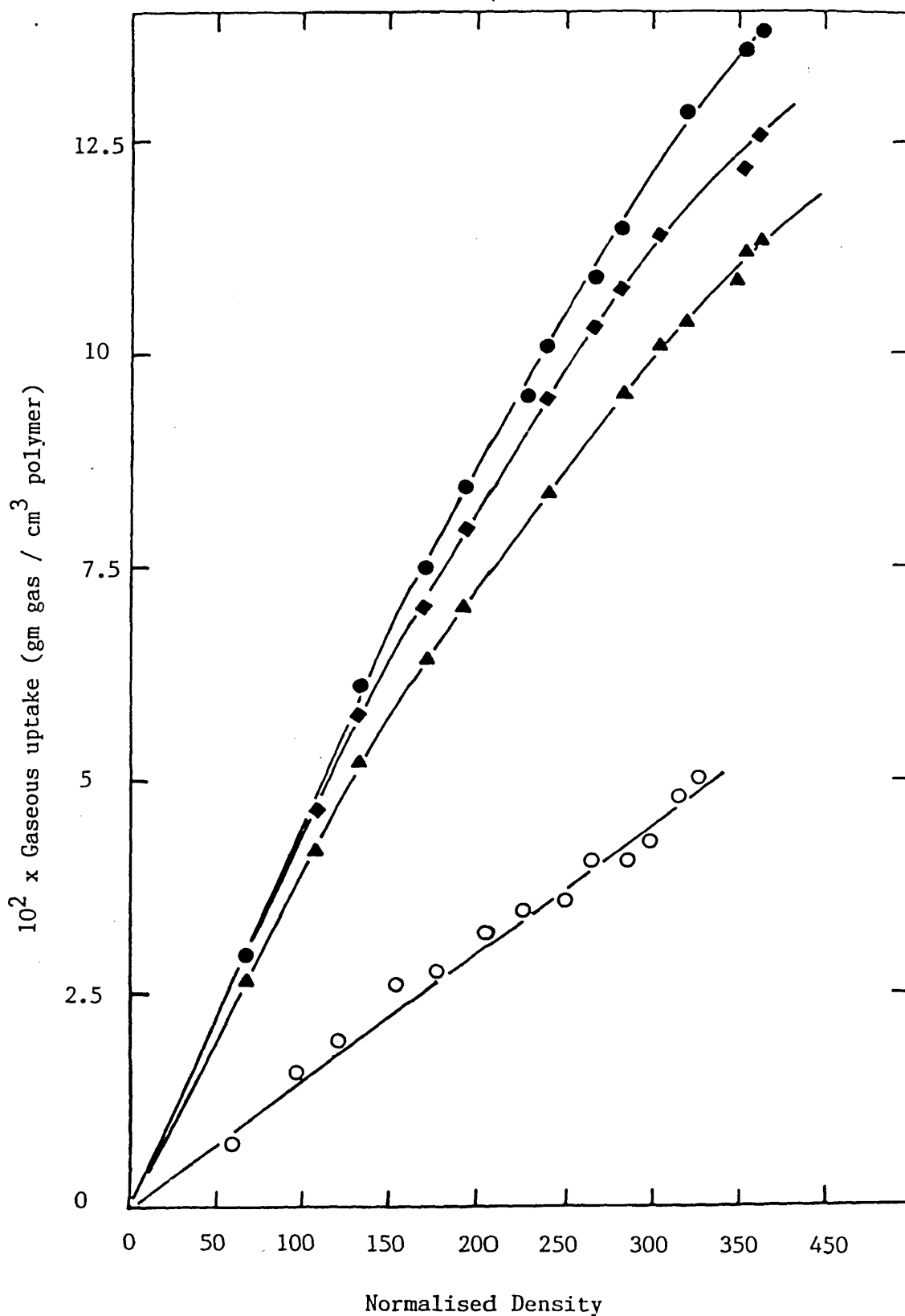
Figure 9.15. N_2 uptake versus gaseous normalised density up to a maximum pressure of 51 MPa at $17^\circ C$: ● ,PP(0.886 gcm^{-3}); ◆ ,HDPE(0.921 gcm^{-3}); ▲ ,PMMA (1.171 gcm^{-3}); ○ ,PTFE(2.157 gcm^{-3}).

C H A P T E R   1 0

MEASUREMENT OF THE LINEAR CONTRACTION OF ORGANIC
POLYMERS UNDER THE INFLUENCE OF HYDROSTATIC OR
PNEUMATIC PRESSURES

10.1 Introduction

In Chapter 9 it was shown that for a number of organic polymers significant gas absorption occurs in a high-pressure environment. The extent of this mass absorption was found to depend on the type, pressure and temperature of the gas medium, but was rather independent of the morphology of the polymer. An important result was that the mass sorption scales with the density of the gaseous medium.

These results produced a dilemma; gas is absorbed under the action of a pneumatic stress and it is natural to inquire whether this involves an expansion or a contraction of the matrix. The volume change cannot be predicted a priori and the present Chapter describes an experimental method for measuring this volume change. The technique complements the method of measuring mass sorption described in Chapter 9.

Previous dilatometric studies on polymers under pressure have been almost exclusively confined to hydrostatic liquid media. For reference purposes we have carried out a study of this type to contrast the effects produced by liquid and gas pressure transmission fluids. The technique adopted here for liquids is almost identical to that developed for gases and both are different from the methods reported in the literature for use with liquids. In view of this,it is appropriate to review briefly the various limitations associated with the techniques reported by others for use in liquid media as described in Chapter 5.

The basic principle shared in most previously reported dilatometric

techniques involves the confining of the specimen in a suitable pressure transfer medium such as mercury and monitoring the total volume of the system by various means following the application of pressure. The problems associated with such methods are numerous. The effect of the finite compressibility of the confining fluid together with its variation with temperature are significant complications. The change in the volume of the pressure chamber following its thermal or stress expansion is difficult to quantify. Other techniques include the linear variable differential transformer technique employed by Mizouchi (1972). A serious disadvantage in the above is the effect of pressure on the materials used in the measuring devices. This gives rise to hysterisis which in turn limits the experimental accuracy. The method of measuring the polymer compressibility by attaching strain gauges to the polymer specimen (Findley et al, 1968) is limited by the quality of adhesion between the strain gauge and the polymer. This is particularly problematical for PTFE where good adhesive junctions cannot be readily produced.

This Chapter describes what is believed to be a novel technique of general value. The method has been evaluated using PTFE and a high density poly(ethylene), HDPE, in a pressure range of ca. 0.1 to 52 MPa using different gases such as N_2, He, H_2/He (1:1 Vol/Vol) and Ar and a commercial hydraulic oil at temperatures between $0^{o}C$ and $45^{o}C$. The method is based upon the measurement of the electrical capacitance between two conductive plates attached to a polymer specimen. The change in capacitance is then related to the length of the specimen. In practice a correction has to be made due to the changes in the dielectric constant of the pressure transmitting medium. This correction factor is found by performing reference experiments using incompressible

reference specimens. The calibration technique provides approximate data for the relative permittivity of gases at high pressures.

10.2 Experimental Methods and Materials

10.2.1 Specimens

The HDPE specimen was the BP type XH100 with a density ca. 0.921 g cm^{-3}. The PTFE specimen was chosen from the medium crystallinity batch (ca. 2.157 g cm^{-3}). Nitrogen gas was white spot oxygen free. The hydraulic oil used was type NS41 (Shell).

(I) Gas measurements

Figure 10.1 shows a dimensioned drawing of the sample cell housed at the base of the gas pressure vessel. The polymer specimen, in the form of a cylindrical rod (ca. 16mm in diameter and 50mm long), was machined at one end as shown to accommodate a brass plate. This plate served as one of the capacitance probes. Brass (type α) was selected as the material of construction for all metallic parts in the cells because of its low thermal coefficient of expansion (ca. 18 x 10^{-6} ^{o}C^{-1}). A 2.2mm diam. clearance hole was drilled along the major axis of the polymer specimen. The screw (ca. 30mm long) which passed through this hole supported the polymer and also provided the other connection for the second element of the capacitance probe. Another 1.3mm diam. clearance hole (ca. 5mm deep) was drilled through the bottom of the polymer. This hole accommodated a second screw threaded into the support plate. This connection prevented the rotation of the polymer about its axis. The support plate was attached to the bottom of the containing chamber (actually the second probe) via three spring loaded 1.3 mm diam. screws. These determined the separation (and hence the sensitivity of measurement), d, between the top plate (mobile) and the bottom (stationary) plates. The value of d is obtained from capacitance measurements (this procedure requires a separate measurement

of the capacitance of the media).

Figure 10.2 shows the apparatus used to monitor the changes in the relative permittivity of the pressure medium under conditions which are nominally identical to those used in the study of the dimensional changes in the polymer specimen. Basically, the system is similar in design to the sample cell described above, with the exception that Pyrex glass tubes were substituted for the polymer specimen and the containing chamber. Glass was chosen because of its negligible electrical conductivity (ca. $3 \times 10^{-8} ohm^{-1} m^{-1}$) and its very low coefficient of thermal expansion (ca. $9 \times 10^{-6} {}^{0}C^{-1}$). This arrangement provides a partial thermal compensation. I have supposed that the glass was incompressible. The support plates of both devices described above were supported by suitably machined electrically insulating PTFE caps.

(II) Liquid measurements

In practice a separate vessel (see Chapter 6) and a set of different capacitance cells were to be used for measurements in liquid environment. Only a brief account is given as the methods adopted are similar in design and operating principle to those used for gases (see Figure 10.3). A number of rather basic geometric modifications were necessary to accommodate these cells in the liquid pressure vessel. This new configuration is not as flexible as the one described in the gaseous studies. It also produces a different capacitance response to specimen dimension changes.

(III) The electrical detection system

The electrical capacitance and hence a value of d was measured using a type 1620-A General Radio capacitance measuring assembly. The operating procedures are described elsewhere (Collins et al, 1973, pp 266-9). Briefly the system consists of a transformer-ratio-arm

bridge, an audio-oscillator (fixed at 1.5 kHz), a tuned amplifier and a null detector. Temperature was monitored by measuring the potential across a platinum resistance film (type 158-328) supplied by Radio Spares with an accuracy of $\pm 0.1^{\circ}C$. This was placed near the specimen in the sample cell.

10.3 Data Analysis

To a first order, the capacitance of a parallel plate capacitor of an area A and a plate separation, t, is (Grant and Phillips, 1975):

$$C = [K_0 K(T,P)A]/t \qquad (10.1)$$

where K_0 is the permittivity of free space and K(T,P) is the relative permittivity or the dielectric constant of the medium which is both a function of temperature and pressure (Buckingham and Pople, 1955). In practice the actual plate area is an underestimate because of edge effects (Blyth, 1980 and ASTM D150, 1980). A precise knowledge of the magnitude of the edge correction is not required in this experiment although an estimate is useful for calculating approximate values of the relative permittivity of the pressure media. The method first requires a precise measurement of the capacitance, C_r, (C_{ro} at one atmosphere) of a reference cell of plate separation, t, (see Figure 10.2). This value of t is fixed and denoted t_r. A precise measurement of the capacitance of the cell containing the polymer, which has the same nominal capacitance area A, as the reference cell but a different value of plate separation, t (t_o at one atmosphere) then provides a measurement of linear strain. The capacitance of this cell is denoted as C_p (C_{po} at one atmosphere). Then

$$t = (C_r/C_p)t_r, \qquad (10.2)$$

assuming that the effective capacitance area is not a function of the plate separation and environment in the ranges of separation adopted.

The linear strain, ε, generated in the polymer axis is

$$\varepsilon = (\frac{1-1_o}{1}) \qquad (10.3)$$

where 1_o is the original axial length of the polymer and 1 is the new length.

For the gas cell (see Figure 10.1), assuming negligible thermal expansion of brass and using equation (10.2) we have

$$1_o - t_o = 1 - t = H \qquad (10.4)$$

or

$$1_o = H + (C_{ro}/C_{po})t_r \qquad (10.5)$$

and

$$1 = H + (C_r/C_p)t_r \qquad (10.6)$$

where H is the distance between the base and the bottom capacitance plates. Combining equations (10.2) to (10.6) and rearranging, the compressive strain of the polymer in the gas pressure vessel is given by:

$$\varepsilon_g = \frac{C_{po}t_r}{C_{ro}t_r + C_{po}H} (\frac{C_r}{C_p} - \frac{C_{ro}}{C_{po}} \qquad (10.7)$$

Similarly for the liquid cell (see Figure 10.3)

$$l_o + t_o = l + t = L \qquad (10.8)$$

Following exactly the same procedure as above, the compressive strain of the polymer in the liquid cell is given by:

$$\varepsilon_l = \frac{C_{po}t_r}{L(C_{po} + C_{ro}t_r)} \left(\frac{C_{ro}}{C_{po}} - \frac{C_r}{C_p}\right) \qquad (10.9)$$

The individual values of t_r, H and L were measured using a travelling microscope to ± 0.01 mm. This was performed by rigidly clamping the cells and measuring each distance at three different positions around the axis of the cell and averaging the results. The quantities $C_r(T,P)$ and $C_p(T,P)$ were measured as a function of T and P.

The calculation of the linear strains ε_l (hydraulic fluid) and ε_g (gas medium) is obtained by insertion into equations (10.7) and (10.9) respectively. This may be achieved by point by point evaluation as a function of temperature and pressure but since the values of capacitance for the reference and the polymer cells are not obtained at precisely the same pressure it is expedient to express the capacitance data $C_g(T,P)$ and $C_p(T,P)$ in the form of a suitable polynomial. It was found that second degree polynomials of the form:

$$C = a + bP + cP^2$$

provide an adequate description of the experimental data (C denotes C_g and C_p). The quantities a, b and c are functions of the medium and

numerical values are given in Tables 10.1 and 10.2. A simple computation then gives discrete values for $\varepsilon_1(T,P)$ and $\varepsilon_g(T,P)$. For presentation purposes these strains are also expressed as:

$$\varepsilon = a + bP + cP^2$$

and values of a, b and c are given in Table 10.3. The use of these polynomials is not intended to provide data averaging; they are required simply because it is impracticable to reproduce precisely equivalent pressures in the sample and reference cells in separate experiments. However some data smoothing is produced.

The data fitting was carried out using a commercial least squares package on an Apple IIe microcomputer.

10.4 Typical Experimental Data and Analysis

10.4.1 Gas and liquid data

Figure 10.4 to 10.8 show data for apparent capacitance for gaseous (N_2, He, Ar and N_2:He (1/1)) and liquid (hydraulic oil) pressure media obtained with the appropriate calibration cells at $0^\circ C$ and $45^\circ C$ up to a maximum pressure of ca. 51 MPa. Figure 10.9 represents the same data but plotted on the same axis for comparison. It may be observed that for all media the capacitance is a function of pressure and temperature. All capacitance data were fitted to second order polynomials (Table 10.1). It is interesting that, to a good approximation, the gas capacitance results (excluding argon) are a linear function of the gas density for a fixed temperature; Figure 10.10. The gaseous densities as a function of temperature and pressure were taken from Din (1961) and Angus et al (1975).

Although these data are primarily intended as calibrations and

corrections for the polymer deformation data to be described in the next section, they may be used to obtain approximate values of gaseous relative permittivity as a function of pressure. The major uncertainty in this exercise is the precise value of the effective plate area. The calculation of the effective area is necessary since guardrings (Blyth, 1980, pp 72-3) were not incorporated in the construction of the present capacitance cells. ASTM, D150 (1980) provides expressions for the calculation of the added equivalent capacitance of simple cells but unfortunately the current cases are not described. However, using Table 10.1, approximate values of the relative permittivity of the gases may be calculated. The values of the constants k in the Table were determined from a knowledge of the gas relative permittivity at 101 kPa (Gregg, 1972) and a calculation of the corresponding effective area using equation (10.1). This area was assumed to be independent of gas pressure. The error introduced by this approximation cannot be computed accurately but it is not considered to be large (less than 10%). Typically, the added equivalent capacitance is ca. 30% which corresponds to an effective plate area 30% greater than the nominal area. Johnston et al (1960) have reported permittivity data on nitrogen, helium and argon using a capacitor cell incorporating guardrings. Their system was however not temperature compensating. The data (though only evaluated to ca. 12.4 MPa)were based on absolute capacitance values measured with an order of magnitude higher in precision compared to the present data. Unfortunately, it was not possible to make direct comparisons; these data were evaluated at different temperatures; the present data are however comparable in magnitude.

10.4.2 Polymer studies

The effect of different pressure media on the apparent capacitance of cells containing the PTFE specimens are shown in Figures 10.11 to 10.15. Figure 10.16 represents the same data but plotted on the

same axis. The results for HDPE using N_2 and an hydraulic oil pressure medium are represented in Figure 10.17. It will be seen later that these data correspond to a contraction of the polymers. The data are fitted to second order polynomials; Table 10.2. Before presenting the calculated linear strain from the data shown in Tables 10.1 and 10.2 using equations (6) and (8) it is appropriate to mention briefly the time dependence of the capacitance data shown in Figures 10.16 and 10.17. The gaseous measurements attained an equilibrium value within ca. 7 minutes and prolonged exposure to the pressure media (up to 24 hours) resulted in no detectable change. The initial variation in capacitance is probably due,in the main,to thermal fluctuactions. The equilibrium times for liquid medium were significantly longer and typically 30 minutes although after extensive exposure (ca. 48 hours) to the liquid a significant re-expansion of the compressed sample is observed; a value of 10% is typical so that only 90% of the original linear strain is preserved. Comparison of the measured values of the capacitance of the polymer cells before and after each compression cycle indicate permanent densification of the polymers (see Chapter 11); the magnitude being slightly larger (ca. 1.5 folds) for PTFE than for HDPE. It was therefore decided to use a new (no pressure exposure) polymer specimen for each experiment.

The equilibrium linear strains for PTFE as a function of pressure using a hydraulic fluid and various gaseous media at two temperatures are represented in Figure 10.18. Figures 10.19 to 10.23 represent the same data but plotted separately for each pressure medium in order to facilitate data analysis. The calculated values of compressive strain data are fitted to second order polynomials (Table 10.3). These were found to give adequate description of the data (ca. $\pm 1 \times 10^{-2}$%

maximum deviation from measured values of capacitance). The results for liquid media (Figure 10.19) show the expected trend (Passagli and Martin, 1963); the compressibility increases with increasing temperature. The gas data (Figure 10.20) were unexpected; first the compression in nitrogen medium exceeds that in liquid medium and second there is only a small and positive temperature dependence in the gas data which changes sign at above 25 MPa pressure. In this region, the compressibility, in contrast to a liquid medium, decreases with increasing temperature.

Figure 10.21 represents the variation of the linear strain induced in PTFE with increasing pressure using He as a pressure medium. The compressibility in He exceeds that in low temperature (0°C) liquid medium and follows the same pattern as in N_2. However, the transition in the temperature dependence of compressibility occurs as a somewhat higher pressure (ca. 35 MPa) than in N_2. Also PTFE is more compressible in a nitrogen pressure environment. This is consistent with the previous observation that the volumetric uptake of N_2 in PTFE is smaller than that in He (see Figure 9.12). The polymer in a N_2 pressure medium is exposed to a larger effective triaxial pressure. The reduction in the linear strain with increasing temperature at high N_2 and He pressures (25 and 35 MPa respectively) is also consistent with the previous observation that the gaseous uptake increases with increasing temperature (see Figure 9.15) and pressure (see Figure 9.11). The polymer therefore becomes progressively more difficult to compress once any of the above two parameters are increased. The transition pressure of the temperature dependence of compressibility is larger for He than it is for N_2 (Figures 10.20 and 10.21) due to the smaller temperature coefficient of the volumetric uptake of He in PTFE (see

Figure 9.15). Figure 10.22 represents the compressibility data obtained

using a 1:1 Vol/Vol mixture of N_2 and He pressure medium at two

temperatures. In this case, the low temperature compressibility is

larger than the corresponding high temperature value at all pressures.

It is also interesting to note that the magnitude of the high and low

temperature compressibilities in the gaseous mixture are similar to

those in pure N_2 and pure He respectively (c.f. Figures 10.20 and

10.21).

Figure 10.23 represents the PTFE compressibility data obtained in

an Ar pressure medium. Surprisingly, the behaviour in Ar is similar

to that in a liquid pressure medium, i.e. the compressibility is larger

at the higher temperature isotherm. This may be explained by specula-

ting that the uptake of Ar in PTFE is comparatively small. This view

is partially supported following the observed comparatively large com-

pressibility of PTFE in Ar. No gaseous uptake measurements using this

gas were carried out.

The equilibrium linear compressive strain of HPDE as a function

of pressure is shown in Figure 10.24 for liquid and N_2 media at $0^{o}C$

and $45^{o}C$ up to a maximum pressure of ca. 51 MPa. The coefficients for

the fitting curves are given in Table 10.3. The results follow exactly

the same trend as those for PTFE (see Figures 10.19 and 10.20).

HDPE is however less compressible than PTFE. In the case of gaseous

media this may be attributed to the larger gaseous uptake in HDPE than

for PTFE (see Figure 9.16).

10.4.3 Accuracy of data: sources of error in the measurement of linear

strain

Certain errors arise from imprecise linear measurements; the

error in measuring the plate separation, t_r, amounted to 0.5% for an

average distance of 2mm on the basis of the assumption that it was measured to ± 0.01mm. The corresponding errors in the measurements of H and L (ca. 5mm long each) amounted to 0.02% (see Figures 10.1 and 10.3). The additional error introduced following the thermal expansion (or contraction) of the above two members over a temperature range of $50^{\circ}C$ was 0.09% in both cases. The error introduced in t_r following the thermal expansion (or contraction) of the glass tube (ca. 45mm long) in the liquid calibration cell (see Figure 10.3) amounted to 1%. The corresponding error introduced following the differential thermal expansion (or contraction) of glass tubes in the glass calibration cell (see Figure 10.2) was negligible (2×10^{-2}%). The error introduced by the precision of the capacitance measurement is trivial (0.01%).

The maximum total error in the measurement of the linear compressive strain from these sources in the gas and liquid cells is calculated as ca. 0.12%.

There are also uncertainties in the absolute values and reproducibility of pressure and temperature measurements. The temperature measurements were accurate to better than $0.2^{\circ}C$. The comparable error in pressure does not exceed 0.35 MPa.

10.5 Summary

The various effects of a pneumatic and hydrostatic pressure media on the volumetric strains induced in PTFE and HDPE are compared and contrasted in some detail. The results reveal that under the influence of a N_2 or He pressure media a volumetric contraction of the polymers is produced. This is despite the fact that relatively large volumes of gas are dissolved in the polymer matrix. The volumetric contraction induced in gaseous media is found to be, to a first order, comparable to that produced in a liquid (hydraulic oil) medium

and to a second order, dependent on the type and temperature of the pressure media. The contraction induced in a gaseous pressure environment is found to decrease with increasing temperature (more gaseous uptake). This is in direct contrast to the effect produced in a liquid pressure medium. Also the polymers are found to be more compressible in a N_2 than a He (larger volumetric uptake) pressure medium. The behaviour of PTFE in Ar is unusual. In contrast to the response in He and N_2, the compressibility of PTFE in an Ar pressure medium increases with increasing temperature; a response similar to that observed in a liquid medium. This may be attributed to the small volumetric uptake of Ar in PTFE with increasing pressure. No gaseous uptake measurements in an Ar pressure medium were obtained.

These results are consistent with a view that the less gas that enters, the greater is the triaxial compression experienced by the polymer. It is also suggested that if a gas molecule cannot enter a site it will produce a triaxial stress on the void. The net result is a similar but not an identical reduction in free volume as that expected in a purely triaxial pressure environment.
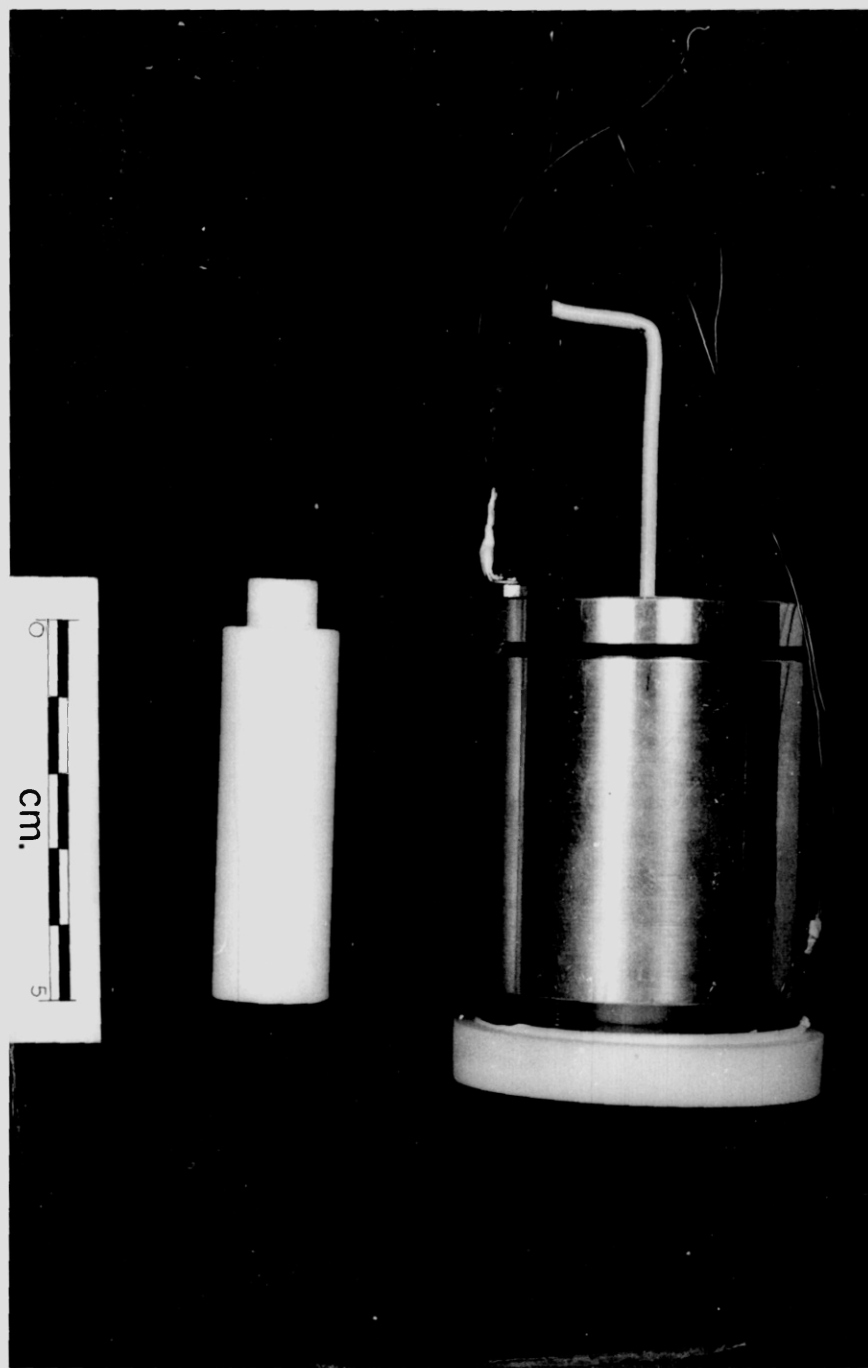
A photograph of the polymer capacitance cell (see opposite page for details).
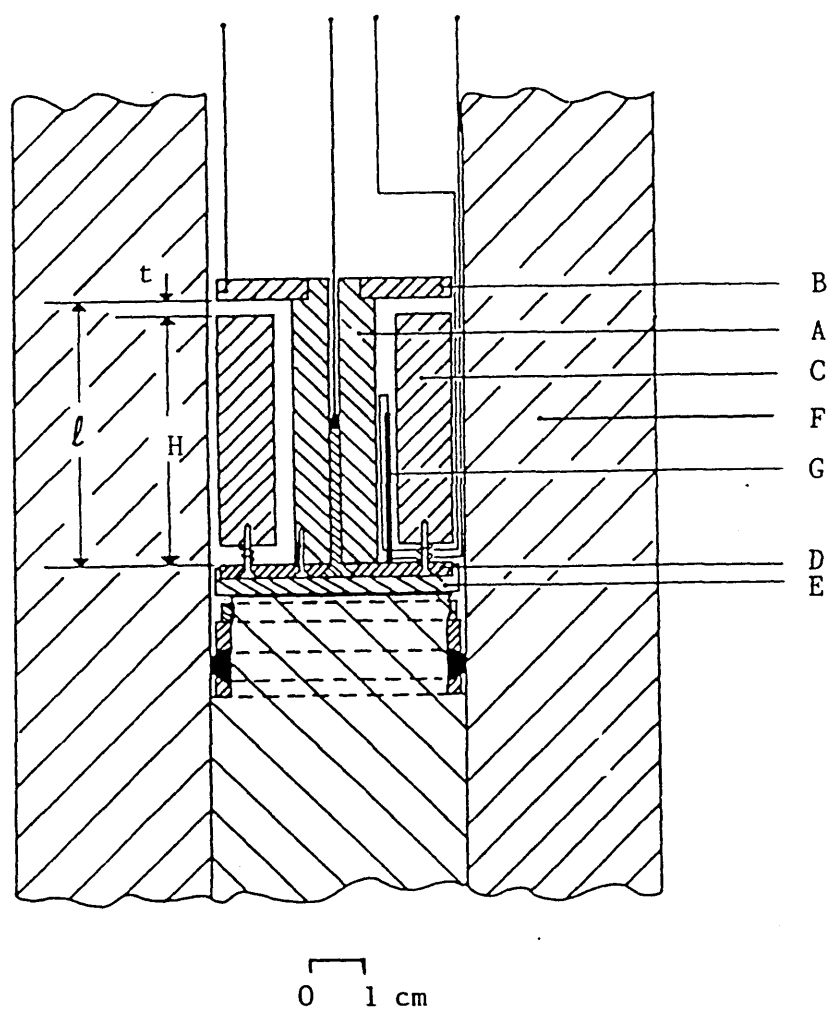
Figure 10.1 . Schematic diagram of the cell used to detect changes in
the linear strain of a polymer rod (A) as a function of
pneumatic stress. The capacitance plates are formed by
a brass ring (B) attached to the polymer rod and a
brass tube (C) screwed to a base plate (D) upon which
the polymer rests. The base plate is electrically
insulated (E) from the pressure vessel (F). A temperature
probe (G) is placed near the polymer specimen.
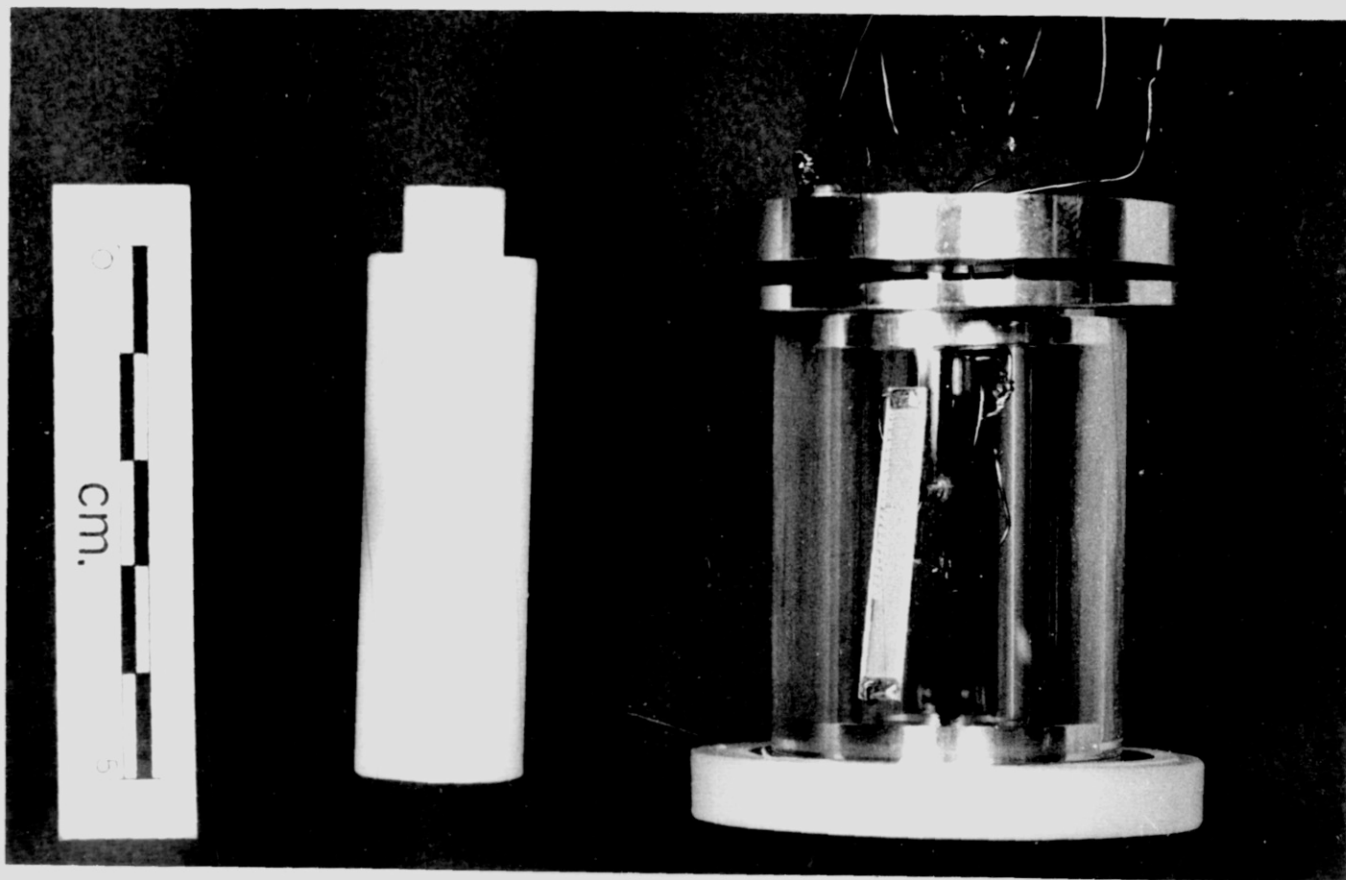
A photograph of the glass capacitance cell (see opposite page for details).
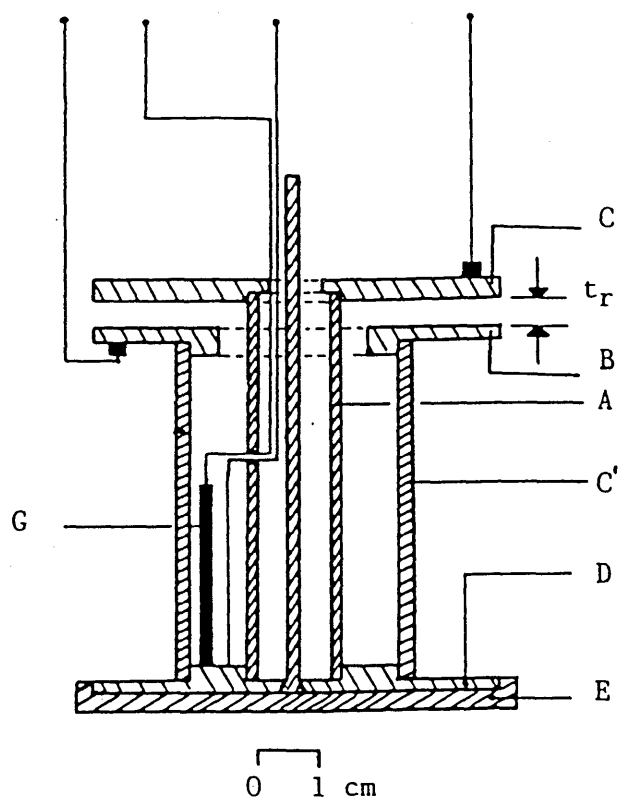
Figure 10.2 . Schematic illustration of the calibration cell used
for pneumatic studies. The two brass plates (B) and
(C) produce a geometry which is nominally identical
to that formed by (B) and (C) in Figure 10. 1.Glass
tubes(A)and(C')replace the polymer specimen (A) and
the bulk of the brass tube (C) in Figure 10.1.Other
symbols as in Figure 10.1.
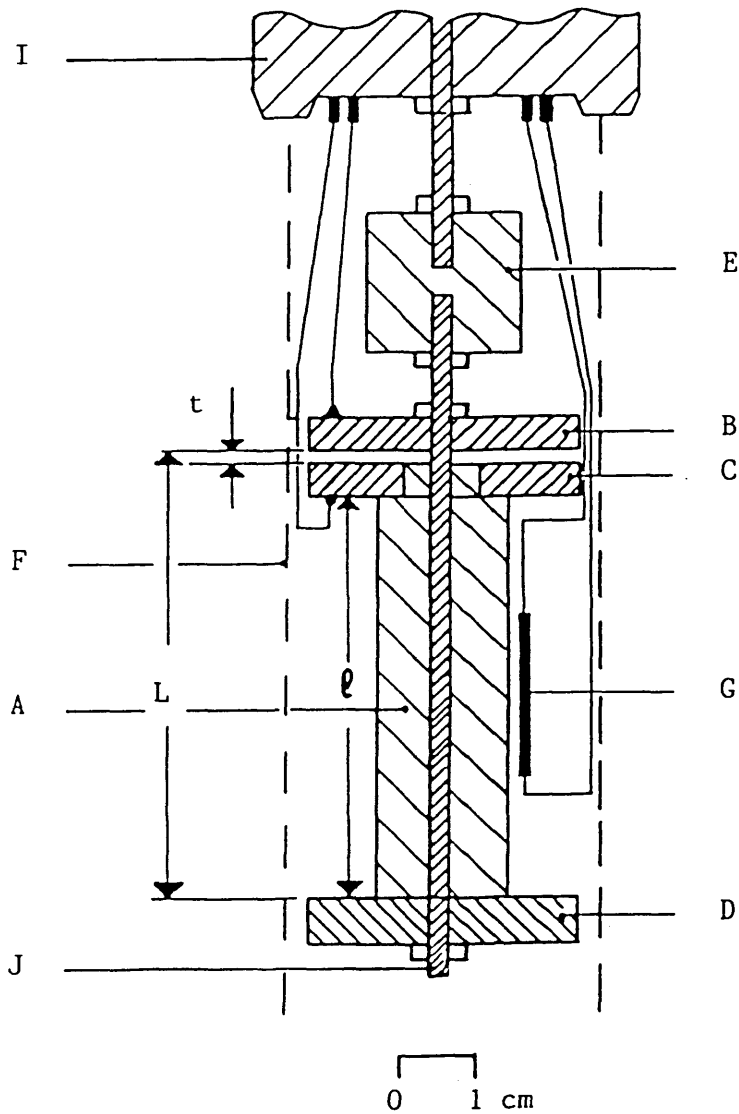
Figure 10.3. A modified version of Figures 10.1 and 10.2 for use in
hydraulic media. The equivalent capacitance plates
are (B) and (C). When (A) is of glass the cell
measures the dielectric properties of the media.
Replacing (A) by the polymer allows the measurement
of the linear strain. The whole assembly is mounted
to the top cap (I) of the pressure vessel (F) via
a 4BA screw (J). Other symbols remain as in Figure 10.1.
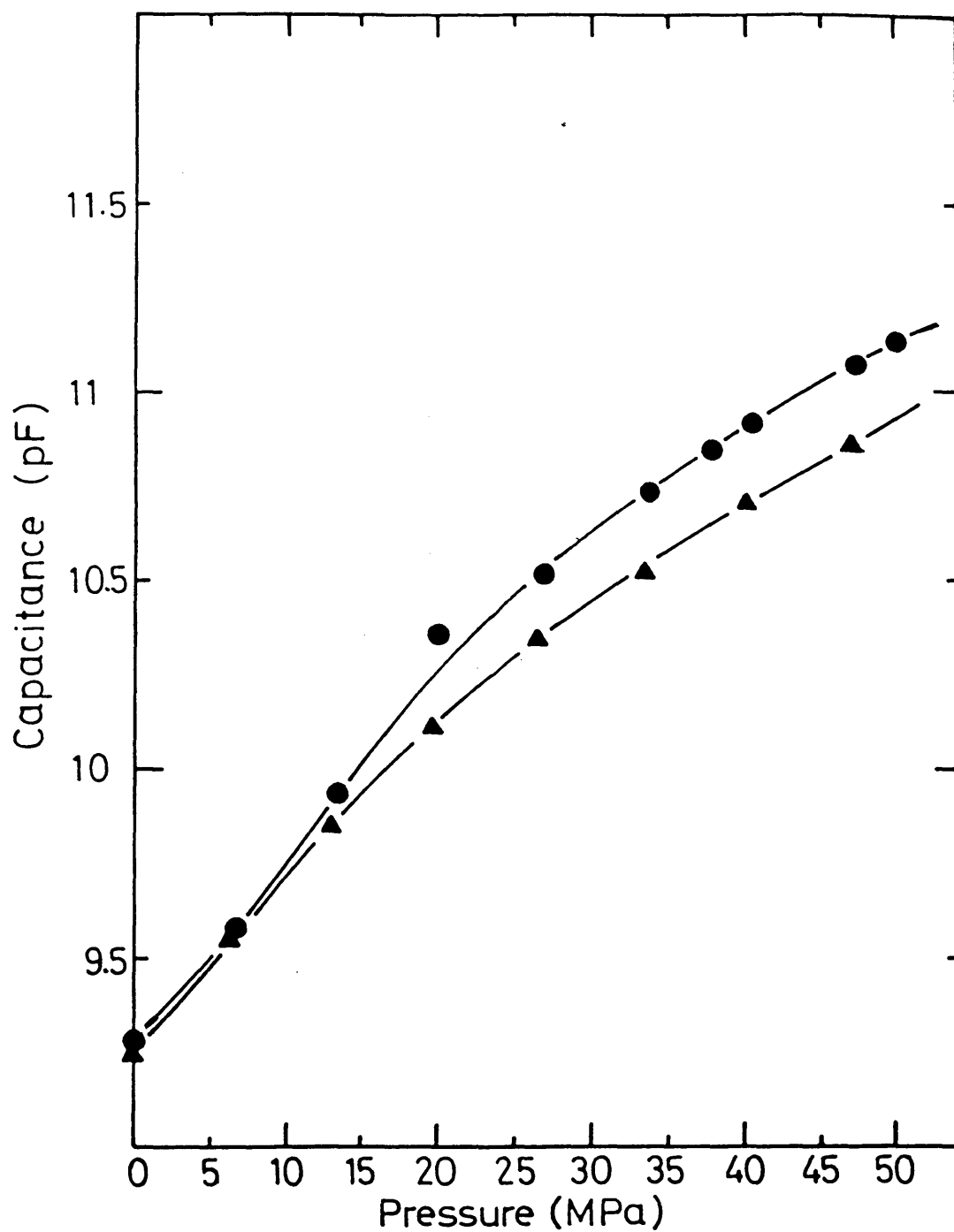
Figure 10.4. The influence of pressure on the electrical capacitance of a N_2 pressure medium: ● ,0°C; ▲ ,45 °C.
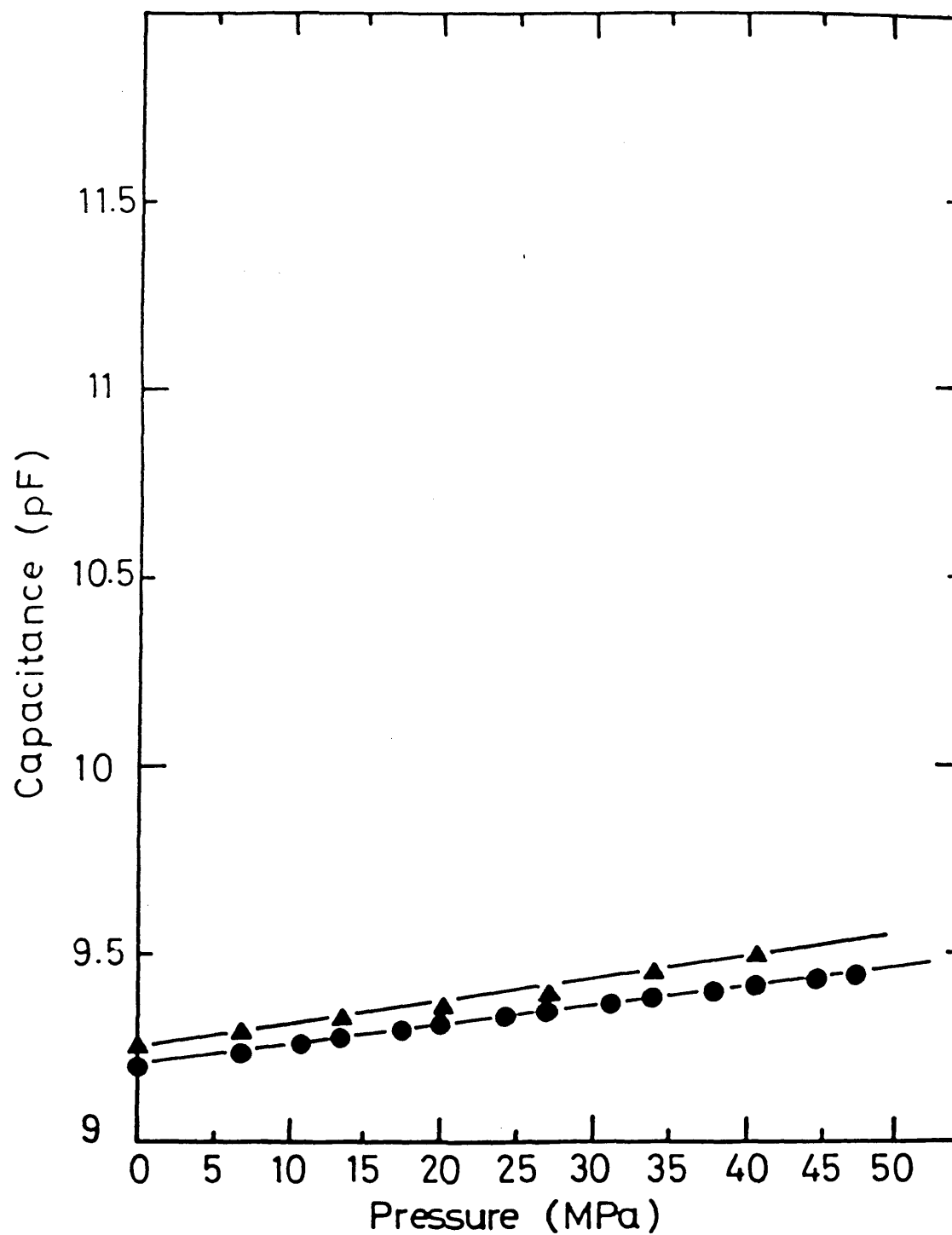
Figure 10.5. The influence of pressure on the electrical capacitance of a He pressure medium: ● ,0 °C; ▲ ,45 °C.
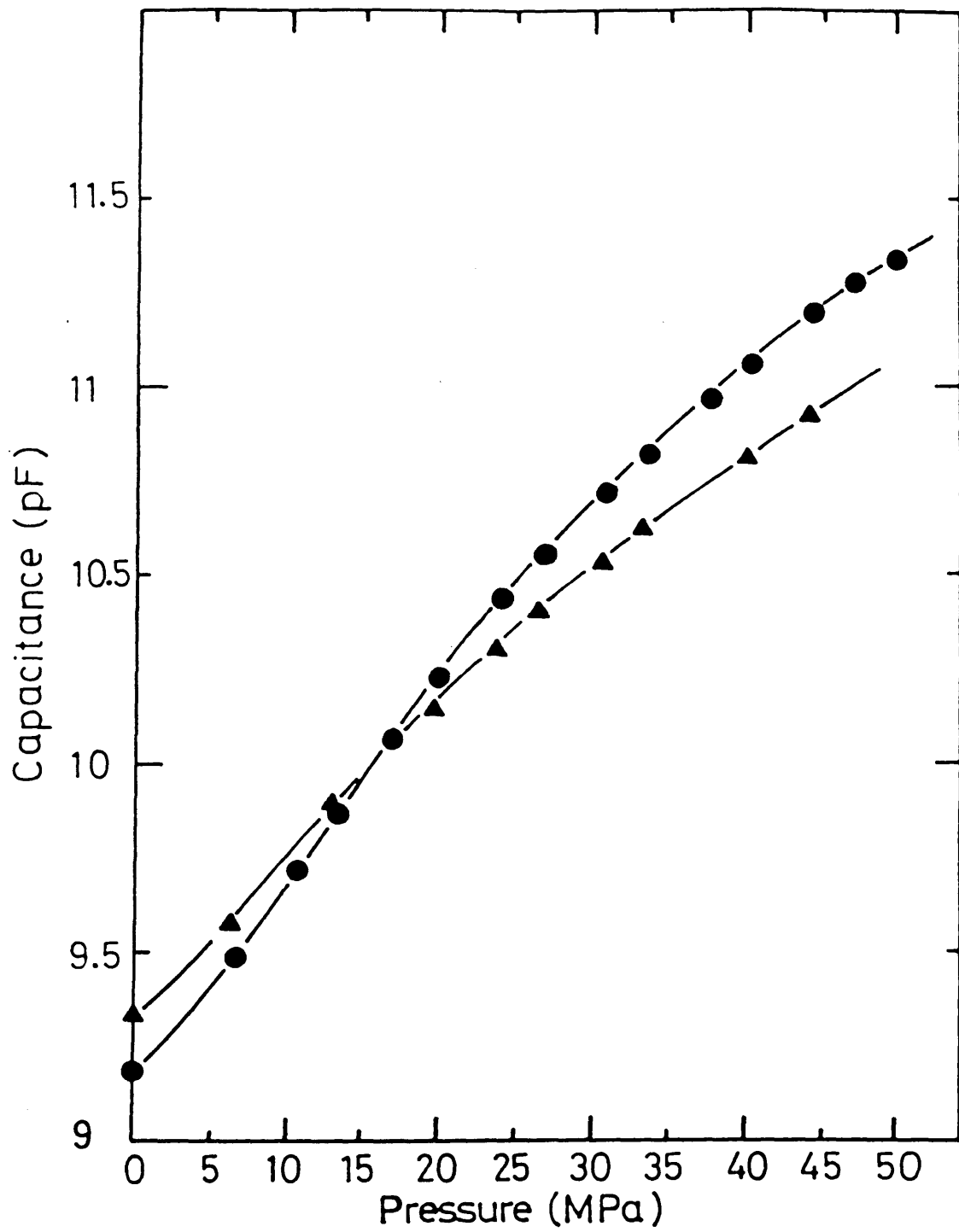
Figure 10.6. The influence of pressure on the electrical capacitance of an Ar pressure medium: ● ,0 °C; ▲ ,45 °C.
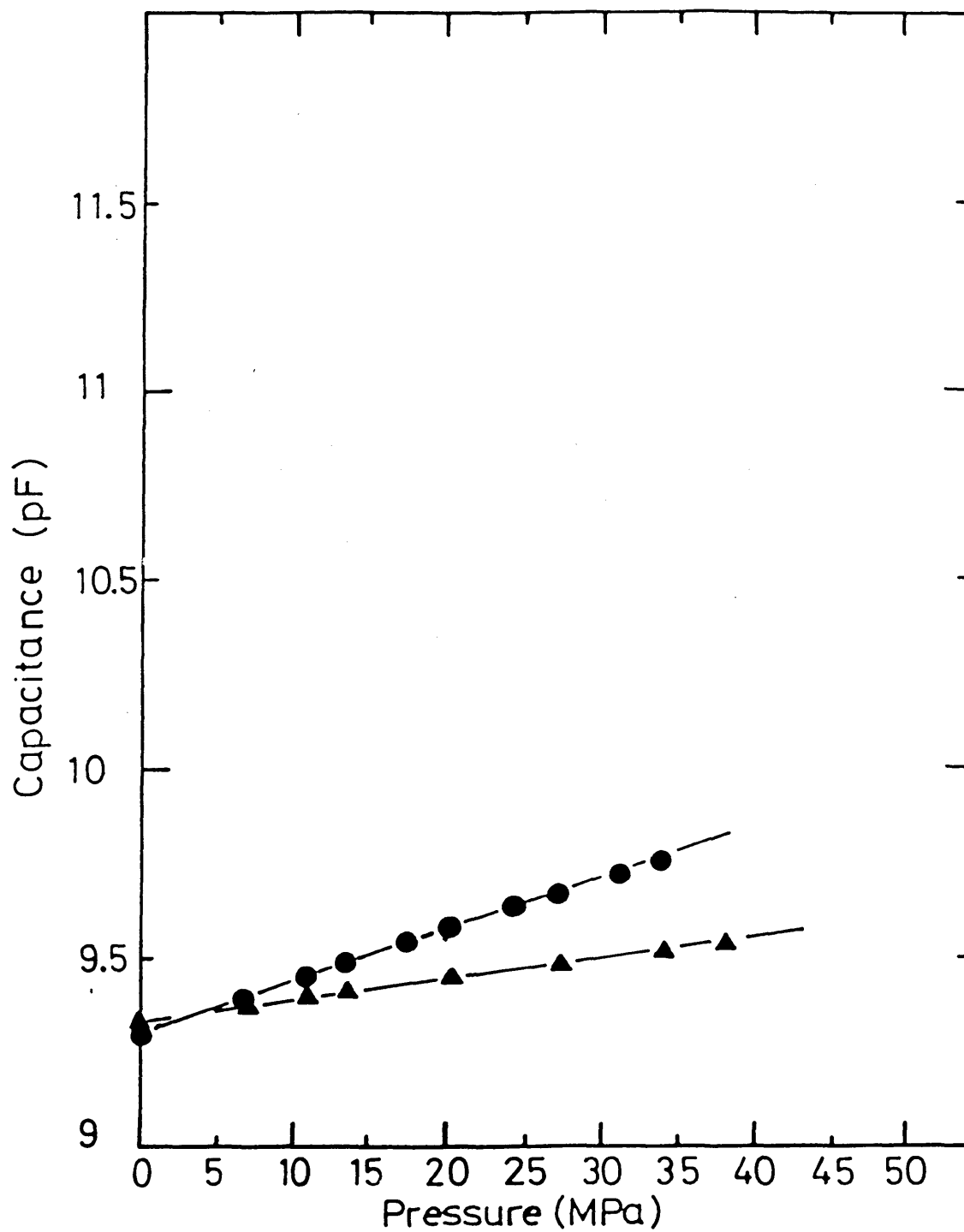
Figure 10.7. The influence of pressure on the electrical capacitance of a 1:1 v/v mixture of N_2 and He pressure medium: ● ,0 °C; ▲ ,45 °C.
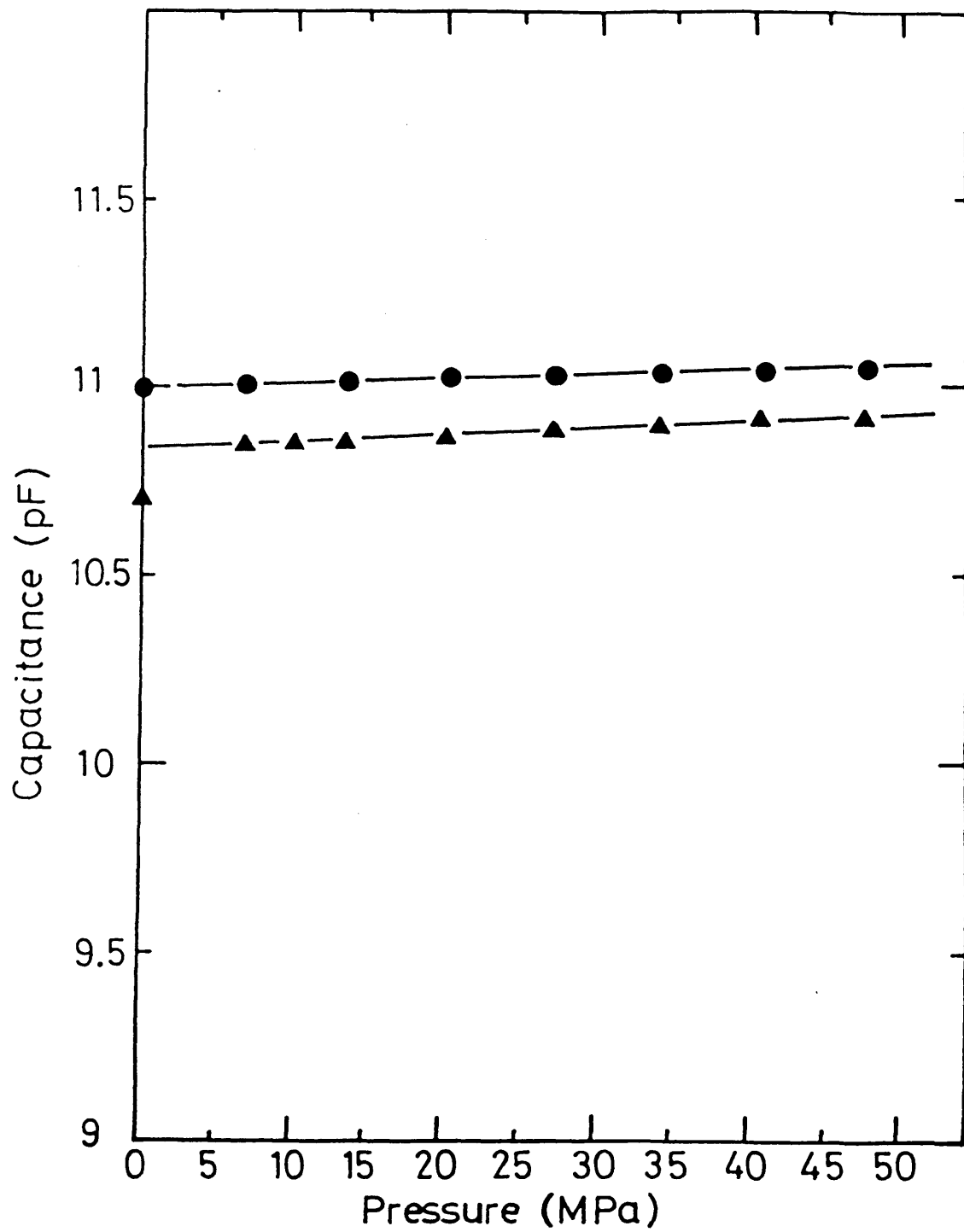
Figure 10.8. The influence of pressure on the electrical capacitance of an hydraulic oil pressure medium: ● ,0 °C; ▲ ,45 °C.
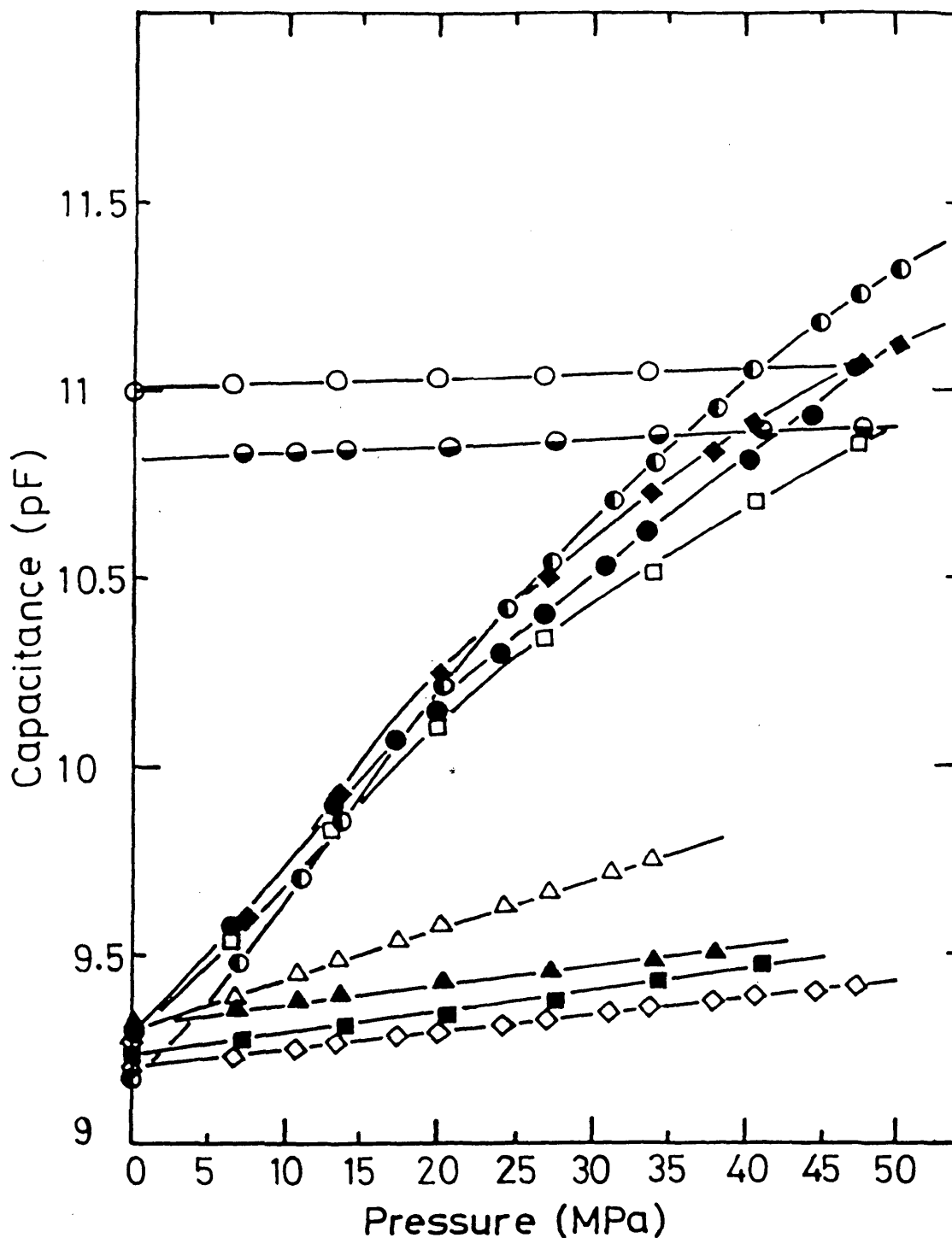
Figure 10.9. The influence of pneumatic or hydrostatic pressure on the electrical capacitance of the pressure transmitting medium: O ,hyd.oil 0 °C; ◒ ,hyd.oil 45 °C; ◐ ,Ar 0 °C; ● ,Ar 45 °C; ◆,N_2 0 °C; □ ,N_2 45 °C ; △ ,N_2/He(1:1 v/v) 0°C; ▲ ,N_2/He(1:1 v/v) 45 °C; ◇ ,He 0 °C; ■ ,He 45 °C. The appropriate coefficients for the fitting curves are given in Table 10.1.
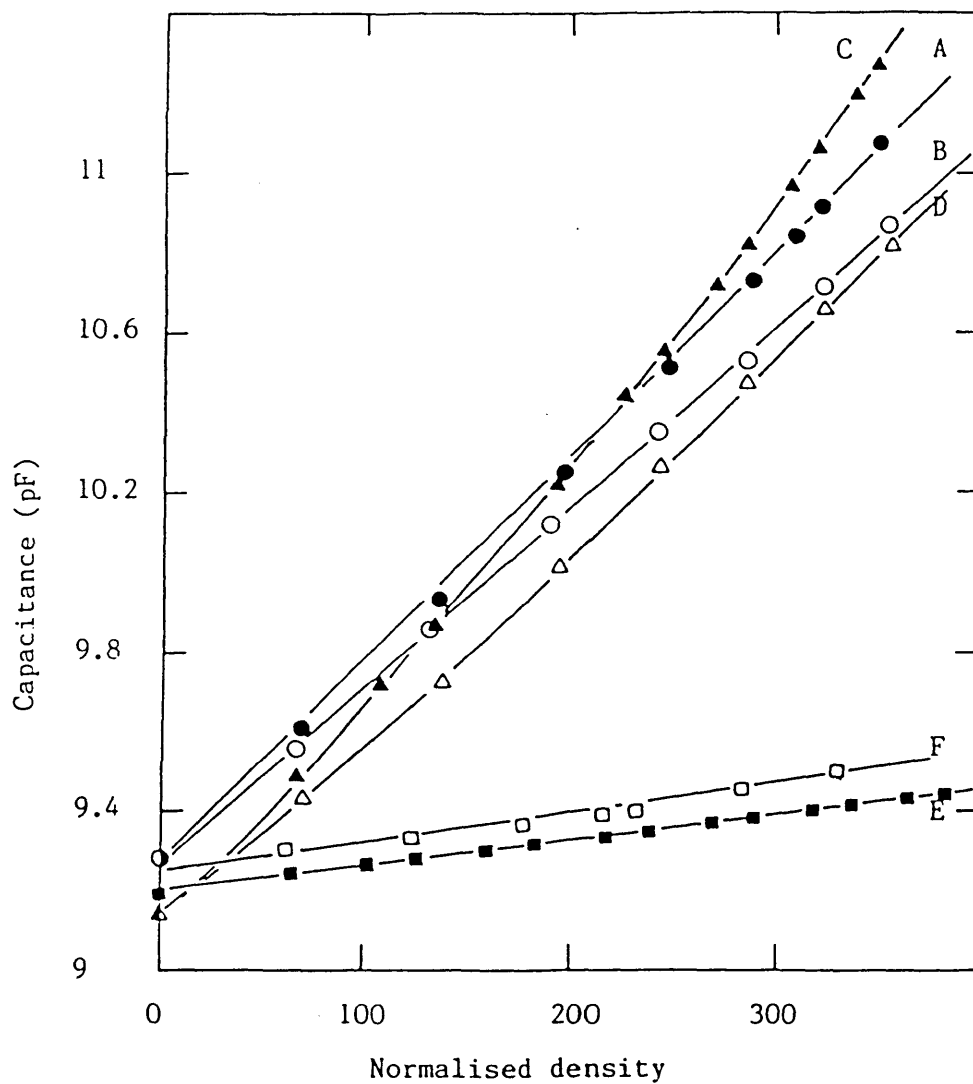
Figure 10.10. Capacitance as a function of normalised gas density
at different temperatures: curve A, N_2 $0^{\circ}C$; curve B,
N_2 $45^{\circ}C$; curve C, Ar $0^{\circ}C$; curve D, Ar $45^{\circ}C$, curve E,
He $0^{\circ}C$; curve F, He $45^{\circ}C$.
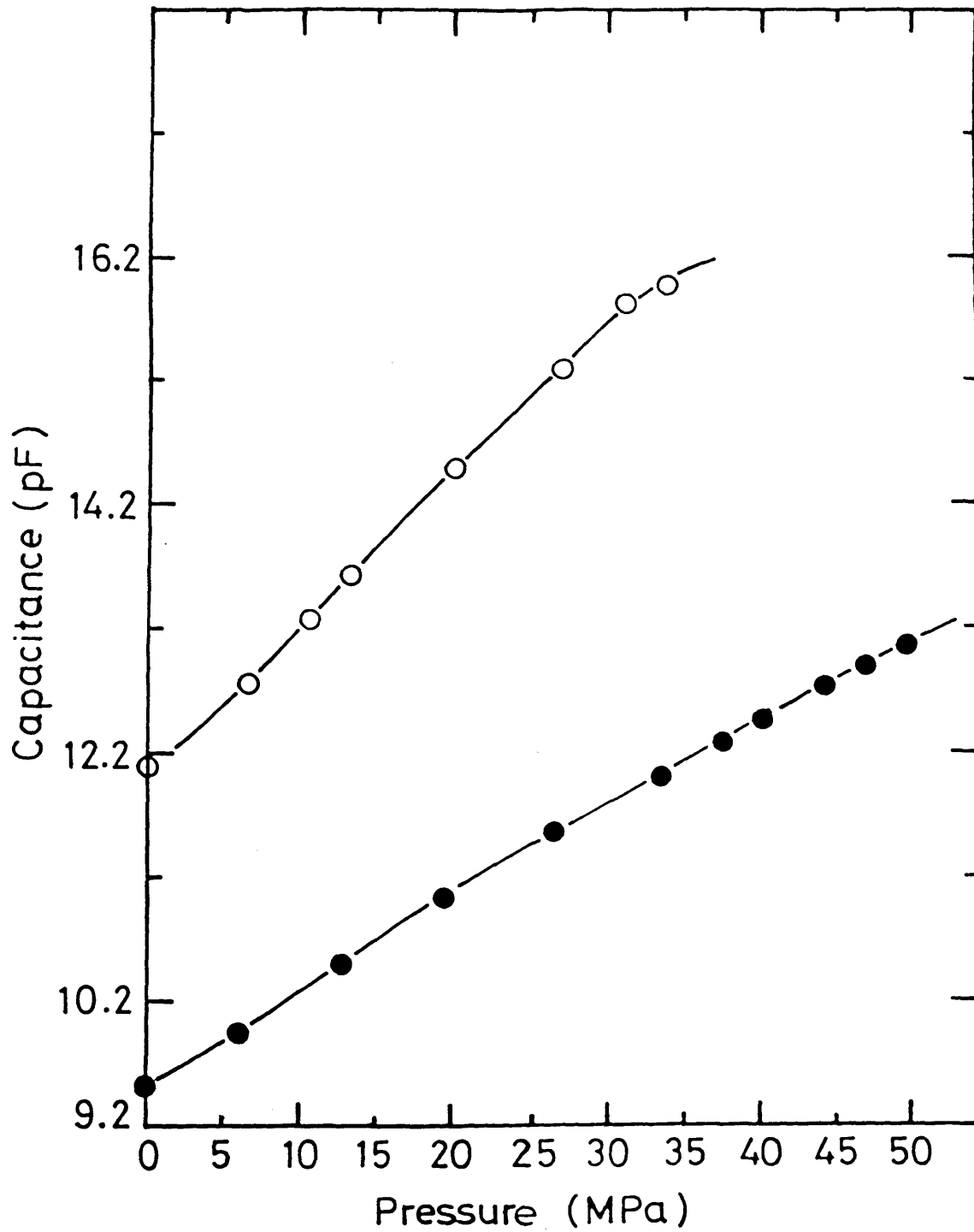
Figure 10.11. Electrical capacitance as a function of pressure using PTFE specimen: O ,N$_2$ 0 $^{\circ}$C; ● ,N$_2$ 45 $^{\circ}$C.

Figure 10.12. Electrical capacitance as a function of pressure using PTFE specimen: O ,He 0°C; ● ,He 45°C.
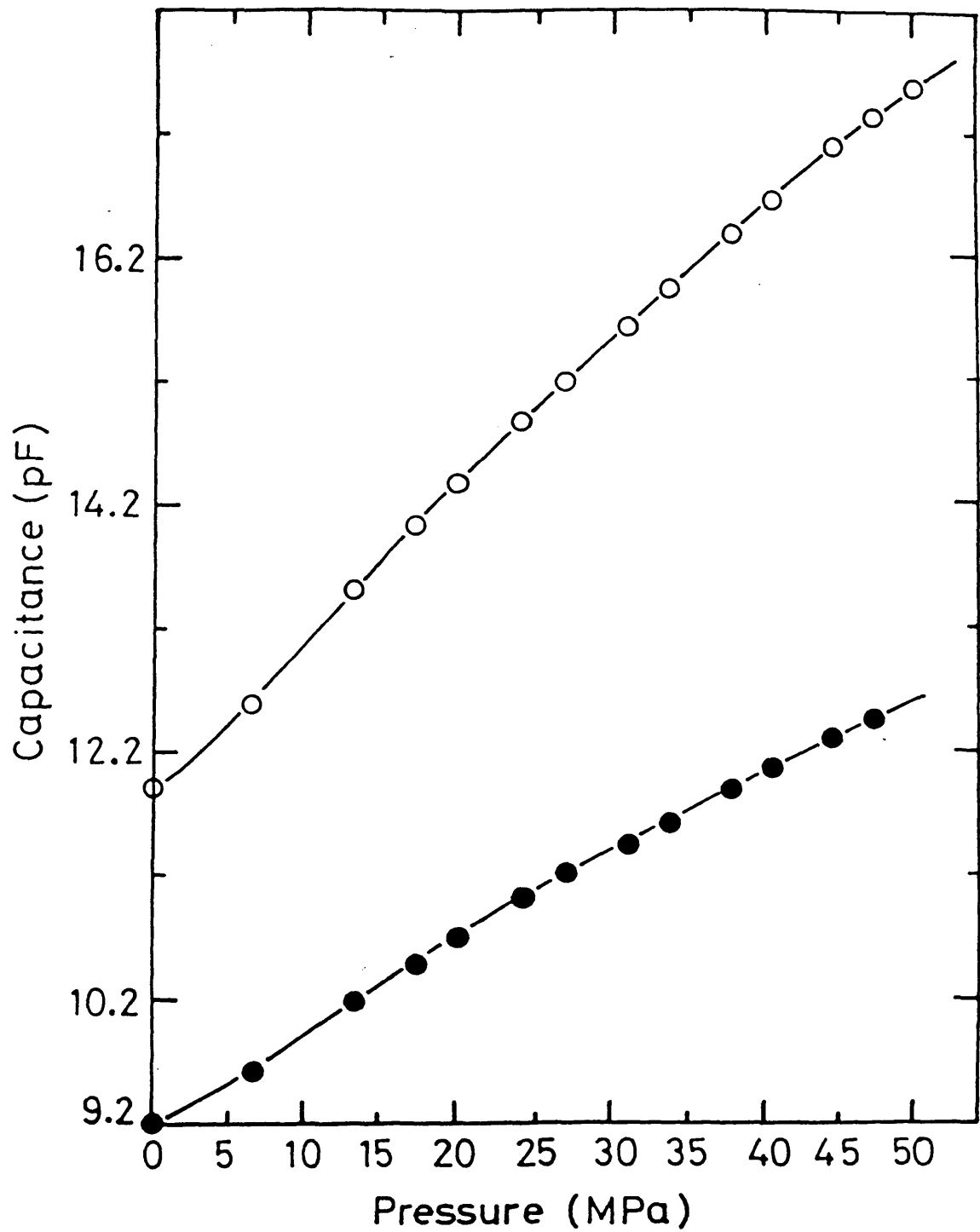
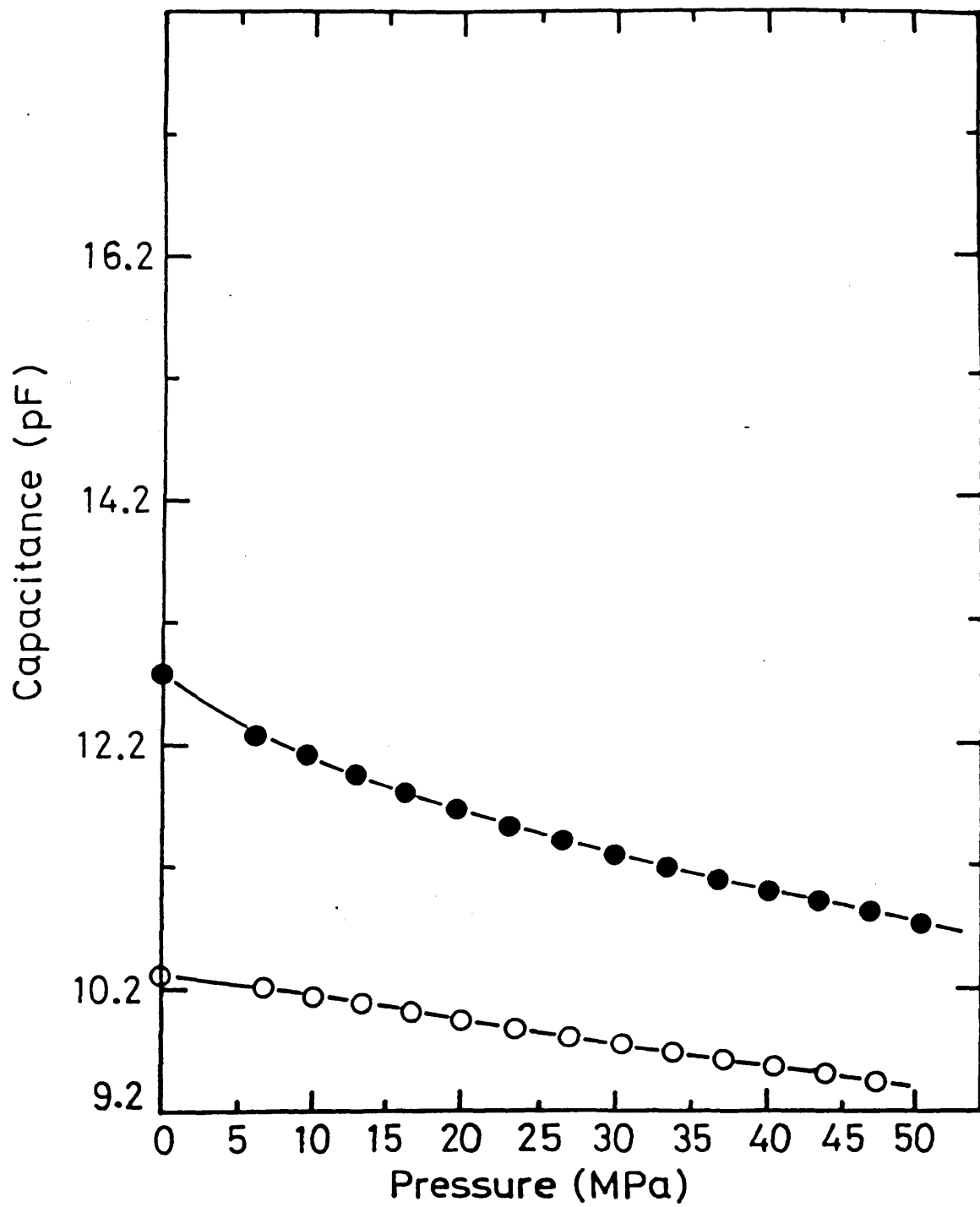Figure 10.13. Electrical capacitance as a function of pressure using PTFE specimen: O ,Ar 0°C; ● ,Ar 45°C.

Figure 10.14. Electrical capacitance as a function of pressure using PTFE specimen: O ,N_2/He(1:1 v/v) 0°C; ● ,N_2/He(1:1 v/v) 45°C.

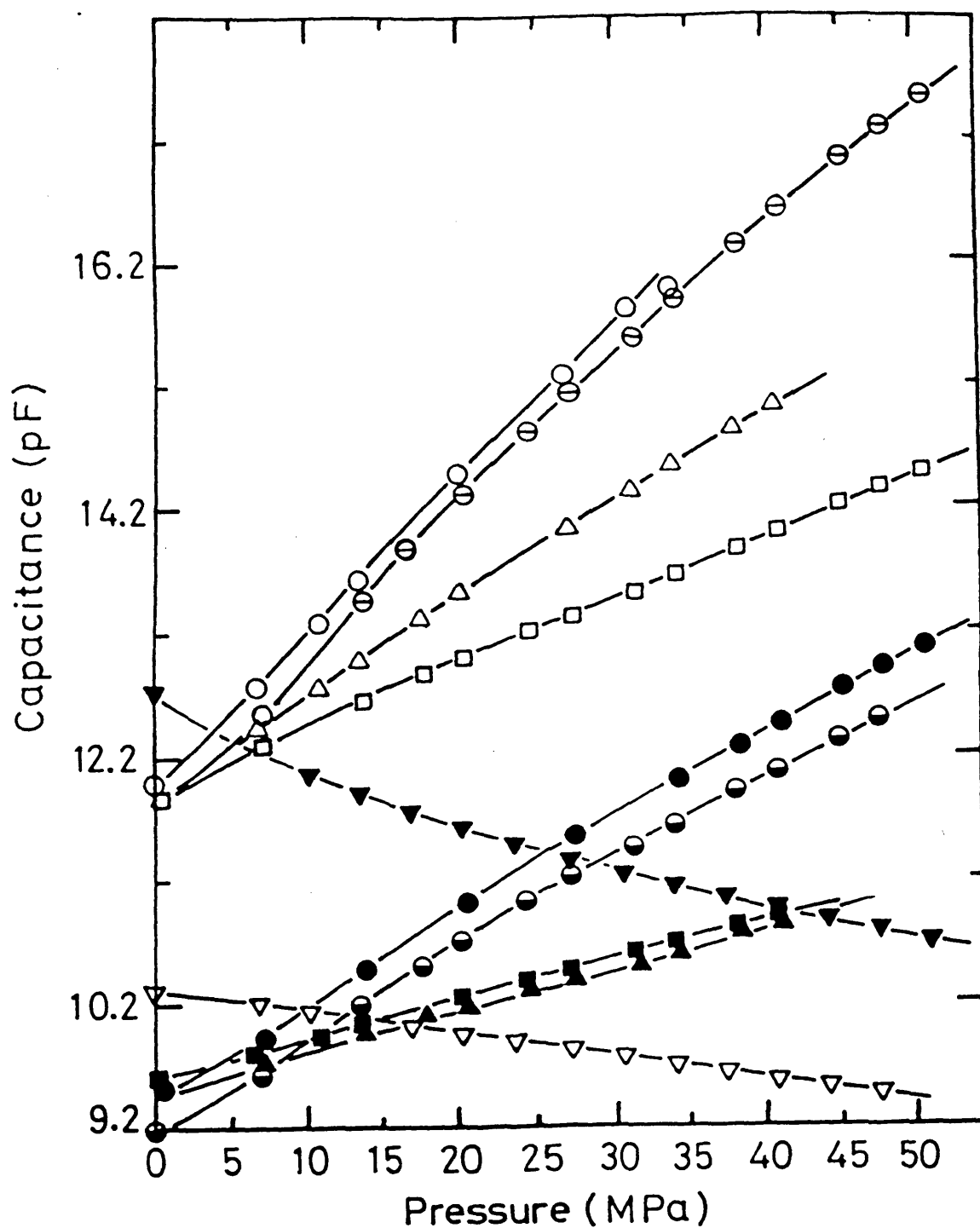Figure 10.15. Electrical capacitance as a function of pressure using PTFE specimen: O ,hyd.oil 0°C; ● ,hyd.oil 45°C.

Figure 10.16. Electrical capacitance as a function of pressure using PTFE specimen: O ,N_2 0^oC; $\bullet$,N_2 45^oC; $\ominus$,Ar 0^oC; $\ominus$,Ar 45^oC; $\triangle$, $N_2/He(1:1$ v/v) 0^oC; $\blacktriangle$,$N_2/He(1:1$ v/v) 45^oC; $\square$,He 0^oC; $\blacksquare$,He 45^oC; $\triangledown$,hyd.oil 0^oC; $\blacktriangledown$,hyd.oil 45^oC. Table 10.2 lists the appropriate coefficients for the fitting curves.
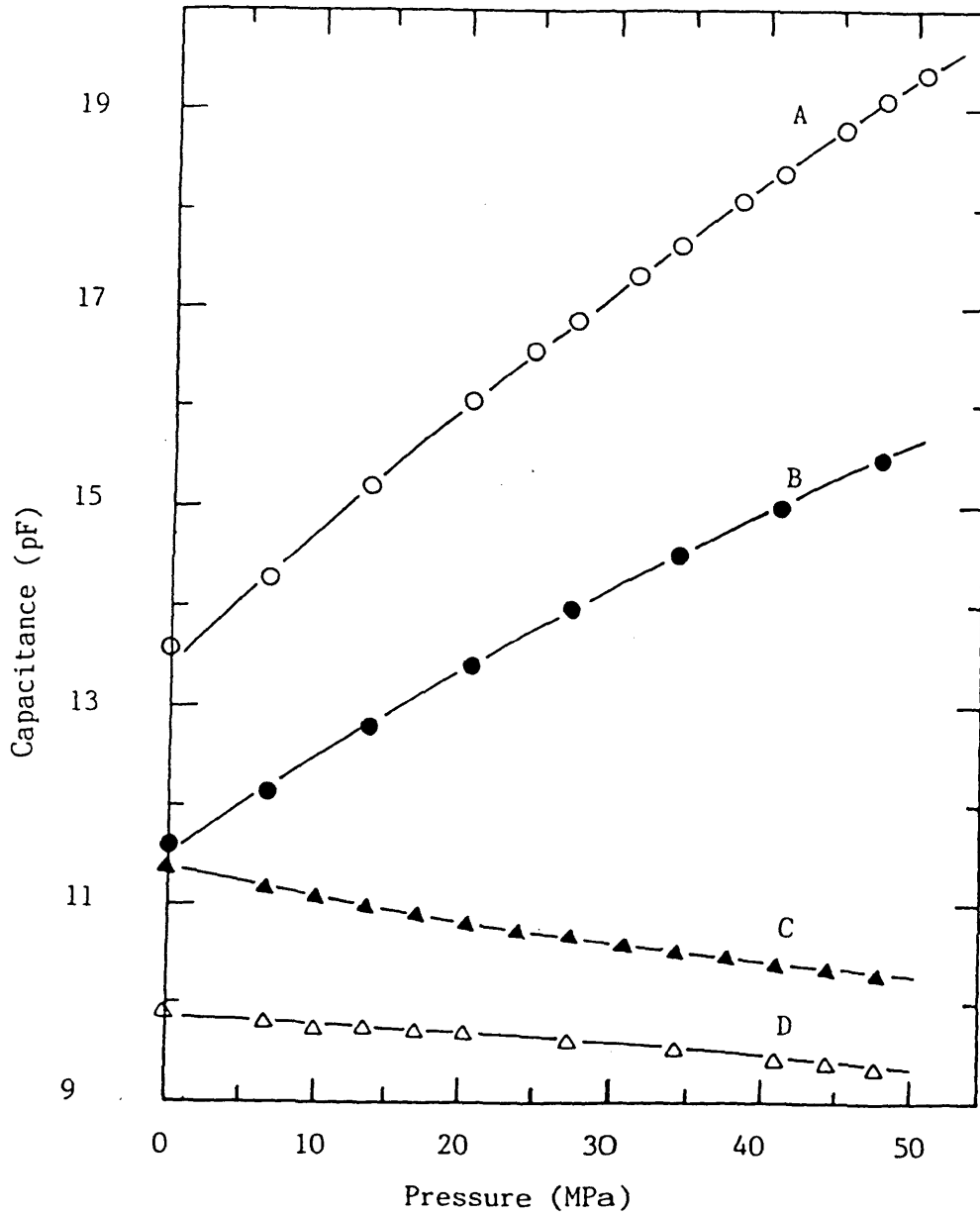
Figure 1C.17. Capacitance as a function of pressure using HDPE specimen
curve A, N_2 $0^{\circ}C$; curve B, N_2 $45^{\circ}C$; curve C, hydraulic oil
$0^{\circ}C$; curve D, hydraulic oil $45^{\circ}C$.
These data reflect changes in the geometry of the polymer
and the dielectric constant of the pressure media.
The appropriate coefficients for the fitting curves
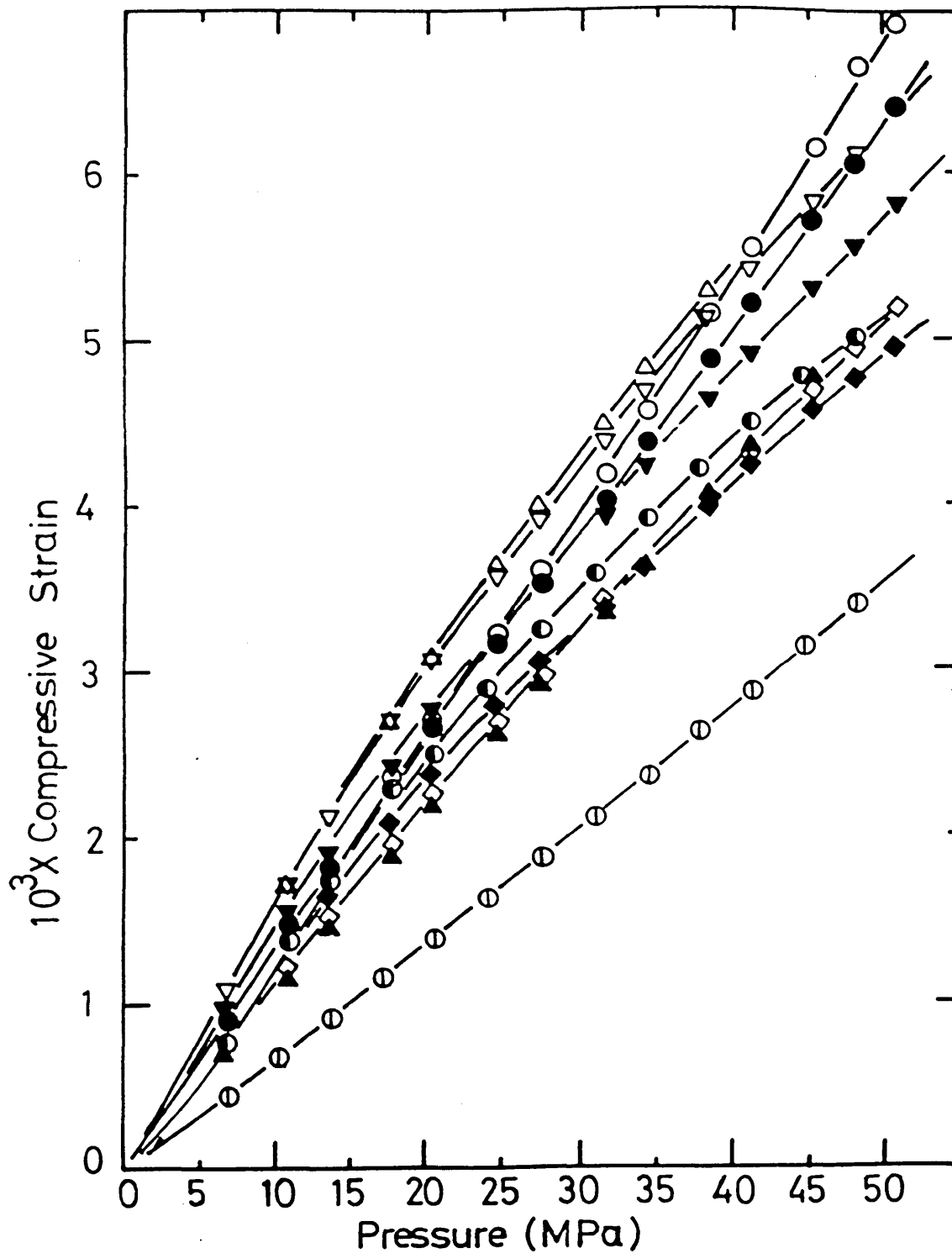are presented in Table 10.2.

Figure 10.18. Computed linear strain as a function of pressure for PTFE specimen: △ ,N₂/He(1:1 v/v) 0°C; ▲ ,N₂/He(1:1 v/v) 45°C; ○ ,N₂ 0°C; ● ,N₂ 45°C; ▽ ,Ar 0°C; ▼ ,Ar 45°C; ⊕ ,hyd.oil 0°C; ◐ ,hyd.oil 45°C; ◇ ,He 0°C; ◆ He 45°C. The appropriate coefficients for the fitting curves are given in Table 10.3.
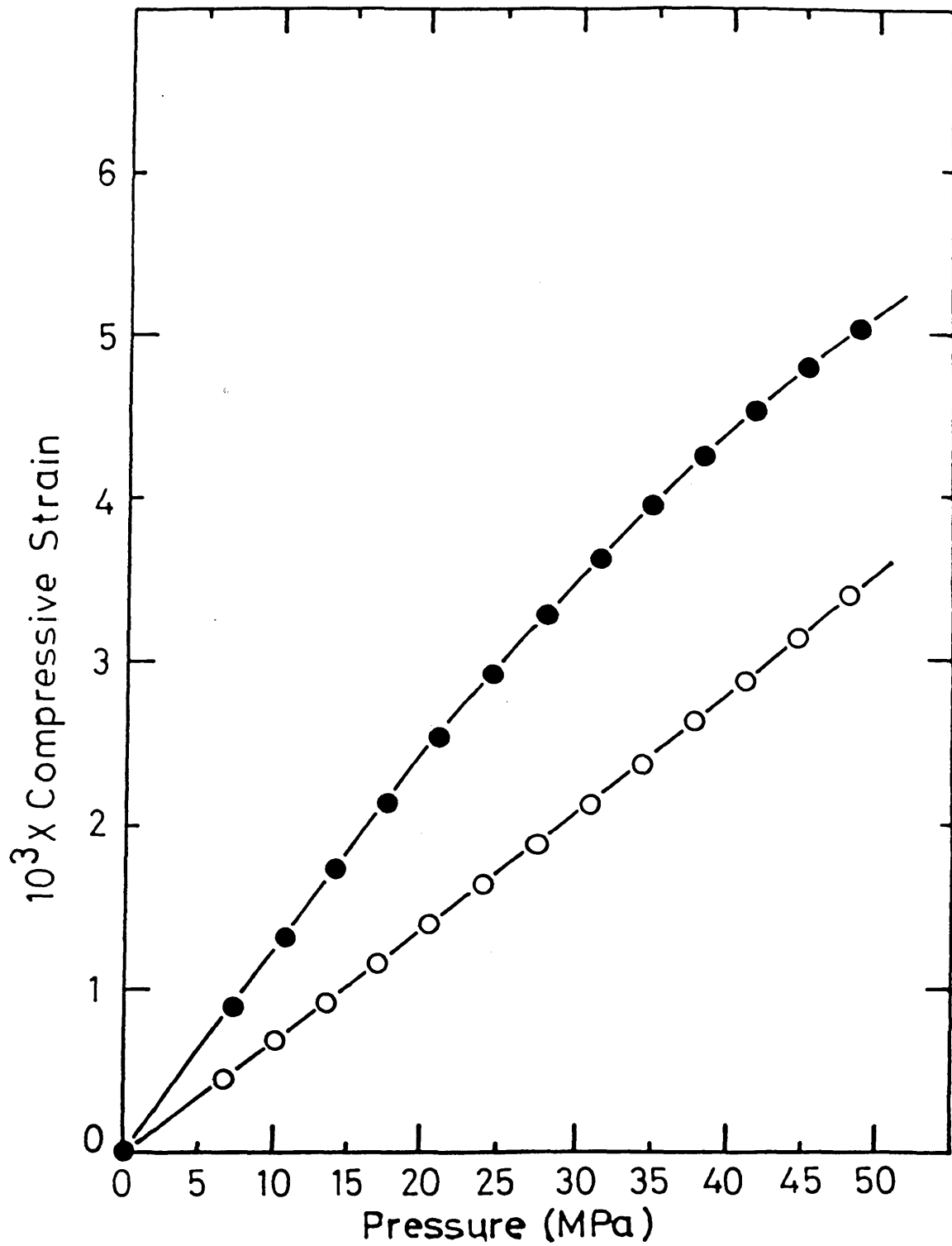
Figure 10.19.   Computed linear strain as a function of pressure for
PTFE specimen: O ,hyd.oil 0°C;   ● ,hyd.oil 45°C.

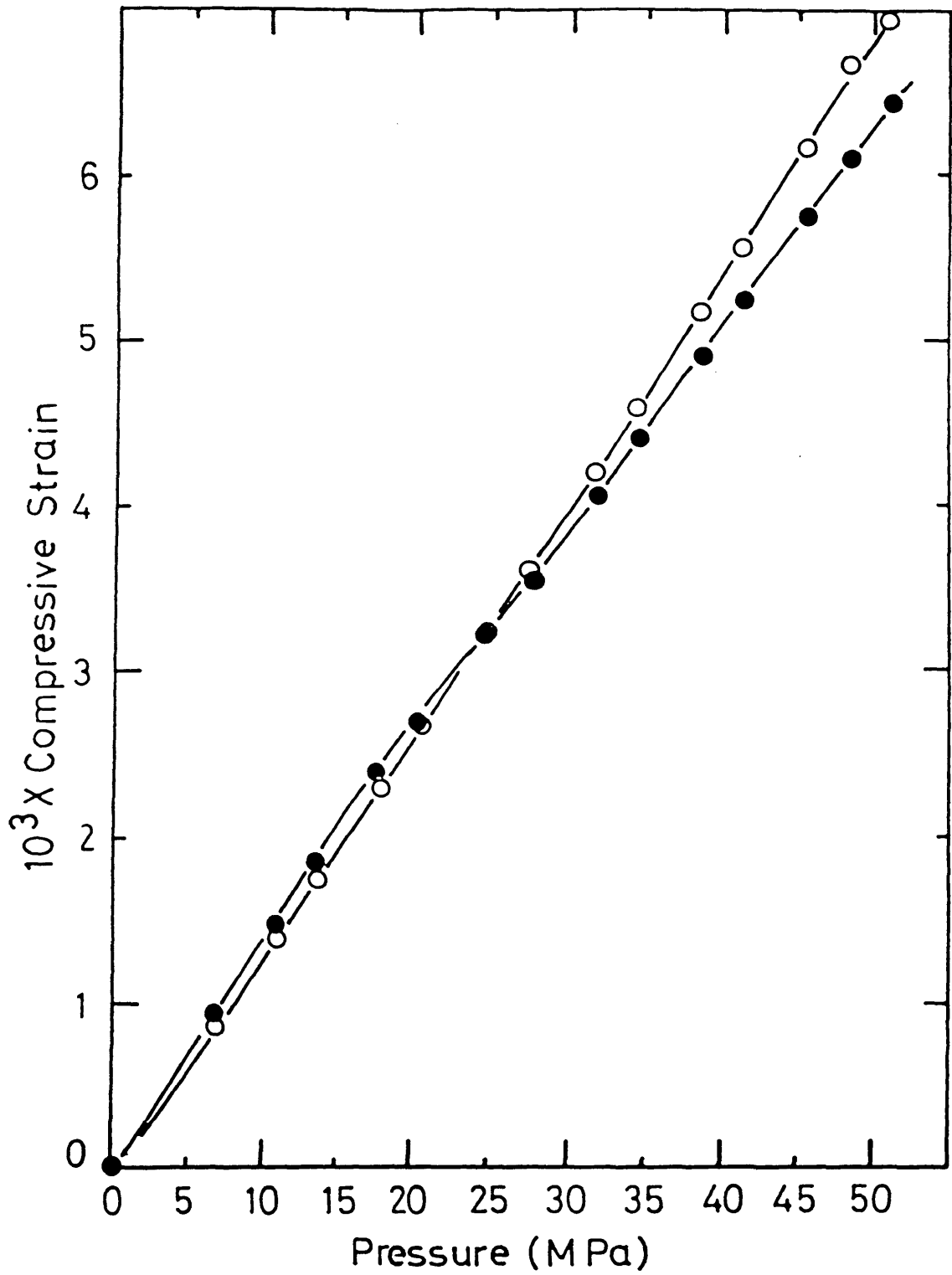Figure 10.20. Computed linear strain as a function of pressure for PTFE specimen: $\bigcirc$,N_2 $0^{\circ}C$; $\bullet$,N_2 $45^{\circ}C$.
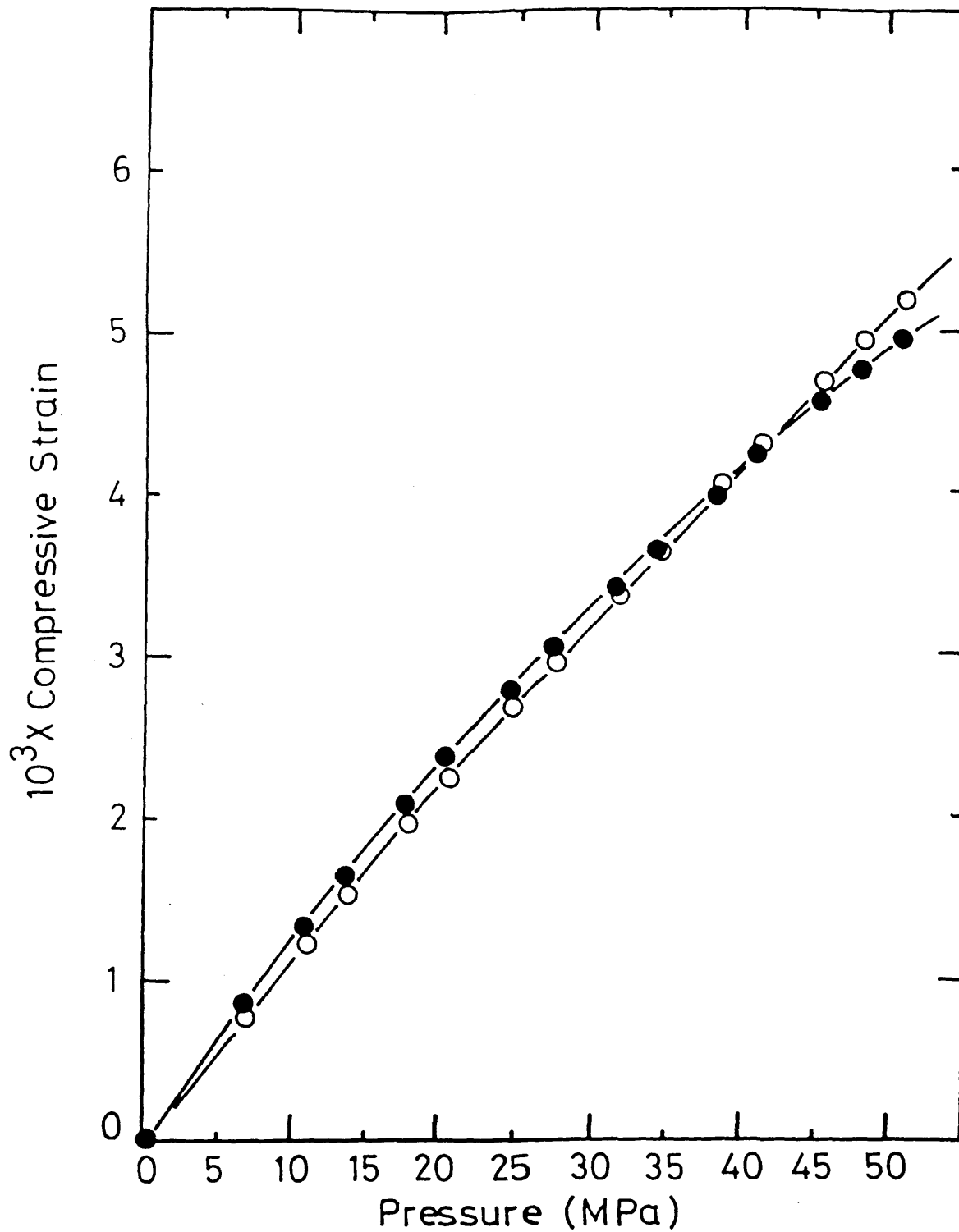
Figure 10.21.   Computed linear strain as a function of pressure for PTFE specimen: O ,He 0°C; ● ,He 45°C.
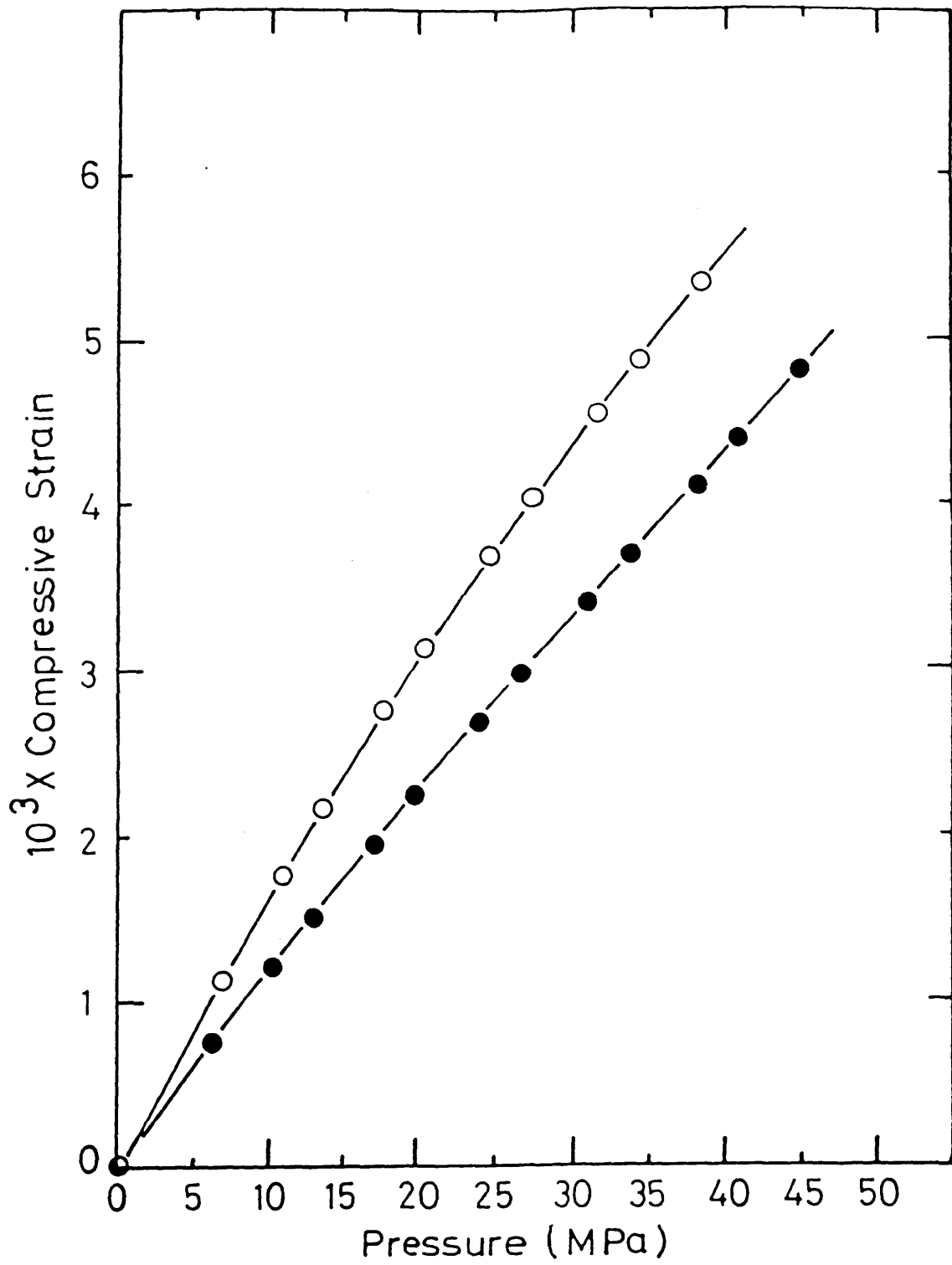
Figure 10.22.   Computed linear strain as a function of pressure for
PTFE specimen: O ,N$_2$/He(1:1 v/v) 0°C; ● ,N$_2$/He(1:1 v/v) 45°C.

Figure 10.23. Computed linear strain as a function of pressure for PTFE specimen: $\triangledown$,Ar 0°C; $\blacktriangledown$,Ar 45°C.
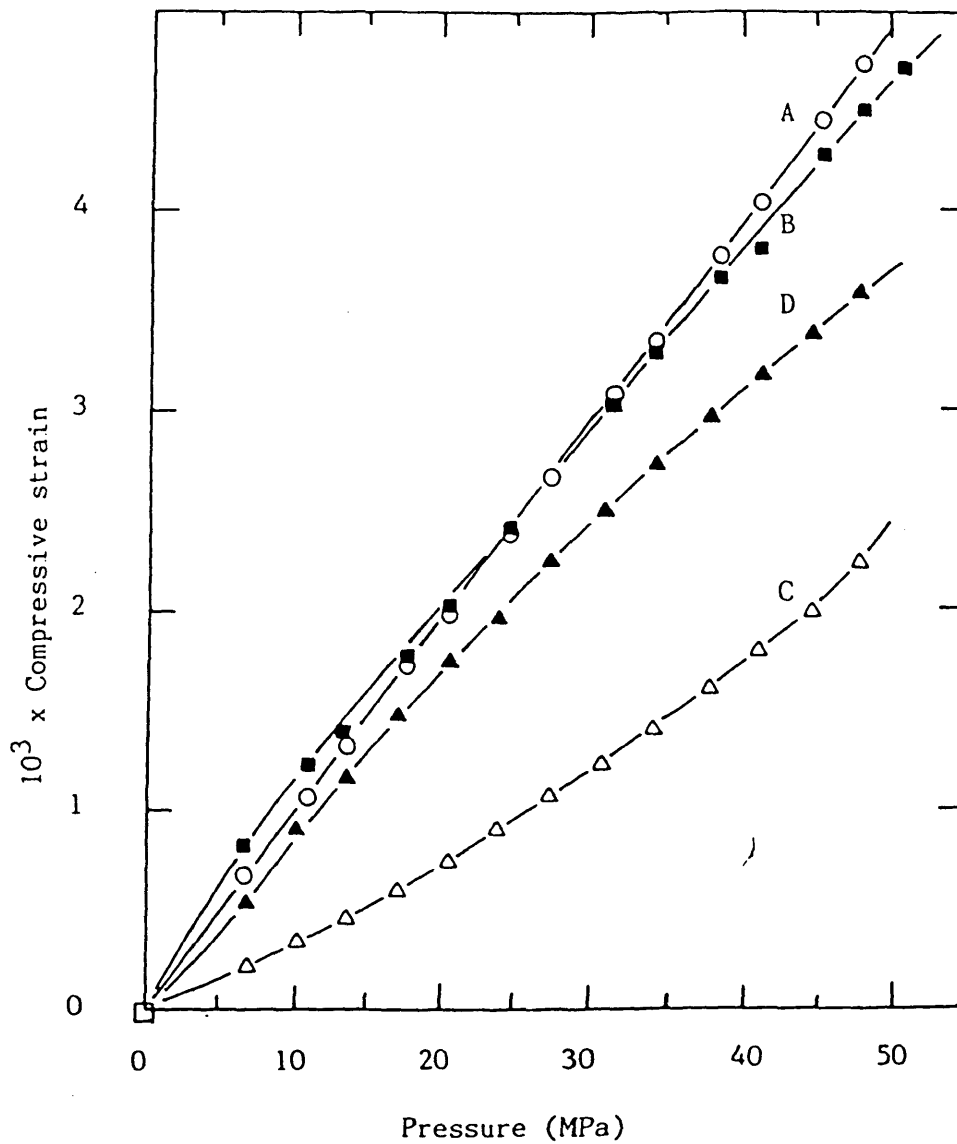
Figure 10.24. Computed linear compressive strain for HDPE as
function of pressure:curve A, N_2 $0^{\circ}C$;curve B,N_2
$45^{\circ}C$;curve C, hydraulic fliud $0^{\circ}C$;curve D,hyd-
raulic fluid $45^{\circ}C$. The data are for apparent
equilibrium for both cases. The appropriate coe-
fficients for the fitting curves are given in
Table 10.3.

Table 10.1   Values of the constants a, b and c in the second order
polynomials used to present the variation of electrical
capacitance C_g, with pressure P, using the glass cells:
$C_g = a + bP + cP^2$. Plate separations t_r are 2.7 mm and
1.59 mm for gas and liquid cells respectively.

Medium	$T(^oC)$	a(pF)	10^{10} x b(pF/Pa)	10^{18} x c(pF/Pa^2)	k(pF^{-1})†
N_2	45	9.2536	477	-297	0.12014
N_2	0	9.2515	571	-402	0.12017
He	45	9.2778	33.5	52.2	0.11977
He	0	9.2077	56.4	-14.8	0.12068
N_2/He(1/1)	45	9.3313	61.8	-27.1	-
N_2/He(1/1)	0	9.2950	140	-21	-
Ar	45	9.3072	448	-203	0.11944
Ar	0	9.1397	590	-307	0.12162
Hyd.oil	45	10.8457	7.11	22.7	-
Hyd.oil	0	10.9950	16.7	-8.8	-

†Approximate values of the dielectric constants of the gases may be
calculated from $K = k(a + bP + cP^2)$.

Table 10.2   Values of the constants, a, b and c in the second degree polynomials used to present the variation of the electrical capacitance, C_p with pressure using the polymer cell;

$$C_p = a + bP + cP^2.$$

Medium	T(°C)	a(pF)	$10^9 \times$ b(pF/Pa)	$10^{18} \times$ c(pF/Pa^2)	Polymer
N$_2$	45	9.5024	78.60	-146.9	PTFE
N$_2$	0	12.036	116.5	28.54	
He	45	9.601	32.65	-31.86	
He	0	12.0405	47.39	31.87	
N$_2$/He(1/1)	45	9.5711	30.45	24.00	
N$_2$/He(1/1)	0	11.9401	76.25	-30.52	
Ar	45	9.1498	79.46	-216.9	
Ar	0	11.8245	129.8	-317.2	
Hyd.oil	45	12.677	-59.13	418.2	
Hyd.oil	0	10.333	-18.29	0	PTFE
N$_2$	45	11.5886	92.91	-250.8	HDPE
N$_2$	0	13.5129	128.7	-278.3	
Hyd.oil	45	11.395	-32.39	196.2	
Hyd.oil	0	9.865	-6.65	-87.6	HDPE

Table 10.3   Values of the constants a, b and c in the second order polynomials used to present the variation of the compressive strain, ε, with pressure, P;

$$\varepsilon = a + bP + cP^2.$$

Medium	T(°C)	$10^7 xa(pF)$	$10^{11} x$ $b(pF/Pa^2)$	$10^{20} x$ $c(pF/Pa^2)$	Polymer
N_2	45	60.49	13.20	-12.74	PTFE
N_2	0	-141.3	12.48	24.69	
He	45	118.4	12.72	-58.89	
He	0	-36.92	11.44	-24.43	
N_2/He(1/1)	45	-91.00	11.10	-11.68	
N_2/He(1/1)	0	8.20	16.72	-74.90	
Ar	45	259.3	16.46	-80.31	
Ar	0	-368.6	14.44	-60.97	
Hyd.oil	45	-389.5	13.93	-70.21	
Hyd.oil	0	-73.80	6.57	10.19	PTFE
N_2	45	131.09	9.86	-15.73	HDPE
N_2	0	14.51	10.09	-5.31	
Hyd.oil	45	-321.7	9.35	-38.76	
Hyd.oil	0	7.28	2.93	34.49	HDPE

C H A P T E R   1 1

THE EFFECT OF VARIOUS PRESSURE MEDIA ON THE

$20^{o}C$ AND $30^{o}C$ TRANSITIONS IN PTFE

11.1 Introduction

Significant gaseous sorption occurs at high pressures in all the

polymers studied including PTFE. In the case of PTFE, preliminary

calculations of the estimated volumetric uptake is up to 17% V/V. It

is therefore not possible to accommodate these relatively large volumes

of gas in the normally accepted free volume spaces in the polymer mat-

rix without matrix expansion. For example, a PTFE specimen exposed to

a N_2 pressure of 51 MPa is thus expected to expand by 7% at room

temperature. Direct measurements on PTFE and HDPE (see Chapter 10) show

a contraction of the polymers, the magnitude of which is to a first

order comparable to that in a liquid pressure environment and to a second

order rather dependent on the type of pressure medium used. Surprisingly,

the polymers are found to be more compressible in gaseous pressure media.

Typically, a PTFE specimen is found to contract linearly by ca. 0.5%

when compressed to a maximum pressure of 51 MPa using a He pressure

medium. The corresponding value in the case of N_2 pressure medium is

larger (ca. 0.8%) but in hydraulic fluid the value is ca. 0.5%.

This Chapter reports the results of various experiments on the

effect of different pressure environments such as He, N_2, Ar and a

hydraulic oil on the crystalline $20^{o}C$ and $30^{o}C$ transitions in PTFE up

to a maximum pressure of 51 MPa. These results reveal that the shift

in the room temperature transition, dTg/dP and the transition volumes

are dependent on the type of the pressure medium used, the magnitude

of dTg/dP being smaller in the case of gaseous media. Values of dTg/dP

for a hydraulic oil, He, N_2 and Ar pressure media are 0.21, 0.20, 0.19

and $0.16^{o}C/Mpa$ respectively. Also, in the case of the gaseous media, the transition volume increases with increasing pressure. This is in direct contrast to the behaviour in a liquid pressure medium.

11.2 Results

Figures 11.1 to 11.4 represent the results of capacitance measurements using the polymer capacitance cells (see Figures 10.1 and 10.3) incorporating medium crystallinity $(2.157$ g cm^{-3}; 70% crystallinity) PTFE specimens in a temperature range of 0 to $55^{o}C$ at various isobars of 0.101 to 48.2 MPa using a hydraulic oil, N_2, He and Ar pressure media respectively. It should be borne in mind that the liquid polymer cell (Figure 10.3) produces an inverse response to that of the gas polymer cell (Figure 10.1) following an expansion or contraction of the polymer. The temperature of the polymer at each isobar was increased at an average rate of ca. $6^{o}C/hr$. Also, at the end of each temperature run, the polymer specimen was slowly (ca. 10 minutes) depressurised and cooled to $0^{o}C$ for no less than 18 hrs before moving to a higher isobar. A new polymer specimen was used for each pressure medium to avoid any complications associated with the permanent densification of the polymer (see later).

The sudden change in capacitance (Figures 11.1 to 11.4) with increasing temperature for each isobar is associated with a rapid expansion of the polymer around the atmospheric $20^{o}C$ and $30^{o}C$ transitions although their precise location in the above data is uncertain. Before attempting to determine the location of these transitions, it is interesting to note some important features in these data. Figures 11.5 and 11.7 are the variation of the temperature dependence of the capacitance data, dC/dT with increasing pressure before and after the completion of each transition respectively. These data were obtained by measuring the slopes of the best straight lines through both tail

ends of each isobar (see Figure 11.1 as an example). As in the case of the gaseous pressure media,an expansion of the polymer corresponds to a reduction in capacitance (see Figure 10.1),it is prudent to invert the data for gases to obtain a relative measurement of the coefficient of the thermal expansion of the polymer in these media. These are represented in Figures 11.6 and 11.8. It is fair to assume that these data represent a measure of the change in the coefficient of thermal expansion of the polymer with increasing pressure $((dV/dT)/dP)$ as the variation of the capacitance of the pressure media with temperature is relatively small (see Figure 10.9).

Some interesting features of the data in Figures 11.7 and 11.9 may be summarised in the following sections:

(a)   For all media, the thermal expansivity (dV/dT) decreases with increasing pressure. In the case of the gaseous media, it may be argued that as pressure and temperature increase, the polymer is exposed to an external triaxial compression opposed by an internal expansion due to an increase in gaseous uptake. The former effect is however the predominant factor.

(b)   The pressure dependence of the polymer thermal expansion data before the initiation of transitions $(dV/dT)/dP$ (Figure 11.6) and the values of dV/dT in the pressure media decrease in the following order; $He < N_2 < Ar <$ hyd. oil. It is interesting to note that in the case of the gaseous media, the pressure dependence of the room temperature transition in PTFE increases in the same order as above (see later).

(c)   The values of $(dV/dT)/dP$ following the completion of transitions (Figure 11.8) is approximately the same for all pressure media. This time, however, dV/dT in 'all' pressure media decreases in the same order as the pressure dependence for the room temperature transition increases, i.e. hyd. oil $< He < N_2 < Ar$.

Finally, Figure 11.9 describes the variation of the induced

volumetric strain at transition (ΔV) with increasing pressure for PTFE

in various pressure media. The values of ΔV were approximated as 3 x

the linear strain calculated from equations (10.7) and (10.9). These

calculations were carried out on the basis of the assumption that the

variation of the capacitance of the pressure media during the transition

with temperature was small and linear. This was a necessary assumption

as the data relating to the change in the electrical capacitance of the

pressure media with pressure in the region of the transition temperatures

were not available. These assumptions are probably partly responsible

for the wide scatter in the data. However, the best straight lines

fitted to the above data using root mean squares reveal some interesting

features. First, the values of ΔV at various pressures are specific

to the type of the pressure medium employed and in the case of the

gaseous media, ΔV increases with increasing pressure. The reverse is

true in the case of the liquid pressure media. Also, ΔV in gaseous

environments at all pressures is always more than the corresponding

values in a liquid pressure medium. In the liquid case, it can be

argued that as ΔV decreases with pressure some of the required free

volume is accommodated not by matrix expansion which requires the

system to do work but by local reordering, i.e. the matrix densifies

in some regions (amorphous regions) to provide extra space. The gas

case is clearly different; the matrix volume change increases with

pressure. The phenomenon may be argued in two ways. As the gas enters

the matrix the effective triaxial stress is less; this is not consis-

tent however with the observation that in gases more "overall" matrix

contraction is observed. Alternatively, since the gas is in the matrix

it now prevents the sort of matrix volume restructuring invoked for

the liquid medium. The vacant volume which could provide the free

volume by reordering is no longer present. N_2 seems to inhibit the supposed ordering more than He which is not what would be expected on the grounds of simple gas concentration. Also the N_2 data are distinctly non-linear. The above cannot be explained unequivocally but can be ascribed to specific interactions of N_2 with sites of volumes close to their molecular size.

Going back to Figure 11.2, curve A' is the response of a PTFE specimen at atmospheric pressure which has already completed the full N_2 pressure cycle. The upward shift of this curve relative to the response of the virgin specimen (curve A) represents a permanent densification of PTFE.

Figures 11.10 to 11.13 describe the variation of the temperature dependence of the capacitance data, $\frac{dC}{dT}$ (second order variation) with temperature for a hydraulic oil, N_2, He and Ar pressure media at various pressures up to 51 MPa. These data were obtained by fitting various degree polynomials to each isobar in Figures 11.1 to 11.4 and evaluating values of $\frac{dC}{dT}$ at temperature intervals of $0.1^{\circ}C$. Each three values of $\frac{dC}{dT}$ corresponding to three consecutive temperatures were then averaged and presented as one data point in the Figures. This latter procedure greatly reduced the amount of scatter in the data. The results show two peaks at each isobar. The first, occurring at around $20.7^{\circ}C$ at atmospheric pressure, is more pronounced and is associated with the room temperature transition of PTFE (Rigby and Bunn, 1949). The second peak, which is much broader and shallow, occurs at ca. $31^{\circ}C$ at atmospheric pressure and was first reported by Quinn et al (1959). It should be pointed out that the height of these peaks not only depends on the magnitude of the particular molecular relaxation but also depends, to some extent, upon the temperature interval at which the capacitance data were recorded especially around the transition temperatures. It

is therefore unwise to place any profound significant emphasis on the

heights of these peaks. This is especially true in the case of the 30°C

transition. However, as expected, the data indicate an increase in

the transition temperatures with increasing pressure. Also the rela-

tive heights of the room temperature transition peaks increase with

increasing pressure in almost all cases. This is consistent with a view

that at a constant rate of increase in temperature, the molecular rela-

xations at the transition become more rapid as pressure increases.

Figure 11.14 shows the variation of $\frac{dC}{dT}$ with increasing temperature

at atmospheric pressure using the polymer capacitance cell used for

gaseous measurements. Curve A represents the results for a virgin

PTFE specimen, whereas curve B represents the behaviour of a PTFE speci-

men which has previously been exposed to the full N_2 pressure cycle.

As it is evident from the data, within experimental error (± 0.2°C),

the position of the room temperature transition of PTFE is unaffected

by the polymer's pressure and thermal history.

Figure 11.15 describes the variation of the rise in the room

temperature transition of PTFE with increasing pressure using different

pressure media. The data indicate an approximately linear relationship

between the two variables in the case of the gaseous media (curves B,

C and D). The pressure coefficients of the transition temperature,

dT/dP for He, N_2 and Ar pressure media are 0.20, 0.19 and 0.14°C/MPa

respectively. In the case of liquid pressure medium (curve A), the

pressure dependence of the transition temperature although larger than

those in gaseous media (the best straight line has a slope of ca. 0.21°C/

MPa), increases less rapidly than linearly. This is somewhat unexpected

and may be associated with non equilibrium effects in this pressure

medium.

Yasuda and Araki (1961) reported a shift of ca. 0.20°C/MPa in

the room temperature transition dilatometrically by directly compressing the PTFE specimen without a fluid medium. This is in good agreement with the corresponding value obtained from the present data (ca. 0.21°C/MPa) using a liquid pressure medium. Interestingly, Billinghurst and Tabor (1971) on the other hand used a torsion pendulum to report a lower value of 0.18°C/MPa in a He pressure environment. The corresponding value from the present data is 0.20°C/MPa.

In contrast, the analysis of the 30°C transitions failed to reveal any obvious trends between the shift in the transition temperature and increasing pressure. Also, the effect of various pressure media on the proximity of the 20°C and 30°C transitions was random.

11.3 Summary

An increase in the room temperature transition temperature of PTFE with increasing pressure in a liquid pressure environment may be predicted from the Clapyeron Glausius equation in the form:

$$\frac{dTg}{dP} = \frac{T\Delta V}{\Delta Q} \qquad (11.1)$$

where Tg is the transition temperature and ΔV and ΔQ are the volume change and enthalpy changes at transition respectively. The above equation is consistent with a generally accepted mechanism of an increase in the transition temperature due to a reduction in free volume following the application of an external pressure. This may be the case for a pure triaxial pressure medium such as a liquid. In the case of a gaseous pressure environment both gaseous sorption (Chapter 9) and volumetric contraction occur (Chapter 10). Surprisingly, the net result is, to a first order, similar to that observed in a pure triaxial liquid pressure environment. The shift is however dependent on the type of the pressure medium employed. This second order dependence

is reflected in a smaller increase in the transition temperature in

a gaseous environment in the order He > N_2 > Ar. This is perverse.

The gases seem to not only compress the polymer but also interstitially

and reversibly occupy the intermolecular and intramolecular spaces

in the polymer chains and also reduce the energy barrier required for

chain movement at transitions by effectively "lubricating" the polymer

chains. The magnitude of this effect depends on the size and the

nature of the gaseous atoms and molecules. The increase in the atmos-

pheric room temperature transition volume of PTFE with increasing

pressure in gaseous environments is in direct contrast to the behaviour

observed in a liquid pressure medium. The above lends further support

to a view in which different mechanisms are responsible for the way in

which gas and liquid pressure media modify the relaxation processes
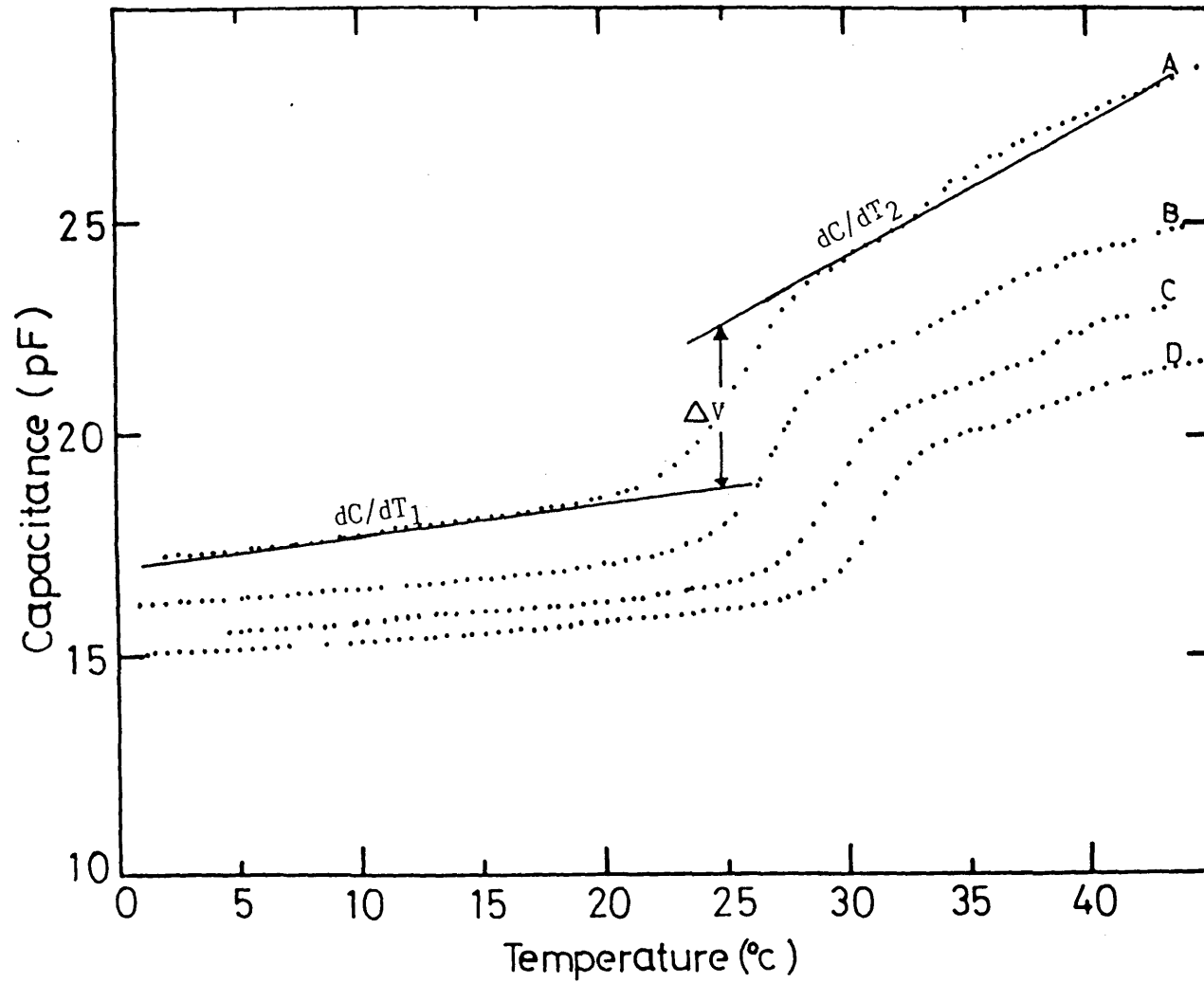
in polymers.

Figure 11.1. The effect of temperature on the measured electrical capacitance using PTFE specimen in a hydraulic pressure medium at various pressures: Curve A,13.8 MPa; Curve B, 27.6 MPa; Curve C,41.3 MPa; Curve D,51.7MPa.
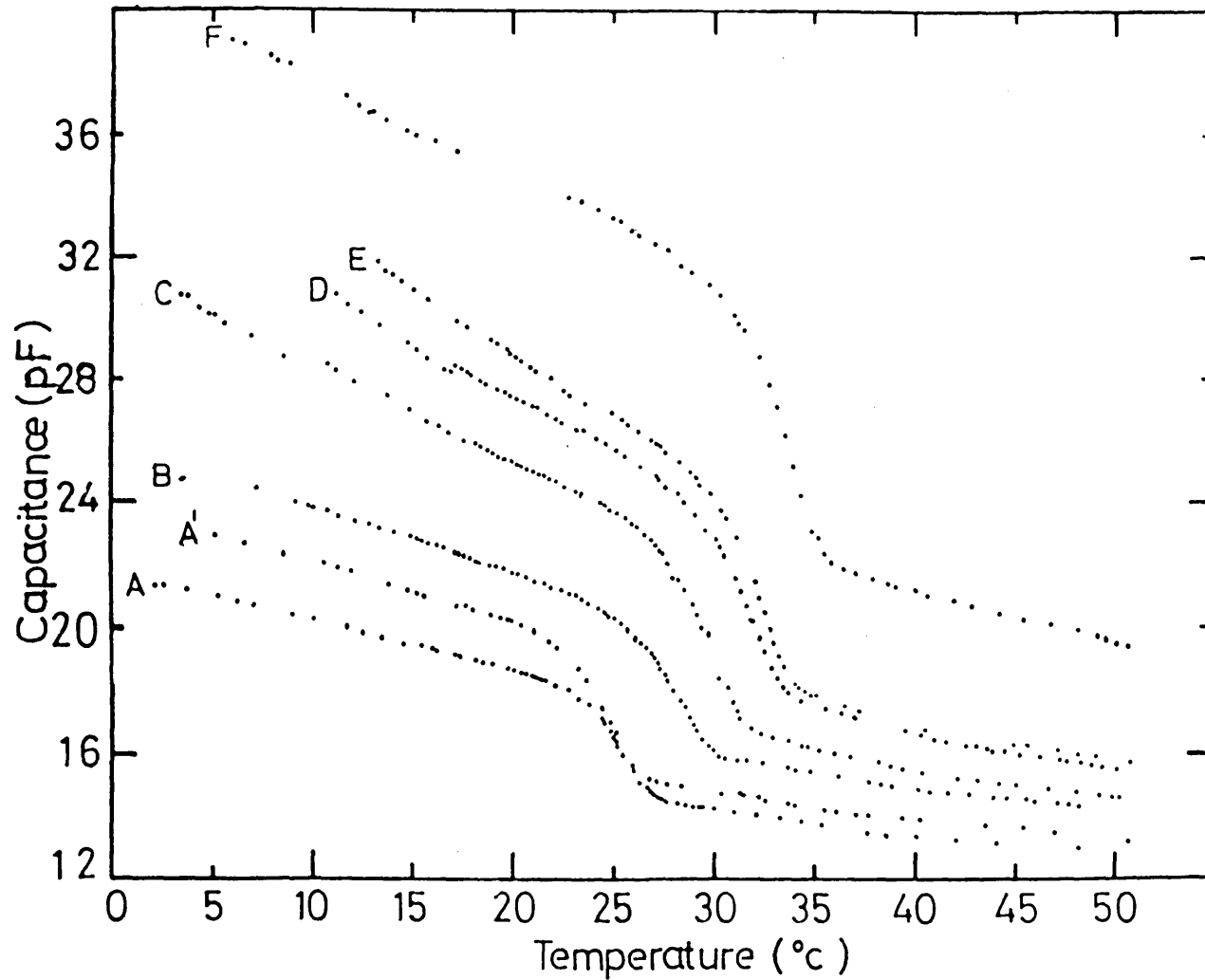
Figure 11.2. The effect of temperature on the measured electrical capacitance using PTFE specimen in a N_2 pressure medium at various pressures: Curve A,0.1 MPa; Curve B,13.8 MPa ; Curve C,20.7 MPa; Curve D,34.5 MPa; Curve E, 41.3 MPa; Curve F,48.2 MPa; Curve A',0.1 MPa (pressurised specimen).
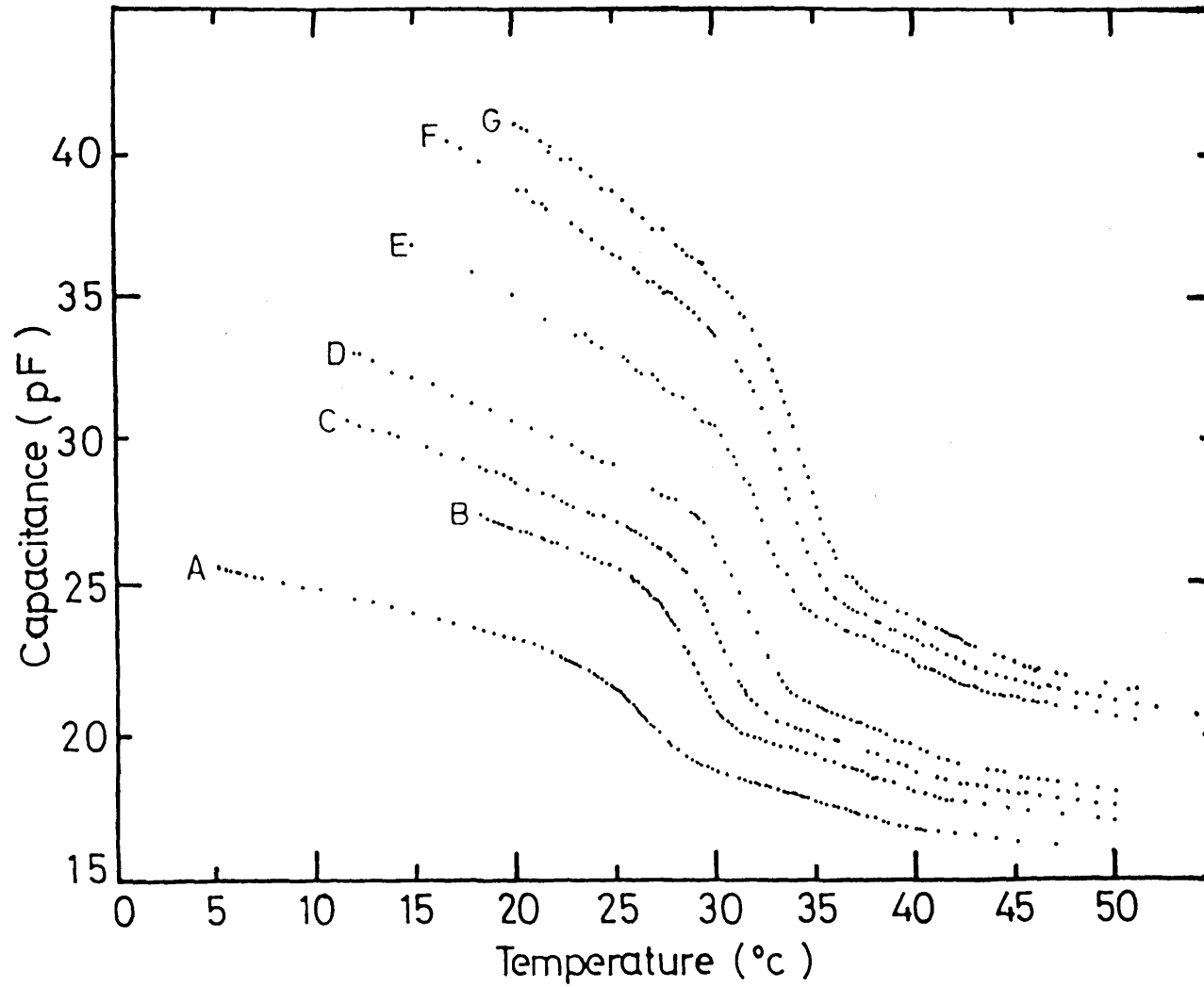
Figure 11.3. The effect of temperature on the measured electrical capacitance using PTFE specimen in a He pressure medium: Curve A,0.1 MPa; Curve B, 13.8 MPa; Curve C, 20.7 MPa; Curve D, 27.6 MPa; Curve E, 34.5 MPa; Curve F, 41.3 MPa; Curve G, 48.2 MPa.
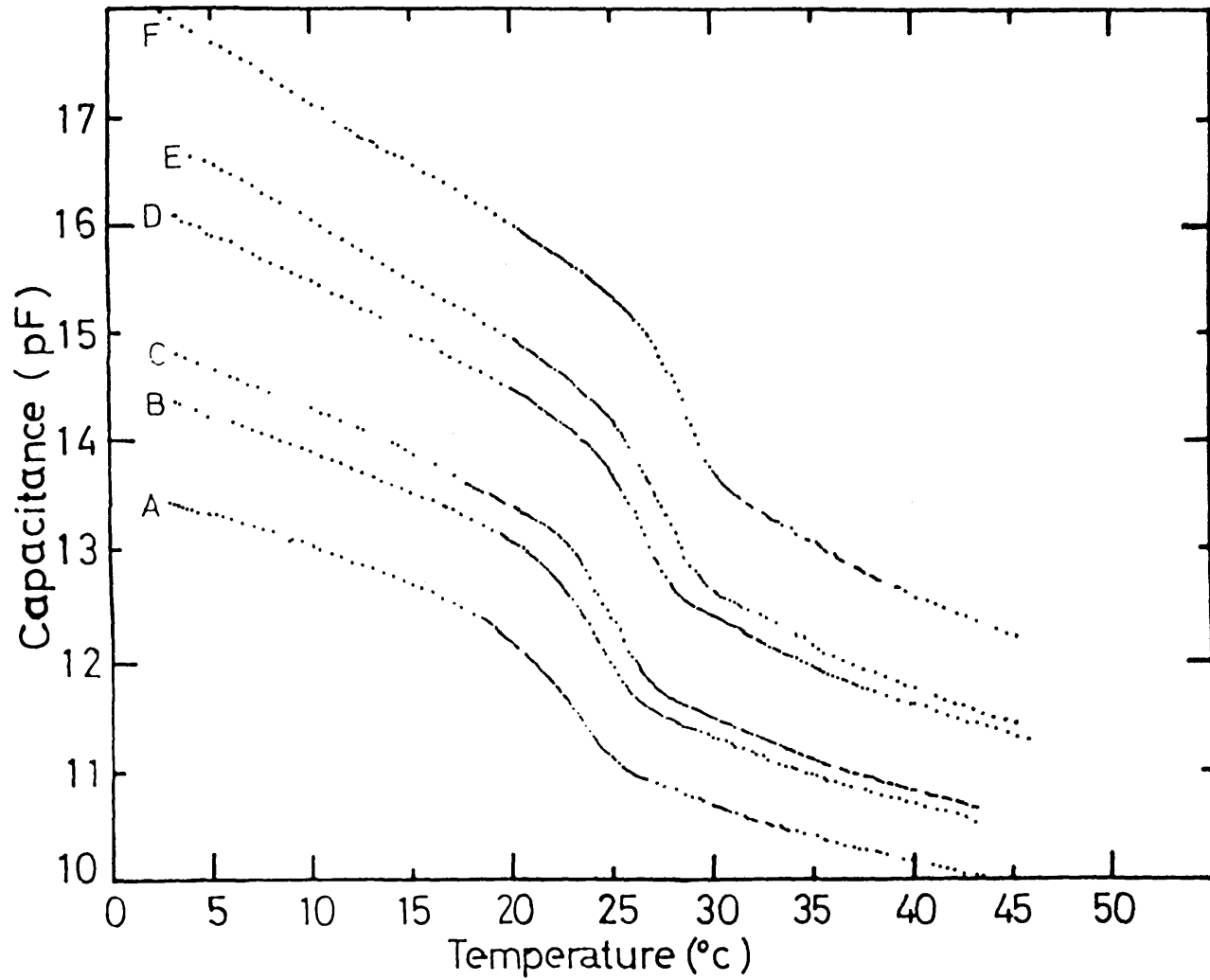
Figure 11.4. The effect of temperature on the electrical capacitance using PTFE specimen in an Ar pressure medium at various pressures: Curve A, 13.8 MPa; Curve B, 20.7 MPa; Curve C, 27.6 MPa; Curve D, 34.5 MPa; Curve E, 41.3 MPa; Curve F, 48.2 MPa.

Figure 11.5. The variation of the temperature dependence of PTFE capacitance data (dC/dT_1) before the initiation of the room temperature transition with increasing pressure in various pressure media.
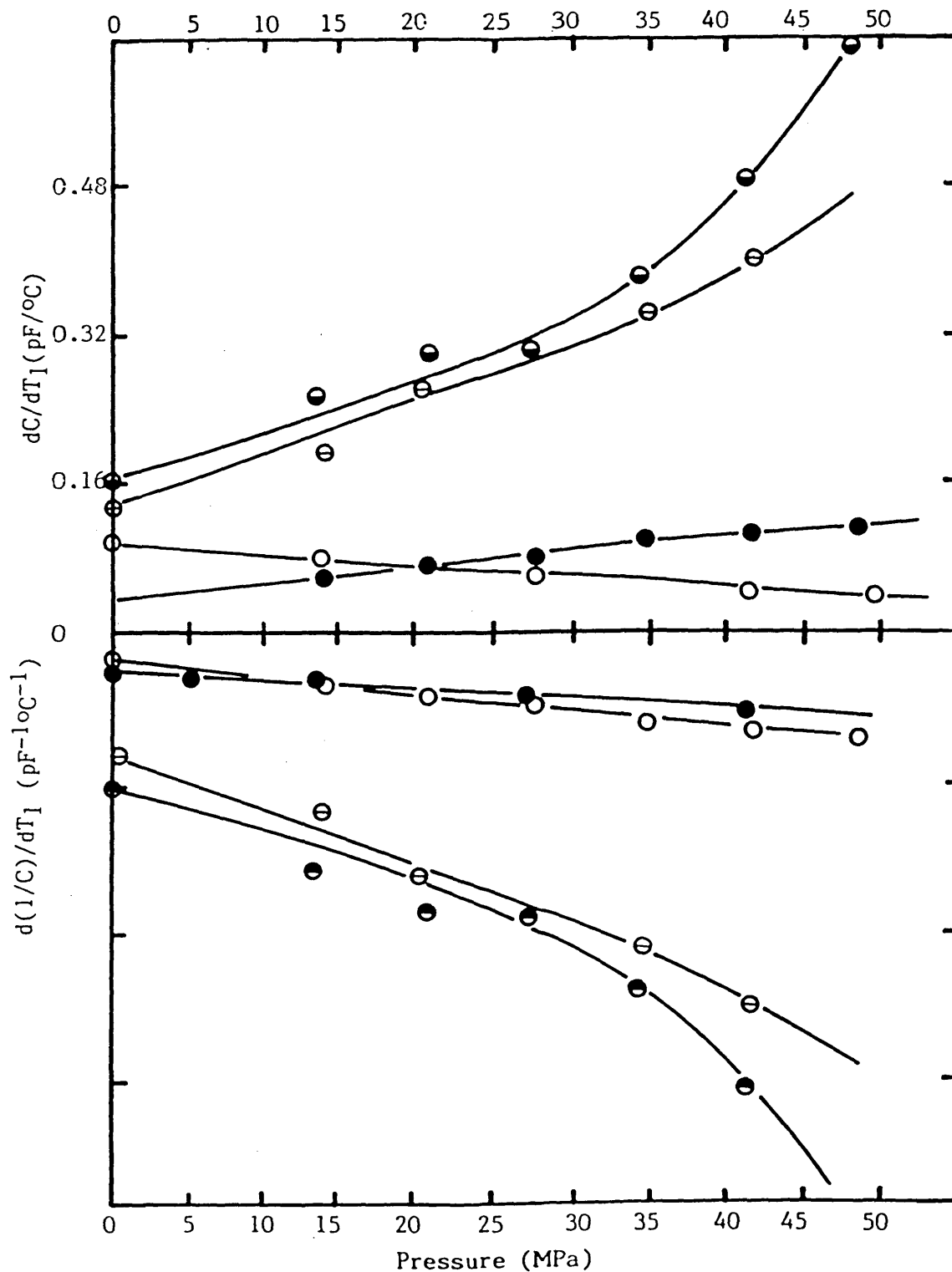

Figure 11.6. The effect of pressure on the thermal expansion coefficient ($d(1/C)/dT_1$) of PTFE before the initiation of the room temperature transition in various pressure media: $\mathbf{O}$,hyd.oil; ⊖,He;⊖,N_2; ● ,Ar.

Figure 11.7. The variation of the temperature dependence of PTFE capacitance data (dC/dT_2) after the completion of the room temperature transition with increasing pressure in various pressure media.
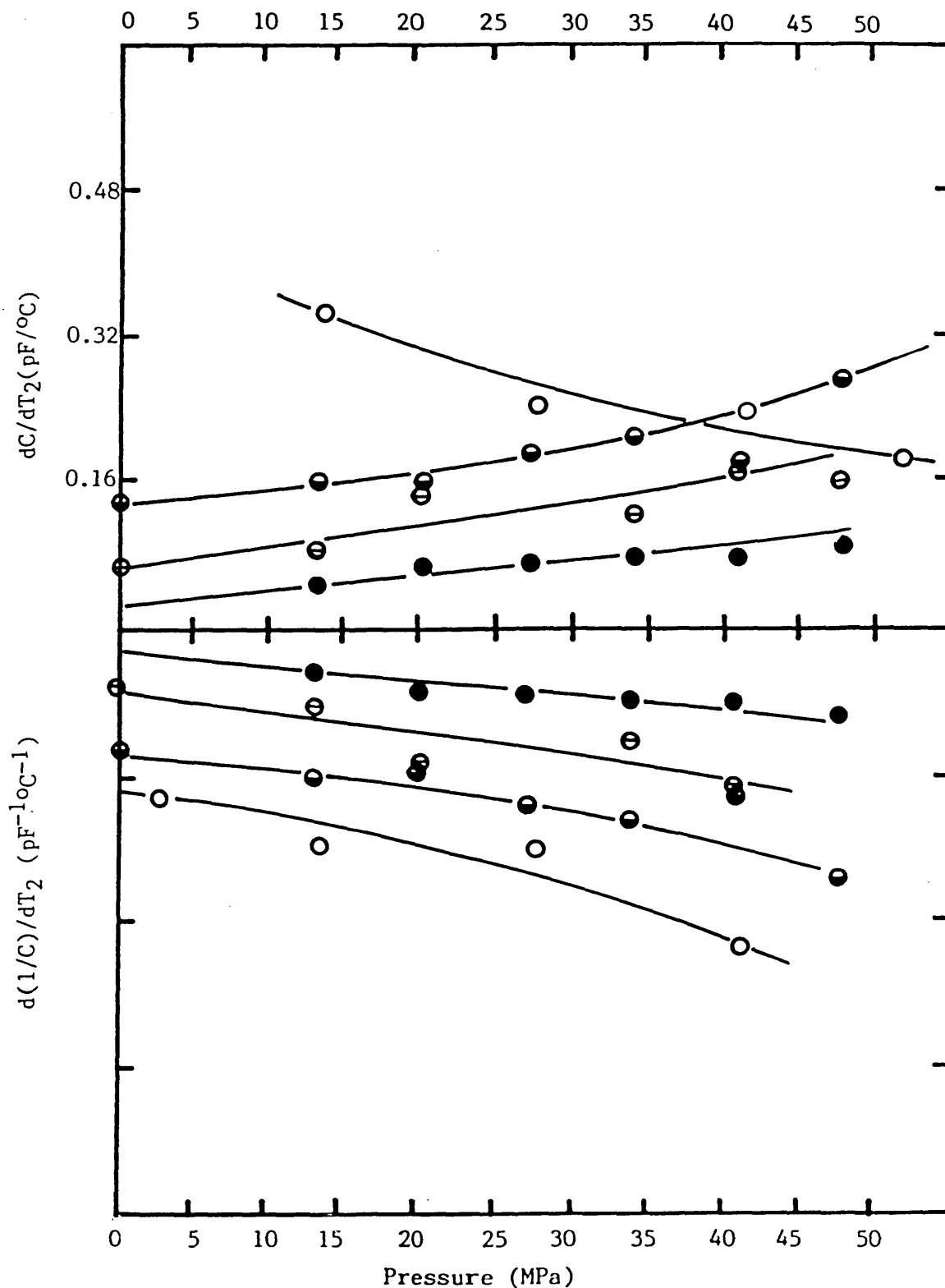

Figure 11.8. The effect of pressure on the thermal expansion coefficient $(d(1/C)/dT_2)$ of PTFE after the completion of the room temperature transition in various pressure media: O ,hyd.oil; ⊖ ,He; ⊖ ,N_2; ● , Ar.
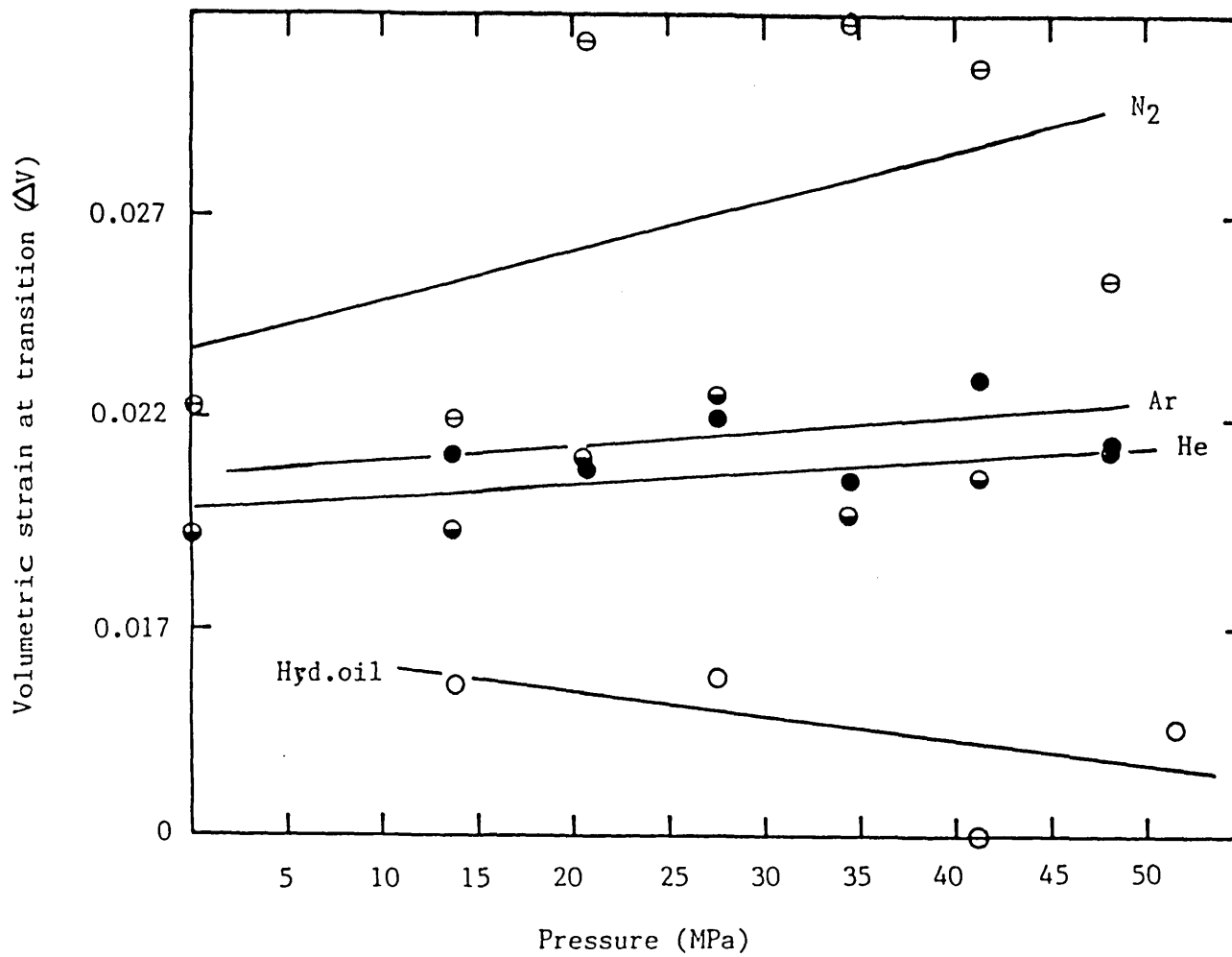
Figure 11.9. The effect of pressure on the transition volumetric strain(ΔV) induced in PTFE in various pressure media: $\bigcirc$,hyd.oil; $\ominus$,He; $\ominus$,N_2; $\bullet$,Ar.

Figure 11.10. The variation of the temperature dependence of the PTFE capacitance data (dC/dT) with temperature for an hyd.oil pressure medium at various pressures: ○ ,0.1 MPa; ⦶ ,13.8 MPa; ⦷ ,27.6 MPa; ⊖ ,41.4 MPa; ● , 48.2 MPa.

Figure 11.11. The variation of the temperature dependence of the PTFE capacitance data (dC/dT) for a N$_2$ pressure medium at various pressures: O ,0.1 MPa; ⦶ ,13.8 MPa; ◑ ,20.7 MPa; ⊖ ,27.6 MPa; ⊕ , 34.5 MPa; ◓ ,41.4 MPa; ● ,48.2 MPa.
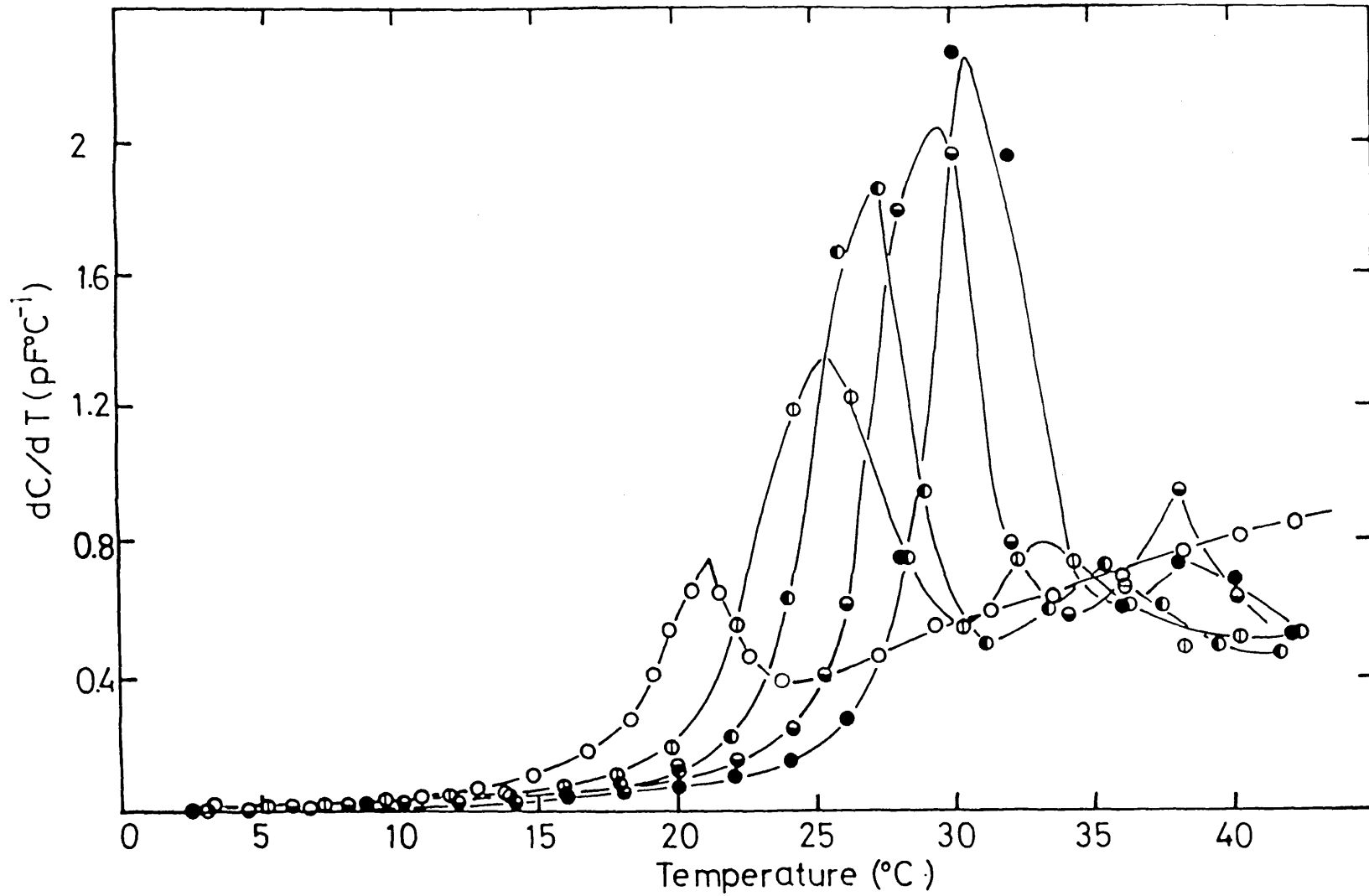
Figure 11.12. The variation of the temperature dependence of the PTFE capacitance data (dC/dT) with temperature for a He pressure medium at various pressures: ○ ,0.1 MPa; ⓓ ,13.8 MPa; ◑ ,20.7 MPa; ⊖ ,27.6 MPa; ⊕ ,41.4 MPa; ● ,48.3 MPa.
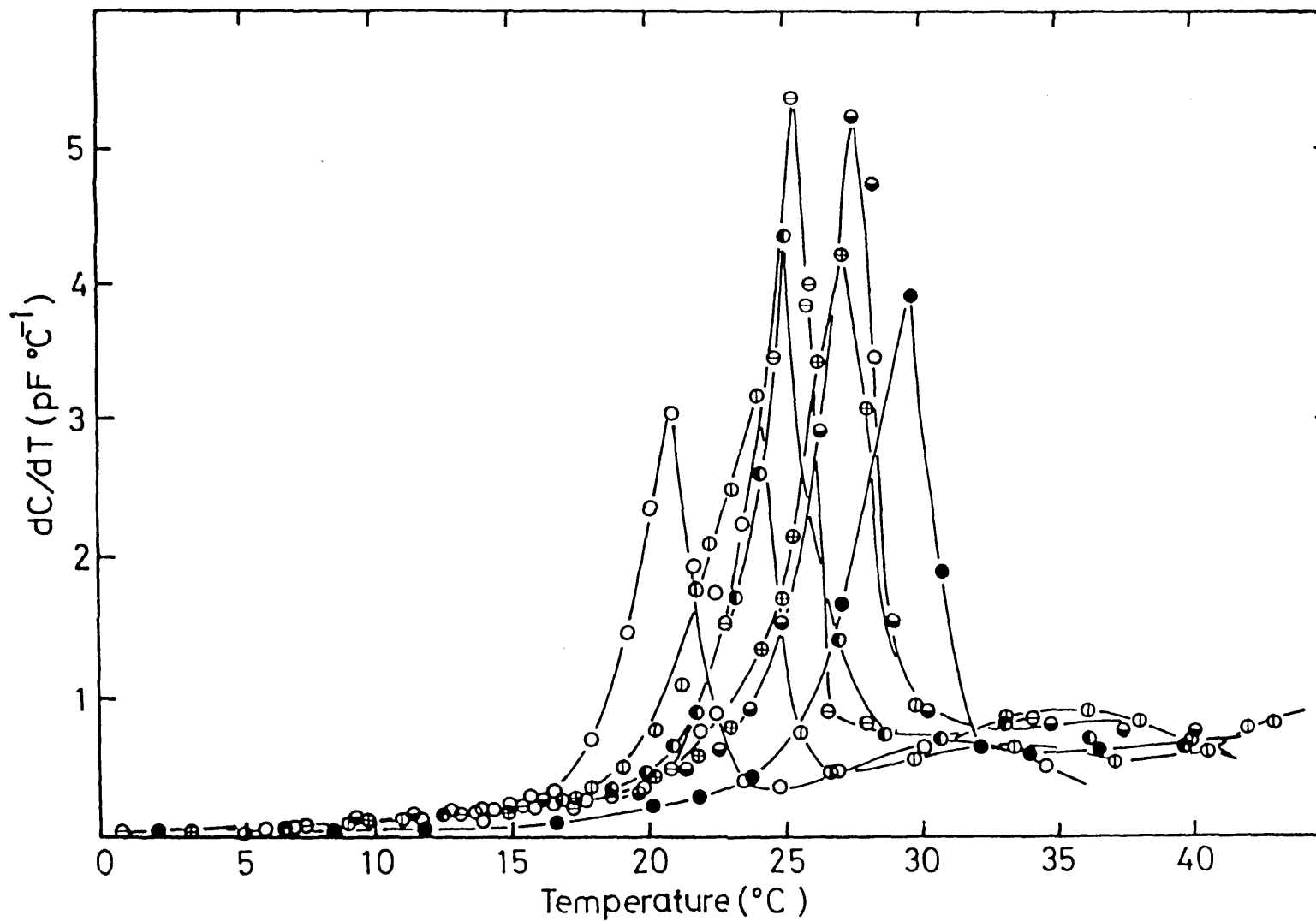
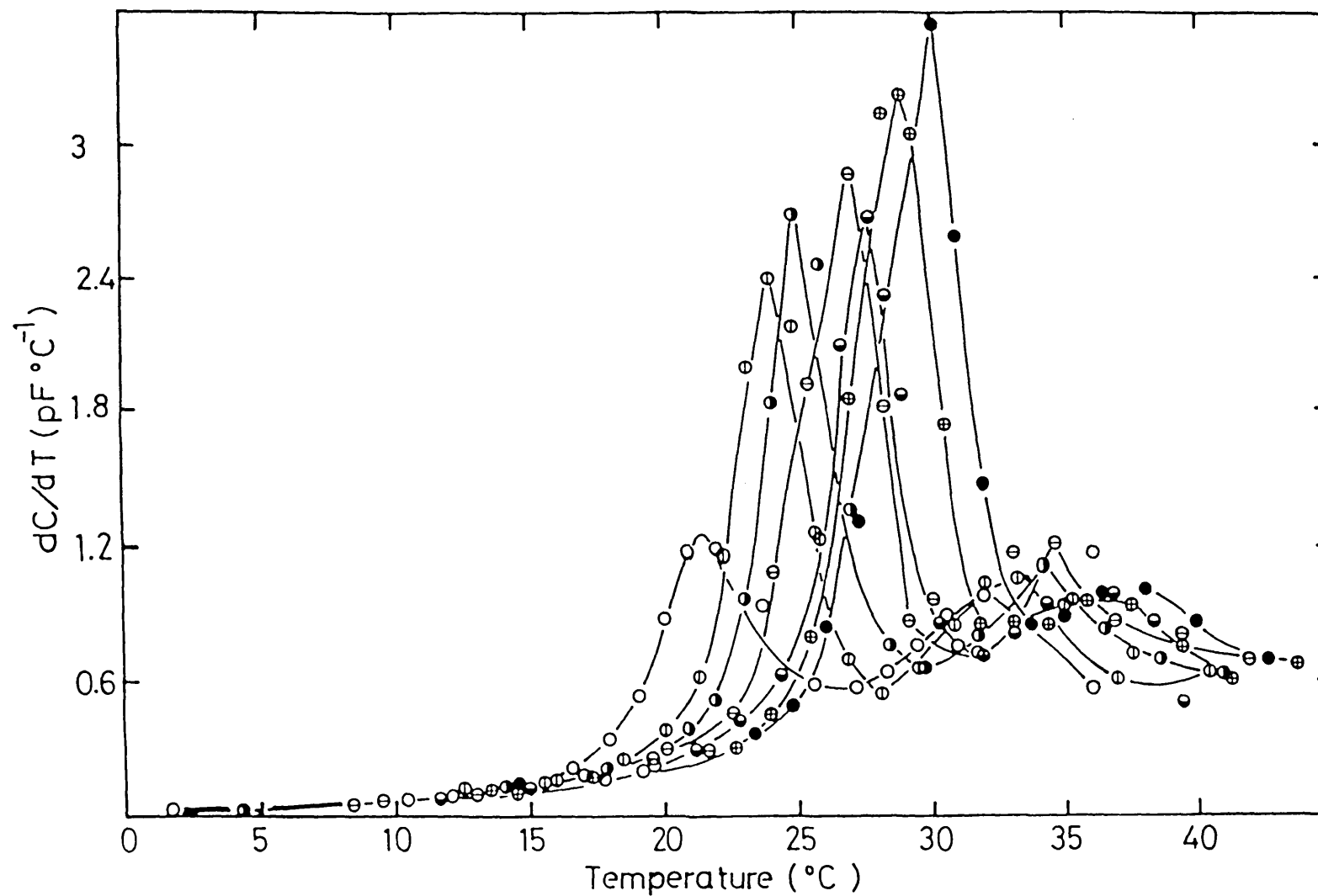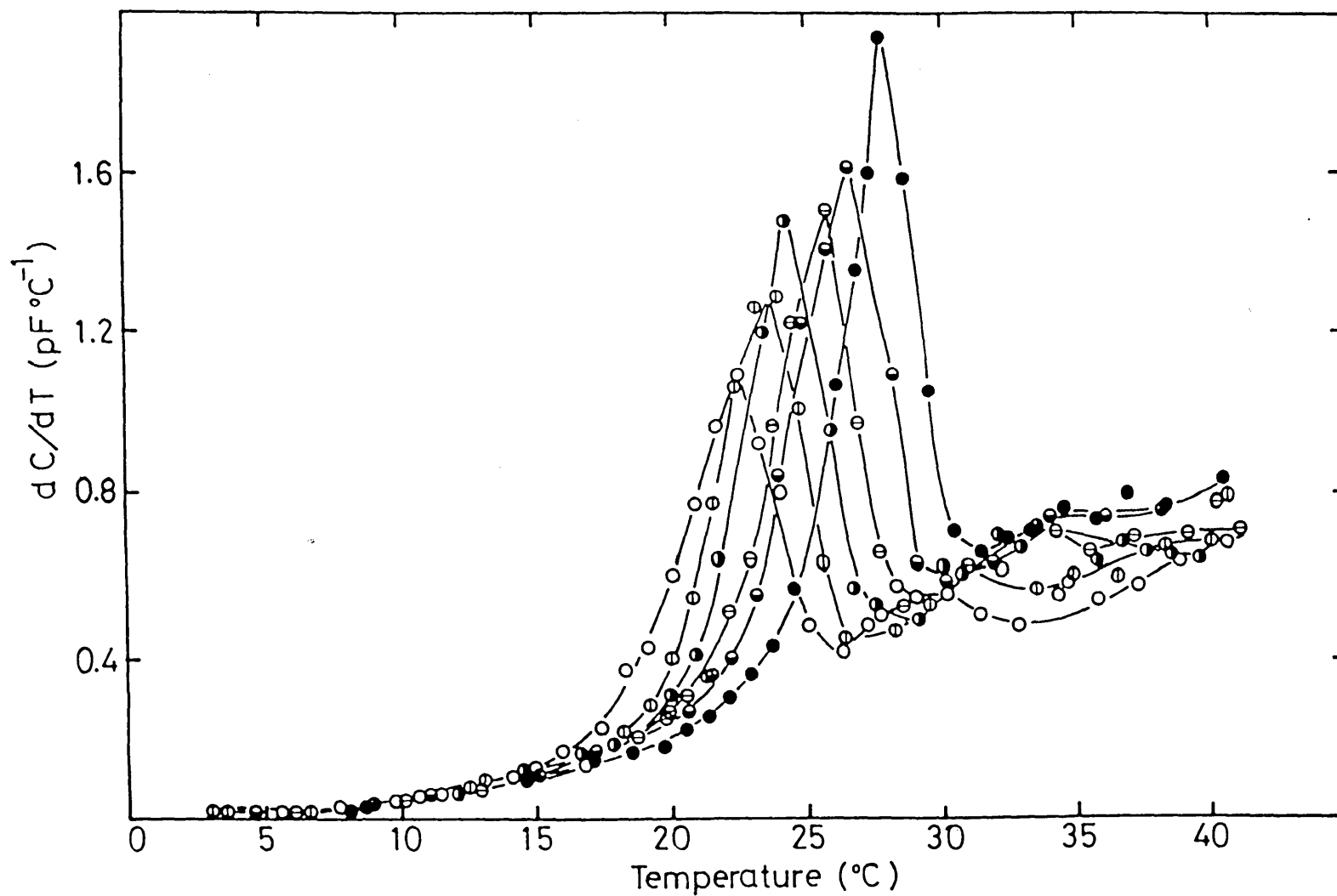Figure 11.13. The variation of the temperature dependence of the PTFE capacitance data (dC/dT) with temperature for an Ar pressure medium at various pressures: ○ ,13.8 MPa; ⦶ ,20.7 MPa; ◑ ,27.6 MPa; ⊖ ,34.5 MPa; ◒ ,41.4 MPa; ● ,48.3 MPa.
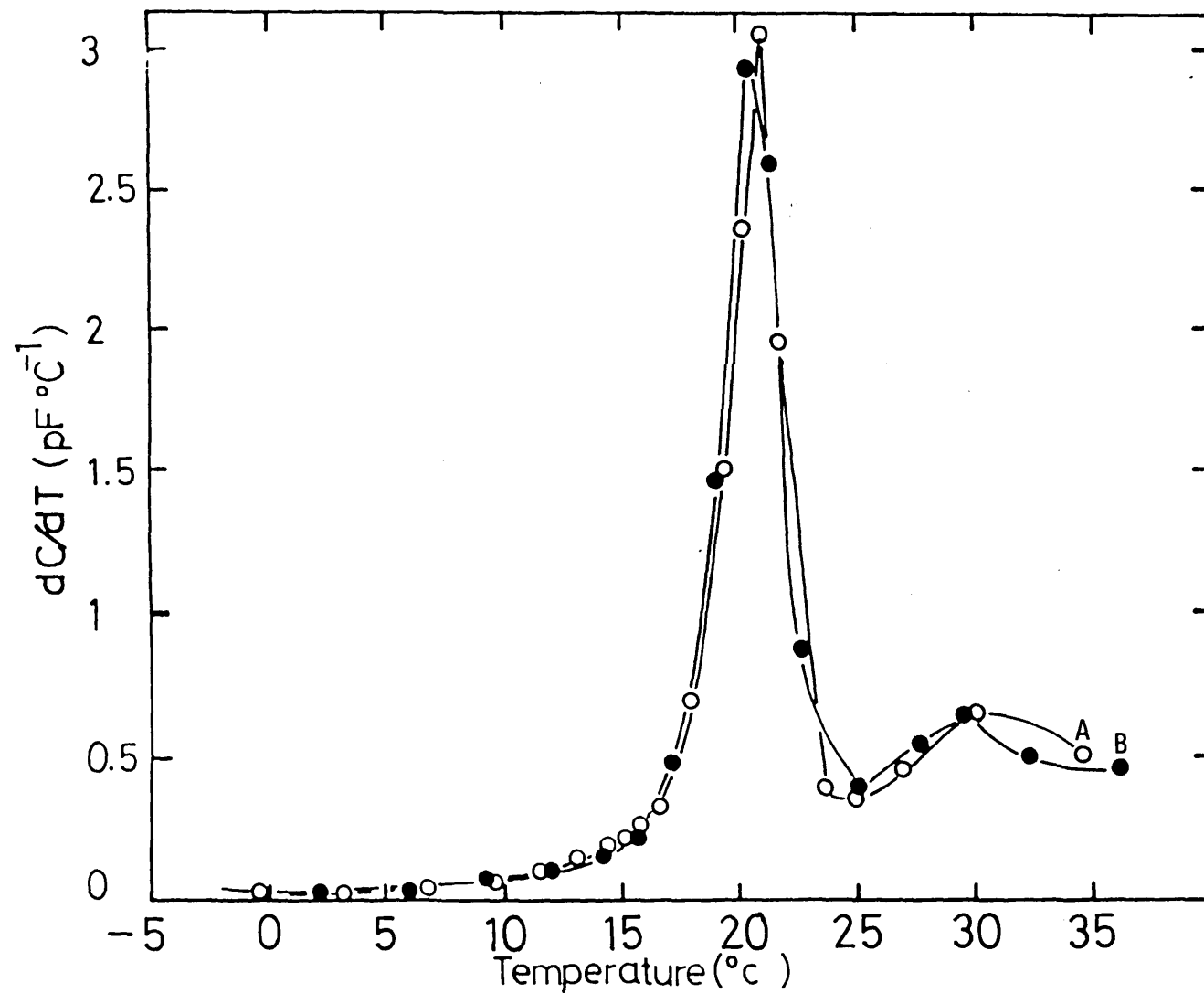
Figure 11.14. The variation of the temperature dependence of the PTFE capacitance data with temperature at atmospheric pressure: O ,virgin specimen; ● ,pressurised specimen.
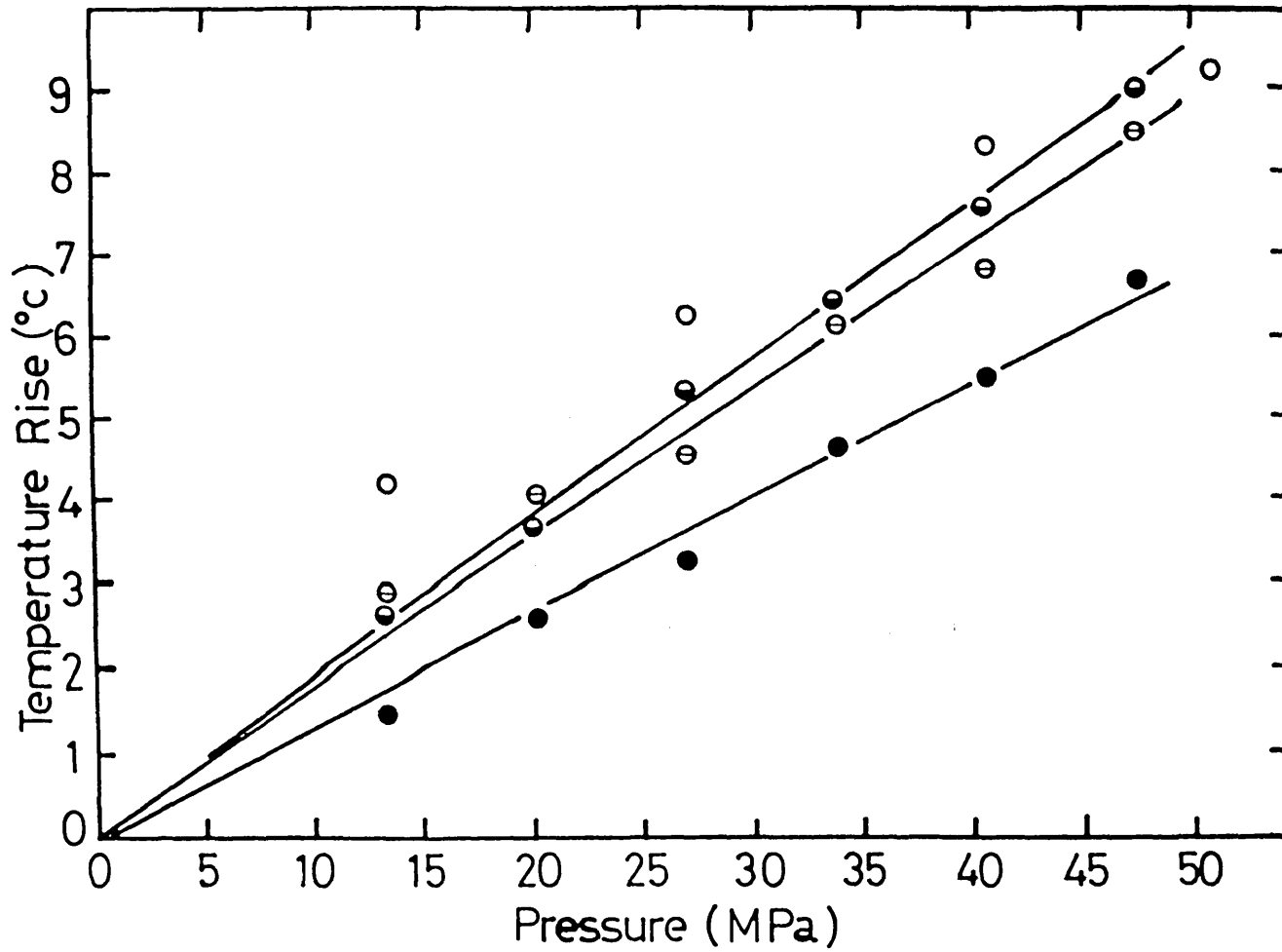
Figure 11.15. The effect of various pressure media on the position of the room temperature transition in PTFE: O ,hyd.oil; ◒ ,He; ⊖ ,N_2; ● ,Ar.

C H A P T E R 1 2
CONCLUSIONS

The work described in this thesis naturally falls into two parts.
One part deals with what may be called dynamic phenomena, in particular
thermal effects, and is treated rather explicitly in Chapter 8 in the
context of apparent plasticisation of PTFE. Similarly this concept also
enters into both the mass sorption data and to a greater extent, in the
volumetric strain studies reported in Chapter 10. This area of work has
not been as extensive as that which is reported in what may be regarded
as the equilibrium studies which are involved with estimates of mass
sorption and equilibrium volumetric strain measurements. This also applies
to Chapter 11 which deals with the effect of various pressure media on
the pressure dependence of the room temperature transition in PTFE. In
this conclusion both of these topics will be reviewed in some detail
and an attempt will be made to draw various parts of the thesis together
under these headings. Before doing so, it is appropriate to note that
the experimental techniques which have been developed during this work
have additional value insofar as that they may be used to measure the
properties of gases and liquids under high pressures. A substantial
part of Chapter 9, for example, reviews the use of a probe which can
accurately and rapidly measure the density of gases over a wide range
of temperatures and at high pressures. Similarly, the linear contrac-
tion measurements described in Chapter 10 produce a first order result
for the influence of pressure on the permittivity of both liquids and
gases. However, as the capacitance probes employed in these studies
only produce a first order estimate, it is not appropriate

to discuss this further in the conclusions but it is worth summarising in more detail the potential and characteristics of the gas density probe.

The gas density probe reported in Chapter 9, which is an essential calibration for the gas mass sorption technique, has been shown to operate very satisfactorily over a wide range of conditions in a number of gases. Whilst the physical principle of the technique is not properly understood, it appears that its operation depends upon the fact that a vibrating reed will entrain, under certain conditions, a constant volume of gas. The entrained mass will attenuate the natural frequency of a vibrating reed and hence the frequency will be accurately proportional to the density of the ambient. The same approach may also be used to measure the mass of any type of specimen in an aggressive or high pressure environment. The potential accuracy is high, the response time is short and the long term stability is excellent. At present it appears that one calibration will survive for a wide range of gases.

The dynamic studies reported throughout this thesis indicate two general effects. First that in any experiment which involves the rapid application of pressure to an organic polymer there is an inevitable rise in temperature. This rise in temperature will include a contribution from the work done within the polymer as it accommodates the triaxial stress, as well as the work done on the pressure transmitting medium. In the case of liquids, the latter is relatively modest but nevertheless an important contribution. In the case of gases, the temperature rise associated with an adiabatic compression can be an enormous factor and it was this contribution which led to the Billing-hurst and Tabor supposition that nitrogen gas could isothermally

plasticise PTFE. Chapter 8 deals with this problem and indicates

that there is no significant intrinsic isothermal plasticisation of

PTFE that would warrant its development as a commercial process. What

is significant in this context, however, is that a large amount of gas

is absorbed (Chapter 9) and this gas will invariably be sorbed at an

elevated temperature. The diffusion of a hot flux of gas into the poly-

mer matrix is rather rapid, typically a few minutes will be sufficient to

saturate the matrix with hot gas and maintain the gas at equilibrium with

the environment. This produces a remarkably efficient heat transfer

medium for what would otherwise be a very poor thermally conducting material.

Chapter 10 also indicates that the application of a pneumatic

gas stress produces a significant volume contraction which would

naturally improve the thermal conductivity of the polymer. The prece-

dents in the area of the effect of pressure on thermal conductivity

of polymers have been reviewed in Chapter 3. The initial plastisisation

data provided by Billinghurst and Tabor is presented in Chapter 4 along

with other data which are possibly now susceptible to criticism because

of similar adiabatic thermal heating effects (see Chapter 2). It has

not proved possible to examine and analyse the subtleties associated

with the transport of hot flux into polymeric matrices in detail as

the boundary conditions for the problem are not well defined. In

addition, a very significant amount of additional data would be required

in order to characterise the thermal response of the temperature probes.

Nevertheless, it can be shown that the application of a transient

pneumatic stress leads to a very efficient thermal annealing of the

polymer in a very short time. This annealing would not occur to the

same extent in an hydraulic oil pressure medium. The effect of hydro-

static pressure on the mechanical properties and compressibility of polymers is reviewed in Chapters 4 and 5 respectively. The increases in density observed in PTFE following the removal of the pressure environment are quite significant and correspond to an effective increase in crystallinity of ca. 6% up to the highest pressures imposed.

Additional information on dynamic effects are also contained in the Chapters dealing with mass sorption and volumetric strain measurement. As far as can be detected, there are no significant time dependent effects associated with gaseous sorption. However, these data have been selected with the data in Chapter 8 in mind in order to remove any potential problems associated with adiabatic effects. The sorption data can therefore be regarded as isothermal. The time dependent data associated with the linear contraction measurements do indicate some interesting features both in gas and liquid pressure media. The data in a liquid medium are interesting insofar as the volume contraction does take a finite time to reach an equilibrium value but on protracted exposure to a high pressure ambient, the volume actually relaxes again. It may be that this behaviour is associated with a time dependent viscoelastic rearrangement in the molecular architecture of the polymer matrix in response to the applied external pressure. Whilst there are some very interesting areas in the kinetics of both gas sorption and the accommodation of triaxial stress in gaseous media, these have not been explored fully primarily because of the problems associated with adiabatic heating effects. Much of the data of real interest in this study has emerged from studies where it is assumed that the system has attained equilibrium. In this context, equilibrium would mean the absence of any detectable changes in either compressibility or mass sorption or indeed in the time dependence of the $20^{\circ}C$ transition within reasonable time scales; in this

study this refers to a period of up to 8 hours.

The equilibrium measurements are therefore divided into three parts: the mass sorption data, the linear contraction data and the influence of various pressure media on the $20^{o}C$ and $30^{o}C$ transitions in PTFE. These data, together with the appropriate experimental methods are described in Chapters 9, 10 and 11 respectively. These Chapters also contain preliminary discussions of these data. There are many subtleties but the important features may be listed as follows:

(1) The amount of gas sorption in mass terms is large and when this mass is converted into volumetric terms, assuming ambient densities pertain in the interior of the polymer, the volume sorptions are very large. For PTFE, the mass sorption accurately scales with the ambient density up to the highest pressures imposed. In the case of PMMA, HDPE and PP, there is evidence that the absorption begins to increase more slowly than the ambient density at pressures in excess of 45 MPa. This is indicative of saturation. The amount of gas sorption also appears to decrease with the density of the polymers.

(2) As far as can be detected, the amount of gas sorption is virtually independent of the morphology, that is the thermal history, the crystallinity, the density or the pressure history of PTFE. This is also probably true for the other polymers studied.

(3) The amount of gas absorbed in volumetric terms is greater for smaller gas molecules.

(4) The amount of gas sorption for pure gases increases with temperature at a rate which is dependent upon the type of gas employed. For PTFE for example, the sorption of N_2 is very sensitive to temperature but the sorption of He is much less so. The behaviour

of mixtures is rather peculiar and indicates the existence of a spectrum of various sized sites in the PTFE matrix available for the inclusion of gaseous atoms and molecules. This size distribution changes with temperature.

(5) The rapid volumetric expansion of PTFE around its room temperature transition is not reflected in an abrupt increase in gaseous uptake. This may be explained in terms of the relatively small size of the gaseous atoms and molecules compared to the average site size distribution in the PTFE matrix involved around its room temperature transition.

(6) A more detailed study reveals that the greater the mass sorption or volumetric sorption of the gas, the less is the compressibility of the polymer. In most cases the compressibility is nearly a linear function of pressure.

(7) In contrast to the gas sorption data, the volumetric contraction in polymers is sensitive to the morphology and the pressure history of the polymer. What is more, a significant volumetric change is noted for the room temperature transition in PTFE.

(8) A detailed inspection of the temperature and pressure dependencies of the compressibility of polymers in gaseous and liquid pressure media does indicate some rather subtle trends. However, these may be generally interpreted using the model that the more gas that enters the less is the effective triaxial stress. It is, however, difficult to reationalise the fact that in spite of the delicate balance between sorption and triaxial stress, a gaseous pressure medium compresses the polymers to an amount which is generally comparable to that obtained in an hydraulic pressure medium. This is despite the fact that a significant amount of

gas enters the polymer matrix. At this point it is worth pointing
out that it is extremely likely that the system has reached an
equilibrium compressibility in gaseous media, but there must be
some concern in the case of the hydraulic medium. This thesis
does not produce any strong evidence that the hydraulic oil com-
pressibility data may be non equilibrium, but it is a factor which
should be borne in mind with regard to this work and other published
data.

(9) The pressure dependencies of the room temperature transitions in
PTFE are found to be linear and also sensitive to the type of the
pressure medium employed. To a first order, the data for gases and
liquids are rather similar but a trend can be seen with the gases.
Values of the pressure dependencies for the room temperature transi-
tion in PTFE in various media increase in the order:hyd. oil > He >
N_2 > Ar.

(10) Within the set of data obtained for the pressure dependence of
the room temperature transition in PTFE, it is interesting to note
that the volume change associated with the transition increases
with pressure for gaseous media but decreases in the case of a
liquid pressure medium.

Taking the sorption and the compressibility data together, two
major points emerge. First, gas molecules of the types studied here
do not distinguish large volumes within the polymer matrix and hence
are not sensitive to the morphology of the system. The gas molecules
seem to be associated with sites along the molecular chains which are
comparable to their own size. The data discussed in Chapter 9 exemplify
this point. Also, it appears that the voids which are effective for

absorbing N_2 into PTFE are relatively sparse at $20^{\circ}C$ but at $70^{\circ}C$, the matrix expands sufficiently to allow the N_2 molecules to be incorporated in the structure of PTFE. The PTFE is behaving somewhat like a molecular sieve and in principle could be used to effectively separate He from N_2. This model would therefore explain the unexpectedly large volumes of gas absorbed. The volumes greatly exceed the conventional values of the free volume in the matrix; the free volume in this context is assumed to represent the specific volume difference between the perfectly ordered or crystalline species and the specific volume of the polymers employed. With regard to gas sorption, the gas does not seem to distinguish the amorphous from the crystalline domains. This would then explain the apparent insensitivity of the amount of gas sorption on the morphology of the polymers. Clearly the use of larger gas species would be required in order to sense the volumes which are conventionally denoted as free volumes. It can be envisaged that this gas sorption technique would provide a very useful probe for examining the free volume size distributions in polymeric matrices in a very similar way to that which is used to investigate the pore size distribution in porous carbons.

The second major point of interest involves the rather surprising results that the polymers studied are compressed in gaseous media to the same extent as in the case of an impermeable hydraulic oil. Ignoring, for the moment, the problems associated with non equilibrium effects in the hydraulic oil cases, it is reasonable to assume that the gaseous atoms and molecules that enter the polymer matrix are at equilibrium with the ambient and presumably have the same pressure in the matrix. Hence a simple physical argument would require that no triaxial stress could be applied to the polymeric matrix. Thus, it would be difficult

to envisage that a compression could occur. The experimental data do however indicate that the more the mass sorption, the less is the compressibility of the matrix. This would support the view that the presence of the species hinder the compression of the matrix; this would fit the conventional picture. At present the only realistic model would assume that the absorption of the gas on the polymer chains is a localised process and hence it would not produce a pressure within the matrix, i.e. the gas molecules are immobile and cannot convey their kinetic energy to the matrix to produce an internal pressure. This would be a satisfactory explanation for the small molecular sites but it is clear that the gas can also enter the relatively large voids associated with the disordered regions where it would have a density comparable with the ambient. It is difficult to see how gas could be immobilised in these regions. Presumably the triaxial stress could not be transmitted through these regions.

The data in Chapter 11 indicate that the volumetric change associated with the room temperature transition in PTFE and the pressure dependence of this transition is gas specific. A review of these data does not reveal the existence of a simple trend that can be drawn between these data and the data presented in Chapters 9 and 10. It is suggested in Chapter 11 that the gas molecules can actually lubricate transitions insofar as their absorption can facilitate the movement of chains in the same way that a monomolecular lubricant might facilitate the sliding of solid bodies over one another. This is tantamount to arguing for localised plasticisation which was in fact the initial notion to be explored in this thesis. The evidence for chain plasticisation by discrete gas absorption at well-defined molecular sites is not strong

but in the absence of any better explanation it cannot be discounted.
The literature on this topic is not particularly helpful (see Chapters
2 to 5). In the main, the trends in mechanical properties, solubility,
diffusion and thermal conductivity can either be interpreted, to a first
order, in terms of density or simply the action of the hydrostatic
environment. The gas can produce a volumetric contraction comparable
with that of a liquid and hence it is reasonable to suppose that the pres-
sure dependence of the modulus or the thermal conductivity will be simi-
lar to that seen in a liquid medium. It is only the second order effects
as seen in, for example Chapter 11, (the pressure dependence of the room
temperature transition in PTFE) which can distinguish the presence of
the gas molecules in the matrix and here the absence of any well-defined
trends, within the limited data available, does not allow specific lubri-
cant effects to be proposed.

Before concluding this general discussion and review of the
trends in the data, it is appropriate to speculate on the meaning of
the term lubrication as introduced in this Chapter and also in Chapter
11. The idea of a boundary lubricant as popularly regarded in the
lubrication of metallic or solid contacts is clearly inadequate and
and it is worthwhile exploring what it could mean in this particular
context. In the case of normal plasticisation, chain lubrication is
usually analogous with an increase in temperature which can be asso-
ciated with a volumetric expansion of the matrix. This is the case for
plasticised PVC, for example. Here, no such effects are present and
the matrix is actually compressed and somehow the gaseous species can
apparently modify the chain mobility. If the idea that the molecules
actually reside in sites comparable with their own dimensions is correct,

and the gases kinetic energies are significantly less than that in the ambient, then one might suppose that these species might have a reduced mobility. Perhaps then, the gas molecules would move along the chains, and thereby operate in a fashion which is not dissimilar to the movement of a dislocation or a point defect. The gas molecules may be able to move along the chain carrying the defects and opening up, perhaps like a wedge, the local volumes and hence facilitate the relaxation of the chains and thereby encourage intra-molecular motions (see Figure 7.2). The idea of gas molecules acting in this fashion is highly speculative and additional experimental investigation would be required to confirm or discount this type of idea. In the present work, it has not proven useful to use the pressure dependence of the room temperature transition as a discriminative tool and early studies on dielectric loss in gaseous media proved inconclusive. An interesting prospect would be an attempt to undertake some type of spectroscopic studies with a wider range of gaseous species in order to detect whether there are any modifications to the chain mobility in the matrix in the presence of gas species. Similarly, if a suitable probe could be developed to measure the mobility or the kinetic energy of the gaseous species in the matrix, useful information could be produced. The central problem associated with ascribing a suitable volume in the matrix for the gas could then be examined in more detail. Finally, it is worth mentioning that attempts to use molecular models to evaluate the likelihood of discrete domains between chains which could incorporate gas molecules have proven inconclusive and hence an investigation which involved a study of dynamic rather than a static chain might be more appropriate.

APPENDIX

SAFETY AND DESIGN CRITERIA FOR THE GAS PRESSURE VESSEL

1. Pressure Vessel Chamber

The chamber had an aspect ratio, K of 2.5, and was 61 cm long. The material's hardness was 380 Hv corresponding to a yield stress, σ_y and an ultimate tensile strength, σ_u of 1.15×10^8 Kgm^{-2} and 1.23×10^8 Kgm^{-2} respectively (Smitchells, 1967).

1.1 Maximum Allowable (Safe) Working Pressure

According to the High Pressure Safety Code, HPSC (Saville, 1975), for vessels of O.D. less than 15 cm, the yield pressure P_y and the burst pressure P_b are given by

$$P_y = \frac{\sigma_y}{2} \left(\frac{K^2-1}{K^2}\right) \quad \text{and} \quad P_b = 2\sigma_u \left(\frac{K-1}{K+1}\right)$$

The maximum allowable working pressure is the lesser of 0.67 P_y and 0.25 P_b. In this case this is equal to ca. 260 MPa. The vessel's safety factor is therefore given by:

$$\frac{\text{Maximum allowable working pressure, } P_{max}}{\text{Maximum working pressure, } P_w} = \frac{260}{55} \approx 5$$

2. Safety and Design Criteria for the Pressure Vessel Cap

The hardness of the pressure vessel cap material was 250 Hv. This corresponded to a σ_u and σ_y of 9.5×10^7 Kgm^{-2} and 8.7×10^7 Kgm^{-2} (Smitchells, 1967) respectively. The cap was held to the chamber via six bolts. A dimensional drawing of one such bolt connecting the cap and the chamber is shown in Figure I. Possible modes of failure of the cap and bolts are discussed in the following sections.

2.1 Failure due to the Shearing of Cap

Assuming that the maximum allowable shear stress on each cap hole is half the ultimate tensile strength of the cap material, the maximum shear load allowed on the cap is therefore:

$$\tfrac{1}{2}(6 \ A\sigma_u) = 1.7 \times 10^6 \ Kg \qquad \text{where } A = \pi Dh \ \text{(see Figure I)}$$

For a maximum working pressure of 55 MPa, the maximum load a cap is subjected to through a bore of 5.08cm is ca. $1.1 \times 10^4 Kg$. The corresponding safety factor with respect to shear is given by:

$$\frac{\text{maximum allowable load } (=1.7 \times 10^6 \ Kg)}{\text{maximum working load } (=1.1 \times 10^4 \ Kg)} \ >> \ 4$$

which is the specified minimum by the HPSC.

2.2 Failure Due to the Bending of Cap

Figure II represents a proposed mode of failure of cap due to bending. The maximum displacement, W_{max} and the maximum stress, σ_{max} due to this failure mode are given by (Benham et al, 1980):

$$W_{max} = C' \ \frac{a'P}{Eh^3} \quad \text{and} \quad \sigma_{max} = C'' \frac{a^2 P}{h^2}$$

where a, b and h are respectively 5.8 cm, 2.5 cm and 5.8 cm. P is the maximum working pressure and E is the Young's modulus for the cap material $(6.8 \times 10^8 \ Kgm^{-2})$. For a/b = 2, the constants C' and C'' are 0.0877 and 0.753 respectively, from which W_{max} and σ_{max} are 0.04 mm and $4.14 \times 10^7 \ Nm^{-2}$. The corresponding safety factor for bending is:

$$\frac{\sigma_y}{\sigma_{max}} = \frac{8.7 \times 10^8}{4.14 \times 10^7} \approx 22$$

2.3 Failure Due to the Shearing of Bolt Heads

The maximum force at which all six bolts can be subjected to before the shearing of their heads is (see Figure I):

$$\tfrac{1}{2}(6\sigma_u A) = 9.9 \times 10^6 N$$

(where A is the shear area of each bolt head $= 2.7 \times 10^{-3} m^2$).

The corresponding safety factor concerning the shearing of all six bolt heads is given by:

$$\frac{\text{maximum allowable shear force}}{\text{maximum working force}} = 90$$

2.4 Failure Due to the Shearing of Bolt Threads

From Figure I, the shear area, A, of bolts in the threaded section

$= \pi \times 2.6 \times 5.5 \times 10^{-4} \times 6$

$= 0.027 \ m^2$.

The maximum design force on the threads $= \tfrac{1}{2}A\sigma_u$

$$= 1.7 \times 10^7 N.$$

The corresponding safety factor with respect to the shearing of all six bolt threads = 150.

3. Design of a Blast Box

The following section undertakes to determine the thickness of a mild steel cubical blast box required to safely contain both the shock wave and any projectiles ejected in case of pressure vessel failure.

3.1 Evaluation of System Energy

The system energy released as a result of vessel failure is:

$$E_s = E_1 + E_2 + E_3$$

where

E_1 = fluid expansion energy

E_2 = chemically released energy

E_3 = elastic strain energy of the vessel (assumed to be negligible)

3.1.1 Calculation of fluid expansion energy, E_1

This is the internal energy change, ΔU, for a process. It is given by the following expression:

$$\Delta H = \Delta U + \Delta(PV)$$

where ΔH is the enthalpy change and P and V are the pressure and volume of gas respectively.

Now consider a catastrophic failure leading to either:

(a) pressure vesel rupture in which all the energy of gas is released in the form of a shock wave;

or

(b) a less likely case in which the system energy is used up in ejecting a lid.

(a) Pressure Vessel Rupture, Shock Wave Containment

Assume the pressure vessel rupture leads to a reversible isentropic expansion. At a maximum hypothetical pressure P_1 of 172 MPa (ca. 3 x P_{max}) and a temperature T_1 of 323.15 K and using the PREPROP/UN=UMECLB computer program stored at Imperial College, the thermodynamic properties of gaseous nitrogen are as follows:

Density, RHO_1 = 2.45 x 10^4 mole/m^3 (=1/V_1)

Enthalpy, H_1 = 2216.51 J/mole

Entropy, S_1 = 126.45 J/mole K

Computer input: - RHO_1, H_1 and T_1. Evaluate T_2, H_2

and RHO_2 for a final condition P_2 = 1 atm and $S_2 = S_1$

Computer output: - using iteration, $T_2 = 47K$, $H_2 = -7920$ J/mol

and $RHO_2 = 4.65 \times 10^2$ mol/m^3 $(= 1/V_2)$

The internal energy change, ΔU and hence the energy of the shock wave for 11 modes of gas is

$$\Delta U = 11 |(H_2 - P_2 V_2) - (H_1 - P_1 V_1)| = -36685 \text{ J}$$

The equivalent static pressure of a shock wave of energy ΔU is given by (Saville, 1975):

$$P = 7.6 \ |(\Delta U/10^6)/V|^{0.72} = 0.72 \text{ bar}$$

This is the equivalent static pressure that the blast box should be able to withstand for a complete containment of the shock wave.

(b) Lid Ejection: Penetration of Projectile Through Mild Steel

In this case, the energy released by the gas following an explosion is assumed to be totally consumed in ejection of lid. Assuming that the plug clears the orifice by an amount equal to its diameter just after the explosion, then $RHO_2 = \frac{1}{2}RHO_1 = 1.225 \times 10^4$ mol/m^3.

Computer input: $P_1 = 1.72 \times 10^8$ N/m^2, $S = 126$ j/mol K

Computer output: $T_2 = 180K$, $H_2 = -5694$ j/mol and $P_2 = 1.37 \times 10^7$ N/m^2

The equivalent energy release is:

$$U_2 = H_2 - P_2 V_2 = -74936 \text{ J}$$

Assume that in case of failure, there is also spontaneous reaction between PTFE and N_2 leading to the release of an energy equal to exploding and equivalent mass of tri-nitroglycerene, TNT. 1 Kg TNT releases 4.5×10^6 J energy following explosion. The maximum chemically

released energy for 2 gms of PTFE is therefore 9×10^3 J.

The total kinetic energy of lid is therefore:

$$E_{KE} = 74936 + 9 \times 10^3 = 83440 \text{ J}$$

The velocity of a projectile (the lid) of an equivalent energy is given by:

$$V = (\frac{2E_{KE}}{M})^{\frac{1}{2}} = 167 \text{ m/sec where M} = \text{mass of lid} = 6 \times 10^3 \text{ g.}$$

The thickness of mild steel required to stop the above projectile is given by (Saville, 1975):

$$t = \frac{CM}{A} \log_{10} (1 + 5 \times 10^{-5} V^2)$$

where

A = projected impact area of projectile = $1.54 \times 10^{-2} \text{ m}^2$

and C = 0.5×10^{-4} for mild steel.

Substituting the corresponding values in the above equation, the thickness of a mild steel blast box required to contain the ejected cap in case of pressure vessel failure is 0.75 cm.

4. Reaction of Pressure Vessel on Ejection of Lid

Assume that following explosion, the kinetic energy of vessel lid = kinetic energy of the recoil (i.e. pressure chamber + bottom lid) = 8.4×10^4 J.

Now following exactly the same procedure as above, the thickness of mild steel support table required to stop the penetration of recoil of mass 40 Kg is 0.87 cm.

5. Summary

Following the above investigation, it is concluded that the most likely cause of failure is that leading to pressure vessel rupture. The corresponding safety factor is 5 which is well above the specified minimum by the HPSC. The vessel is therefore exposed to a hydraulic test pressure of 250 MPa (ca. 5 x maximum working pressure) for 24 hrs. A 0.74 cm thick walled steel cabinet is required to contain both the shock wave and any projectile in case of pressure vessel failure.
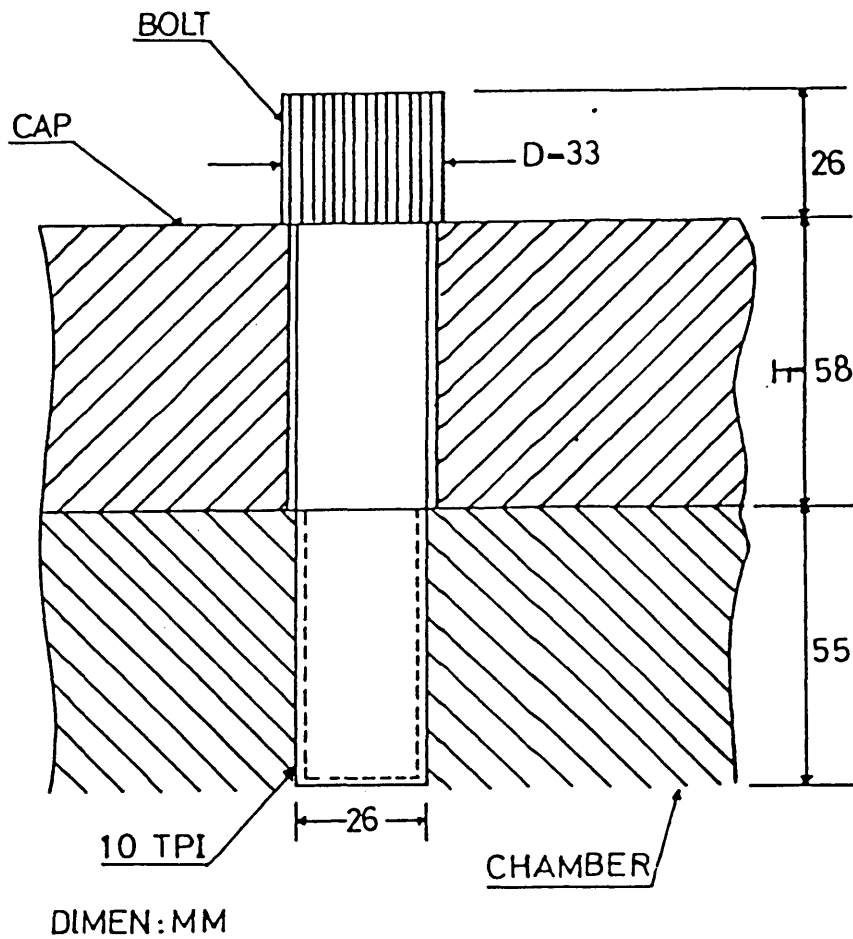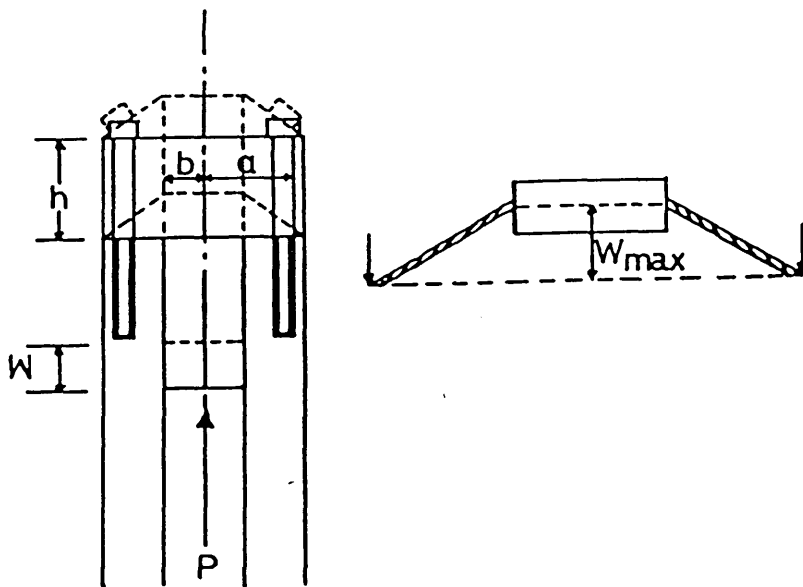
FIG I : PRESSURE VESSEL BOLT ASSEMBLY

FIG II : SYSTEMATIC REPRESENTATION OF CAP
FAILURE DUE TO BENDING

REFERENCES

Ainbinder, S.B., Laka, M.G. and Maiors, I.Y., 1965, J.Polym.Sci., 1, 65.

Albright, L.F., 1974, Processes for Major Addition Type Plastics, (McGraw-Hill: New York), 72.

Andersson, P. and Backstrom, G., 1972, High Temp-High Press., 4, 101-9.

Andersson, P. and Backstrom, G., 1973a, J.Apply.Phys., 44 (2), 705.

Andersson, P. and Backstrom, G., 1973b, J.Apply.Phys., 44(6), 2601.

Andersson, P. and Backstrom, G., 1976, Rev.Sci.Instrum., 47(2), 205-9.

Andersson, P. and Sundquist, B., 1975, Polym.Phys.Ed., 13, 243.

Angus, S., Reuck, K.M. and McCarty, R.D., 1975, Helium International Tables (London: Pergamon Press), pp.150-93.

Assael, M., 1980, Ph.D. Thesis (Accurate Measurements of the Thermal Conductivity of Gases), Imperial College, London, pp.108-22.

Atkinson, E.B., 1977, J.Polym. Sci., 15, 795.

Auerback, I., Miller, W.R., Kuryla, W.C. and Genham, S.D., 1958, J.Polym.Sci., 28, 129.

Baheteja, S.K., Pae, K.D. and Sauer, J.A., 1974, J.Appl.Polym.Sci., 18, 1319.

Barham, P.J. and Arridge, R.G.C., 1979, Polym., 20, 509.

Barker, P.E., Chen, R.Y.S. and Frost, R.S., 1977, J.Polym.Sci.:Polym. Phys.Ed., 15, 1199.

Barrer, R.M., 1939, Trans.Farad.Soc., 35, 628.

Beards, C.F., 1981, Vibration Analysis and Control System Dynamics (Cichester: Ellis Horwood), pp.44-5.

Beecroft, R.I. and Swenson, C.A., 1959, J.Appl.Phys., 30, 1973-8.

Benham, P.P. and Warnock, F.V., 1980, Mechanics of Solids and Structures (London: Pitman), pp.382-3.

Bett, K.E., Rowlinson, J.S. and Saville, G., 1975, Thermodynamics for Chemical Engineers (London: Athlone Press), pp.84-86.

Bernett, M.K. and Zisman, W.A., 1959, J.Phys.Chem., 63, 1911.

Billinghurst, P.P., 1961, Ph.D. Thesis (The Effect of Hydrostatic Pressure on Viscoelastic Properties of Polymers), Cambridge University, Cambridge, p.71.

Billinghurst, P.P. and Tabor, D., 1971, Polym., 12, 101-118.

Blyth, A.R., 1980, Electrical Properties of Polymers (Cambridge: Cambridge University Press), pp.72-3.

Bonner, C.D. and Cheng, Y.L., 1975, Polym.Lett., 13, 259-64.

Boyer, R.F., 1966, J.Polym.Sci., C14, 1966.

Bridgeman, P.W., 1948, Proc.Am.Acad.Arts.Sci., 76, 71.

Bridgeman, P.W., 1952, Studies in Large Plastic Flow and Fracture (New York: McGraw Hill), p.90.

Bridgeman, P.W., 1953, J.Appl.Phys., 24, 560.

Brown, N., 1981, J.Macromol.Sci.Phys., B19(3), 387.

Brown, N. and Metzger, B.D., 1980, J.Polym.Sci.:Polym.Phys.Ed., 18, 1979.

Bryant, W.M.D., 1962, J.Polym.Sci., 56, 277.

Buckingham, A.D. and Pople, E., 1955, J.A.Trans.Farad.Soc., 51, 1179-84.

Bunn, C.W., Cobbold, A.J. and Palmer, R.P., 1958, J.Polym.Sci., 28, 365.

Bunn, C.W. and Holmes, D.R., 1958, Disc.Farad.Soc., 25, 95.

Bunn, C.W. and Howells, E.R., 1954, Nature, 174, 549.

Chen, C.S.H., Colthup, N., Deichert, W. and Webb, R.L., 1960, J.Polym. Sci., 45, 247.

Cheng, Y.L. and Bonner, D.C., 1978, J.Polym.Sci., 16, 319.

Choy, C.L., 1977, Polym., 18, 984-1003.

Christiansen, A.W., Baer, E. and Radcliffe, S.V., 132nd Amer.Chem. Soc. Meeting, New York.

Colbeck, E.W. and Manning, W.R.D., 1953, Trans.Inst.Chem.Eng., 203.

Collins, E.A., Bares, J. and Billmeyer, F.W., 1973, Experiments in Polymer Science (New York: John Wiley), pp.296-9.

Cox, J.M., Wright, B.A., and Wright, W.W., 1964, J.Appl.Polym.Sci., 8, 2935.

Dainton, F.S., Evans, D.M., Hoare, F.E., and Melia, T.P., Polym., 3, 286.

Daynes, H.A., 1920, Proc.Roy.Soc., A94, 286.

Debye, P., 1914, Vortrage Uber die Kinetische (Berlin: Teubner), 108.

Din, F., 1961, Thermodynamic Functions of Gases (London: Butterworth), pp.146-7.

Doak, K.W. and Scharge, A., 1965, Crystalline Olefin Polymers (New York:

Interscience), 301.

Doban, R.C., Knight, A.C., Peterson, J.H. and Sperati, C.A., 1956, Paper: 130th Meeting, Am.Chem.Soc., Atlantic City.

Duckett, R.A. and Joseph, S.H., 1976, Polym., 17, 329-34.

Duckett, R.A., Joseph, S.H., Sumner, H. and Stachurski, Z., 1979, Deformation, Yield and Fracture of Polymers: 4th Int.Conf., 37.1.

Durrill, P.L. and Griskey, R.G., 1966, Am.Inst.Chem.Engnrs.J., 12, 1147-51.

Dzhavadov, L.N., 1975, High Temps-High Press., 7, 49-54.

Ehlich, P., 1953, J.Res.Natl.Bur.Stand., 51,(4), 185.

Eiermann, K., 1964, Kolloid-Z.Z.Polym., 199, 63.

Eiermann, K., 1965, Kolloid-Z.Z.Polym., 201, 3.

Eiermann, K., 1965, Kunstoffe, 55, 355.

Findley, W.N., Reed, A.M. and Stern, P., 1967, J.Appl.Mech., 34, 895.

Findley, W.N., Reed, A.M. and Stern, P., 1968, Modern Plastics, 45, 141-69.

Fluon Technical Service Note, F3, I.C.I. Plastics Division, Hertz.

Fortune, L.R. and Malcolm, C.N., 1960, J.Phys.Chem., 64, 934.

Fourier, J., 1955, The Analytical Theory of Heat (Dover: Englewood), 293.

Frost, R.S., Barker, R.E. and Chen, R.Y.S., 1978, J.Polym.Sci.:Polym. Phys.Ed., 16, 689.

Graham, T., 1866, Phil.Mag., 32, 401.

Grant, I.S. and Phillips, W.R., 1975, Electromagnetism (London: John Wiley), pp.54-5.

Gregg, C., 1972, Dielectric Constants of Gases, Handbook of Chemistry and Physics, (Ohio: CRC Press), p.E47.

Groenewege, M.P., Raff, V. and Doak, K.W., 1965, Crystalline Olefin Polymers (New York: Interscience), 2, 798.

Haldon, R.A. and Simha, R., 1968, J.Appl.Phys., 39, 1890.

Hansen, D., Kantagga, R.C. and Ho, C.C., 1966, Polym.Eng.Sci., 6, 260.

Harris, J.S., Ward, I.M. and Parry, J.S.C., 1971, Mat.Sci., 6, 110.

Heijboer, J., 1956, Kolloid Z., 148, 36.

Hildebrand, J.H. and Scott, R.L., 1950, Solubility of Non Electrolytes (New York: Reinhold), 53.

Kirakawa, S. and Takemura, T., 1968, Jap.J.Appl.Phys., 7(8), 814.

Holliday, L., Mann, J., Pogany, G.A., Pugh, H.L.D. and Gunn, D.A., 1964, Nature, 202, 381.

Howells, E.R., Fluon Technical Service Note, F3, I.C.I. Plastics Division, Hertz.

Jezl, J.L. and Honeycutt, E.M., 1969, Propylene Polymers (New York: Wiley), 11, 597.

Johnston, D.R., Ondemans, G.J. and Cole, R.H., 1960, J.Chem.Phys., 33, 1310-17.

Kantor, S.W. and Osthoff, R.C., 1953, J.Am.Chem.Soc., 75, 931.

Kieffer, S.W., 1976, J.Geophys.Res., 81(17), 3018-24.

Klein, J., 1977, Ph.D. Thesis (Diffusion of Long Molecules through Bulk Polymers), Cambridge University, Cambridge, 5.

Klug, A. and Franklin, E.R., 1958, Disc.Farad.Soc., 75, 104.

Kreith, F., 1973, Principles of Heat Transfer (New York: Intext Educational Publishers), pp.312-15.

Kumins, C.A. and Roteman, J., 1961, J.Polym.Sci., 55, 683.

Kuroda, T. and Sakami, H., 1958, Nagoya Koggs Gijutsu Shikensho Hokoku, 7, 1.

Kolough, R.J. and Brown, R.G., 1968, J.Appl.Phys., 39, 3999.

Langmuir, J., 1918, J.Am.Chem.Soc., 40, 1361.

Lundberg, J.L. and Mooney, E.J., 1969, J.Polym.Sci., 17, 947-62.

Lundberg, J.L., Wilk, M.B. and Huyett, M.J., 1960, J.Appl.Phys., 31(5-8), 231.

Lundberg, J.L., Wilk, M.B. and Huyett, M.J., 1962, J.Polym.Sci., 57, 275-99.

Lundberg, J.L., Wilk, M.B. and Huyett, M.J., 1965, Indust.Eng.Chem.Fund., 2(1), 37.

Manashe, J., 1980, Ph.D. Thesis (Thermal Condctuvity Measurements of Liquids and Gases at High Pressures), Imperial College, London, pp.87-106.

Martin, G.M. and Eby, R.K., 1968, J.Res.Natl.Bur.Stand.-A: Phys.Chem., 72A(5), 467-70.

Matsuoka, S. and Maxwell, B., 1958, J.Polym.Sci., 32, 131.

McCane, D.L., 1970, Encyclopedia of Polymer Science and Technology (London: Wiley), 13, 623.

McCrum, N.G., 1959, J.Polym.Sci., 34, 355.

McKinney, J.E. and Goldstein, M., 1974, J.Res.Natl.Bur.Stand:Sect.A., 78, 331.

Mclaren, K.G. and Tabor, D., 1963, Nature, 197(4870), 856-59.

Mears, P., 1954, J.Am.Chem.Soc., 76, 3415.

Mears, D.R., Pae, K.D. and Sauer, J.A., 1969, J.Appl.Phys., 40, 4229.

Meyer, K.H., 1942, High Polymeric Substances (New York: Interscience), 139.

Michaels, A.S. and Bixler, H.J., 1961, J.Polym.Sci., L, 393.

Mizouchi, N., 1973, Rev.Sci.Instrum., 44(1), 28-31.

Moyniham, R.E., 1958, J.Am.Chem.Soc., 81, 1045.

Nadia, A., 1950, Theory of Flow and Fracture of Solids (New York: McGraw Hill), 138.

Olf, H.G. and Peterlin, A., 1974, J.Polym.Sci., 12, 2209.

Pae, K.D. and Bhateja, S.K., 1975, J.Macromol.Sci., C13, 1.

Park, G.S., 1952, Trans.Farad.Soc., 48, 11.

Parry, E.J. and Tabor, D., 1974, J.Mater.Sci., 9, 289.

Passaglia, P. and Kevorkian, H.K., 1963, J.Appl.Phys., 34, 90.

Passaglia, E. and Martin, M.G., 1964, J.Res.Natl.Bur.Stand:App.Phys. Chem., 68A, 273.

Pasternak, R.A., Burns, G.L. and Heller, J., 1971, Macromol., 4(4), 470.

Pasternak, R.A., Christensen, M.V. and Heller, J., 1970, Macromol., 3, 366.

Pastine, D.J., 1970, J.Appl.Phys., 41, 5085.

Paterson, M.S., 1964, J.Appl.Phys., 35, 176.

Peierls, R., 1929, Ann.Phys.Lpz., 3, 1055.

Peterlin , A., 1970, J.Colloid.Int.Sci., 32, 654.

Peterlin , A., 1974, Pure.Appl.Chem., 39, 239.

Pierce, R.H.H., Clark, E.S., Whitney, J.F. and Bryant, W.M.D., 1956, Abstracts of 130th Amer.Chem.Soc. Meeting, Atlantic City.

Plunkett, R.J., 1941, U.S. Pat: 2230654 (to Kinetics Chemicals Inc.).

Powell, R.L., Rogers, W.M. and Coffin, D.O., 1957, J.Res.Nat.Bur.Stand., 59, 349.

Pugh, H.L.D., Chandler, E.F., Holliday, L. and Mann, J., 1971, Polym. Eng.Sci., 11, 463.

Prevorsek, D. and Butler, R.H., 1972, Int.J.Polym.Mat., 1, 251.

Quach, A. and Simha, R., 1971, J.Appl.Phys., 42, 4592.

Quinn, F.A., Roberts, D.E. and Work, R.N., 1951, J.Appl.Phys., 22(8), 1085.

Rabinowitz, S., Ward, I.M. and Parry, J.S.C., 1970, J.Mat.Sci., 5, 29.

Reding, F.P., Faucher, J.S. and Whitman, R.D., 1961, J.Polym.Sci., 54, 556.

Reese, W. and Tucker, J.E., 1965, J.Chem.Phys., 43, 105.

Renfrew, M.W. and Lewis, E.E., 1946, Indust.Eng.Chem., 38, 870.

Rigby, H.A. and Bunn, C.W., 1949, Nature, 164, 583.

Rodriguez, F., 1982, Principles of Polymer Systems (New York: Hemisphere), 419.

Rossay, B.B., 1964, Prakt.Che., 15(2), 64.

Ryland, A.L., 1958, J.Chem.Educ., 35, 80-6.

Sadar, D., Radcliffe, S.V. and Baer, E., 1968, Polym.Eng.Sci., 8, 290.

Sandberg, O., Andersson, P. and Backstrom, 1977, J.Phys.E:Sci.Instrum., 10, 474.

Sandberg, O. and Backstrom, G., 1980, J.Polym.Sci:Polym.Phys.Ed., 18, 2123.

Sauer, J.A., Mears, D.R. and Pae, K.D., 1970, Eur.Polym.J., 6, 1015.

Saville, G., 1977, High Pressure Safety Code (London: Milner), pp.1-32.

Schonhorn, H. and Ryan, F.W., 1969, J.Adhesion, 1, 43.

Schults, A.K., 1956, J.Chem.Phys., 53, 933.

Seely, S., 1958, Electron Tube Circuits (New York: McGraw Hill), pp.147-51.

Sella, C., 1959, Sompt.Red., 248, 1819.

Shooter, K.V. and Thomas, P.H., 1949, Research, 2, 533.

Silano, A.A., Pae, K.D. and Sauer, J.A., 1977, J.Appl.Phys., 48(10), 4076.

Smith, J.A.S., 1955, Disc.Farad.Soc., 19, 207.

Smitchells, C.J., 1967, Metals Reference Handbook (London: Butterworth), 252.

Speerschneider, C.J. and Li, C.H., 1963, J.Appl.Phys., 34, 3004.

Sperati, C.A. and Starkweather, H.W., 1961, Fortchr.Hoch.Poly.-Forsch., 2, 465.

Spetzler, H.A. and Meyer, M.D., 1974, Rev.Sci.Instrum., 45(7), 911.

Stannett, V. and Williams, J.L., 1966, J.Polym.Sci.C., 10, 45.

Stephens, D.R., Heard, H.C. and Schock, R.N., 1972, UCID-16007.

Timoshenko, S., 1937, Vibration Problems in Engineering (London: Constable), pp.170-2.

Toshihiko, K. and Sakami, H., 1958, Nagoya Kogyo Gignstsu Shikensho Hokou, 7, 1.

Van Amerongen, G.J., 1964, Rubb.Chem.Technol., 37, 1065.

Van Dyke, M., 1982, An Album of Fluid Motion (Stanford: Parabolic), p.22.

Van Krevelen, D.W., 1972, Properties of Polymers (Amsterdam: Elsevier), pp.236-7.

Weir, C.E., 1950, J.Res.Natl.Bur.Stand., 50(2), 85-7.

Wilson, C.W. and Pake, G.E., 1957, J.Chem.Phys., 27, 115.

Wittmann, J.C. and Kovac, A.J., 1969, J.Polym.Sci., C16, 4443.

Wroblewski, S., 1879, Weid.Annln.Phy., 8, 29.

Wunderlich, B. and Dole, J., 1957, J.Polym.Sci., 24, 201.

Wu, J.C.B. and Brown, N., 1982, J.Mat.Sci., 17, 1311.

Yasuda, T. and Araki, Y., 1961, J.Appl.Polym.Sci., 5(15), 331.

Zoller, P., 1978, J.Appl.Polym.Sci., 22, 633.

Zoller, P., Bolli, P., Pahud, V. and Ackermann, H., 1976, Rev.Sci. Instrum., 47(8), 948.

†Michaels,A.S.,and Parker,R.B.,1959,J.Polym.Sci.,41,53.